Master Thesis, Department of Geosciences

Mixed siliciclastic-carbonate sedimentation in the Late Ordovician shallow marine epicontinental sea, Oslo Region

Martin Kjærsgaard

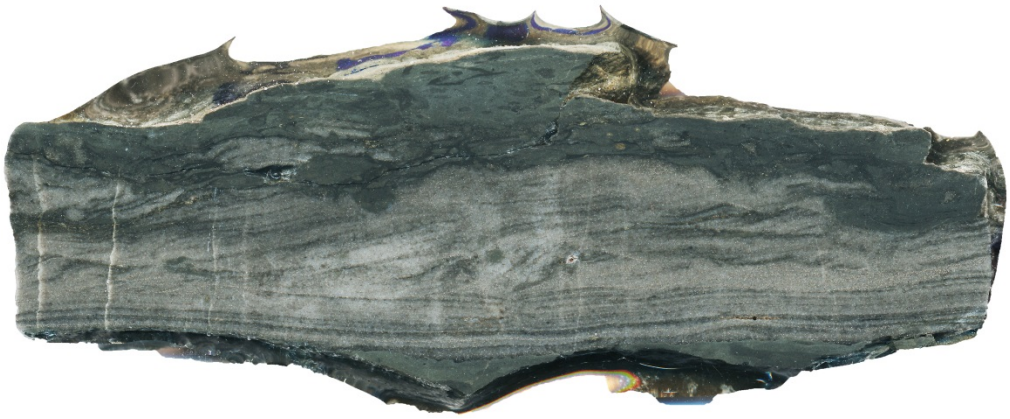

UNIVERSITY OF OSLO

FACULTY OF MATHEMATICS AND NATURAL SCIENCES

Front page: Sample slab suface scan of a tempestite bed. Sample collected on Rambergøya. Length of the sample is approximately 10 centimeters.

Mixed siliciclastic-carbonate sedimentation in the Late Ordovician shallow marine epicontinental sea, Oslo Region

Martin Kjærsgaard

Master Thesis in Geosciences

Discipline: Geology

Department of Geosciences

Faculty of Mathematics and Natural Sciences

University of Oslo

July 4th, 2014

Tutors: Professor Hans Arne Nakrem (UiO), Professor emeritus Johan Petter Nystuen and Johan Fredrik Bockelie (Ithaca Petroleum Norge AS)

This work is published digitally through DUO – Digitale Utgivelser ved UiO

http://www.duo.uio.no

It is also catalogued in BIBSYS (http://www.bibsys.no/english)

Abstract

The Upper Ordovician (Upper Katian to Middle Hirnantian) of the Skogerholmen Formation, Husbergøya Formation and the Langøyene Formation has been studied on the islands Hovedøya, Rambergøya and Langøyene in the inner part of Oslofjorden.

During the Upper Katian to Middle Hirnantian there was a shift from the dominance of calcareous shale and limestone to an increase in coarser siliciclastics with deposition of mainly siltstone-and sandstone beds. Transport and sedimentation have mainly taken place through storm-generated currents and suspensions, with water depths varying from beneath storm-wave base to proximal settings of a prograding shoreface.

The sedimentary logs display an upwards shallowing in the uppermost part of the Skogerholmen Formation by the occurrence of a thin limestone conglomerate. This was followed by a flooding event and a subsequent slow upwards shallowing in the Husbergøya Formation. Rhythmic variations in thickness of storm-deposited beds are observed throughout the Husbergøya Formation and indicate sea-level fluctuations. There is a marked increase in very fine sand fraction at the top of the studied succession. This indicates a rapid fall in sea-level which was most likely controlled by the Late Ordovician glaciation in Gondwana land. A forced regression with progradation of the shoreline is proposed as mechanism for the increasing sand content in the uppermost part of the studied succession.

Five sedimentary logs on three localities were created during the fieldwork. Each log represents approximately 30 meters of succession. Three of the sections are logged in the scale of 1:10 and show measured thickness, lithology, sedimentary structures and fossil content of each individual observed bed. Both siliciclastic and carbonate samples were collected and studied in thin sections and polished slabs.

Acknowledgements

First of all I want to direct a special thank you to my main supervisor Hans Arne Nakrem for all the helpful support and guidance during all stages of writing this master thesis. I would also like to give a special thanks to my second supervisor Johan Petter Nystuen for always having the time to answer all of my questions.

I would also like to thank my third supervisor, Johan Fredrik Bockelie for taking the time to guide us during the fieldwork. I will never forget our interesting boat trip.

A special thanks to Martin Sandbakken. I really enjoyed our interesting talks during the fieldwork and still remember how good our “field-work-taco” tasted.

I would also like to acknowledge Salahalldin Akhavan for preparing my thin sections, Øyvind Hammer for loaning us the susceptibility meter and havnepolitiet in Oslo for taking the time to transport us to Langøyene during the off-season.

I am most grateful to my family for all the help and support you guys have given me throughout my studies.

Finally, my thanks and love goes to Tine Lise Folvik for keeping me well fed and giving me constant moral support during the most stressful periods of my master thesis.

Oslo, July 4^{th}

Martin Kjærsgaard

Contents

1 Introduction

The Upper Ordovician mixed siliciclastic-carbonate successions in the Oslo Area are well known from the earlier work by Kjerulf and Dahl (1857) and Brøgger (1882) to the work by *inter alia* , Bjørlykke (1974a), Brenchley and Newall (1975), Brenchley et al. (1979), Stanistreet (1989).

Mixed siliciclastic-carbonate sedimentary systems are common in shallow-marine environments at low latitudes. The depositional environments include land-attached settings of continental shelves, epicontinental seas, rift- and foreland basins. The interaction of carbonate-producing biogenic processes in the marine realm and processes of influx of terrigenous siliciclastic detritus involves a series of controlling factors. These include type and abundance of carbonate-producing organisms, temperature and climatic changes, changes in relative sea level driven by eustacy or tectonics, or a combination, relief of land areas, storm activity, tidal currents, salinity, pH and others. The Upper Ordovician succession in the Oslo Region was formed in an epicontinental sea at low latitudes and is characterized by various mixed siliciclastic-carbonate facies that illustrate the complexity of this type of sedimentary system. The goal of the present study is to supply with detailed description of the lithology, sedimentary structures, bed thickness, characteristics and the controlling factors in this mixed siliciclastic-carbonate environment and to discuss the impact of various external and internal factors controlling the sedimentation.

This master thesis uses detailed sedimentary logs, sample slab surface scans, microscopic methods and some laboratory work to describe the depositional environment and sedimentary processes of the mixed siliciclastic-carbonate successions from the upper part of the Skogerholmen Formation to the lower part of the Langøyene Formation. All exposed outcrops of the Husbergøya Formation are present in the sedimentary logs and a special emphasis has been put on this part of the succession. The main focus has been the sedimentological aspects of the strata, but fossils and trace fossils have been recorded and are used as palaeoenvironmental indicators.

Data for this work has been collected from three islands in the inner Oslo fjord, Norway. The data has been processed at the Natural History Museum in Oslo.

2 Regional and tectonic setting

Residual patches of the Lower Palaeozoic epicontinental platform sequence are located in different parts in Southern Norway, Sweden and Estonia (Brenchley and Newall, 1977). The total thickness of this remaining platform sequence seen in the Oslo area is about 1550 m and approximately 470 m belongs to the Ordovician(Brenchley and Newall, 1975). The fold axis in these Lower Palaeozoic sediments in the Oslo Area has a NE-SW to ENE-WSW strike, but the deformation style is not completely uniform throughout the Oslo Region (Bruton et al., 2010).

The Caledonian Orogenesis with the closure of the Iapetus ocean and collision between Baltica and Laurentia resulted in folding and shortening of the Lower Paleozoic successions in the Oslo-Asker area (Ramberg and Bockelie, 1981). The collision started during the Tremadocian and the complete closure of the Iapetus Sea occurred in the Late Silurian (Bruton et al., 2010). The collision also led to the formation of thrust sheets that had a present day transport direction approximately to the E or SE, but it was not until Late Llandovery that this nappe translation is recorded to have yielded any indirect effect on the successions in the Oslo Area. The Oslo Region exhibits characteristics that place it within the external zone of the Caledonian Nappe System. Harmonic and disharmonic folds, back-thrusts, deformed foreland basin units, imbricate stacks, duplexes and other characteristics are associated with pronounced basal thrust with splay faults in this area. Local metamorphism in the form Permian intrusions of sills and dykes is also common in these Upper Palaeozoic sedimentary rocks (Bruton et al., 2010). A sole plane is located 1-2 m above the Precambrian basement within the Cambrian black Alum shale. Sediments above this sole are folded, while sediments below has been influenced by Permian block faulting (Bockelie, 1982).

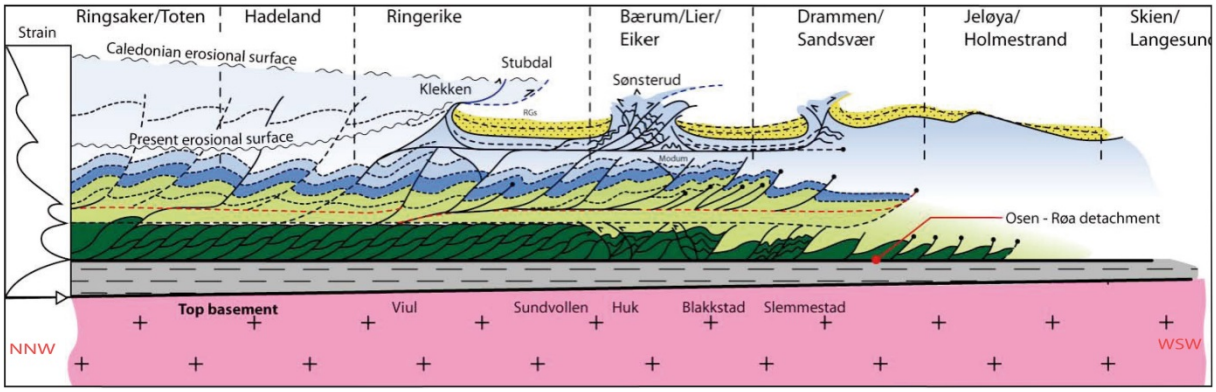

Figure 2.1: *Schematic cross-section of the tectonic morphology of the Oslo Region displaying the different principal structural levels. Figure not to scale. Modified from Bruton et al. (2010).*

2.1 Ordovician Climate

In the Early Ordovician, Baltica was situated about 60° S latitude and during the Ordovician the plate moved northwards towards the equator (Nielsen, 2003). Many reconstructions of the Late Ordovician palaeogeography have been proposed in recent years, and most of them place the Late Ordovician South Scandinavia in the southern hemisphere, more correctly in the tropics (Brenchley et al., 1979). Cocks and Torsvik (2006) proposed one reconstruction that reflect the plate dynamics and positions from Venedian to the end of the Palaeozoic. Parts of this reconstruction are presented in Figure 2.2.

In the Ordovician period, the land areas were generally small and the cratons were more like archipelagos rather than continents. Due to the small land areas and the abundance of epicontinental seas, the Ordovician period was pronouncedly thalassocratic (Jaanusson, 1984). Spjeldnæs (1960) suggested that both equator and the poles had a different position in the Ordovician than present. Indications found showed a trend of the arrangement of the Ordovician climatic zones, from warm to cold, was from N and NW to S in Europe and NW and W to E and S in America. Based on these indications, Spjeldnæs (1960) interpreted that the Ordovician equator was located at the present arctic. Jaanuson (1984) discussed that paleomagnetic data implied an Ordovician North Pole that was situated around the area of the present north-western Pacific. He also argued that since there was free exchange of water between the polar region and the thermal reservoirs of the oceans, it implied an absence of a polar ice cap around the Ordovician north pole (Jaanusson, 1984).

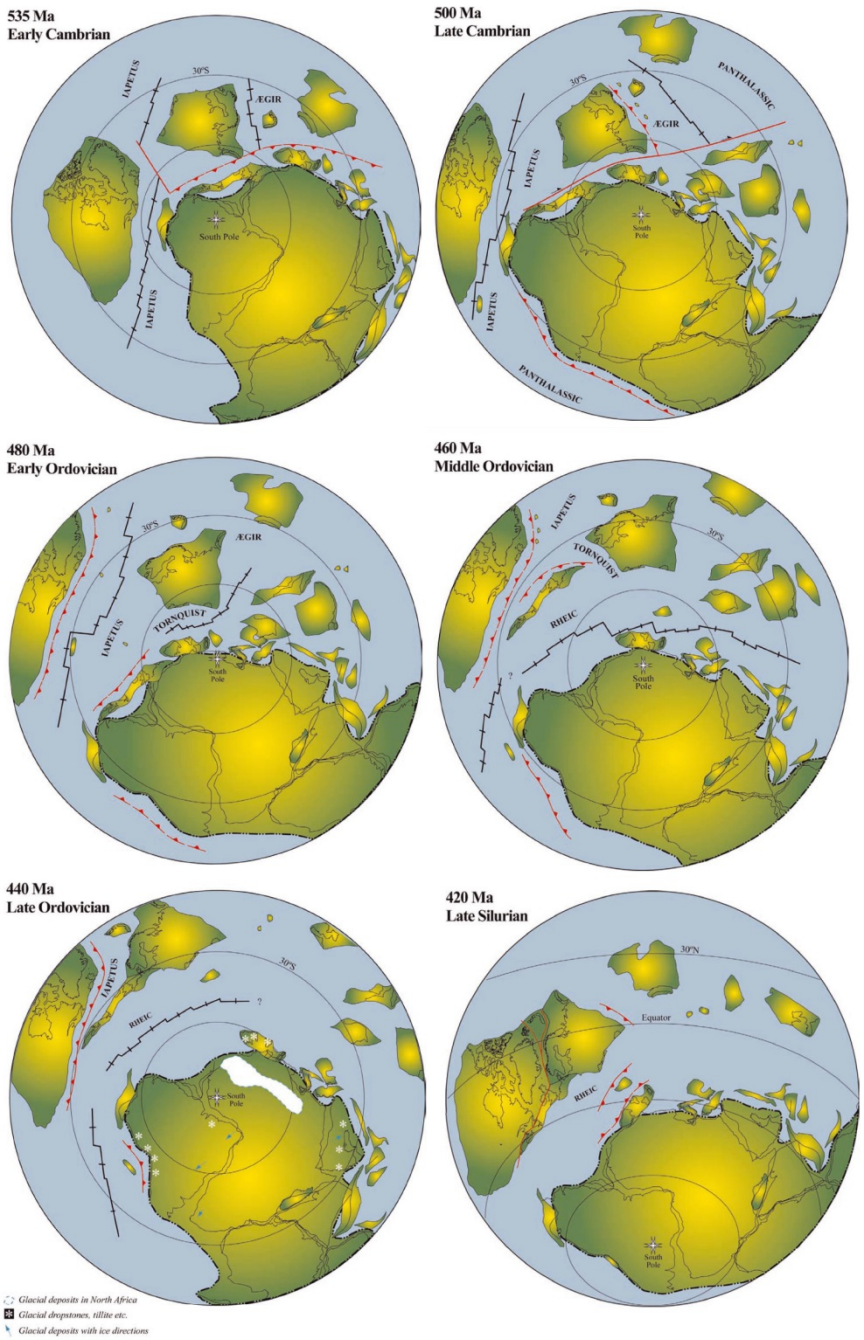

Figure 2.2: *Reconstruction of plate positions from Early Cambrian to Late Silurian with projection center at the South Pole. Black lines shows spreading centers, red lines with ticks shows subduction zones and red lines with no extra ornament shows transform faults. Modified from Cocks and Torsvik (2006).*

2.2 Sedimentation accumulation rates

The average accumulation rates in the Ordovician, recorded from Sweden and East Baltic, were in the order of 1-9 mm/1000 years. This was due to the limited clastic supply, and cold-water conditions during the Early- to Late Ordovician induced slow production of carbonates. Baltoscandia had moved northwards in the Late Ordovician and accumulation rates increased. The limited environment endured and warm water carbonate environment developed (Nielsen, 2004). The average sea floor gradient in this kind of epicontinental sea was substantially low and the water depths rarely reached 200 meter (Bjørlykke, 1974a). This also induced slow sedimentation rates. The clastic supply increased along the western periphery in the Middle Ordovician as the Iapetus Ocean closed and a foreland basin developed adjacent to the Caledonian Orogen in the (Nielsen, 2003).

3 The Baltoscandian Epicontinental Platform

Eustacy in the Early Cambrian raised the sea level over the boundaries of the Late Neoproterozoic basins. At that time, the Oslo Area was part of Baltica which had been eroded down to a peneplane basement. As a result of this inundation, the Baltoscandian Epicontinental Sea was formed. Dark mud now started to deposit, gradually filling up the basin. In the Early Ordovician, carbonate production started to deposit as the sea-level became gradually lower with more oxygenated bottom conditions. In the Oslo Area, sediments were now deposited on an epicontinental platform. Carbonate production gradually increased with a peak of maximum production in the Sandbian-Hirnantian (Nielsen, 2003). This epicontinental platform seemed to have had a palaeoslope that inclined gently to the east or southeast and this are also recorded in earlier parts of this platform(Skjeseth, 1952, Størmer, 1967, Brenchley et al., 1979). A topographic high to the west separated the epicontinental shallow sea from the Iapetus Ocean and the ocean was bounded in the east by the Baltic craton (Størmer, 1967, Brenchley et al., 1979, Brenchley and Newall, 1980, Worsley et al., 1983).

Besides an regression in the uppermost Ordovician that developed shallow water shoreface environments, water depths were probably not greater than 100 meters in the Oslo-Asker area (Brenchley and Newall, 1980). A shift from the mentioned regression to a transgressive phase is located in the Ordovician/Silurian boundary. Changes in facies due to sea-level fluctuations are also closely related to changes in fossil trace assemblages (Stanistreet, 1989).

3.1 Epicontinental seas

An epicontinental or epeiric sea is the result of flooding of continental interiors and is represented by large areas of shallow water.

In general, epeiric seas are characterized by:
1. Vast, flat, shallow subtidal zones with the only relief being inherited from pre-existing topographic lows and scattered skeletal sand shoals;
2. Intertidal zones that may have been tens of kilometers wide; and
3. Wide supratidal zones (Jones, 2010, p.358)

Much research has been done in large shelf areas like the Florida coast, the Bahama Banks and the Persian Gulf, but these are small when compared to the large ancient epicontinental

seas (Irwin, 1965, Shaw, 1964). Shaw (1964) and Heckel (1972) argued that the maximum depth of epicontinental seas probably were less than 200 m and average slopes were potentially not more than 20 cm/km (<1º).

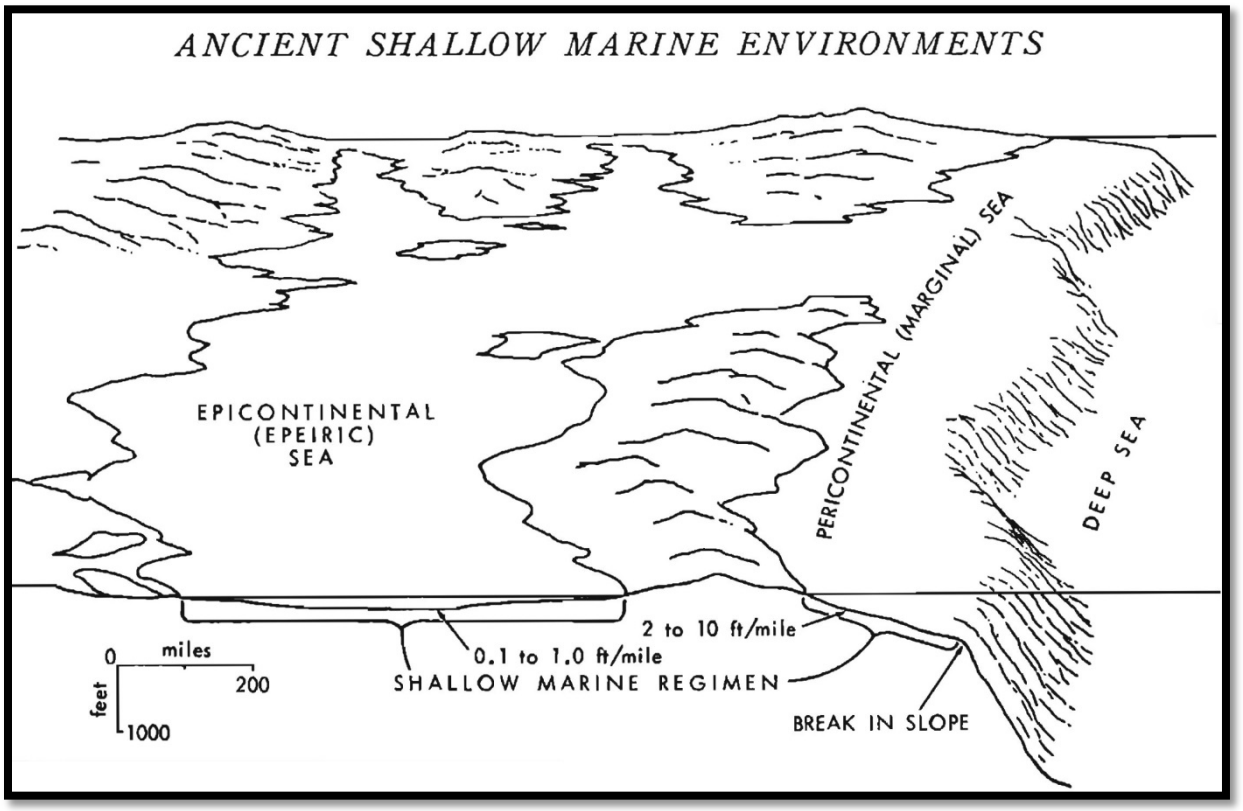

Figure 3.1: *Ancient shallow marine environments. In scale; 1 foot equals ~0, 30 centimeter and 1 mile equals ~1, 61 kilometers. Modified from Heckel (1972).*

3.2 Sedimentation control and dynamics

Ancient shallow marine epicontinental seas differ in their characteristics of distribution of wave and current energy than the most “equivalent” marginal seas in present days (Bjørlykke, 1974a). Several simultaneously different sedimentary environments could be produced at a specific time in an epicontinental sea by lateral variations in temperature, depth, dissolved chemicals, hydraulic energy, organic activity and clarity of water. In each of these environments, different lithofacies are able to form (Irwin, 1965).

3.2.1 Ancient clastic shelves

Three main types of ancient clastic shelf deposits can generally be identified mainly based on sand/mud content and the relative interaction between fairweather and storm processes. These

main types are; tide dominated, storm dominated and mud dominated shelf deposits (Reading and Collinson, 1996). Figure 3.2 show the zonation in a shelf profile. The individual zones have their own facies, morphology and characteristic processes that define them. The offshore zone is a zone that is dominated by fine-grained sediments that settles from suspension as a result of a sea bottom that lies below the mean storm base. Further landward, the offshore transition zone starts at the intersection point between the mean storm wave base and dissipates on the onset of the shoreface zone. During storm events, the offshore transition zone is affected by high energy represented by shoaling waves that is supplemented by currents. During fairweather, this zone is dominated by fine-grained sediments that settles during suspension and bioturbation occur. Thus, this zone is characterized by alternations between high energy and low energy. The nearshore zone starts at the point where the mean fairweather wave base intersects with the sea bottom and dissipates at the mean high water point. This zone is divided into the shoreface and the foreshore. During storms, the subtidal shoreface are affected by erosion by shoaling waves, storm currents and enhanced rip currents. The erosion takes place particularly on the upper shoreface and the sediments are carried either to the beach or swept offshore and redeposited. Oscillatory and shoaling waves operated in the lower shoreface during fairweather, while the break/surf zone processes in the upper shoreface. The intertidal foreshore zone is affected by the daily swash of waves and extends from the mean low water point to the berm (Reading and Collinson, 1996).

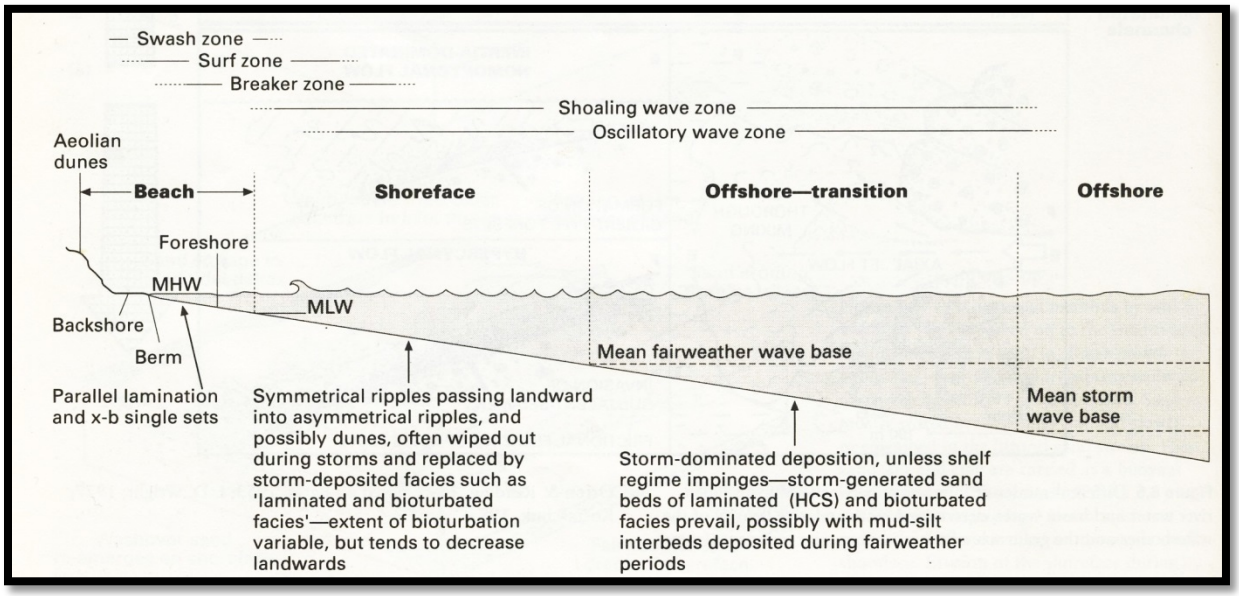

***Figure 3.2**: Processes, facies and subenvironments in a generalized shoreline profile. Modified from (Reading and Collinson, 1996).*

Depositional features on an epicontinental shelf can generally be distinguished by the intensities of tide and wave power and also based on the prograding or transgressive nature of the setting. Progradation takes place in two scenarios, 1; when rate of sediment supply exceeds the rate of relative sea-level rise, or 2; when sea level fall and sediments propagates (Reading and Collinson, 1996).

3.2.2 Shallow clastic seas

Sediment transport, sediment supply and relative sea-level changes are the dominant controls of sedimentation patterns and facies characteristics in shallow clastic seas. In carbonate settings, biological, climate and chemical factors may be equal dominant. In ancient shallow marine successions, the geological history, inherent topography and the influence of tectonic control of sedimentation are also important factors (Reading and Collinson, 1996).

In shallow marine offshore clastic environments, facies are controlled by numerous factors. After (Reading and Collinson, 1996) these controlling factors are:

- Type and rate of sediment supply
- Intensity and type of hydraulic regime and its frequency of reworking
- Water depth
- Relative sea level fluctuations
- Biogenic activity

Some ancient shelves were affected by physical processes such as storms and biogenic processes in fairweather periods. Others were dominated by daily reworking by fairwater tidal currents. In terms of preservation potential, tectonic activity and rate of sea-level fluctuations are also important factors to consider. These allocyclic processes influenced the geometry, size, orientation, depth, sediment supply patterns and the communication with other oceanic basins.

3.2.3Accomodation vs. supply dominated shelves

Factors such as the creation of accommodation space and sediment supply mechanisms are closely related to the nature of ancient shelf sediments, and by taking these into account, characterization of shelves that are supply-or accommodation-dominated can be distinguished.

From the dynamic processes that control the shelf sedimentation patterns, Swift and Thorne (1991) proposed a model for calculating the accommodation/supply ratio. The formula used

for calculating the ratio are; $\frac{R \times D}{Q \times M}$, where R = rate of relative sea level, Q = rate of sediment input, M = type of sediment input, P = fluid power and D = rate of sediment transport. Based on this formula, Swift and Thorne recognized two sedimentary regimes. The supply-dominated regimes are recognized by having a ratio less than 1. In this case the sediment supply and type exceeds the rate of created accommodation space and sediment dispersal. With a ratio greater than 1, the accommodation-dominated regimes is characterized by a rate of sea-level rise and sediment transport/dispersal exceeds the type and supply of sediments (Swift and Thorne, 1991).

3.2.4 Tidal influence in the Baltoscandian Epicontinental Sea

Although tidal currents may not have affected the inner part of ancient epicontinental platforms (see Figure 3.3) the wind stress from storm events or hurricanes may have caused water to pile up and move extensive amounts of sediments. The distribution of waves, currents and also wind from the continents are all important factors for controlling the amount of introduced sediment into an epicontinental platform (Bjørlykke, 1974a). Based on a simple model of the characteristic features on Lower Palaeozoic epicontinental seas, Bjørlykke (1974a) proposed four different mechanisms that produced the energy needed to transport suspended sediments. These mechanisms, as described by Bjørlykke (1974a), are;

> *"(1) Wind blowing from the deep sea will generate large waves which will gradually lose their energy due to friction against the sea floor as they continue across a shallow epicontinental sea. Wind blowing in the other direction will generate only smaller waves because of the shallow water.*
> *(2) Tidal currents which may be strong in deep waters will dissipate their energy along the margin of the epicontinental sea. On the epicontinental shelf there are too small volumes of water relative to the friction against the bottom, so that virtually no tidal energy will be generated.*
> *(3) Ocean currents affected by the Coriolis force will also become negligible on a large shallow shelf.*
> *(4) Evaporation on the continental shelf will generate currents from the deep water to the shelf to replace the volume of water that has evaporated."*

With the interaction of these mechanisms, the trend is that the dominant energy direction that transport suspended sediments are from the deeper throughs around the continental margin moving sediments to the epicontinental sea.

3.2.5 Possible sources of detrital sediments

Størmer (1967) observed extensive amounts of coarse clastic sediments in the Katian/Hirnantian successions around Oslo. These clastic sediments contained inter alia characteristic feldspars from Caledonian nappes, thus he suggested a potential rise of a land to the west. This geographically positive area is referred to as Telemarkland and was situated between the geosyncline and the Oslo area. This was also identified by Skjeseth (1952). The relative supply of sediments from land and adjacent island arcs are to a great extent part of the controlling factors for the composition of the deposited clastic sediment in epicontinental seas. As a result of geochemical and mineralogical analysis, Bjørlykke (1974a) found evidence in the Oslo Area of sediment supply into the Baltoscandian Epicontinental platform derived from island arcs that emerged in the Trondheim Region. These island arcs, which are present along most of the Scandinavian Caledonide strike length, developed during the closer of the Iapetus ocean and range in ages from Late Cambrian to Late Ordovician (Dunning and Pedersen, 1988). Contemporaneous to the uplift and erosion of the basic lavas in the eugeosynclinal Trondheim Region, chlorite appeared to have been introduced in the Baltoscandian Epicontinental Sea (Bjørlykke, 1974a). This evidence suppressed the theory of alternative sources of chlorite rich sediments from nearby sources. Chromite in shales of Middle/Upper Ordovician age in the Oslo area is also quite similar to the serpentinites of the Trondheim Region, and this was also an indication of igneous rock derivation (Bjørlykke, 1974a).

3.2.6 Sediments related to storm events

Sandstone layers that are interbedded in fossiliferous marine shale and silt (sub littoral sand sheets) are interpreted as being deposited from offshore up to the foreshore beach and off-beach in shallow marine environments. These sandstone beds often occur with similar common characteristics and abundant fossils contents, thus makes them useful in paleoecology. They range in thicknesses of about 5-70 cm and they either occur individually separated by interbeds of silt or clay or stacked in groups with little or no mud and silt

between them. Their common characteristics with inferences are summarized after Goldring and Bridges (1973) in Table 3.1.

Table 3.1: *Characteristics with inferences of sediments related to storm events. Modified from Goldring and Bridges (1973).*

CHARACTER	INFERENCE
Erosional features	
Grooves or furrows	Flow oscillatory or unidirectional, but when helical toolmark pattern present, current has net residual.
Toolmarks	Flow oscillatory or unidirectional.
Depositional features	
Sandstones 5-70 cm thick	Requires mechanism that is competent to transport much sediment.
Amalgamated beds up to 5 m	Recurrent sand deposition in area of little mud deposition.
Lateral persistence varies from few m to km bed always terminated by subsequent erosion	Mechanism may operate over a large area.
Horizontal lamination	Sand deposited under transitional flow regime conditions.
Only top of bed may be graded	Slowly decelerating suspension current (Kuenen, 1966).
Bioturbation	
Burrowing decreases downward	Deposition resulted from a single event.
Fauna	
Smothered fauna at base	Not always sufficient power for currents to erode organisms, particularly from muddy substrate, before deposition. Cf. Grooves and tool marks. Currents clearly vary in power.
Mixed fauna assemblage	Life assemblages from variable substrates and wide area mixed together.

Thin, interbedded sandstone layers are a common feature within the typical fine-grained shallow-water sequences of the Lower Palaeozoic in the Oslo area (Brenchley et al., 1979). Sudden influx of coarse sediment into a fine-grained environment can be a result of different

processes such as turbidity-currents, storm surges, tsunamis and also flooded waters from nearby land (Goldring and Bridges, 1973). These sandstone layers, commonly in the order of 0.5-10cm in thickness, are found almost throughout the Husbergøya Formation and in the southeastern lower part of the Langøyene Formation. They appear to have the same characteristics in both formations, but they increase in occurrence and thickness in the Langøyene Formation. This increase in occurrence and thickness is explained by the Late Hirnantian regression that induced higher current velocities. The bedforms change and graded beds and planar lamination are more common. The most prominent sedimentary structures in these sandstone layers are graded bedding, planar lamination, small-scale cross-lamination and siltstone and mudstone interlamination.

3.2.7 Theoretical model

Irwin (1965) described a theoretical model for sedimentation in nondetrital clear water epicontinental seas. He recognized three energy zones and defined them by their characteristic intensities of water agitation resulting from the depth at which waves and currents impinge on the sea bottom (Heckel, 1972). As seen in Figure 3.3, zone X represents the deepest part of the sea. In this environment, fine-grained mud is able to settle because the sea bottom is below wave base. If the bottom is well oxygenated, diverse biota will form and deposit coarser materials in the form of shells (Heckel, 1972). This low energy zone is in the scale of hundreds of kilometers wide and the only energy acting upon the sea floor is marine currents. Zone X dissipates at the point where the effective wave base intersects the sea floor. From that point and basinward, down to the point where waves and tides dissipate due to friction is characterized as zone Y. This is a high energy belt where waves expend their energy on the bottom. In this zone, animal life flourished with reefs on the seaward side and both algae and carbonate sands on the landward side. Thus, the sediments are mainly biogenic. Further landward, in zone Z, very little sediment deposits except fine-grained detritus derived from zone Y. This area is beyond the effects of tidal exchange (Irwin, 1965, Jones, 2010).

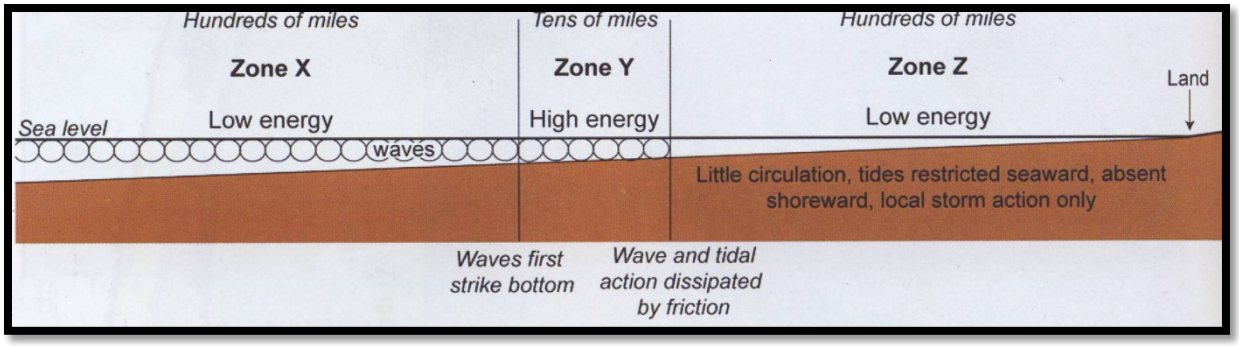

Figure 3.3: *Energy zones in non detrital clear water epicontinental seas. Modified from Jones (2010).*

Even though this model describes the energy systems and sedimentation in nondetrital clear water epicontinental seas, it has close affinity with the land attached epicontinental seas that had low gradients, reduced tidal energy and low wave energy (Eriksson et al., 2008). This makes the model relevant when studying the Baltoscandian Epicontinental Platform.

3.3 Global sea level

The main factors controlling sea-level changes and eustasy are tectonic events and glaciation. Milankovic cycles are also an important factor to consider when studying sea level oscillations. Relative sea level change are according to Swift and Thorne (1991) characterized by as the net effect of eustatic changes in base level as a result of tectonic basin subsidence or uplift and subsidence due to compaction created by fluid escape. The latter sea level change is a result of the weight of the overburden on the sediments.

In the Ordovician Baltica, the rate of deposition was low and there was not extensive tectonic activity until the onset of Silurian. Thus, the sea level record reflects ecstasy. A sea level curve (See Figure 3.4) was presented by Nielsen (2003) based on analysis from different sections of the Baltoscandian Platform.

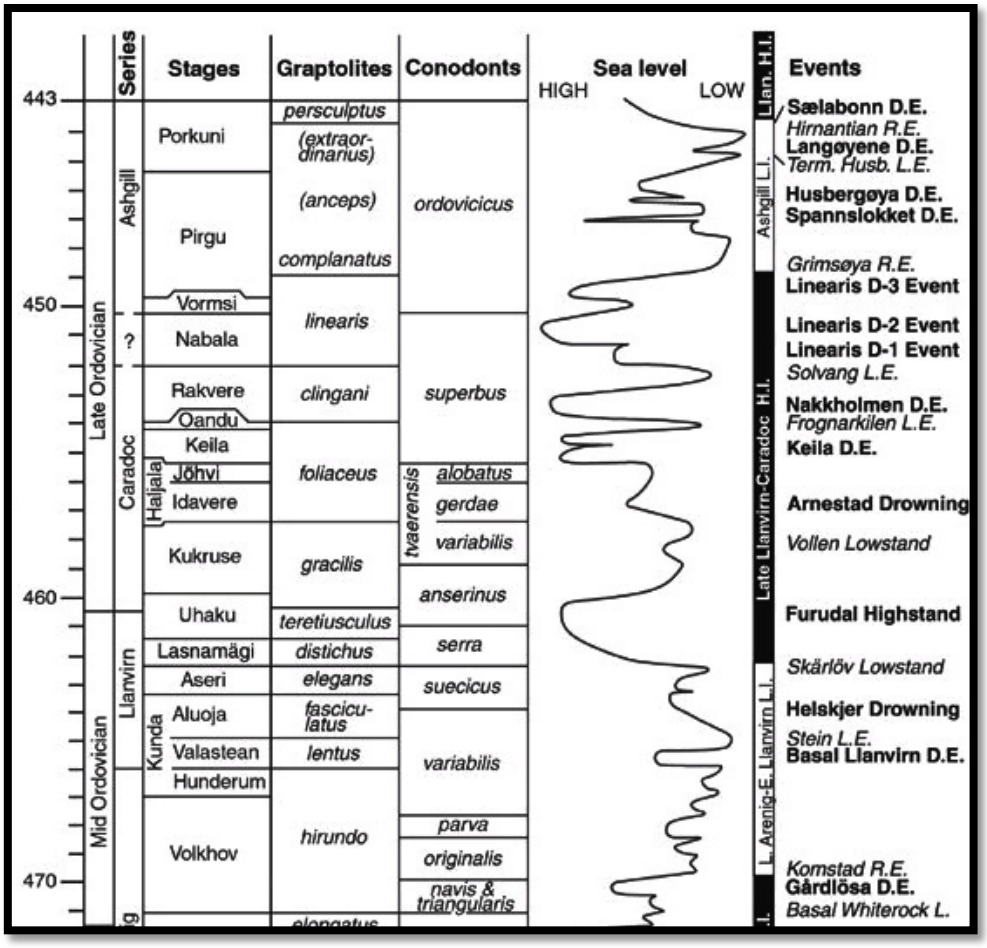

Figure 3.4: *Sea level curve from the middle-to Upper Ordovician with correlative conodont and graptolite zones. Explanation of abbreviations: D.E; "Drowning Event", L.I; "Lowstand Event, L.I; "Lowstand Interval" and H.I; "Highstand Interval". Modified from Nielsen (2003)*

3.3.1 The Skogerholmen flooding event

As seen in Figure 3.4, there was a flooding event in the latest stage of the Spannslokket Member (Skogerholmen Formation in the Oslo Area). This drowning event is marked by the transition from nodular limestones in the upper part of Skogerholmen Formation to shales on the onset of the Husbergøya Formation.

3.3.2 Upper Ordovician regression

The glaciation of the Supercontinent Gondwana in the Late Ordovician – Silurian was a short lived event compared to later Gondwana glaciations. It is also the only glacial event that appear to coincide with a mass extinction (Finnegan et al., 2011).

At the start of the Hirnantian, the glaciation induced a major sea-level fall, but evidence shows that the dramatic lowering of the sea-level appeared to have been at the end of the

Hirnantian (Brenchley et al., 2006, Brenchley and Newall, 1980). The regression is best represented in the sedimentary succession of the topmost Langøyene Formation in the Oslo Area by channels related to erosion. Erosional surfaces connected to the regression are also identified in Central Wales by Brenchley et al. (2006). The regression was followed by a rapid transgression as a result of the melting of the ice sheet at the Ordovician-Silurian boundary (Brenchley and Newall, 1980). A diagram after Brenchley et al. (2006) is presented in Figure 3.5 and summarizes the different events, biotic changes and sea-level curve of the Late Ordovician.

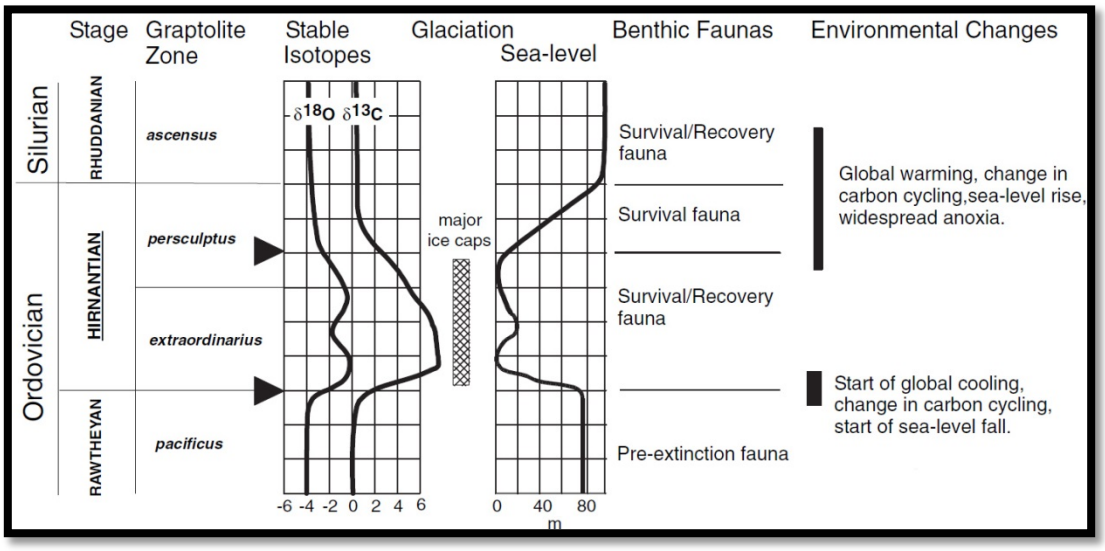

Figure 3.5: *Simple diagram showing sea level curve, events, stratigraphy and environmental changes in the Late Ordovician. Modified from Brenchley et al., (2006).*

Global facies changes in sedimentary sequences reflect the different phases of the Late Ordovician Gondwana glaciation, but there are uncertainties in the pattern and magnitude of the sea level-changes caused by this event (Brenchley et al., 2006).

3.4 Upper Ordovician carbonates in the Oslo Area

Generally, the carbonate sediments in the Ordovician Epicontinental Sea show a mixture of skeletal sand and carbonate mud (Jaanusson, 1973). There are notable depositional rhythms that are characteristic of the Upper Ordovician succession in the Oslo Area. These rhythms are characterized by shale that passes upwards into shales with limestone nodules. The factor controlling these rhythms or cycles has been suggested by Brenchley and Newall (1980) as being local tectonism. Bjørlykke (1974a) interpreted the origin of these cycles as probably

being glacio-eustatic. The frequency of nodular limestones increases upwards, sometimes containing benthic shelly fauna, overlaid by a new sequence of shale.

The regressive phase mentioned above is represented in the carbonate facies in the Upper Ordovician by autochthonous carbonate mud mounds, growth of corals and development of ooide shoals. These carbonates show lithification and emergence of these facies are indicated by their karstic surfaces. A comparable lithified carbonate platform are studied from the Gulf Coast in Bahamas (Brenchley and Newall, 1980).

3.5 The Origin and deposition of carbonate mud

The most common carbonate minerals in ancient carbonates are aragonite and calcite. The environments in which these carbonates form can be defined and characterized by the different factors that control the minor ion substitution. Examples of such factors is water composition, pressure and temperature (Blatt et al., 1972).
According to Blatt et al. (1972), organisms that produces carbonates prolifically are fundamental in the formation of carbonate platforms. These organisms are light dependent, thus the area of the carbonate platform are shallow, ideally with abundant detrital sediments. High influx of detrital sediments dilutes the carbonate production, and if the detrius are silicates, the water gets muddy and light penetration depth is reduced. Carbonate production is therefore facilitated in environments that have a low influx of silicate detrius. The amount of detrital silicate particles in ancient carbonates is as little as 5% (Blatt et al., 1972).

3.6 Nodular limestones

Earlier studies done by different authors (e.g. Brøgger (1882), (Bjørlykke, 1973), Henningsmoen (1974) and Möller and Kvingan (1988)) have resulted in an ongoing discussion about the origin of nodular limestone in the Early Palaeozoic in the Oslo Area. Möller and Kvingan (1988) argued that all occurrences of nodular limestones must be considered individually, since there is no evidence of a single mechanism that is responsible for their overall creation. Taken this into account, it is important to clarify and summarize the different theories and suggestions from earlier studies and in that way compare this information to the nodular limestones described later in this thesis.

Bjørlykke (1973) argued that the origin of these nodular limestones was a result of subsolution of continuous carbonate layers prior to burial but after deposition, and that the

nodules was the remains of this continuous layer. He recognized that the Ordovician limestones consisted mainly of biomicrite in a matrix of calcareous shale and that, in contrary to the Cambrian alum shale where carbonates and calcareous tests of fossils are absent, subsolution had been more selective and less complete. In a comment to the work in Bjørlykke (1973), Henningsmoen (1974) explained that the origin of nodular limestones was due to concretionary growth, and that continuous layers of carbonate were formed by the coalescence of these concretions. More recent studies done by Möller and Kvingan (1988) supports this explanation and characterized the origin of the nodular limestones within the area as being formed centimeters to decimeters below the sediment/water interface by early digenetic concretionary carbonate cementation.

3.7 Stratigraphic history

The stratigraphic nomenclature of the uppermost Ordovician formations, Husbergøya, Langøyene and Langåra was earlier split up in different stages. All three formations were parts of Stage 5 and represented 35-80 meters of sedimentary succession. As seen in Figure 3.6, Stage 5 is again divided into Stage 5a and Stage 5b. Kjerulf was the first to introduce the term “Stage” in 1857 (Kjerulf and Dahl, 1857). In later years, it has been modified to modern use.

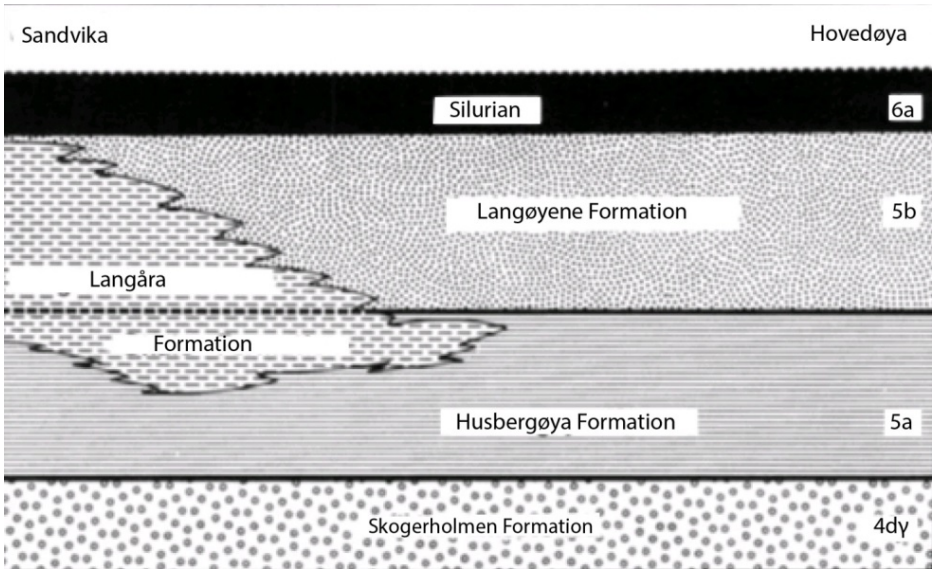

Figure 3.6: *Illustration of the different stages in Upper Ordovician/Silurian in relationship with formations (Brenchley and Newall, 1975).*

Brenchley and Newall (1975) proposed the three new formation names. Two of these formations, the Langøyene Sandstones and the Husbergøya Shales, define the boundary

between Stage 5a and Stage 5b. Westward into the Asker district the Langåra Limestone-Shale formation is in between Stage 5a and Stage 5b. The names of the formations are taken from the type localities of where the rock is best exposed (Brenchley and Newall, 1975).

3.8 Upper Ordovician units

Thorough description of the depositional environment, ecology and successions of the Upper Ordovician in the Oslo Area has been done by different authors (Brenchley and Newall, 1975, Brenchley et al., 1979, Brenchley and Newall, 1980, Brenchley and Cocks, 1982, Owen et al., 1990). The general depositional environment in the Upper Ordovician in the Oslo area are described by Brenchley and Newall (1980) as representing a shelf environment with moderate depths. A detailed stratigraphic correlation between the Ordovician succession of the Oslo Area and the standard British and Baltic sequences are presented in Figure 3.7.

3.8.1 Skogerholmen Formation

The Shogerholmen Formation comprises two members, the lowermost Hovedøya Member and the overlying Spannslokket member. The lower part of this formation marks a change from shales of the underlying Skjerholmen Formation to a more limestone dominated succession. The thickness of this formation in its type locality is approximately 38.50 meters with 43 meters on Hovedøya and 33.06 meters on Skogerholmen. Both members of this formation consist of alternating limestone, siltstone and shale beds. The difference between the members is the occurrence of thicker siltstone beds (up to 30 centimeters) in the Spannslokket Member, in contrary to the Hovedøya Member that contains thinner siltstone beds. There is also a transition from bedded limestones in the lower part of the Spannslokket member to the occurrence of nodular limestones in the upper part. The frequency of siltstone beds is also reduced upwards in the upper part of this member. The lower Hovedøya Member has a sparse fauna. Burrows are quite common in the upper Spannslokket Member and examples of these are *Chondrites* and *Planolites (Owen et al., 1990).*

3.8.2 Husbergøya Formation

The lower part of the Husbergøya Formation consists of gray, silty shales that overlie the nodular limestone in the top of Spannslokket Member in the Skogerholmen Formation. The color and crude fissility of these gray shales are, according to Brenchley and Newall (1975),

probably due to bioturbation by *Chondrites*. Upwards in the formation, calcareous sandy horizons get progressively more common with interbedded bioturbated mudstones, siltstone and nodular limestone (Owen et al., 1990, Stanistreet, 1989). On the top of the formation, nodular limestone and layered limestone overlie brown sandstone that varies in thickness from 1 m to 4 m (Stanistreet, 1989). The "brown-weathered" sandstone is massively bioturbated and marks the boundary between the Husbergøya Formation and the Langøyene Formation. Internal lamination is destroyed by bioturbation, and Brenchley and Newall (1975) suggested that a pause in sedimentation occurred. Stanistreet (1989) interpreted this pause as being a transitional phase from offshore to shoreface sedimentation. The type section thickness of the formation is 18.5 m with a minimum thickness of ca 10m in Asker and as much as 35 m in Bærum (Brenchley and Newall, 1975). It passes laterally into the Langåra Formation to the west (Owen et al., 1990) .

3.8.3 Langøyene Formation

As mentioned, the "brown-weathered" bioturbated sandstone at the top of the Husbergøya Formation marks the boundary to the Langøyene Formation. Brenchley and Cocks (1982) provided evidence indicating that the Langøyene Formation was deposited within a regressive phase. The base of the formation shows shales, laminated sandstone beds and thin limestone beds. Further upwards, contorted units of shale and sand layers occur. These contortion structures are argued in Brenchley and Newall (1977) to be a result of high sedimentation rate that can be connected to storm-events and/or seismic shocks. Examples of these contortion structures are e.g. load casts, ball-and-pillow structures, slumps, convolute bedding and sand rolls. Conglomerate layers in the upper part of the Langøyene Formation are evidently deposited in channel systems due to their erosional surfaces that cuts down into the underlying sandstone (Brenchley and Newall, 1975, 1980). The top of the formation most commonly contains beds of oolite limestone with a bioclastic limestone in some locations (Brenchley and Newall, 1975). The type section thickness at Langøyene of the Langøyene Formation is 51 m with a maximum thickness of 60 m in the east. The upper part of the formation passes laterally into the Langåra Formation where it thins to 8 m. The minimum thickness of the Langøyene Formation is as little as 50 cm in Sandvika where it is represented as a oolite conglomerate layer (Owen et al., 1990).

3.8.4 Langåra Formation

The upper part of the Husbergøya Formation and the Langøyene Formation passes gradually into the Langåra Formation and is restricted to the western part of Oslo-Asker. The maximum thickness of this formation is 35 m at Sandvika with a type thickness of 13 m at Langåra.

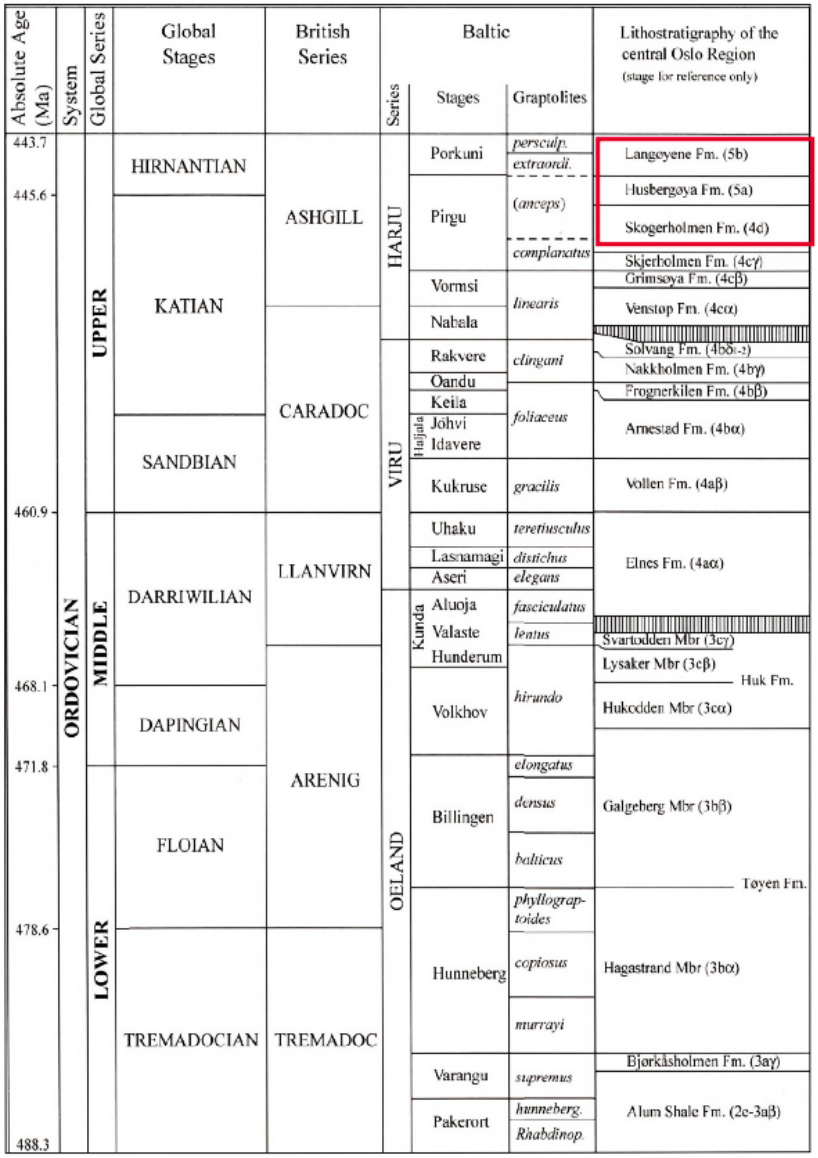

Figure 3.7: *Stratigraphic correlation between the Ordovician succession of the Oslo Area and the standard British and Baltic sequences. Modified from (Bruton et al., 2010).*

4 Methods

4.1 Field work

The field work for this master thesis was done in the summer and autumn season of 2013 at three islands in Oslo Fjord, Langøyene, Gressholmen/Rambergøya and Hovedøya respectively, see Figure 4.1

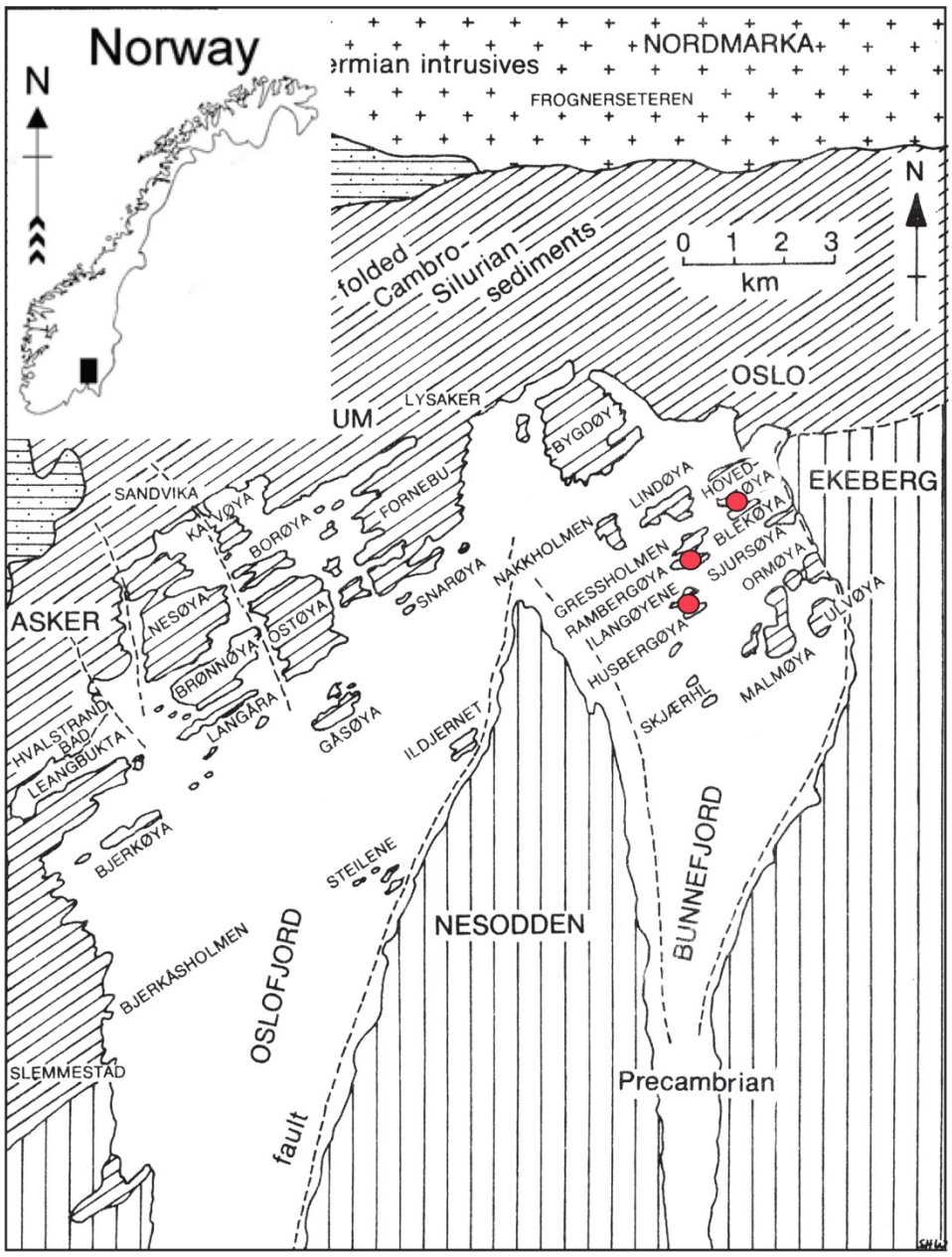

Figure 4.1: *Geological map of Oslo and Asker. Red dots shows localities studied in this master thesis. Modified from Bruton and Williams (1982).*

Due to the large number of people visiting the island, particularly in the outcrop areas of the actual stratigraphic section in sunny and warm periods, the summer season was devoted to observational work at the logged localities with supervision by Professor Hans Arne Nakrem (University of Oslo), Professor emeritus Johan Petter Nystuen and Johan Fredrik Bockelie (Exploration Advisor hos Ithaca Petroleum Norge AS). An additional day of observational fieldwork was carried out by boat, distributed and directed by Johan Fredrik Bockelie, in company with Hans Arne Nakrem, Johan Petter Nystuen and peer student Martin Sandbakken. During this day, other equivalent localities was visited and observed with the intention of using the localities further in the thesis. These localities were unfortunately not studied in more detail due to time limitations and the volume of work this would implicate, but it gave great insight when studying the lateral distribution of the Upper Ordovician stratigraphy in the Oslo Area. The field work with geological logging and sampling was carried out in a timeframe of approximately eight weeks. The first couple of days of geological logging were followed-up and supervised by Hans Arne Nakrem and Johan Petter Nystuen. Collaboration in field between the author and a fellow student, Martin Sandbakken, assured that safety was well attended to. Both Martin Sandbakken and the author focus on the Upper Ordovician in the Oslo area and collaboration was consequently done to maximize the total obtained data.

4.2 Geological logging

Geological logging was carried out on all three localities mentioned above, and the profiles were chosen on the criteria of the outcrop visibility, accessibility and minimum degree of weathering. In agreement with supervisors and peer student Martin Sandbakken, a point zero was set in the boundary between the nodular limestone of the Skogerholmen Formation and the overlying mudstone of the Husbergøya Formation. On all localities, the stratigraphy from point zero throughout the Husbergøya Formation and the first four to five meters of the Langøyene Formation has been logged. The last four or five meters of the nodular limestones of the Skogerholmen Formation below point zero have also been logged on all localities. All profiles were measured in meters up front with point zero as a reference point. Due to the folded nature of the exposed rock strata with varying inclination of the layers, thickness corrections were done before the actual logging took place. The grain size of the limestones shown in the logs with scale of 1:10 is not representative of the real grain size, as can be estimated in thin sections. This is because the fellow peer student Martin Sandbakken and the author wanted to highlight these layers to better detect them when interpreting the logs further.

The layers in the succession that represent nodular limestone according to the legend (see APPENDIX A), represents a dominance of limestone nodules interbedded with other lithology. This was done to maximize the accuracy of the logging and due different degrees of weathered and well exposed outcrops. During the geological logging, the grade of bioturbation observed was classified into three different groups; “Little”, “medium” and “heavy”. Later, when observing polished slabs, the grade of bioturbation was enhanced according to the semiquantitative field classification proposed by Droser and Bottjer (1986), see Figure 4.2. Two different logging templates were used based on the scale of the logged profile. These logging sheets are shown in APPENDIX F.

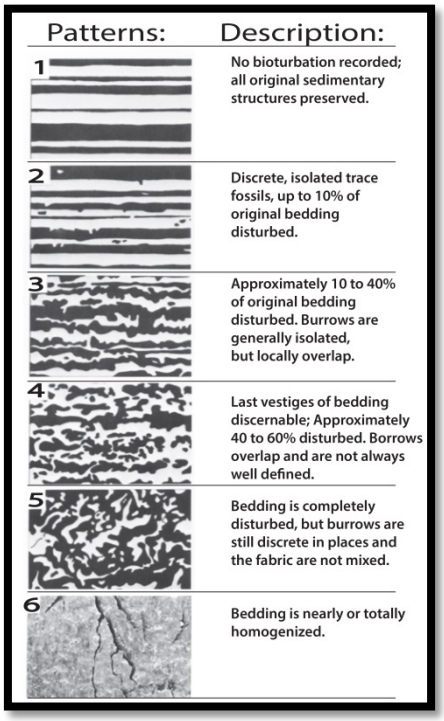

Figure 4.2: *Semiquantitative field classification of ichnofabric. Modified from Droser and Bottjer (1986).*

Langøyene:

Three profiles were logged from separate localities on Langøyene. Two logs, L.Ø Profile 2 and L.Ø Profile 3, with the scale of 1:100, and one log (L.Ø Profile 1) with the scale of 1:10. All logs on this locality were done in collaboration with Martin Sandbakken. In L.Ø Profile 1, all beds and layers were measured separately and plotted in the log sheet. The two logs (L.Ø Profile 2 and L.Ø Profile 3) with a larger scale of 1:100 were logged in sections where the ratio between the different lithologies were registered and plotted. These two logs do not

reveal details for correlation and comparison of e.g. changes in formation thicknesses. A map of the location of the logged profiles is shown in Figure 4.3.

Figure 4.3: *Map of Langøyene showing the locations (red circles) of the profile that were logged during the field work. Map acquired from http://kart.finn.no/*

Rambergøya:

On Rambergøya, R.Ø profile 1, with the scale of 1:10 in collaboration with Martin Sandbakken. A planned work on an additional log in the scale of 1:100 on a different locality was cancelled due to observed complex structural features within this section of the succession and also due to strong weathering of the outcrops here. In R.Ø Profile 1, all beds and layer thicknesses and lithologies were measured and observed separately and plotted in the log sheet. A map of the location of the logged profile is shown in Figure 4.4.

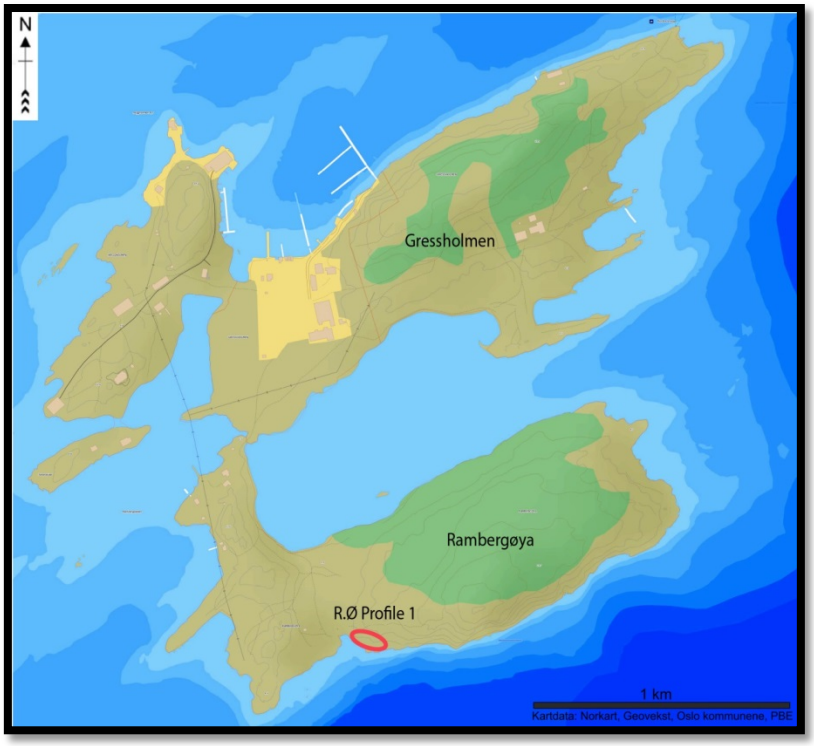

Figure 4.4: *Map of Gressholmen and Rambergøya. The location of the logged profile is marked with a red circle. Map acquired from http://kart.finn.no/.*

Hovedøya:

Additional logging was done by the author on Hovedøya. This was carried out in the course of two weekends during the spring season of 2013. This resulted in a geological log in the scale of 1:10 from this location (see APPENDIX A). In H.Ø Profile 1, all beds and layer thicknesses and lithologies were measured and observed separately and plotted in the log sheet. A map of the location of the logged profile is shown in Figure 4.5.

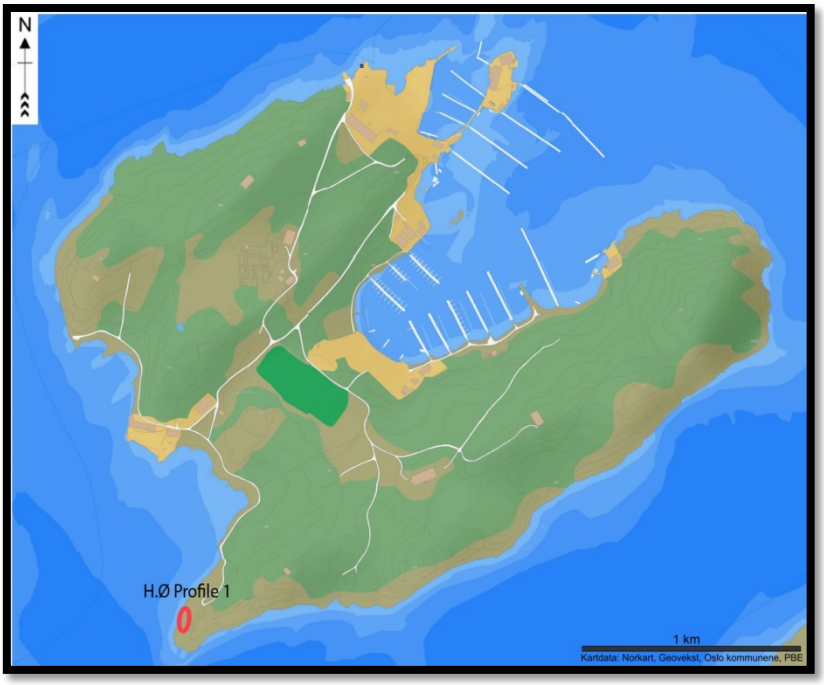

Figure 4.5: *Map of Hovedøya. The location of the logged profile is marked with a red circle. Map acquired from http://kart.finn.no/.*

4.2.1 Susceptibility measurement

A susceptibility measurement was carried out on Rambergøya Profile 1 by peer student Martin Sandbakken and the author. One measurement each 10 centimeter was done from 0,98 meter below point zero to 23,98 meter above point zero with the intention of correlating this data with Milankovic cyclicity. The measurements were done using a Terraplus kappameter model KT-10, provided by Øyvind Hammer at the Natural History Museum at Tøyen, Oslo. This was, due to time limitations, unfortunately not studied any further. The measurements are presented in APPENDIX G.

4.3 Log digitalization

All the logs from the different localities were digitized using Adobe Illustrator CS6.

Profile 1 on all three localities (L.Ø Profile 1, R.Ø Profile 1 and H.Ø Profile 1) is digitalized in the true scale of 1:10. The two logs from Langøyene (L.Ø Profile 2 and L.Ø Profile 3) are also digitized in their true scale of 1:100. All these logs and legend are presented in APPENDIX A. The digitized logs with scale of 1:10 are also simplified and stacked with the

intention of correlating the logged profiles. Sedimentary structures, observed fossils and comments are removed in the logs presented in Chapter 6. This means that, when the logs are shown and described, information presented is collected from APPENDIX A, raw logs, general observations, samples, thin sections and acetate peels.

4.4 Sampling

The total of 91 samples were collected in Profile 1 on Langøyene and Profile 1 on Rambergøya. These samples were collected by the author, peer student Martin Sandbakken and main supervisor Hans Arne Nakrem at the locality. These were brought to the Natural History Museum at Tøyen in Oslo. All samples were given a sample indentificator reflecting the locality, an arrow showing right way up and characterized by their level (in meters) from point zero. The aim during the sampling was to get a representative selection of rock samples that could show all the aspects of the depositional history. All sample pictures in any form throughout this paper are portrayed right way up.

4.4.1 Sample preparation

All the samples collected were cut in 1 centimeter thick slabs at the Natural History Museum at Tøyen in Oslo by peer student Martin Sandbakken and the author. Due to the brittle character of many of the samples, two-component epoxy glue was used to glue together parts of samples that fractured during the cutting process. In agreement with supervisors, 33 representative samples from Profile 1 on Langøyene were prepared further to make thin sections, and 21 representative samples from Profile 1 on Rambergøya were prepared to make acetate peels. These samples were polished with silicon carbide paper until satisfactory surface of sample was achieved. This meant that each sample had to be polished several times with minimum grit size of the silicon carbide of P1200. All the selected samples were given PMO (“Paleontological Museum Oslo”) numbers at the Natural History Museum, and the samples are kept in the museum’s collection of scientific material. These numbers refers to both the sample scan pictures, the thin sections and the acetate peels. The sample scan pictures are referred to as “PMO-number”-SS, the thin sections are referred to as “PMO-number”-TS and the acetate peels are referred to as “PMO-number”-AP. The samples from Langøyene Profile 1 have PMO-numbers from 227.434 to 227.464 and the samples from Rambergøya Profile 1 have PMO-numbers from 227.465 to 227.485. A list of “PMO” material is presented in APPENDIX B.

Figure 4.6*: A: Rock saw machine at the Natural History Museum at Tøyen in Oslo. B: Red arrow shows the rock polishing machine at the Natural History Museum at Tøyen in Oslo.*

4.5 Scanning and sample scan editing

After cleaning, cutting and polishing, the samples were flat-bed scanned using a Canon Canoscan 4200 F at the Natural History museum by peer student Martin Sandbakken and the author. To achieve good quality and clear pictures, boiled water was used on top of the scanner glass and the samples were laid on the scanner in a way that removed all air bubbles. All samples were scanned two times, one scan showing the scale of the samples and one without. A sample scan picture example is shown in Figure 4.7.

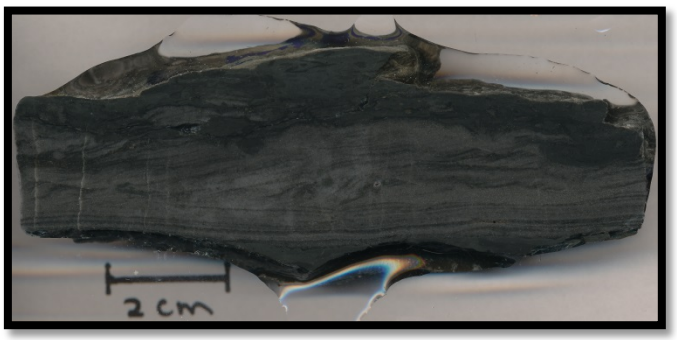

Figure 4.7: *Example of sample 227.470-SS with scale from Rambergøya Profile 1, 5.90 meter above point zero.*

Photoshop was used on all samples to remove sample background and to enhance the quality by changing brightness and contrast. Figure 4.8 shows the same sample from Figure 4.7 at the two stages of editing in Photoshop.

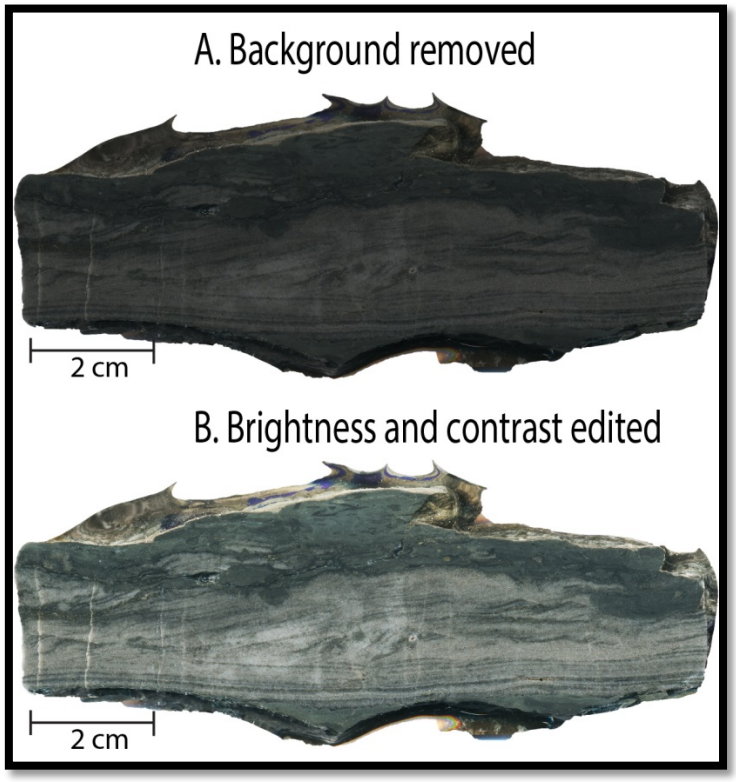

Figure 4.8: *A: Background removed in a Rambergøya Profile 1 sample (5.90 meter above point zero). B: Brightness and contrast edited in the same sample.*

The polished sample slab surface scan pictures (before and after brightness and contrast enhanced) and a table with observational descriptions of the samples is presented in APPENDIX C. The location of these samples in the logged profile is presented in APPENDIX D. All polished sample slab surface pictures presented further in this master thesis is brightness and contrast enhanced.

4.6 Thin sections

After scanning, the 33 samples from Profile 1 on Langøyene were sent to professional thin section laboratories for thin section production. 23 of these samples were prepared by Salahalldin Akhavan at the Department of Geoscience (University of Oslo), and 20 of the

samples were sent to Lars Kirksæther at Petro-sec/IFE (Kjeller) for preparation. The outline of the area on the sample that was to be made thin sections of was drawn by peer student Martin Sandbakken and the author. One sample could contain more than one outline, and the end result was 43 thin sections. The samples were polished to a thickness of 30 μm and prepared as standard petrographic thin sections. A summary of the PMO-number and location in correlation with point zero of these thin sections are shown in APPENDIX B.

4.6.1 Grain size counting

28 of the 43 thin sections were used in the grain size counting. The counting was done under the light microscope with an attached 3.1 USB2.0 Microscope Camera. The program ScopeView was used to measure the longest axis of 100 random grains in each sample. It must be taken into account that the longest axis of the grains was measured, with no corrections for skewness. The author tried to use a modified version of program GRADISTAT.v8, but due to technical problems, the results were not properly plotted and were discarded.

All the plots made from the grain size counting follows the Udden (1914) classification which is more detailed than the classification used during the fieldwork.

4.7 Acetate peels

The author prepared acetate peels out of the 21 samples collected on Rambergøya. These samples were first polished and then immersed into an acid bath with 4% HCl concentration for 4-5 seconds. The samples were then flushed in hot water and laid on a sheet of paper to dry. After drying, acetone was put on the polished surface of the sample and then an acetate sheet was applied. The samples were then left for several minutes before the acetate sheet was taken off and placed in a slide frame.

By using this method, carbonate components can be identified in the sample. The acid dissolves the carbonate content of the polished surface and will appear dark in the microscope. Silicate components such as quartz appear lighter. The acetate peels were mainly used to identify the fossil content in these samples. A list of the PMO-number and depth of these acetate peels is presented in APPENDIX B.

4.8 Facies description and facies associations

The different facies are defined on the basis of field observations and by studying polished sample scans and field pictures. The different facies contain lithologies with structures that are related to a specific depositional event. Different facies that relate to a specific depositional environment are defined as a facies association. The classification of the sedimentary rocks in facies description and facies associations follows the Wentworth grain-size classification and are shown in Table 4.1 (Wentworth, 1922).

Table 4.1: *Grain size classification. Modified from Wentworth (1922).*

Size range (mm)	Phi units	Wentworth size class
256 – ∞	∞ – -8	Boulder
64 – 256	-6 – -8	Cobble
4 – 64	-2 – -6	Pebble
2 – 4	-1 – -2	Granule
1 – 2	0 – -2	Very coarse sand
0,5 – 1	1 – 0	Coarse sand
0,25 – 0,5	2 – 1	Medium sand
0,125 – 0,25	3 – 2	Fine sand
0,0625 – 0,125	4 – 3	Very fine sand
0,039 – 0,0625	5 – 4	Silt
∞ – 0,0039	1/∞-8	Clay

A more detailed classification of sedimentary rocks was provided by Folk (1954). This classification also includes mixtures of sand, silt and clay content. In the description and classification of the carbonate rocks, the Folk (1962) classification and terminology has been used. This classification is presented in Figure 4.9.

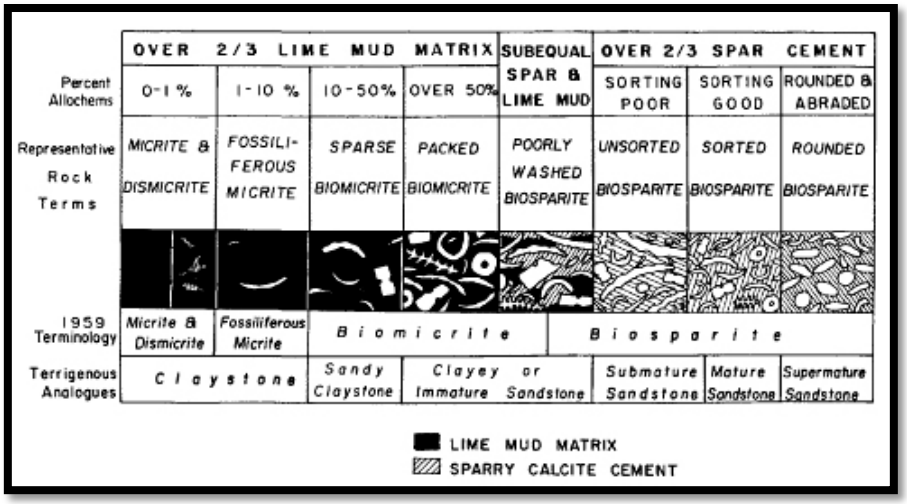

Figure 4.9: *classification of limestones. From Folk (1962).*

The location of the facies associations in simplified and stacked logs from Hovedøya Profile 1, Rambergøya Profile 1 and Langøyene Profile 1 are presented in APPENDIX E.

5 Results

5.1 Facies and facies association

5.1.1 Facies description

Facies has been defined based on the criteria from Chapter 4.8. The facies description is solely based on field observations, pictures and sample scan pictures, and not laboratory work and fossil content. The fossil content of the logged profiles is presented in Chapter 5.4. Table 5.1 shows an overview of the different facies and figures related to the different facies. Photographs are oriented right way up unless otherwise specified.

Table 5.1*: An overview of the different facies defined by field observations, pictures and sample scan pictures.*

Facies nr.	Description	Physical structures	Figure
I	**Mudstone**		
Ia	Grey fissile calcareous mudstone	Diffuse laminae. Bioturbation: 1-5.	Fig. 5.1, 5.2
Ib	Dark grey/black fissile calcareous mudstone	Diffuse laminae. Bioturbation: 1-5.	Fig. 5.3
Ic	Black fine-grained laminated shale	Laminated.	
Id	Structureless siltstone	Bioturbation: 3-6. Some loading structures observed.	Fig. 5.4, 5.5
Ie	"Brown weathered" siltstone/very fine sandstone	Bioturbation: 6.	Fig. 5.6, 5.7
II	**Silstone/sandstone**		
IIa	Internally laminated siltstone/sandstone	Parallel lamination, interbedded sand and mudstone, current ripple lamination, erosional bottom contacts, water escape structures, soft sediment deformation, loading structures, convolute	Fig. 5.8, 5.9, 5.11, 5.12, 5.13

		bedding, escape burrows, bioturbated top. Often seen with micro hummocky cross stratification. Slumping of whole layers observed.	
IIb	Massive sandstone	Massive sandstone. Parallel lamination and grading are common, cross lamination is observed.	Fig. 5.14
IIc	Slumped sandstone	Slumping structures. Often multiple layers of sandstone and shale.	Fig. 5.15
III	**Carbonate**		Fig. 5.16
IIIa	Nodular limestone	Isolated and coalesced nodules.	Fig. 5.17
IIIb	Continuous limestone beds	No laminae observed.	

Facies I: Mudstone

Ia: Grey fissile mudstone

Description: This facies is present in all localities and occur interbedded with Facies IIIa below point zero. It is also observed as the dominant lithology in the first 5 to 15 meter above point zero on all localities. The sediments in this facies show clay to silt size of grains, with various degrees of bioturbation. Units observed from this facies vary in thickness from ~2 centimeter to 20 centimeter. Brown, small (mm) clasts of siderite are common.

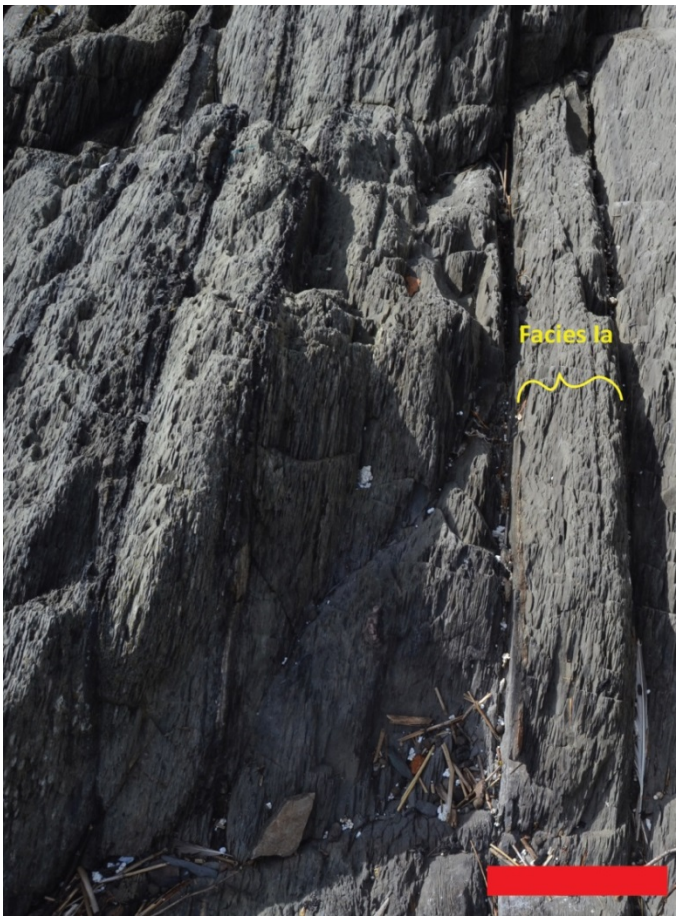

Figure 5.1: *Facies Ia are dominant with some interbedded siltstone/sandstone layers of facies IIb. Facies Ib is also present and show darker layers. The picture illustrates the first 1 meter above point zero of facies association FA2. One of the layers of Facies Ia is marked in yellow. Scale: 50 centimeter. Position: L.Ø.P1, 1 meter above point zero. Right way up is to the right.*

Figure 5.2: *Facies Ia interbedded with isolated and coherent nodular limestone (Facies IIIa). This succession represents FA1 (see chapter 5.2). Scale: 5 centimeter. L.Ø.P1, 1 meter below point zero.*

Interpretation:

Fine particles are carried in suspension by water. When the water mass flow carrying the suspended material enters quieter water or slows down, these particles settles and mud is deposited (Collinson et al., 2006). High grade of bioturbation has most likely altered sedimentary lamina. It is also possible that massive mudstone is formed by continuous deposition of clay and silt particles. The lack of obvious grain-size differences suggest that fissility is due to grain size orientation (Collinson et al., 2006).

Ib: Dark grey/black fissile mudstone

Description*:*

This facies is present in all localities and occurs interbedded with Facies Ia above point zero. The samples collected from this facies show no internal lamination but crude fissility is observed. The sediments in this facies show clay to silt size of grains, with various degrees of bioturbation. Brown clasts of siderite/pyrite are common. Units observed from this facies vary in thickness from a few centimeters to approximately 0.5 meter. No fossils are observed in this facies.

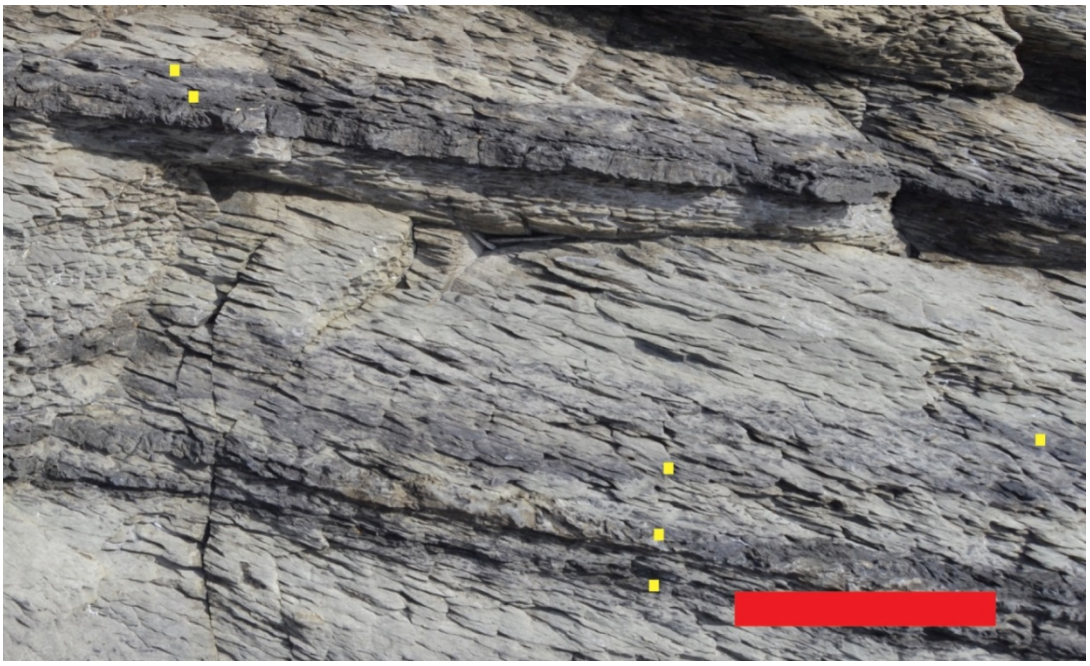

Figure 5.3: *The location of layers belonging to Facies Ib is marked with yellow squares. The facies is interbedded between the more calcareous shale of Facies Ia and Facies IIa and represent facies association FA2. Position: L.Ø.P1, 1 meter above point zero. Scale: 15 centimenters.*

Interpretation:

Fine particles are carried in suspension by water. When the water mass flow carrying the suspended material enters quieter water or slows down, these particles settles and mud is deposited (Collinson et al., 2006). The lack of obvious grain-size differences suggest that fissility is due to grain size orientation (Collinson et al., 2006). The darker color compared to Facies Ia is probably due to the lack of available oxygen needed in the production of carbonate.

Ic: Black parallel laminated fine-grained shale

Description:

This facies is observed interbedded predominantly between the sandstone layers of Facies IIb. The sediments in this facies show clay size of grains and no bioturbation is observed.

Interpretation:

Fine particles are carried in suspension by water. The mud is deposited as described in Facies Ib. Primary laminae are preserved probably due to the absence of bioturbation caused by a reduction in available oxygen.

Id: Structureless siltstone

Description:

This facies has some similarities with Facies Ia and Ib with the occurrence of crude fissility, but appear with a brown color. The sediments in this facies show grain sizes that correspond to a very coarse siltstone according to the Wentworth grain-size classification. Loading structures down into underlying sediment are observed in sample 227.462SS and shell fragments are observed in sample 227.474SS. This facies is observed in all localities, primarily from 5 meter to approximately 22 meter above point zero where it is interbedded between different other facies. It is absent within Facies Ie. Bioturbation grade is in the order of 3-6.

Interpretation:

Mud is deposited as particles falls out of suspension during fairweather conditions (Collinson et al., 2006). Bioturbation may have altered primary laminae.

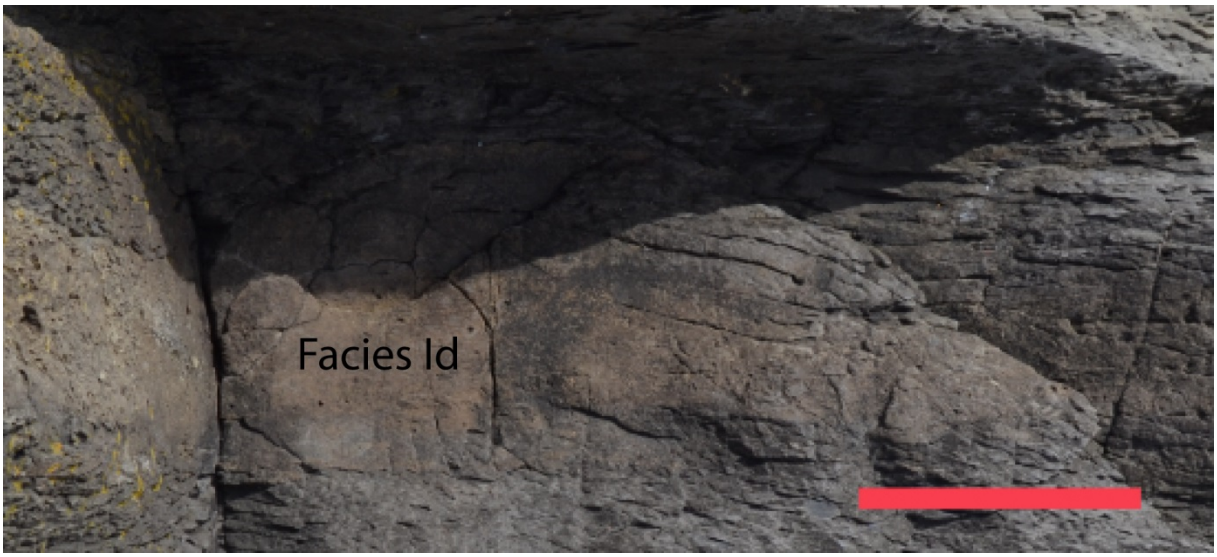

Figure 5.4: *Facies Id; Structureless bioturbated siltstone. Position: L.Ø.P1, 4.5 meter above point zero Scale: 15 centimeter. Right way up is up.*

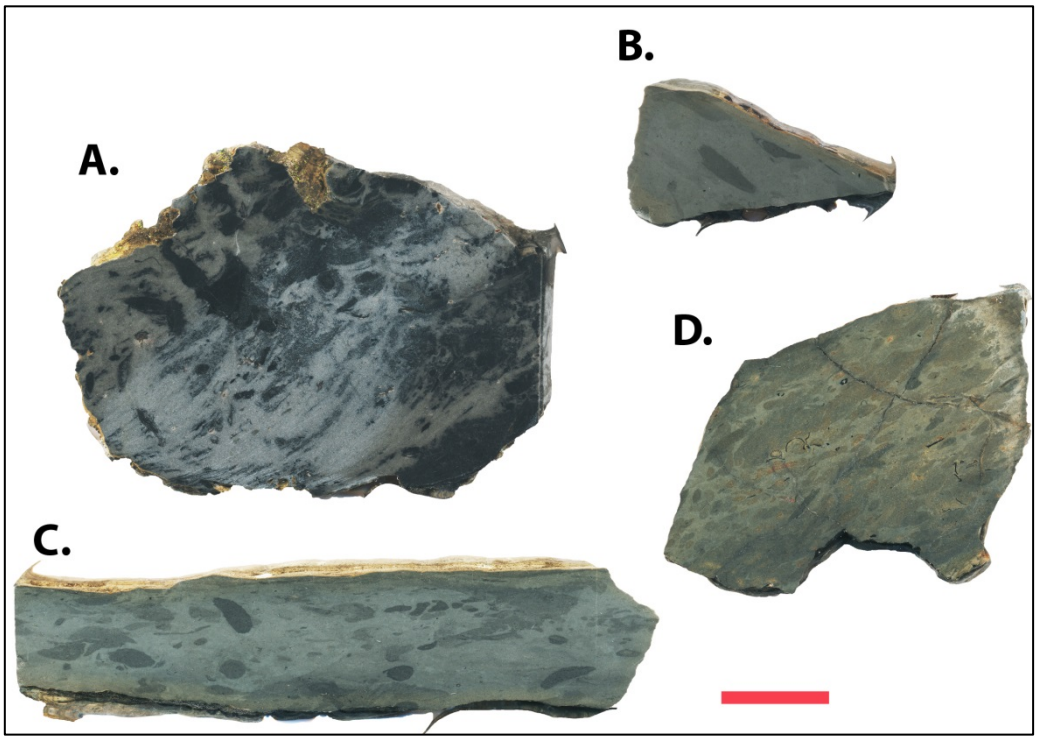

Figure 5.5: *Four different samples showing facies Id with different grade of bioturbation. A: Sample 227.441SS (L.Ø.P 1, 3.50 m.a.b); bioturbation grade; 4. Soft sediment deformation is shown as slump structures in the middle of the sample. B: Sample 227.444SS (L.Ø.P 1, 7.00 m.a.b); bioturbation grade: 6. All internal structures are altered by bioturbation. C: Sample 227.471SS (R.Ø.P1, 6.80 m.a.b); bioturbation grade; 5-6. D: Sample 227.474SS (R.Ø.P1, 10.40 m.a.b); bioturbation grade; 5. Sample contains shell fragments. Abbreviation m.a.b: Meter above basis (meter above point zero).*

Ie: “Brown-weathered” siltstone

Description:

This facies is observed in all profiles on all localities. It is situated in the upper part of the Husbergøya, approximately 17-19 meter above point zero. The thickness varies from ~1.5 meter to ~3 meter dependent on in which locality the facies is observed in. Bedded massive units with alternating lighter and darker brown colors are observed within this facies. The thicknesses of these bedded units vary from 5 – 40 centimeters. This facies shows similarities with facies Id, but stands out visually with its “brown-weathered” color. The sediments of this facies show grain sizes ranging from very coarse siltstone to very fine sandstone. The grade of bioturbation is substantially high with a value of 6, and no internal structures are observed.

Interpretation:

The unlaminated character of this facies is due to extensive bioturbation. As also proposed by (Brenchley and Newall, 1975), a pause in sedimentation resulted in extensive bioturbation by organisms that destroys primary lamination.

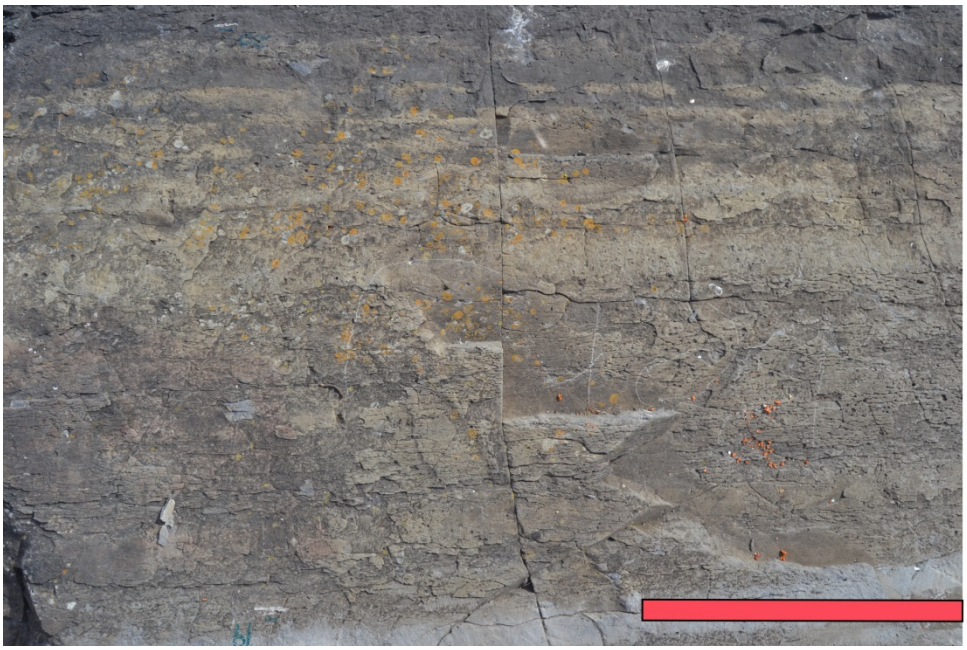

Figure 5.6: *Facies Ie; bioturbated very coarse siltstone to very fine sandstone 19.5 meter above point zero. Underlying facies Ie is a continuous limestone bed. Picture is taken on Langøyene Profile 1 and the succession represents the lowest part of facies association FA4. Scale: 30 centimenter.*

Figure 5.7: *Facies Ie; sample 227.481-SS (R.Ø.P1, 17.10 m.a.b) collected on Rambergøya in Profile 1. The sample has no internal lamination and the bioturbation grade is 6.*

Facies II: Siltstone/very fine sandstone

IIa: Internally laminated siltstone/very fine sandstone

Description:

The sedimentary rocks in this facies show grain size that represents very coarse siltstone to very fine sandstone. The facies occurs interbedded between different other facies throughout the logged profiles in all localities, but it is not observed interbedded in Facies Ie. The thickness of these layers ranges from 1 centimeter to maximum 5 centimeter. A common feature in the samples studied from this facies is interbedded sand and mud. Samples studied show most often a sharp erosional base with loading structures down into the underlying sediment. From the sharp base and upwards, the best represented samples from this facies show parallel lamination that is overlain by micro hummocky cross stratification structures. The top section shows current ripple lamination and, in some samples, climbing ripples. Other characteristic structures and processes observed in this facies are water escape structures, soft sediment deformation and escape burrows. Beds of Facies IIa have large lateral distribution, but pinching beds observed as lenticular features are also observed. Some of the beds of Facies IIa have undergone slumping and up to a few centimeters thick clasts of pyrite are observed in some occasions.

Figure 5.8: *Facies IIa; represented as very fine sandstone in the middle of the picture, interbedded between Facies Ia and Ib. From Langøyene Profile 1, approximately 2 meter above point zero. Scale: 15 centimeter. Right way up is up.*

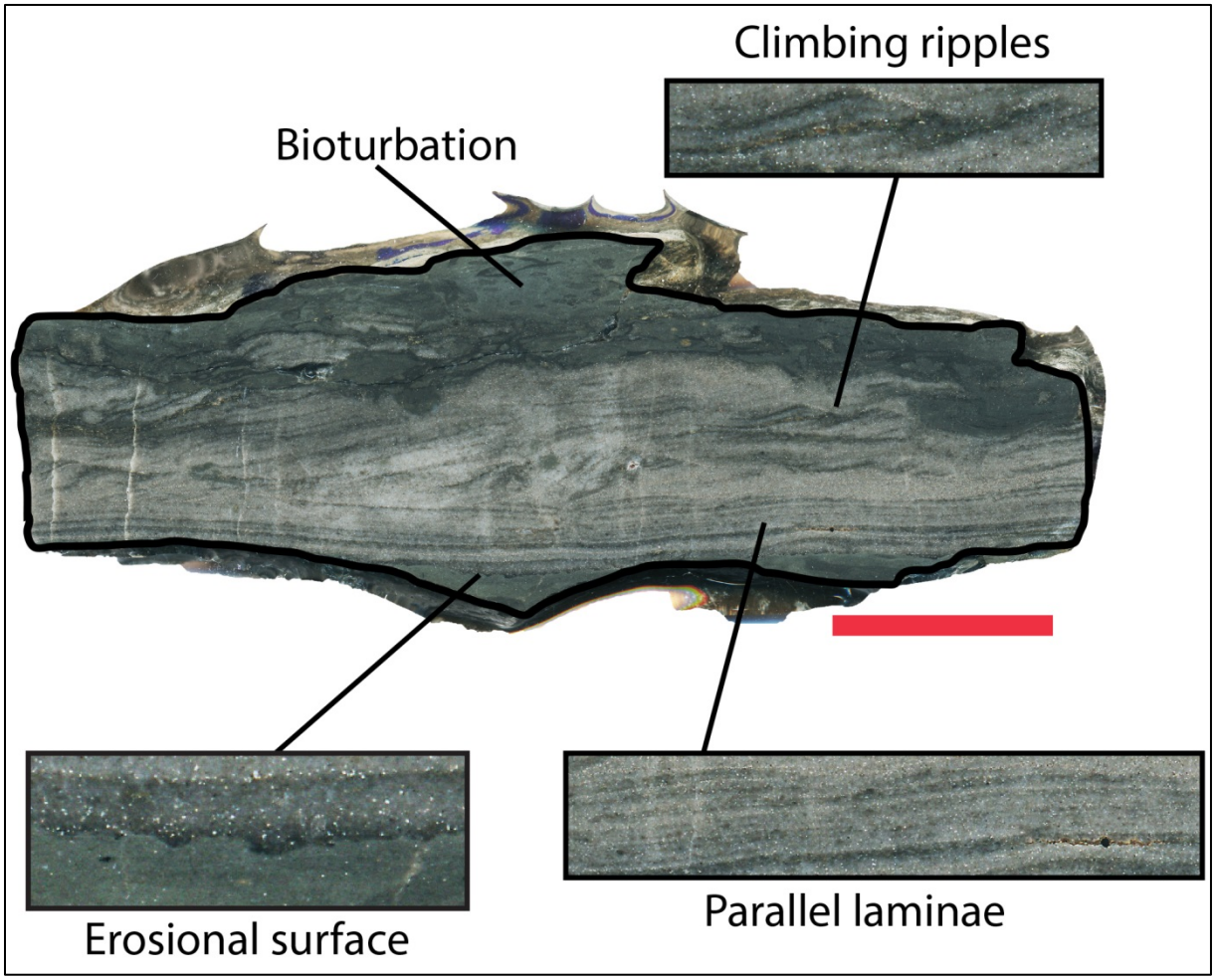

Figure 5.9: *Charateristical structures of Facies IIa from sample 227.470-SS (R.Ø.P1, 5.90 m.a.b). Hummocky cross stratification can be observed in the middle of the picture.*

Interpretation:

Sand in suspension can be transported from the coast to the open shelf by storm or tsunami induced turbulent waters. As the energy decreases, the suspension cloud descends and form parallel laminae. Fine-grained sediments settles as the energy decreases further and a graded rhytmite of sand and mud is formed. Storm-sand layers in ancient sediments can show planar lamination in the lower part and ripples in the upper part (Reineck and Singh, 1972). Reineck and Singh (1972) explained this phenomenon by the laminated part as being deposited by a suspension cloud during a heavy storm leading to increase in water level. Ripples are formed as the water level falls and the sea bottom get exposed to waves again.

Water moves downwind during a storm due to frictional coupling between wind and the sea surface. Water moving towards the shore can cause the sea surface to rise as much as several meters. This “piling-up” of water is better known as a “storm surge”. As the sea surface is elevated, a bottom current moving sea-wards down the pressure gradient is produced. This geostrophic flow moves obliquely offshore due to the Coriolis force. During a storm, both geostrophic flows and wave induced oscillatory flows operate together moving the sediments (Swift et al., 1986). The height, wavelength and type of bedforms are a result of variations in the orbital diameter and velocity of the oscillatory current and the velocity of superimposed unidirectional currents (Dumas et al., 2005, Dumas and Arnott, 2006). Hummocky cross-stratification forms most likely above storm wave base where the oscillatory component is strong and the unidirectional component are weak (Plint, 2010).

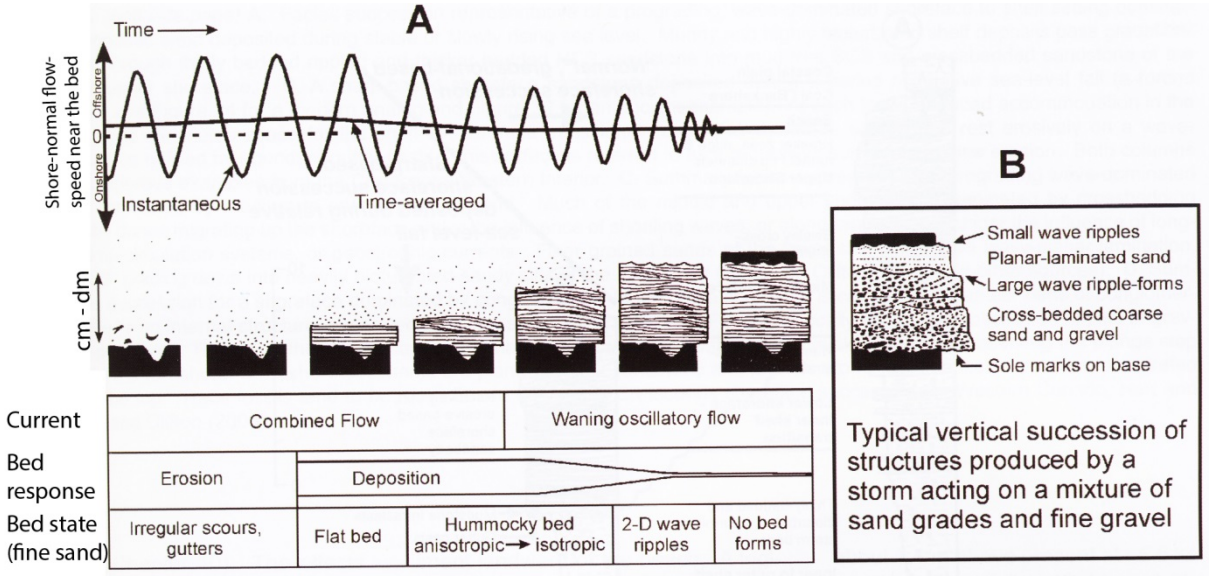

Figure 5.10*: **A**. Development of an idealized fine sandstone event bed, resulting from a storm-generated combined flow.* **B**. *The development in the same conditions, but here, the substrate is a mixture of sand and fine gravel. Modified from Plint (2010).*

As seen in Figure 5.10, planar lamination is deposited as the storm starts to wane. This occurs under powerful combined flow. The planar lamination may develop into anisotropic hummocky cross-stratification due to the influence of the unidirectional flow component. Isotropic hummocky cross-stratification develops as the storm continues to wane and the oscillatory flow component is dominant. Small scale ripples forms on top of the hummocky cross-stratification as the energy in the oscillatory flow decreases. The frequently observed sharp and erosive surfaces form during the rising phase of the storm. As seen in Figure 5.10, the formation of sole marks and gutters are common in the initial phase (Plint, 2010).

Some of the observed samples from this facies show soft-sediment deformation structures. Unconsolidated sediment being in a weak condition is often exposed to this kind of deformation (Collinson et al., 2006). According to Owen et al. (2011), the stresses that typically drive soft-sediment deformation include; “(1) gravity acting on slopes; (2) unequal loading caused by topographical irregularities in the sediment-water interface (including bedform topography); (3) gravitational instabilities due to a reverse density gradient where denser sediment overlies less dense sediment; (4) shear by aqueous or other currents; and (5) biological and chemical agents”. If a shock is applied to loosely packed, waterlogged sediment it can undergo liquefaction where the sediment and water act as a liquid. An example of a slump structure, where the whole bed or part of the bed has moved and

deformed is presented in Figure 5.11. Internal soft sediment deformation structures in some of the samples collected are presented in Figure 5.12.

Figure 5.11: *Slump structure of facies IIa. Position: L.Ø.P 1, 12.95 meters above point zero. Scale: 2 centimeters. Right way up is up.*

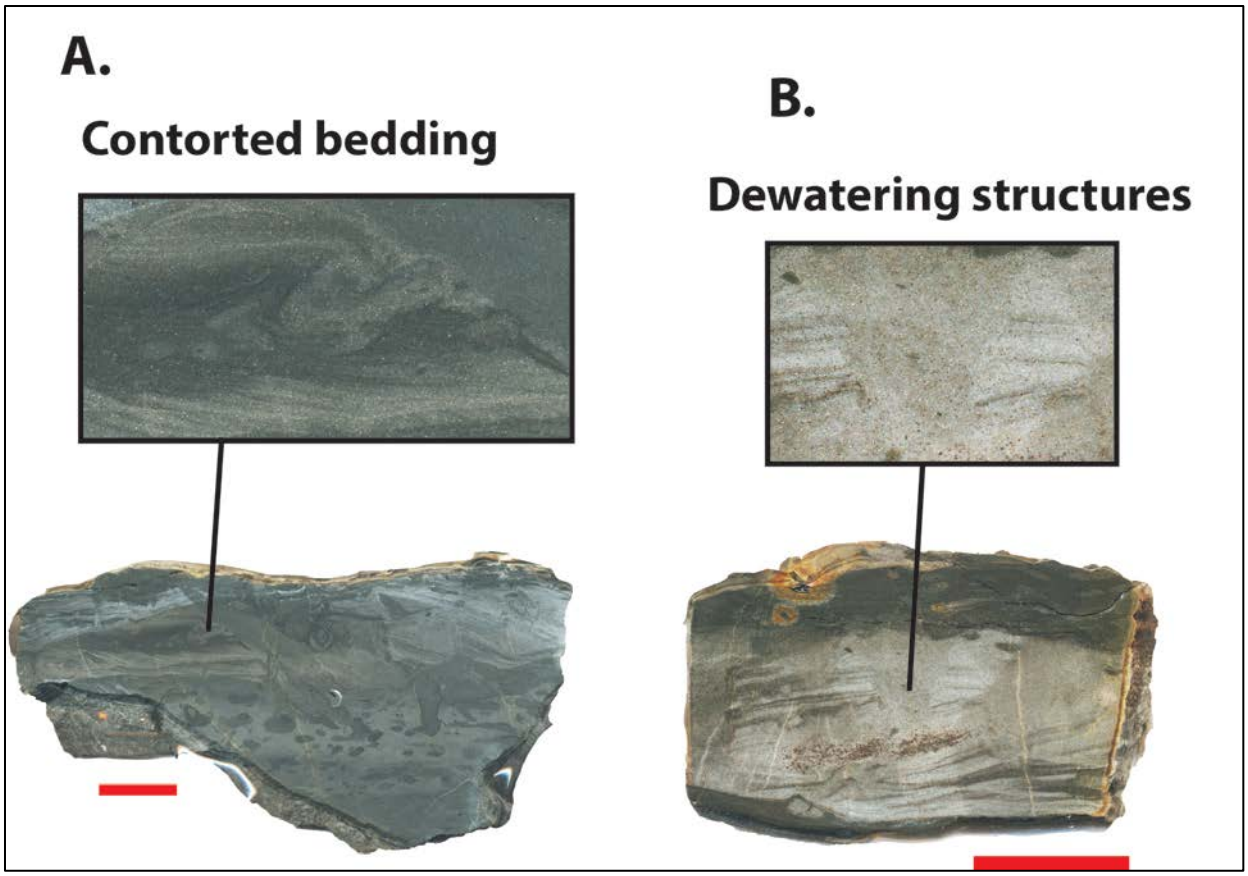

Figure 5.12: *Examples of soft-sediment deformation structures observed in sample scans.* **A:** *Facies IIa showing soft-sediment deformation structures in the form of contorted bedding. From Sample 227.446-SS (L.Ø.P1, 9.35 m.a.b). Scale: 2 centimeter.* **B.** *Facies IIa showing soft-sediment deformation structures in the form of water escape structures that have altered primary sedimentary structures (dewatering structures). From sample 227.448-SS (L.Ø.P 1, 11.85 ma.b). Scale: 2 centimeters.*

Recolonization of the top section of Facies IIa and in the overlying layer is observed as horizontal grazing of organisms (high grade of bioturbation). Many of the samples collected from Facies IIa also shows horizontal escape borrows and this indicates that Facies IIa developed during a rapid event. An example of a vertical escape burrow penetrating the whole sample is presented in Figure 5.13.

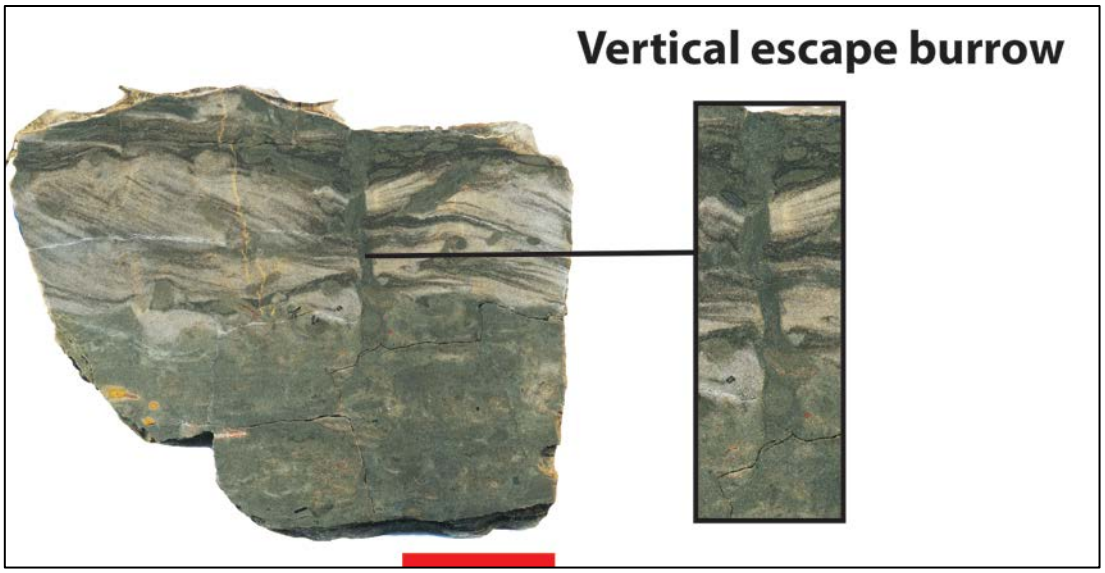

Figure 5.13: *Vertical escape-burrow penetrating the bed of Facies IIa. From Sample 227.473-SS (R.Ø.P.1, 10.00 m.a.b). Scale: 2 centimeters.*

IIb: Massive sandstone

Description:

Facies IIb is observed above Facies Ie in the succession on all localities. It is most often observed with grading and planar lamination and cross lamination occurs in some of the layers. The thickness varies from 10 centimeter to approximately 1.5 meter. Facies IIb is observed interbedded with facies Ia, Ib and Ic, has sharp bottom boundary surfaces and erosional structures are observed in some of the underlying beds of this facies. Bioturbation occur in some beds.

Figure 5.14: *Facies IIb with a sharp erosional contact to the underlying bed. Position: L.Ø.P1, 22.5 meters above point zero. Scale: 15 centimeters.*

Interpretation:

Sand in suspension can be transported from the coast to the open shelf by storm or tsunami induced turbulent waters. As the energy decreases, the suspension cloud descends and form parallel laminae (Reineck and Singh, 1972).

IIc: Slump sandstone

Description:

Facies IIIc consists of multiples layers, commonly Facies Ia, Ib Ic and IIIa, which are slumped. This facies is observed in all localities, on all logged profiles. This facies is not logged on Hovedøya Profile 1 as it is seen higher up in the stratigraphy than what was logged. The slumped packages show a variation in thickness between 0.5 to 5.5 meters.

Figure 5.15: *Facies IIc (facies association FA5); interbedded layers of different facies (dominantly Facies IId) are slumped. Position: L.Ø.P1, 24 meters above point zero. Scale: 15 centimeters.*

Interpretation:

According to Owen et al. (2011), the stresses that typically drive soft-sediment deformation include; "(1) gravity acting on slopes; (2) unequal loading caused by topographical

irregularities in the sediment-water interface (including bedform topography); (3) gravitational instabilities due to a reverse density gradient where denser sediment overlies less dense sediment; (4) shear by aqueous or other currents; and (5) biological and chemical agents". If a shock is applied to loosely packed, waterlogged sediment it can undergo liquefaction where the sediment and water acts as a liquid.

Facies III: Carbonate

IIIa: Nodular limestone

Description:

Facies IIIa consists of nodular limestone. It is present below point zero in all profiles on all localities but is also observed above point zero interbedded with other facies. The nodules occur in different sizes, isolated or coalesced to almost continuous beds (facies IIIb). It is observed mostly interbedded with facies Ia and IIIb, but also higher in the succession, mainly interbedded with Facies IIIb and Id.

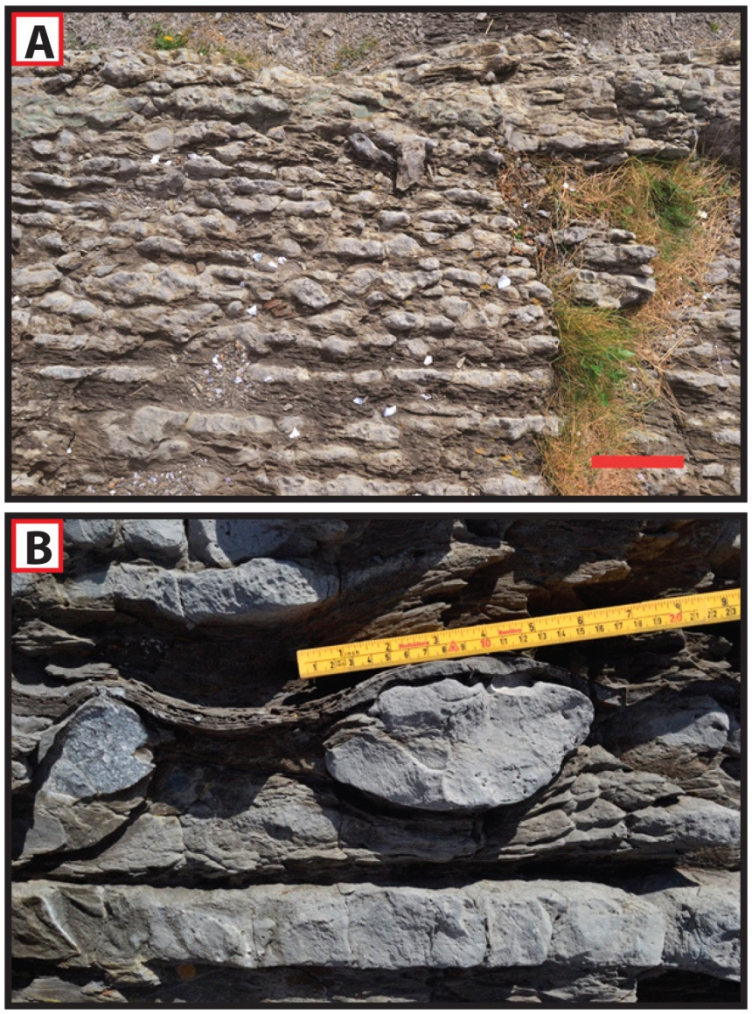

Figure 5.16: A: *Nodular limestones of Facies IIIa interbedded with the fissile shales of Facies Ia. Top section of the picture represents point zero. The succession is the uppermost part of FA1. Position: Langøyene Profile; 1 meter below point zero. Scale: 15 centimeter.* **B:** *Alternating continuous beds of limestone (Facies IIIb), limestone nodules (Facies IIIa) and grey calcareous shale beds (Facies Ia). A storm deposited siltstone/very fine sandstone bed (Facies IIa) drape over an erosional surface on the underlying limestone nodule. Position; 3 meters below point zero on Rambergøya Profile 1.*

Interpretation:

Carbonate is formed by carbonate producing organisms which is facilitated in environments with low influx of siliciclastic detrius. According to Blatt et al. (1972), the origin of clay size mud can have three sources; (1) abrasion of larger carbonate particles, (2) direct inorganic precipitation of aragonite from seawater, or (3) the production of aragonite needles within the tissues of calcareous algae. The origin of limestone nodules is caused either as a result of subsolution of continuous carbonate layers prior to burial but after deposition (Bjørlykke, 1973), or by early diagenetic concretionary carbonate cementation (Henningsmoen, 1974, Möller and Kvingan, 1988).

IIIb: Continuous limestone

Description:

This facies consists of continuous limestone beds and appear in the Sedimentary succession in all localities. It occurs frequently below point zero interbedded between Facies Ia, Facies Ib and Facies IIa, but also interbedded between other facies above point zero. No laminae are observed in this facies.

Figure 5.17: *Facies IIIc seen in the middle of the picture as a continuous limestone layer. Below lies an isolated limestone nodule of facies IIIa and above the continuous limestone layer are Facies Id and Ie. Picture taken 19 meter above point zero on Langøyene, Profile 1. Scale: 15 centimeter. Right way up is up.*

Interpretation:

As previously mentioned when describing Facies IIIa, carbonate is formed by carbonate producing organisms and is facilitated in environments that have a low influx of silicate detrius (Blatt et al., 1972). According to Blatt et al. (1972), the origin of clay size mud can have three sources; (1) abrasion of larger carbonate particles, (2) direct inorganic precipitation of aragonite from seawater, or (3) the production of aragonite needles within the tissues of calcareous algae.

5.2 Facies associations

Five facies associations are constructed based on the different facies described in Chapter 5.1 (see Table 5.1). These facies associations are presented in Table 5.2 and will be described further in Chapter 5.2. A description of the different facies association and their position in the logged successions are presented. The description is based on the different facies presented in Chapter 5.1, observations during field work, sedimentary logs, scanned sample surfaces, grain size measurement in thin sections. Due to the high amount of data, the simplified and stacked sedimentary logs with facies associations are presented in APPENDIX E.

Table 5.2: *An overview of the five different facies associations proposed based on the different facies presented in Chapter 5.1.1*

Facies Association	Facies nr.	Located	Description
FA1	Ia, IIa, IIIIa, IIIb	Skogerholmen Formation	Interbedded nodular limestone, continuous limestone beds, grey fissile shale and internally laminated very fine sandstone/silt.
FA2	Ia, Ib, Ic, IIa	Husbergøya Formation	Interbedded grey and dark grey/black fissile mudstone and internally laminated siltstone/very fine sandstone.
FA3	Ia, Ib, Id, IIa, IIIa, IIIb	Husbergøya Formation	Interbedded grey and dark grey/black fissile mudstone, bioturbated siltstone, internally laminated siltstone/very fine sandstone and continuous limestone beds. Limestone nodules observed.
FA4	Ia, Ie, IIa, IIIa, IIIb	Husbergøya Formation	"Brown-weathered" calcareous siltstone/very fine sandstone, nodular limestone and continuous

			beds of limestone. Interbedded storm deposited beds observed.
FA5	Ic, Ib, IIb, IIc	Langøyene Formation	Interbedded massive/laminated sandstone, bioturbated siltstone and fine-grained laminated black shale. Slump structures.

5.2.1 FA1

Observation:

FA1 represents alternations between calcareous shale, nodular limestone (both isolated and coalesced) and continuous limestone layers (see figure 5.2 and 5.17). The storm deposited siltstone/very fine sandstone layers of Facies IIa occur sporadically in the succession with planar laminae and cross lamination. The limestone nodules vary in size and lateral extent, and overlying planar elements are often deformed and bent around the nodules. Some the observed nodules are coalesced and show a flaser structure. A conglomerate layer with limestone clasts in matrix of calcareous mud occurs at the top of this facies (Figure 5.18). The diameter of the clasts in the conglomerate varies with diameter from 5 centimeter to a few millimeters. From the studied thin sections in light microscope, the carbonate particles that are present in this facies association are micrite. The fossil content in this facies association is low.

Interpretation:

Rhythmic alternation of limestone and shale was observed in the Lower Palaeozoic of the Oslo Region by (Bjørlykke, 1973) and he interpreted this as being possibly controlled by climatic cycles. As all observed limestones in this facies occur alternating with fissile shale, the depositional environment must have been quiet and below fairweather wave base where fine-grained sediments settles from suspension (Collinson et al., 2006). Möller and Kvingan (1988) interpreted from their studies of the nodular limestones in the Ordovician and Silurian of the Oslo region that carbonate platform sediments with shale contents around 50% or more, represent quiet environments where the dominance of the limestone content appear most often as nodules. The continuous beds were thus more commonly observed in the succession in which represents shallower environments and higher energy.

***Figure 5.18**: Limestone conglomerate in the topmost part of facies association FA1 on Langøyene Profile 1.*

Hovedøya Profile 1

Five meters of FA1 is logged on Hovedøya Profile 1, from -5 meters below point zero to point zero. As seen in Figure 5.19, grey fissile calcareous shales of Facies Ia dominate with ~55 %. The limestones of Facies IIIa and IIIb represent a percentage of ~42 while the storm deposited siltstones/very fine sandstones (Facies IIa) represent approximately 3 % of the total logged succession. Six layers with thicknesses that vary from 1 to 6 centimeters, representing Facies IIa, are observed in this succession. The conglomerate layer has a thickness of 3 centimeter. Horizontal cracks are observed in some parts of this succession. These cracks are restricted to single layers and show no characteristics of being faults. They contain calcite, whereas neither slickensides nor displacement are observed.

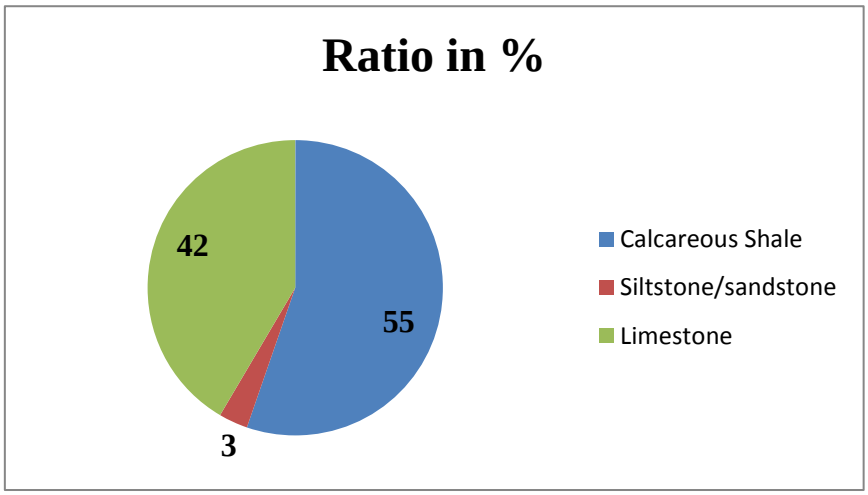

Figure 5.19: *Ratio between calcareous shale, siltstone/sandstone and limestone presented in a pie-diagram of FA1 on Langøyene Profile 1.*

Rambergøya Profile 1

Four meters of succession belonging to FA1 are logged on Rambergøya Profile 1. The characteristics of the different facies in this profile are quite similar to those observed and described on Hovedøya Profile 1. The limestone nodules of Facies IIIa are mostly elongated with diameters that vary from 0.5 centimeter to approximately 10 centimeters. With an exception of four thin siltstone/very fine sandstone beds that is interbedded within a 10 centimeters thick shale unit, Facies IIa is absent in the logged succession. The limestone conglomerate layer, as previously described from Hovedøya, is 10 centimeters thick. The diameters of the limestone nodules decrease towards point zero within the topmost 60 centimeters of the succession.

Calcareous shale dominates FA1 with ~50% and the ratio of limestone and siltstone/sandstone are ~4% and ~46% respectively.

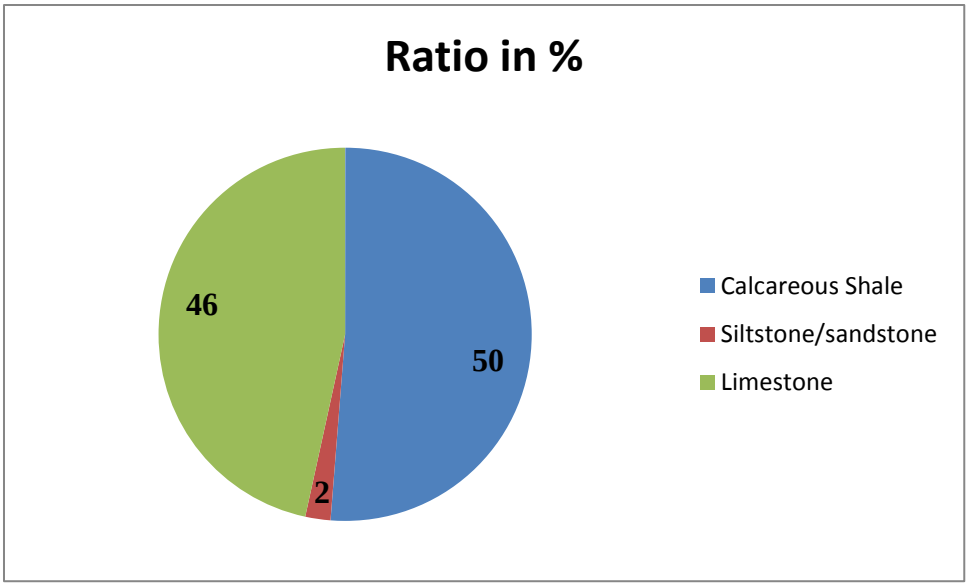

Figure 5.20: *Ratio between calcareous shale, siltstone/sandstone and limestone presented in a pie-diagram of FA1 on Rambergøya Profile 1.*

Langøyene Profile 1

The succession where FA1 is located on Langøyene Profile 1 is logged with fewer details than on Rambergøya and Hovedøya. There is a variation from isolated nodules to almost coherent limestone layers in the succession. Only one continuous limestone bed is observed in the succession. The limestone conglomerate layer is located in the topmost (underlying point zero) section and has a thickness of 2 centimeters. There is observed only one internally laminated siltstone/sandstone layer (Facies IIa) with a thickness of 10 centimeters. There is heavy bioturbation in the last 2 meters of this succession. The sedimentary logs illustrating FA1 in Hovedøya Profile 1, Rambergøya Profile 1 and Langøyene Profile 1 are presented in Figure 5.21.

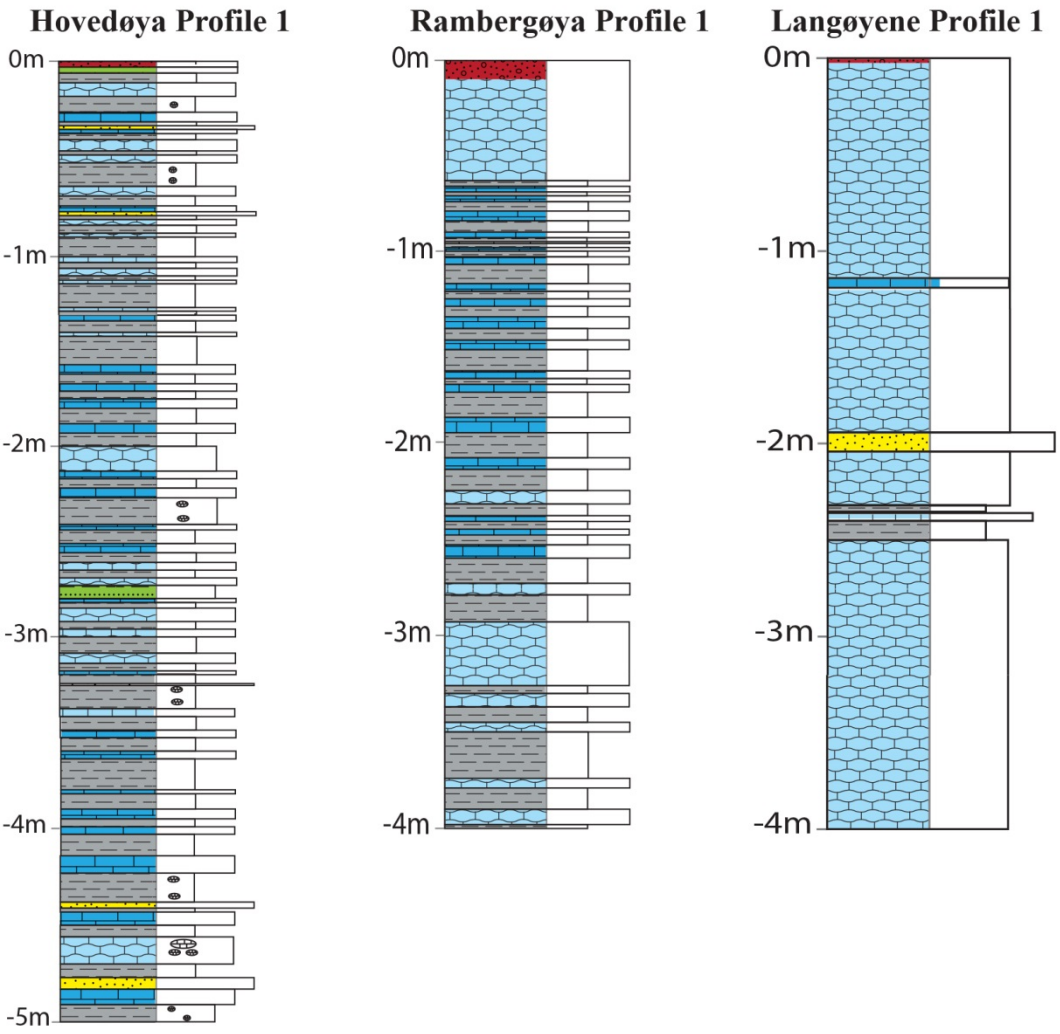

Figure 5.21: *FA1 represented by sedimentary logs from Hovedøya Profile 1, Rambergøya Profile 1 and Langøyene Profile 1.*

5.2.2 FA2

Observations:

As seen in Figure 5.1 and Figure 5.3, the characteristics of this succession are alternating grey fissile shale (Facies Ia), dark grey/black fissile shale (Facies Ib) and internal laminated siltstone/very fine sandstone (Facies IIa). There is also observed some few centimeters thin black very fine-grained laminated shale beds belonging to Facies Ic interbedded with the calcareous shales of Facies Ia and Ib.

Interpretation:

Deposition at moderate shelf depth is proposed by Stanistreet (1989) with water depth values of about 100 meters (Brenchley et al., 1979). The thin siltstone/very fine sandstone beds represent distal storm-generated current deposits (Brenchley et al., 1979). Evidence in

sedimentary successions from the Middle Devonian muddy epeiric sea in the western and central New York, presented by Miller et al. (1988), showed that the depth do not only control the mudstone/storm deposited sandstone thicknesses and the relative significance of winnowing and blanketing, but also control the frequency of storm-generated deposits, and their probability of preservation.

Hovedøya Profile 1

FA2 can be seen in the logged profile from point zero (0 meter) to approximately 3.3 meters above point zero. This facies association starts as calcareous shales of facies Ia with a sharp contact to the underlying FA1. FA2 shows shale layers with thicknesses of 3 centimeters to 1.5 meters. Facies IIa comes in four times as thin beds (4 – 0.5 centimeters) every 40-50 centimeters, both as continuous beds but also as laminated pinching beds. The last 1.7 meters of this facies is calcareous shale that shows little bioturbation in the bottom section with increasing bioturbation towards the top (medium bioturbated).

Figure 5.22 shows that the ratio of mud versus siltstone/very fine sandstone in this facies association is as high as ~97 percent.

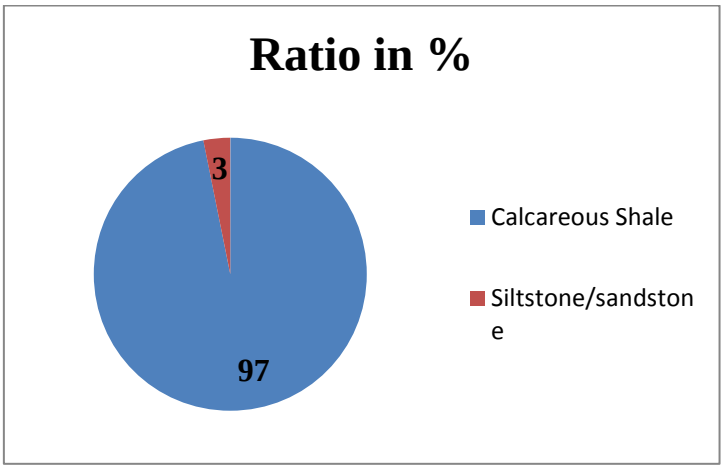

Figure 5.22: *Calcareous shale and siltstone/sandstone ratio in FA2 from Hovedøya Profile 1.*

Rambergøya Profile 1

FA2 can be recognized from point zero to approximately 1.72 meters on Rambergøya Profile 1. There are not observed any storm deposited siltstone/sandstone beds in the FA2 succession

and only a few beds of Facies IIb are observed. Facies IIa is heavily bioturbated on this locality.

Langøyene Profile 1

FA2 can be recognized from point zero to approximately 3.5 meters. There are four storm deposited very fine sandstone beds with thicknesses of 2 to 5 meter observed in the succession. Thin sand lenses are also observed quite near point zero. The grade of bioturbation vary from medium in the shale to heavy on the top of the sandstone layer located 1 meter above point zero. The ratio between shale and siltstone/sandstone shows ~ 92 % shale and 8 % siltstone/sandstone.

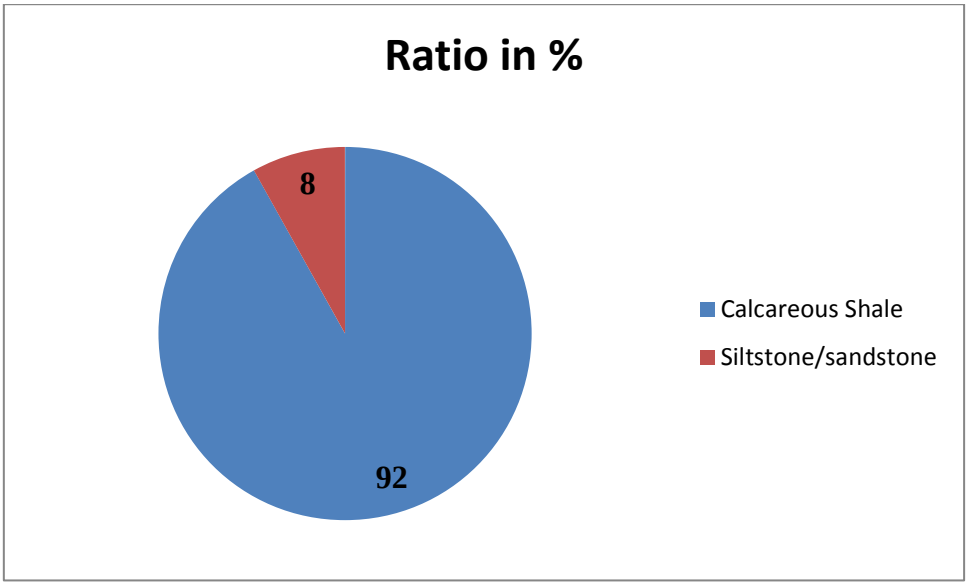

Figure 5.23: *Calcareous shale and siltstone/sandstone ratio in FA2 from Langøyene Profile 1.*

5.2.3 FA3

Description:

This facies association consists of grey calcareous fissile shale (Facies Ia), dark grey/black calcareous fissile shale (Facies Ib), structureless siltstone (Facies Id), limestone nodules (Facies IIIa) and continuous limestone beds (Facies IIIb). Facies IIIa and Facies IIIb are only absent on Rambergøya Profile 1. A common feature in FA3 that is observed in all localities are the progressively increase in the occurrence and thicknesses of internally laminated siltstone/very fine sandstone beds. The grade of bioturbation also increases upwards with

some exceptions in different beds of Facies Id. There is observed cyclicity of a progressively increase in occurrence and thickness of Facies Id and Facies IIa.

Interpretation:

According to Thorne et al. (1991), storm-deposited beds, tempestites, get progressively thinner with increasing depth of the sedimentary basin. Thus, the observed increase in occurrence and thickness of the storm deposited siltstone/very fine sandstone beds throughout FA3 favors an overall upward shallowing of the actual part of the basin represented by this section of the Upper Ordovician in the Oslo Region.

Hovedøya Profile 1

FA3 is seen from approximately 3.3 meters above point zero where the first bioturbated siltstone beds occur, until approximately 16.5 meters above point zero. Facies Ia is representative throughout the succession with maximum thicknesses of 60-70 centimeters in the lower section of this facies association to a minimum thickness of 4-5 centimeters in the upper part. Three continuous limestone layers interbedded with Facies Ia, Facies Id and Facies IIa are observed 15 meters above point zero. These continuous limestone beds often contain shell fragments and are 5-7 meters thick.

Rambergøya Profile 1

FA3 starts in the transition from calcareous shale to the first bioturbated siltstone layer, 1.7 meters above point zero. The facies association can then be traced 13.2 meters up in the succession. The different facies show highly varying thicknesses, but a general trend of decreasing occurrence and thicknesses of Facies Ia and increase in occurrence and thicknesses of Facies IIa are observed.

Langøyene Profile 1

FA3 is first recognized by a bioturbated siltstone bed, 3.5 meters above point zero. The facies association covers an interval of the succession of a total thickness of 14.1 meters. Alternating limestone and shale beds are located 2 meters up in FA3. There are five observed limestone layers with thicknesses of 5-9 meters. Underlying the alternating limestone and shale beds is a 3.5 meters thick shale layer with limestone nodules. These limestone nodules have a diameter of 5 centimeters and are elongated in shape. There is a rhythmic increase in the occurrence and thickness of the storm deposited siltstone/very fine sandstone beds (Facies IIa) and structureless siltstone beds (Facies Id) in the succession. Four separate rhythmites are located throughout facies association FA3.

5.2.4 FA4

Description:

The lithology of FA4 represents dominantly "brown weathered" siltstone/very fine sandstone that is highly bioturbated (see Figure 5.6). Alternating structureless siltstone (Facies Id), continuous limestone beds (Facies IIIb) and some observed nodular limestone beds (Facies IIIa) are in most cases located both below and above the "brown weathered" siltstone/very fine sandstone unit. Interbedded storm-deposited beds with internal laminations are observed in Langøyene Profile 1. The fossil content is commonly high (see Chapter 5.4).

Interpretation:

Brenchley and Newall (1975) suggested a pause in sedimentation with extensive bioturbation and reworking of the sediment as a possible factor resulting in the brown appearance of this succession.

Hovedøya Profile 1

FA4 is located from 16.5 meters to 22.2 meters above point zero on Hovedøya. The "brown weathered" siltstone/very fine sandstone has a thickness of 3.3 meters, while the successions of alternating limestone (Facies IIIb) and structureless siltstone beds below and above Facies Ie account for 1.55 meters and 85 centimeters, respectively. The high degree of weathering of the "brown weathered" siltstone/very fine sandstone unit makes it hard to observe any fossils or grading.

Rambergøya Profile 1

FA4 starts at the transition from alternating grey fissile shale, structureless siltstone and storm deposited siltstones to a thick (1.7 meters thick) bioturbated structureless siltstone approximately 14.9 meters above point zero. The latter succession is abundant in fossil content compared to the underlying FA3. FA4 is approximately 6.1 meters thick on Rambergøya Profile 1. There is only one observed (4 centimeters thick) limestone bed underlying the "brown weathered" siltstone/very fine sandstone succession (Facies Ie). Above Facies Ie are alternating limestone and structureless siltstone beds that has maximum thicknesses of 15 centimeters in the lower part and end with two thicker limestone and structureless siltstone beds that are 50 and 30 centimeters thick, respectively. There are also observed seven interbedded thin (2-5 centimeters) storm deposited beds in this succession. The total thickness of this succession is 2.7 meters. The "brown weathered" siltstone/very fine sandstone has a thickness of 1.6 meters on this locality.

Langøyene Profile 1

The transition from FA3 to FA4 in this profile is similar to what was described above. This transition occurs 17.6 meters above point zero with a 60 centimeters thick structureless siltstone bed. Towards the "brown weathered" siltstone unit (facies Ie) there are thinner (10 – 2 centimeters) alternating limestone and structureless siltstone beds. The total thickness of the succession below Facies Ie is 1.55 meters, while Facies Ie show a thickness of 2.3 meters. Some bedding is observed in Facies Ie. A "bed" of isolated limestone nodules are observed right below the "brown bioturbated" unit. Above Facies Ie are alternating 7-10 centimeters thick beds of limestone and structureless siltstone. The top of FA4 in this locality is represented by a 3 centimeters thick nodular limestone layer. The total thickness of FA4 in this locality is 4.4 meters.

5.2.5 FA5

Description:

FA5 consists of interbedded massive/laminated very fine to fine sandstone and fine-grained internally laminated shale. Slump structures occur in some parts of the succession. Bioturbated siltstone beds are observed in some localities. This facies is first recognized from the many sharp erosional surfaces overlying FA4, and the characteristic slumped layers. The overall grade of bioturbation is very low compared to the underlying FA4, and fossils are abundant. Normal grading is observed in some of the sandstones.

Figure 5.24: *Lowest part of FA5 from Langøyene Profile 1. Position: 22 meters above point zero. Scale: 15 centimeter.*

Interpretation:

This facies association is dominated by sandstone, so the amount of siliciclastic detrius has increased. This may be ascribed to an advance of land-areas that have introduced more sand to the basin. Either this is caused by tectonics in the Caledonian Orogen or by regression due to fall in eustasy, or just be due to increasing energy in the epeiric basin, allowing more sand to be transported and deposited.

Hovedøya Profile 1

FA5 is located approximately 22.2 meters above point zero in this profile, and only 1.1 meters of this facies association is logged on Hovedøya Profile 1. This was due to observed faults in the succession in which the author found hard to correlate over.

Rambergøya Profile 1

FA5 is located approximately 21 meters above point zero on Rambergøya Profile 1. Approximately 3 meters belonging to this facies association was logged. The massive sandstone beds in this facies have thicknesses of 2-5 centimeters and increases in occurrence upward in the succession. The structureless siltstone beds are 30-40 centimeters thick in the lower part of the succession, but their thicknesses decrease upwards to 4-15 centimeters. Vertical burrows are often observed in the top section of the sandstones. The first slumped layer is observed from 1.6 meters up this succession, and has a thickness of 10 centimeters. There is also second slumped layer at the end of the logged succession that has a thickness of 60 centimeters.

Langøyene Profile 1

FA5 is located in the transition from the alternating limestone and structureless siltstone beds in the top of FA4 to a more sandstone dominated lithology 22 meters above point zero. 3 meters of FA5 are logged in this profile. The sandstone beds increase rapidly in thicknesses from 2-15 centimeters at bottom section of the succession to 10-30 centimeters within a stratigraphic level three meters above. The first observed slumped layer consists of two layers, sandstone and shale, and are 10 centimeters thick. At the top of the succession there are observed two slumped sandstone layers that are approximately 25 centimeters thick.

5.2.6 Position of facies associations

Table 5.3 summarizes the positions of facies associations in correlations with point zero on Hovedøya Profile 1, Rambergøya Profile 1 and Langøyene Profile 1. The position of facies associations in simplified sedimentary logs is presented in APPENDIX E.

Table 5.3: *The positions of facies associations in correlation to point zero on Hovedøya Profile 1, Rambergøya Profile 1 and Langøyene Profile 1.*

	Hovedøya Profile 1		**Rambergøya Profile 1**		**Langøyene Profile 1**	
Facies association	**Start**	**End**	**Start**	**End**	**Start**	**End**
FA1	Logged from (-5,00 m)	0 m	Logged from (-4,00 m)	0 m	Logged from (-4,00)	0 m
FA2	0 m	3,30 m	0 m	1,72 m	0 m	3,50 m
FA3	3,30 m	16,50 m	1,72 m	14,90 m	3,50 m	17,60 m
FA4	16,50 m	22,20 m	14,90 m	21,00 m	17,60 m	22,0 m
FA5	22,20 m	Logged to 23,28 m	17,60 m	Logged to 24,0m	22,00 m	Logged to 24,00 m

5.3 Grain size measurement

As described in Chapter 4.6.1, 28 thin sections of samples collected on Langøyene (Profile 1) were used in the grain size measurement. The definitions are based on the classification by Udden (1914) (see Table 5.3). The bar diagrams presented in this chapter represents grain size measurements done in thin sections belonging to various facies. The main focus is to give an overall view of the grain size distribution in the succession. A list of PMO numbers and position of the thin sections measured is presented in APPENDIX B.

Table 5.4: *Grain size classification. Modified from Udden (1914).*

µm	Terminology
250-500	Medium sand
125-250	Fine sand
63-125	Very fine sand
31-63	Very coarse silt
16-31	Coarse silt
8-16	Medium silt
4-8	Fine silt
2-4	Very fine silt
0-2	Clay

FA1

One thin section belonging to facies association FA1 was measured. The two other thin sections from this facies association represented micritic limestone and were not taken into account. There is some fractions of very fine sand in the sample, but very coarse silt dominate. The thin section measured represents Facies IIa and are shown in Figure 5.25.

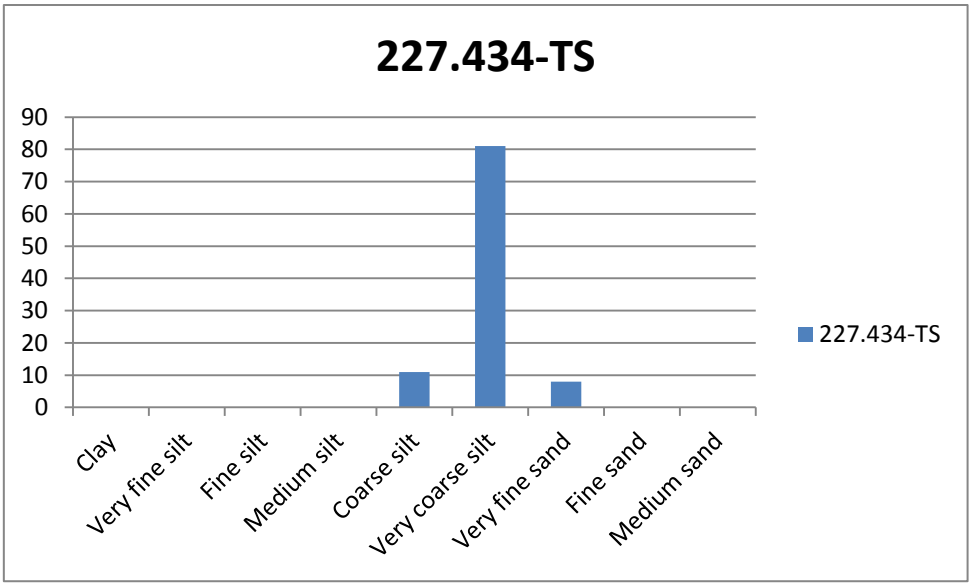

Figure 5.25: *Grain size distribution in sample 227.434-TS (FA1).*

FA2

The total of six thin section from facies association FA2 was measured. The grain size distribution is quite homogenous with very coarse silt as the dominant fraction.

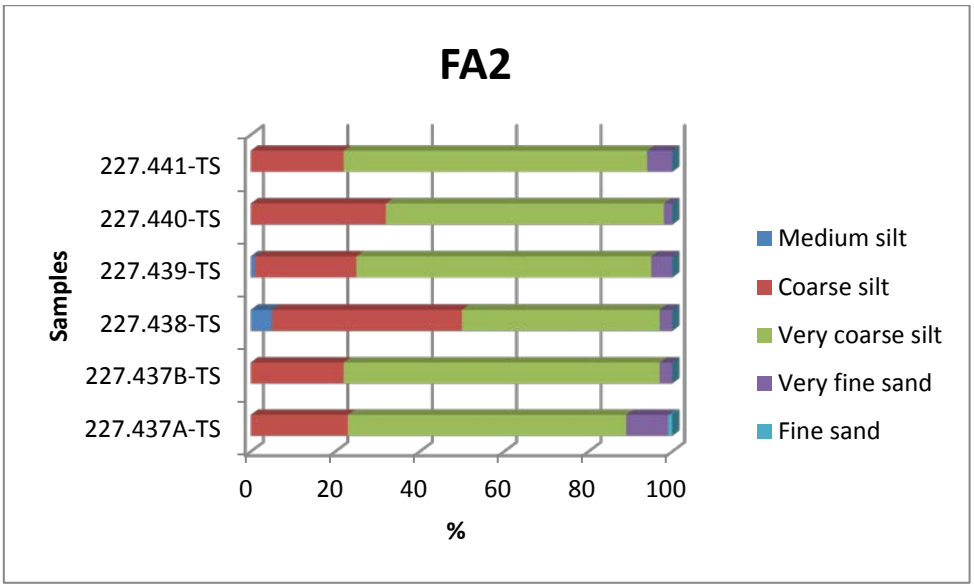

Figure 5.26: *Grain size distribution of the measured thin sections belonging to facies association FA2.*

FA3

As seen in Figure 5.27**,** eleven samples were measured from thin sections belonging to facies association FA3. There is an increase in the very fine sand fraction compared to FA2.

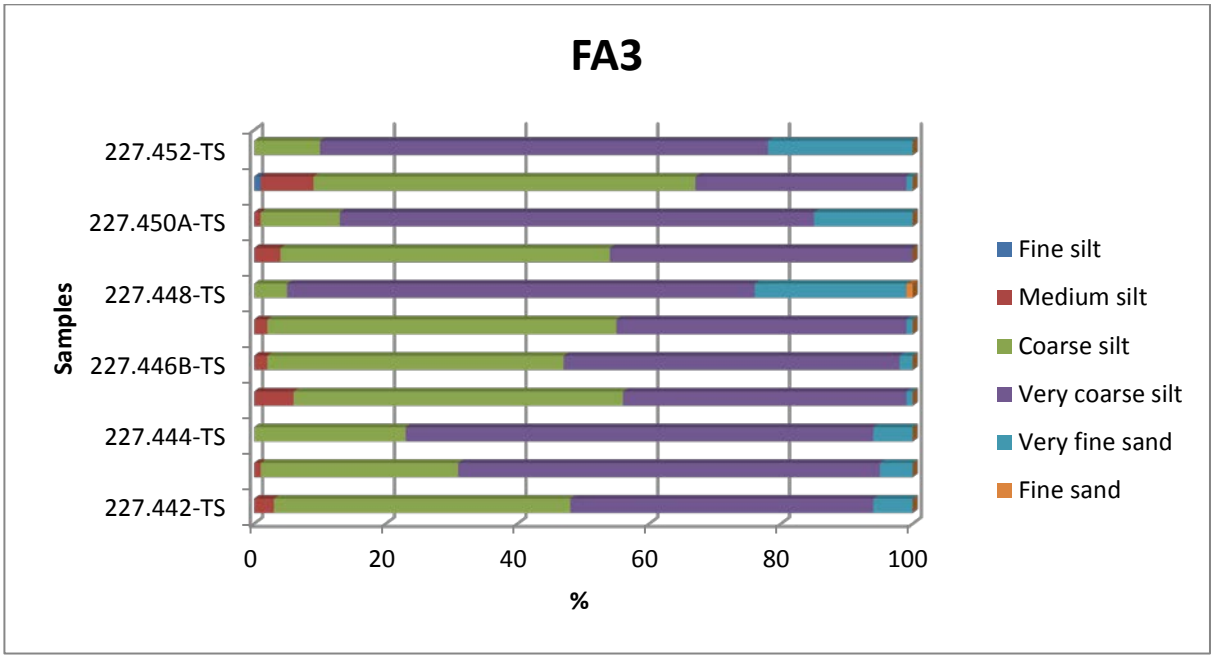

Figure 5.27*: Grain size distribution of the measured thin sections belonging to facies association FA3.*

FA4

Grain size measurement was done in seven thin sections belonging to facies association FA4. As seen in Figure 5.28, the amount of very fine sand has increased compared to FA3 and very coarse silt dominate.

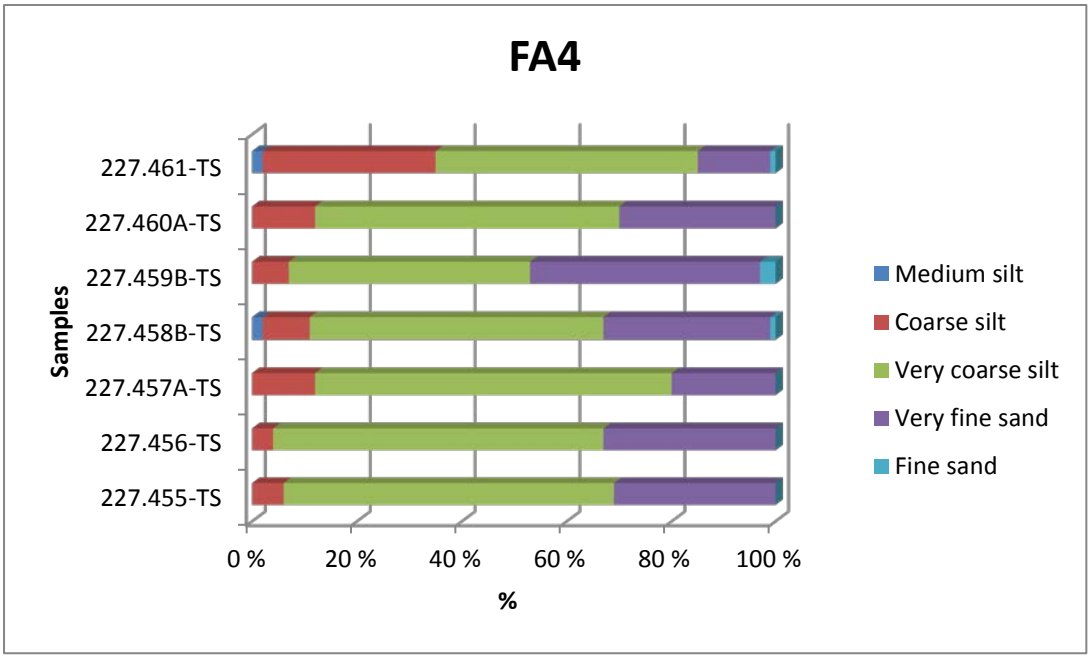

Figure 5.28: *Stacked bar diagram representing the grain size distribution of the measured thin sections belonging to facies association FA4.*

FA5

Three samples belonging to facies association FA5 were measured. The stacked bar diagram is presented in Figure 5.29. The fraction of very fine sand dominates in this facies association while very coarse silt dominates the silt fraction.

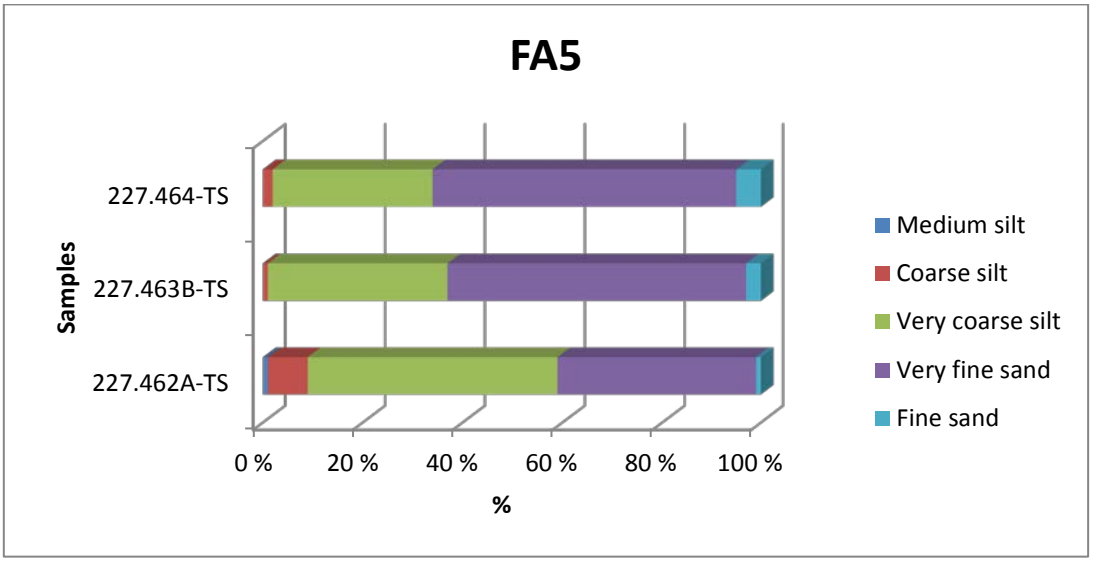

Figure 5.29: *Grain size distribution of the measured thin sections belonging to facies association FA3.*

5.3.1 Summarized grain size data

Figure 5.30 summarizes the grain size distribution of all the measured thin sections. The topmost bar represent the highest position in the succession (approximately 23.20 meters above point zero). There is a observed trend of increasing particle sizes upwards in the succession. This will be discussed further in Chapter 6.

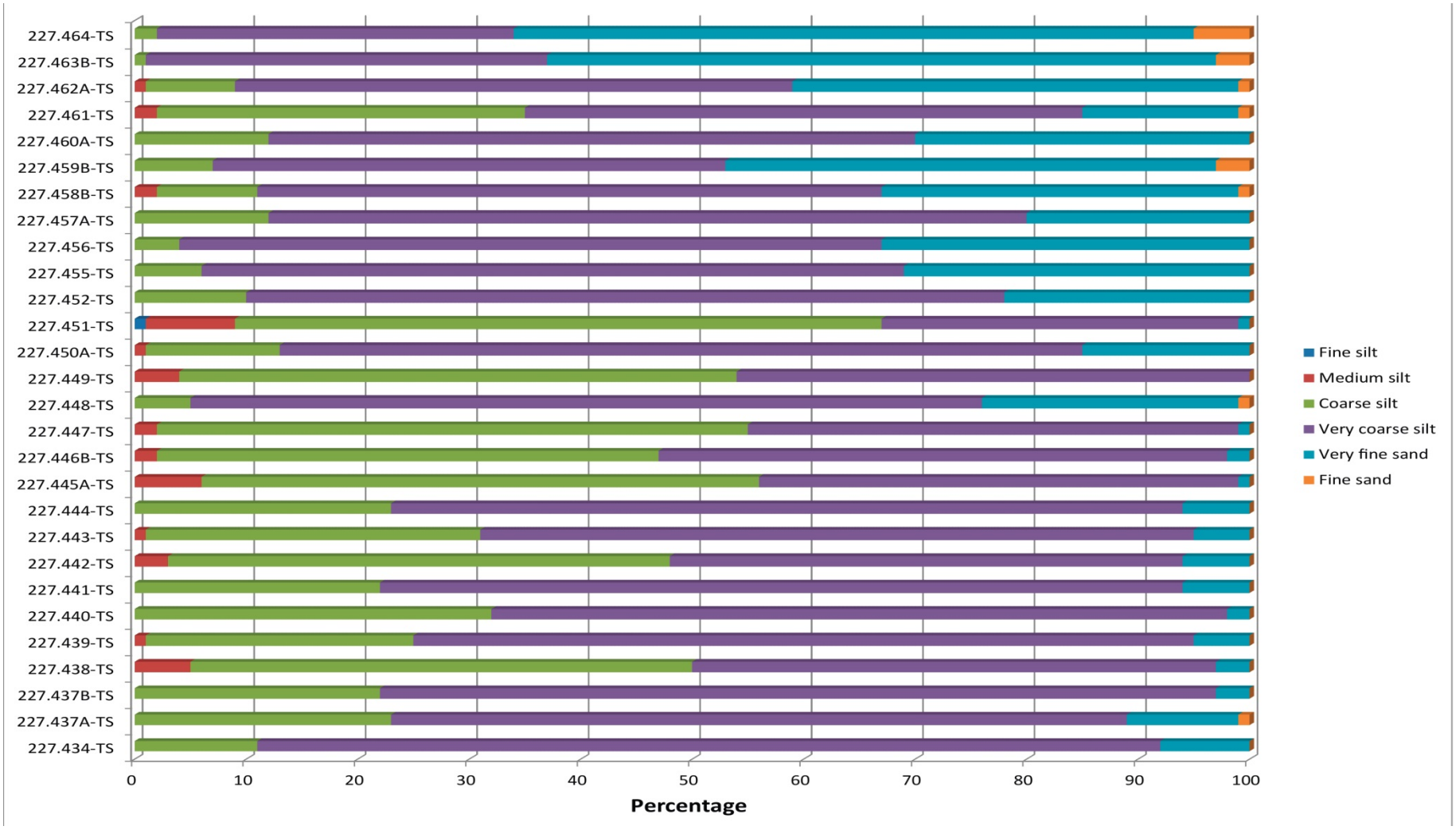

Figure 5.30: *Distribution of grain sizes in all measured thin sections.*

The average and the standard deviation are calculated for each measured thin section. This is done to see if there is coherence between the average grain size and sorting. A trendline is shown as a straight line.

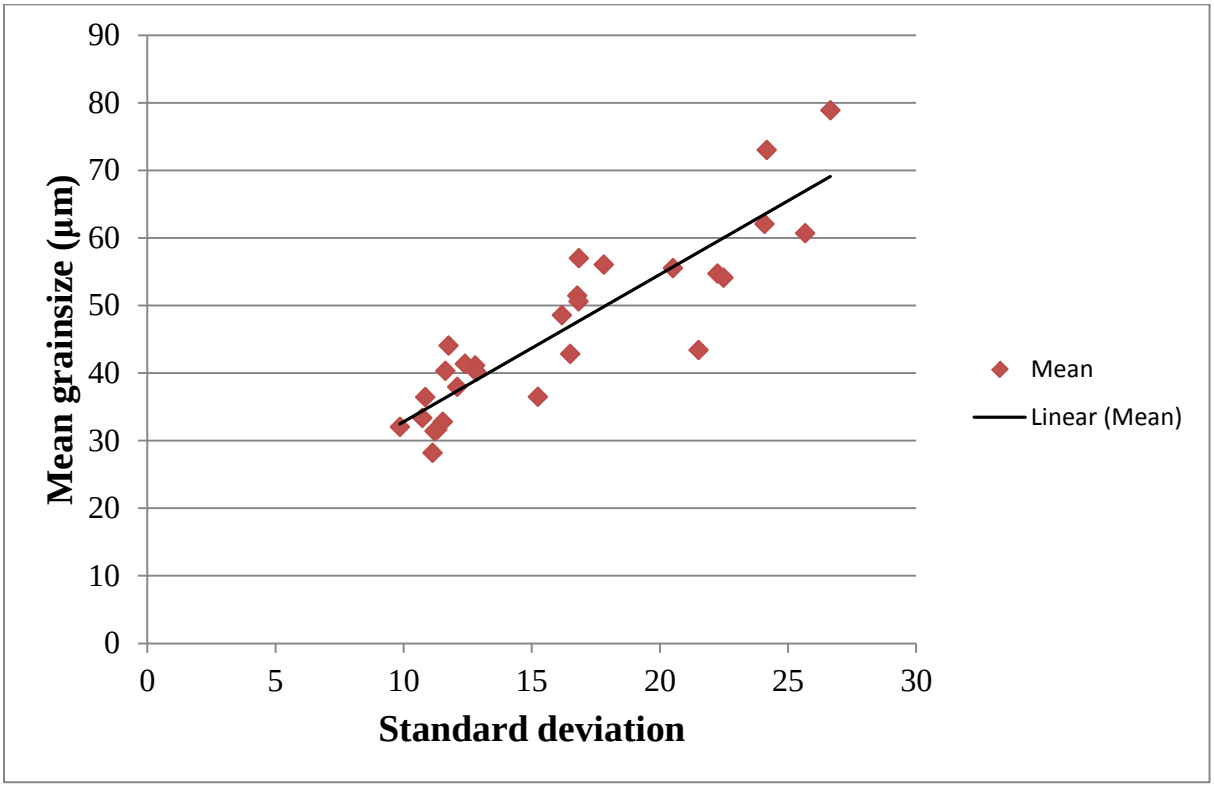

Figure 5.31: *Average grainsize plotted against standard deviation for each measured sample.*

5.4 Fossil content

This chapter summarizes the most common fossil observations in the studied successions. The main focus is to try to find out the depositional environment in which these fossil assemblages represent and their distribution throughout the succession.

Stanistreet (1989) described the trace fossil associations of the Upper Ordovician in the Oslo-Asker area. Figure 5.32 represent the trace fossil assemblages described by (Stanistreet, 1989).

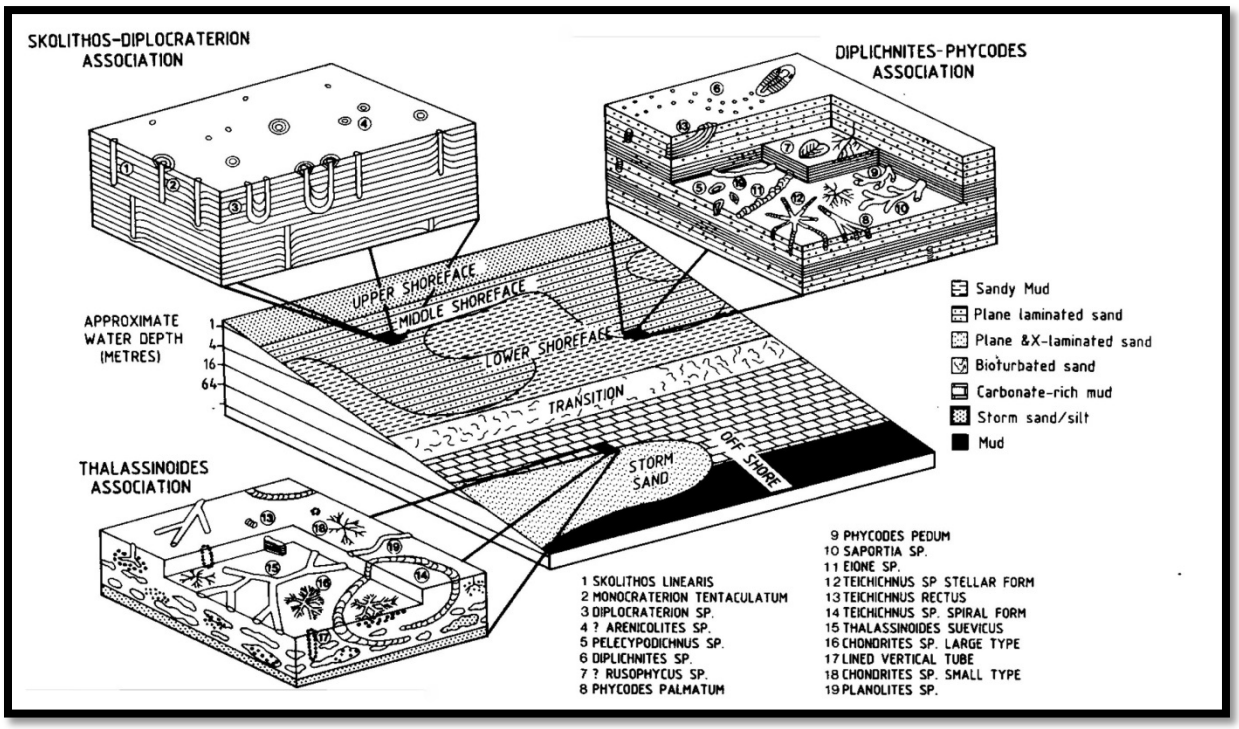

Figure 5.32: *Trace fossil associations in relation to upper Ordovician palaeoenvironments. From Stanistreet (1989).*

FA1

The observed fossil content in this facies association is sparse and only one brachiopod is observed during the fieldwork. Only a few unidentified shell fragments are recognized in the tree thin sections that belong to FA1.

FA2

As described earlier, the grey shales (Facies Ia) that dominate facies association FA2 has crude fissility. Brenchley and Newall (1975) interpreted this as a result of bioturbation by *Chondrites*. *Chondrites* is a branched burrow system that is constructed by deposit-feeding

animals that lived within the sediment or on the sediment surface. These “root like” trace fossils are found in terrigenous and carbonate sediments in Paleozoic, Mesozoic and Cenozoic rocks. Bromley and Ekdale (1984) suggested that the occurrence of these trace fossils in a deposit reflect anoxic bottom conditions. The larger trace fossils described below are also observed in the top section of this facies association.

Even though the fauna are sparse in this facies association, some cross sections of body fossils of brachiopods are observed in thin sections and acetate peels. Figure 5.33 illustrates what is most likely a cross section of a brachiopod with a thin shell.

Figure 5.33: *The middle section of the picture illustrates a cross section of what is most likely a brachiopod. Sample 227.467-AP; 1, 3 meters above point zero.*

FA3

Facies association FA3 is more diverse in fossil content than the underlying FA2. The fossils in this facies association most often occurs individually but there is observed one structureless calcareous siltstone bed on Rambergøya Profile 1, 8.5 meters above point zero, with shell fragments contained in a small life assemblage cluster.

Large trace fossils in the form of spreite are observed on all the studied profiles (see Figure 5.34). Seilacher and Meischner (1965) referred these trace fossils as *Tricophycus* and they are also observed and studied by other authors such as Brenchley and Cocks (1982) and Stanistreet (1989). Most of their occurrence is horizontal with the bedding, but some of them also occur vertically down into underlying shale.

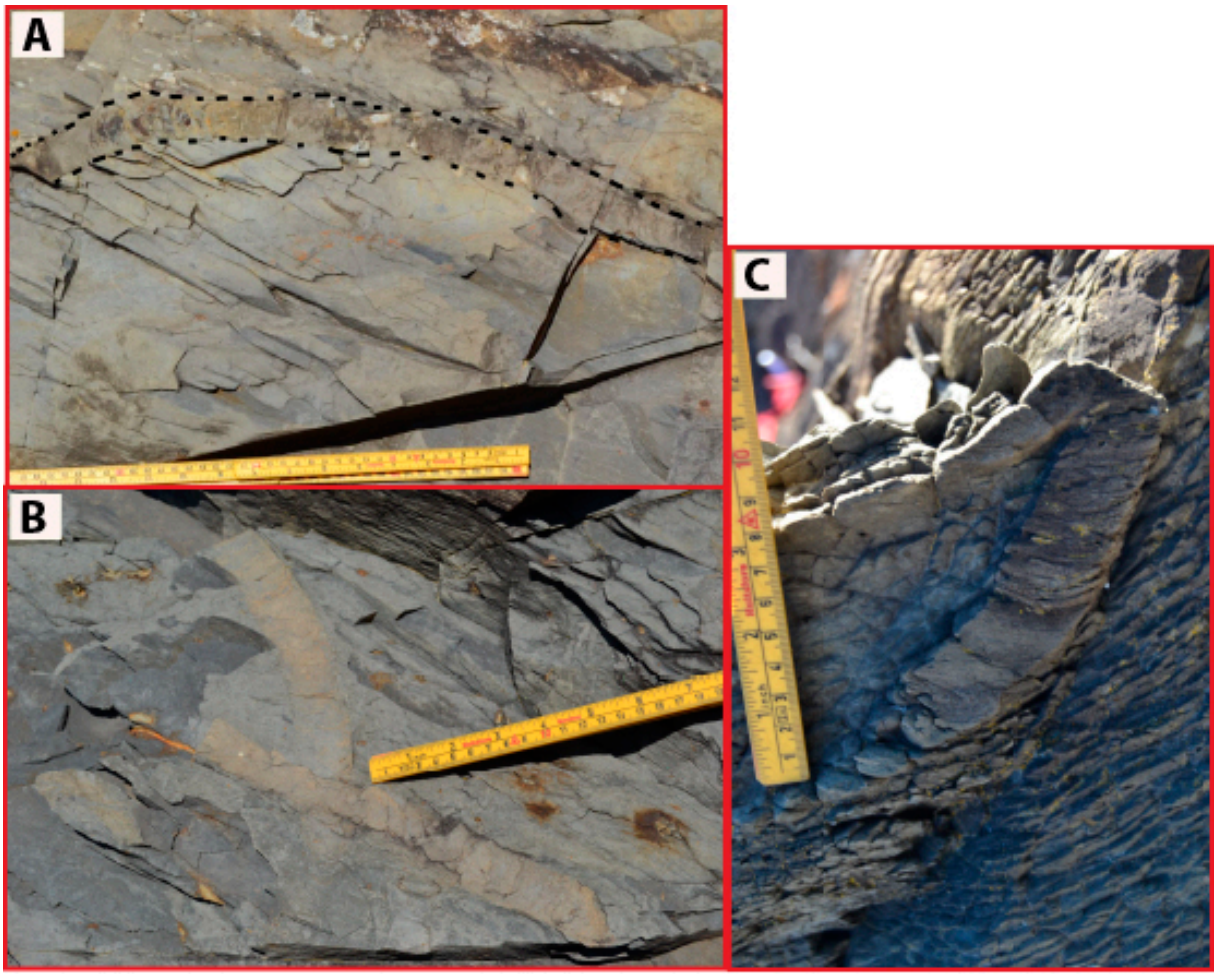

Figure 5.34: *A; Horizontal Trycophycus trace fossil from Rambergøya Profile 1, approximately 4 meters above point zero in facies association FA2. B; two intersected Trycophycus trace fossils from Rambergøya Profile 1, 1.26 meters above point zero. C: vertical Trycophycus trace fossil from Rambergøya Profile 1, 1.20 meters above point zero.*

According to Brenchley and Cocks (1982) the Trilobite association *Tretaspis* occur in sparse but moderately diverse assemblages throughout the Husbergøya Formation. One trilobite specimen was observed in this facies association (Figure 5.35).

Figure 5.35: *Trilobite, 2.3 meters above point zero on Rambergøya Profile 1.*

According to Brenchley and Cocks (1982), several species of gastropods is seen the *Tretaspis* association and the author located one specimen in the upper part of this facies association, close to facies association FA3 on Langøyene Profile 1.

Figure 5.36: *Gastropod located in the upper part (approximately 18 meters above point zero) of facies association FA3 on Langøyene Profile 1.*

FA4

Facies association FA4 show the highest abundance of observed fossils in the studied successions. Due to highly weathered outcrop in this facies association in Profile 1 on Hovedøya, only some fossils were visible on that locality. Both Profile 1 on Rambergøya and Profile 1 on Langøyene show abundance in spherical sometimes elongated fossils with diameters of 1.5 to 4 centimeters. There are most commonly found in the "Brown weathered" siltstone/very fine sandstone unit of Facies Ie, but also in the some are located in the interbedded structureless siltstone and limestone beds both above and below. According to Bockelie (1981), these spherical fossils represents the two species of cystoids, *Tetreucystis* and *Eucystis*. Thus, the "brown weathered" siltstone/very fine sandstone unit was referred to as the cystoid bed by Brenchley and Cocks (1982). There is also observed several brachiopods, tube worms (*Cornulites*) and some corals in this succession.

FA5

The logged successions of facies association FA5 does not show as high abundance of fossil content as the underlying facies association FA4. There is observed some brachiopods, crinoids and *Cornulites*, but these occur individually.

6 Discussion

The discussion is based on field observations, sedimentary logs (APPENDIX A), observations from sample slab surface scans (APPENDIX C), visual interpretation of thin sections, acetate peels, grain size measurements in addition to interpretations of facies and facies associations (Chapter 5).

6.1 Log correlation

As seen in Figure 6.1, the logged successions on Hovedøya Profile 1, Rambergøya Profile 1 and Langøyene Profile 1 correlate well. Stanistreet (1983) inferred syn-sedimentary Upper Ordovician faults in the Oslo Area from lateral facies and thickness variations and thought that the faults were reactivated old faults in the local Precambrian basement. However, the Lower Palaeozoic successions in the Oslo Area are a part of a Caledonian decollement thrust unit (Bruton et al., 2010). Oftedahl (1943) proposed a shortening of 50% due to the deformation, and this was supported by Morley (1986). As there are approximately one and a half kilometers between Hovedøya and Rambergøya, and one and a half kilometer between Rambergøya and Langøyene, this implies an initial distance range of approximately 6 kilometers between these localities in the Upper Ordovician times. This might explain some of the small differences in facies distribution. The logs are also correlated in response to the formations described and proposed by Brenchley and Newall (1975) represented by bars on the left side of each succession in Figure 6.1. A factor of uncertainty is present as parts of the outcrops on Hovedøya Profile 1 were not exposed. The “brown bioturbated” siltstone/very fine sandstone show more variations in thickness than expected. In turn, these successions were logged in the scale of 1:10 and only the parts of facies association FA4 where no distinct bedding was observed, was logged as the “brown weathered” unit. There is a possibility that the “brown weathered” sandstone that was described in Brenchley and Newall (1975), and selected as the top of the Husbergøya Formation, comprised more of the facies association FA4 than what is shown in Figure 6.1.

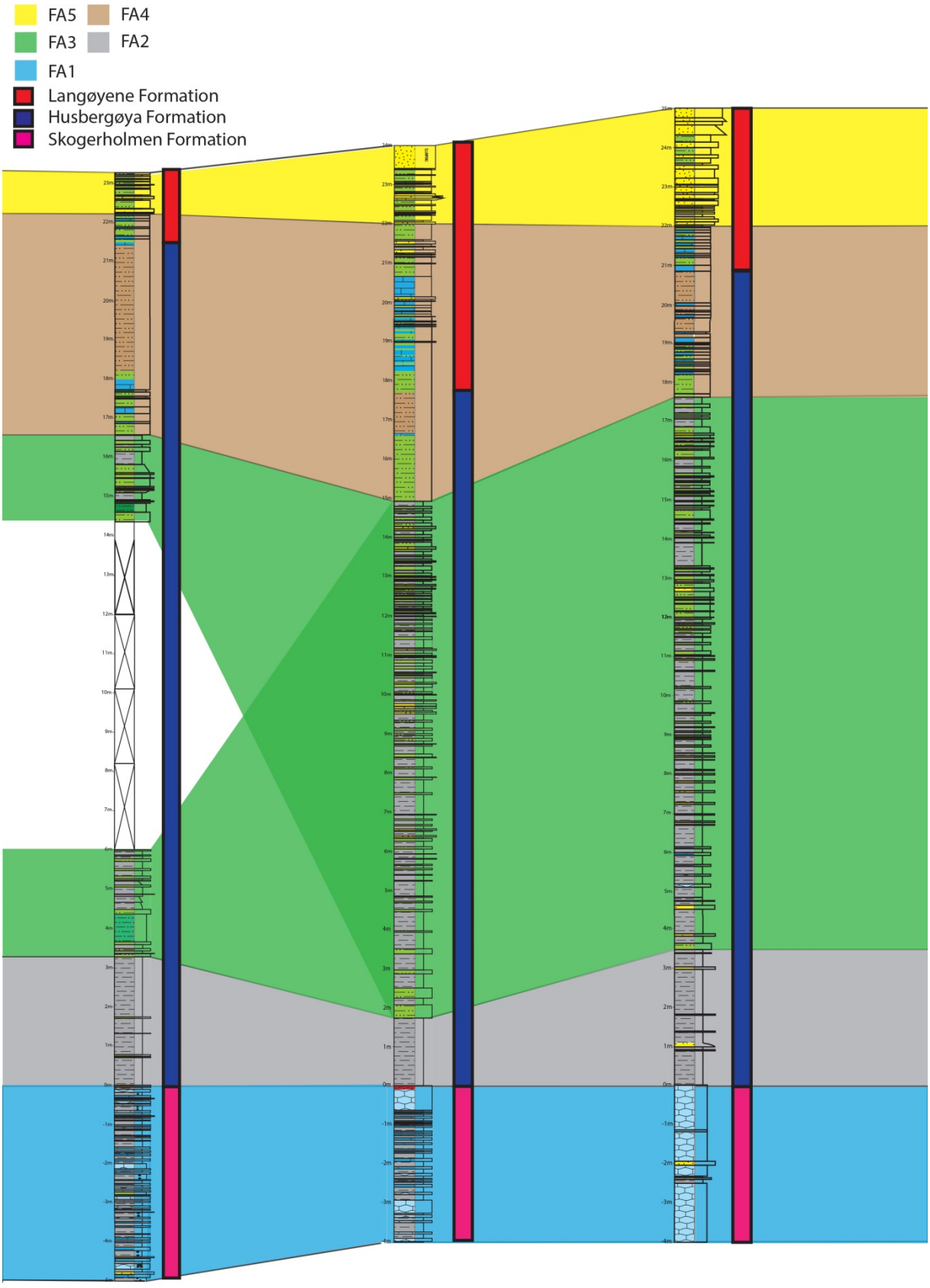

Figure 6.1: *Correlation of (from left to right) Hovedøya Profile 1, Rambergøya Profile 1 and Langøyene Profile 1. Based on the described facies associations in Chapter 5.2 and the distribution of the Upper Ordovician formations described in Chapter 3.8.*

6.2 Continuous limestone and nodular limestone

Nodular limestone are abundant throughout most of the Lower Palaeozoic in this area, but only a small part of the Upper Ordovician limestone succession was studied during this master thesis project. Thus, the author sees it as being important to address attention to the general observations and interpretations of nodular limestones in the Oslo Region done by various authors to see if these coincide with the observations done in this study.

Thin sections of carbonate samples belonging to this facies association show a high grade of bioturbation and only faint remnants of sedimentary lamination are observed. As described by Bjørlykke (1973), the limestone nodules possess distinct bedding when not altered by bioturbation. It is likely that some of the limestone beds (if not bioturbated) in the studied succession have more prominent lamination preserved than recorded in the studied thin sections. The bioturbation consists of *Chondrites* type of burrows and occur both in the limestone nodules, and also as white spots in the grey shaly matrix. Bjørlykke (1973) interpreted the white spots as a result of light lime mud transported into the darker grey matrix by *Chondrites* forming organisms, and he thus suggested that the bioturbation was subsequent to the formation of the limestone nodules. As seen in Figure 5.16 B, the storm deposited siltstone/very fine sandstone (Facies IIa) drapes over an erosional contact to the underlying nodular limestone. Bjørlykke (1973) also observed that some of the nodules had been truncated by erosion beneath overlying calcarenite beds and that the sharp erosional contact indicated that the calcarenite beds had been deposited subsequently to the formation of the nodules. Based on these observations and interpretation of succession of sedimentary events, combined with the fact that the sedimentary and biologically formed structures seen in limestone nodules showed similarities with continuous calcarenite limestone beds, Bjørlykke (1973) suggested that the Upper Ordovician limestone nodules in the Oslo Area were remains of dissolved originally continuous limestone layers, and that lithification occurred after the formation of the nodules.

If the limestone nodules are remains of dissolved continuous limestone layers, one must consider how these carbonates could have been dissolved in the general shallow water environment. As described by Bjørlykke (1973), the solubility of carbonate in ocean water is related to a complex set of parameters such as temperature, pH and alkalinity and not directly related to depth, making dissolution in shallow water possible. The uptake of CO_2 causes pH in the water to decrease and the water gets undersaturated in respect to carbonate minerals

(Morse et al., 2007). A study done by Mucci (1983) also showed that cold water promotes undersaturation in respect to $CaCO_3$. This would imply that if the limestone nodules are remains of dissolved continous limestone beds, the dissolution would be partly restricted to or occur more rapidly in colder periods. As a result of the slow sedimentation rate (2-7 mm/1000 years), the continuous limestone layers would be exposed to the seawater over long periods (Bjørlykke, 1973). He also argued that the colder periods would have induced undersaturation of water in respect to calcium carbonate and thus the continuous limestone beds would start to dissolve; the thermodynamically most stable shape of remaining parts of the limestone bed would be spheres.

The observed limestone beds in the Upper Ordovician in the Oslo Area show all intermediate stages from continuous beds to isolated limestone nodules. Bjørlykke (1973) interpreted this as being a result of selective dissolution of the finer carbonate particles, resulting in a lesser complete dissolution of the continuous limestone beds than of the limestone beds in the Cambrian Alum shale. He also believed that bioturbation by *Chondrites* contributed to the dissolution because the bioturbation would continuously supply the seawater with limestone mud which in turn would dissolve in the water undersaturated with respect to $CaCO_3$.

Henningsmoen (1974) argued that the limestone nodules of the Lower Palaeozoic were formed by concretionary growth, most often around a fossiliferous seam, within the host sediment, and believed that cementation by precipitation of calcium carbonate took place close below the water-sediment interface at an early diagenetic stage. This interpretation was based on the various structures in the dark, bituminous limestones interbedded in the Alum shale Formation, such as bedding planes that were laterally converging, concentric bands around the center, septarian structures, bedding planes that converge laterally etc. He observed uncorroded fossils with well-preserved surface details in the limestone nodules and suggested that dissolution of the carbonate before or during cementation of the nodules could hardly have happened, and that the main concretionary growth would have been taking place prior to any carbonate dissolution. As for the continuous limestone beds, he argued that these were the result of fusion of separate limestone nodules, but in cases where there were no traces of the initial nodules in the continuous bed, there were no evidence of concretionary growth. His interpretation of concretionary growth was later supported by *inter alia* Sramek (1974), Harwood (1985) and Möller and Kvingan (1988).

Contrary to the interpretation by Bjørlykke (1973) of Upper Ordovician limestone nodules, many of the same in which are studied in the present project, as being formed by dissolution of continuous limestone layers and bioturbation, Henningsmoen (1974) found similarities between these nodules and the dark, bituminous limestone nodules in the Cambrian Alum shale. He also suggested the formation of nodules were favourable in bioturbated beds, expecially of *Chondrites* types of burrows because the burrow-innfillings were more favourable to precipitation of calcium carbonate than the matrix surrounding the nodules. Henningsmoen (1974) did agree that some limestone nodules could be solution relics of early consolidated limestone layers, but not from unconsolidated limestone layers. Bjørlykke (1974b) emphasized that some of the Cambrian nodules contained 90 to 95% calcium carbonate, with host sediment of relatively pure carbonate, and he found it difficult to see how these carbonate deposits itself could form discrete clumps on the sea floor. In his reply to Henningsmoen (1974), Bjørlykke (1974b) agreed that dissolution could not have taken place in early cemented limestone, but he suggested that the cementation was most likely irregular, producing discontinuous beds or patchy clumps on the sea bottom and that dissolution would have been taking place in non-cemented parts of these discontinuous beds. This would imply that the cemented parts of the limestone layer would not be deformed during compression, while the unconsolidated parts would be deformed and dissolution would have taken place (Bjørlykke, 1974b).

As described above, the samples collected from this facies association showed no structures indicating concretionary growth, but this could be due to the bioturbated nature of the samples. The interpretation by Bjørlykke (1973) are favored by the observations and interpretations in this master thesis. The dissolution of calcium carbonate is interpreted to probably be a result of variations in the carbonate dioxide content in the water and hence variation in pH. This could be controlled by sea level fluctuations probably due to Milankovic cyclicity. The author also wants to emphasize that only 4-5 meter of the succession representing facies association FA1 on the five different localities was studied, and that a more thorough analysis is needed to fully understand all aspects of the origin of the limestone nodules.

6.3 Storm-deposition

Storms is an important mechanism for transportation of sediment into shallow open shelf environments (Kreisa, 1981). The recognition and significance of major storms have been pointed out and studied in the earlier days by many authors such as Hobday and Reading (1972), Goldring and Bridges (1973), Kelling and Mullin (1975) and Brenchley et al. (1979). This subject has also been studied in a great extent in more modern times with examples such as Duke et al. (1991), Lee and Kim (1992), Molina et al. (1997), Bádenas and Aurell (2001), Purkis et al. (2014) and many others. Many of the siltstone/sandstone layers observed and logged in this master thesis are characterized as storm-deposited tempestites. This is due to their internal structures; often starting with a sharp erosional boundary to the underlying sedimentary rock, parallel lamination in the bottom, small-scale hummocky cross stratification/lamination in the middle and climbing ripples/cross bedding /lamination in the top section (see Figure 5.9 and APPENDIX C). Other characteristics observed in these storm-deposited beds are mud and sand interlamination with bioturbated tops and some vertical escape-burrows (Figure 5.13). Tempestite formation is described in Chapter 5.1.1; IIa: Internally laminated siltstone/very fine sandstone. In modern shelf sands, small-scale storm-generated structures are often destroyed within a few days by weak tidal currents (Butman et al., 1979).

As described in Chapter 3.2.4 and 3.2.7, tidal influence on sediments in a shallow epicontinental sea may have been very restricted, and thus the preservation potential of the thin storm-deposited beds may thus have been rather high. Sediment transport by turbidity current from the nearshore zone down to deeper waters is another single-event process. During fieldwork there is not always easy to detect the differences between tempestites and turbidites, and many ancient storm deposits resemble turbidites (Myrow and Southard, 1996). Although there are similarities between tempestites and turbidites as regards to grading and internal structures, turbidity currents need a sufficient slope gradient to be initiated and to propagate along the sea bed by gravity. Even if initiation takes place, the turbidity current must gain mass through erosion. With a slope gradient >1.5 **°,** erosion will not take place and the current will die out fast (Pratson et al., 2000). It is earlier mentioned that the shelf slope gradient of the Baltoscandian Epicontinental Sea during Late Ordovician times was significantly low and the average slope were probably less than 20 centimeters per kilometer, which corresponds to an angle of ~0.01° (Shaw, 1964, Heckel, 1972). Thus, suspended sediments would most likely not be able to achieve the critical velocity in which

autosuspension occur. Hayes (1967) suggested that turbidity currents are responsible for the transportation and deposition of sand in the offshore shelf regions during storm events such as hurricanes. Reineck and Singh (1972) stated that there has been observed extensive amounts of sand in the form of suspension clouds in the turbulent water during storms in the southern North Sea, thus turbidity currents are not the only factor controlling this transport. Even in the southern North Sea, with a much higher shelf slope gradient (0.75 meters per kilometer), the slope is generally not enough to produce turbidity currents (Reineck and Singh, 1972).

As described and referred in Chapter 2.2, the average accumulation rates in the Ordovician, recorded from Sweden and East Baltic, were in the order of 1-9 mm/1000 years. Storm-deposited siltstone/very fine sandstones are abundant in the studied successions with an upwards increase in occurrence. Even though storm-deposited sandstone beds are abundant throughout the succession, the low sediment accumulation rate clearly indicates that these events were very rare. The storm-deposited beds were probably deposited during major storm or hurricanes. Brenchley et al. (1979) proposed that the deposition of storm beds in the Husbergøya Formation would in average occur approximately every 10 000 to 15 000 years, and that this is incompatible with storm events due to their annual frequency pattern. Thus, they proposed that the frequency of hurricanes matches better to the frequency in which these storm-deposited beds occur.

As there are clear differences between both thickness and occurrence of the storm-deposited sandstone beds in the different localities studied in this project, one must take into account that these successions are folded and the deposition of the storm-deposited beds were probably not uniform over larger distances. Most of the storm-deposited beds are laterally persistent within the outcrop extent of one single locality, but it is impossible to correlate one specific bed from one locality to another. This is probably due to the lack of any distinct character of individual beds. There are also observed many storm-deposited beds that “pinch and swell” laterally in both facies association FA1 and FA2, and this probably indicates that they terminated quite quickly in the distal parts of the open shelf. This is also suggested by Brenchley et al. (1979). Variations in the topography of the sea-bottom and complex turbulent water flows during a major storm may also be a controlling factor.

As described in Chapter 5.2.3, the thickness of storm-deposited beds decreases with increasing depth (Swift and Thorne, 1991). Figure 6.2 illustrates the thickness of the storm-deposited siltstone/very fine sandstone (Facies IIa) beds throughout the logged succession on

Langøyene Profile 1. There should be noted that only the beds that show characteristic sedimentary structures indicating storm-deposition are taken into account, and that the thickness of each individual bed varies laterally. Thus, the diagram only represents an approximation of their real thickness and occurrence of the storm-deposited beds in this succession. The bar diagram is constructed to illustrate if there is a general trend which could coincide with any possible sea level fluctuation and eustacy. The thickness from 1 meter below point zero to approximately 17 meters above point zero show little variation in thicknesses, but one can observe what looks like five distinct rhythms. This may represent sea level fluctuations, possibly due to Milankovich cycles. However, a further statistical analysis of this problem has been outside the scope of this master thesis. If the thickness of the storm-deposited beds reflect proximity to a potential sediment source, a general trend is observed with an upwards increase in thickness from approximately 22 meters above point zero. Here, the thickness of the beds increases from approximately 5-7 centimeters to beds that are approximately 10-25 centimeters thick only a few meters upwards in the succession. This clearly indicates that there is an upward shallowing event.

Many of the structureless siltstone beds of Facies Id show patches of light and black color (see Figure 5.5; A). This may indicate that many of these beds represent bioturbated storm-deposited beds. Thus, the influence of storms in controlling the transportation and deposition of sediments on the shelf seems to have been very high.

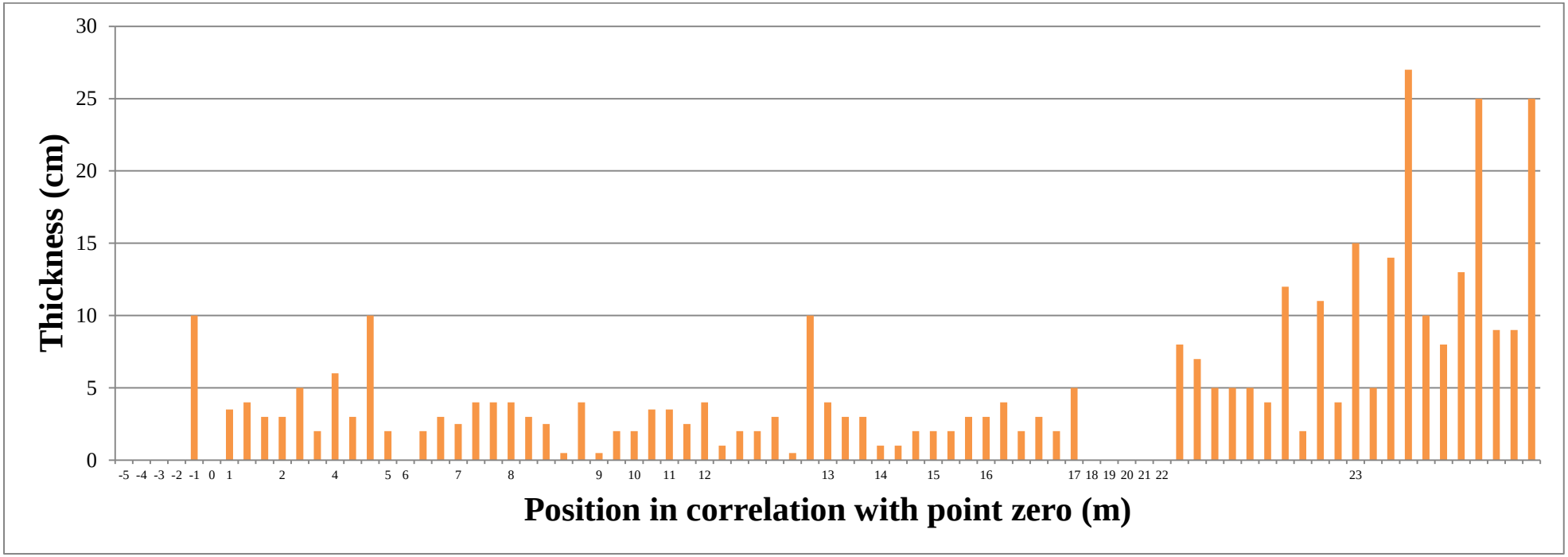

Figure 6.2: *Illustration of the thickness of characteristic storm-deposited siltstone/very fine sandstone beds throughout the succession on Langøyene Profile 1. The gap between 17 and 22 meters are due to highly weathered outcrops (facies association FA4).*

6.4 Facies associations

6.4.1 FA1 (Upper Katian)

The formation of the carbonate content in this facies association could be due to *in situ* production by organisms. By studying the limestone nodules in the black shale matrix in the Cambrian and Lower Ordovician, Bjørlykke (1973) suggested that these limestone layers in the Cambrian and Lower Ordovician in the Oslo Area may have been formed from skeleton fragments of trilobites that were living in ventilated conditions. He also observed that most of the limestone nodules in grey shale facies in Ordovician and Silurian consist of calcareous mud. This latter is consistent with the observations done in this master thesis. Since the calcareous thin sections show abundant micrite content with no indications of recrystallization and sparse fossil content, the corollary has been proposed that this carbonate most likely has been formed by one or a combination of the three factors described by Blatt et al. (1972) (see Chapter 5.1.1; Facies IIIa and IIIb). A well studied form of micritization is the boring into carbonate shell or grains by endolithic (boring) algae. Earlier studies done by Pia (1937) and Hessland (1949) showed that this process can be traced back to the Ordovician or earlier. The algae produce micrite envelopes by boring and infilling of borings by precipitated micrite. Micrite is also produced by the algae outside grains by cementation of exposed dead endolithic filaments (Bathurst, 1964, Kobluk and Risk, 1977).

There is also a presence of a well sorted silt fraction in all the calcareous thin sections. This implies that this silt fraction may have been transported by wind and deposited at the same time as carbonate production took place. Another possibility is that the micrite was produced *in situ* on the shelf but later transported and deposited together with the silt fraction during storm events.

As described in Chapter 5.2.1, the overall depositional environment must have been quiet and below fairweather wave base, where fine-grained sediments settles from suspension (Collinson et al., 2006). There is an upward decrease in the size of limestone nodules towards the base of the facies association FA2, with a limestone conglomerate with limestone clasts in a darker grey matrix at the very top. As seen in Figure 5.18, the conglomerate is matrix supported polymodal and the limestone clasts are of different size. No preferred orientation of the clasts is observed. This could indicate a slight shallowing towards the base of facies association FA2, where there was sufficient energy for erosion of already consolidated

limestone beds, probably during storms. Without having done any grain size measurements in the matrix of this conglomerate, it seems like it contains a higher grain size than the adjacent fissile shale of Facies Ia. Harms (1975) observed clay clasts in isolated cross-stratified sand beds in the Upper Cretaceous Shannon Sandstone, Wyoming. He interpreted limestone clasts as rip-up clasts formed during a severe storm. In forming this limestone conglomerate, high energy waves during a major storm could have scoured the limestone shelf surface and formed rip-up clasts. As the storm started to wane, this could create a lag deposit where winnowing of the finer particles may have occurred. This facies association is thus interpreted to indicate proximal parts of a shallow marine open shelf or platform, dominated by quiet sedimentation, infrequently interrupted by high-energy storm events. As there are recorded only thin and infrequent storm-deposited beds in this facies association, these sediments were most likely deposited close to the storm wave base.

6.4.2 FA2 (Upper Katian)

There is a marked boundary from the limestone dominated facies association to the calcareous shales of facies association FA2. This sharp change represents the boundary between the Spannslokket Member of the Skogerholmen Formation to the shale dominated Husbergøya Formation. The ratio between fissile shale (Facies Ia and Ib) and siltstone/very fine sandstone beds (Facies IIa) presented in Chapter 5.2.2 clearly indicates a more distal position of this facies association than the underlying facies association FA1, and a flooding event is proposed to have taken place. Nielsen (2004) recorded the transition to a condensed shale dominated succession in the Husbergøya Formation from the interbedded shale and limestone beds/nodules of the upmost part of the Spannslokket Member of the Skogerholmen Formation. He described it as the “Spannslokket drowning event”. This is also reflected in the sparse body fossil content, abundant bioturbation by *Chondrites*, the dominance of mudstone and the almost absence of limestone.

A distinct feature observed in the succession representing this facies association is the dark grey/black fissile shale (Facies Ib). This facies is interbedded with grey fissile shale, but their boundaries are often diffuse. This is suggested to represent variations in available oxygen content at the sea bed or/and slighly beneath the water-sediment interface. The darker grey shale might represent periods of oxygenated bottom waters with extensive algal bloom, and the darker color could be due to high organic content in these beds. To confirm this observation, a measurement of the total organic carbon (TOC) would be valuable.

This facies association is thus interpreted as representing the deeper parts of the shallow marine shelf or platform. A water depth of 100 meters was suggested by Brenchley and Cocks (1982). The thin storm-deposited siltstone/very fine sandstone beds are interpreted as indicate distal tempestites.

6.4.3 FA3 (Upper Katian and Lower Hirnantian)

The boundary between facies association FA2 and FA3 is defined as starting from where the first structureless siltstone of Facies Id is observed (see APPENDIX E). As previously described in Chapter 5.2.3, there are observed five rhythms of upward increasing thickness of storm-deposited siltstone/very fine sandstone beds (Facies IIe) and structureless siltstone (Facies Id) from the sedimentary logs. This rhythmic tendency is also reflected in Figure 6.2. A common feature in the figure is the increase in thickness of the storm-deposited beds up to a higher peak, and subsequently the decrease of bed thickness again. What is interesting here is that there seems to be a correlation between the increasing thicknesses of storm-deposited beds presented in Figure 6.2 and the thickness of structureless siltstone beds observed in the sedimentary log from Langøyene Profile 1. This might also indicate that many of the structureless siltstone beds were deposited as tempestites and later bioturbated.

Both continuous limestone beds (Facies IIIb) and nodular limestone (Facies IIIa) are observed approximately 4 meters above point zero on Langøyene Profile 1 and approximately 15 meters above point zero on Hovedøya Profile 1. Limestone beds and nodular limestone in this facies association are not observed on Rambergøya Profile 1. These are in turn recorded on many localities by Brenchley and Newall (1975). There is a possibility that limestone beds and nodules are present, but not logged on Rambergøya Profile 1 due to the grade of weathering of the outcrops. The occurrence of limestone beds/nodules, increased occurrence of storm-deposited beds and increased occurrence and thickness of bioturbated siltstone beds indicate that a slight upward shallowing occurred during this facies association. This is also reflected in trace fossils described in Chapter 5.4 and the increase in bioturbated beds. Thus, this facies association is interpreted as being deposited in intermediate parts of the platform, below fairweather wave base and above the storm wave base.

As described and presented in Chapter 6.3, distinct rhythms of the thickness of storm deposited siltstone/very fine sandstone are observed in Figure 6.2. Four rhythms are observed in this facies association. The interpretation of this as being a result of sea-level fluctuations

coincides well with the occurrence of limestone beds and nodular limestone in this facies association. Figure 6.3 illustrates an approximation of the palaeogeography in the Oslo Area during facies association FA2, FA3, and the lower part of FA4. It should be noted that the calcareous mud with palaeoporella are only representative in the Langåra Formation (see Chapter 3.8.4). Variations in the sea level would most likely have had a severe impact on the facies distribution in consideration with the low slope angle.

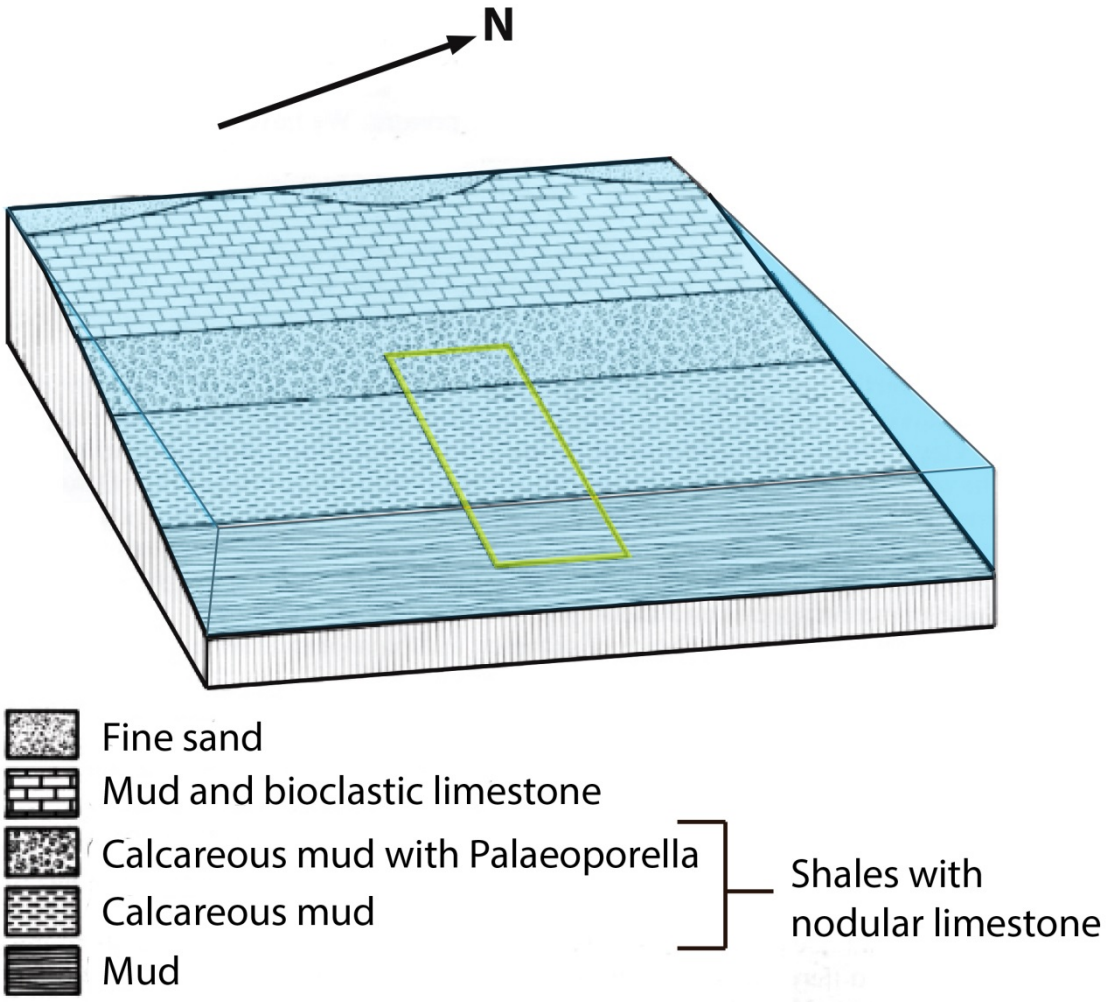

Figure 6.3: Reconstruction of the palaeogeography of the Husbergøya Formation in the Oslo Area. The yellow square is not representative of the successions studied in this master thesis, but marks the area studied in Brenchley and Newall (1975). Modified from Brenchley and Newall (1975).

6.4.4 FA4 (Lower Hirnantian)

The transition from facies association FA3 to FA4 is marked with the sudden absence of shale, extensive bioturbation and the increase in fossil content. The alternating limestone beds, nodular limestone and bioturbated silt show similarities with facies association FA1 and are

interpreted as deposition in proximal parts of the shallow marine open shelf or platform in a period of extensively low rate of sediment accumulation. The dominance of a siliciclastic fraction of very coarse silt to very fine sand in the structureless siltstone beds (Facies Id) could be explained by a sand source that may have moved closer to this area. If this was only a result of a closer proximity to the the shoreline, one might expect to find a coarser particle fraction in facies Ia in facies association FA1. Figure 6.4 illustrates the palinspastic interpretation of the lithofacies distribution during deposition of Husbergøya Formation and the lower part of Langøyene Formation done by Brenchley et al. (1979). They inferred the presence of a sand shoal that formed between the flooded craton and the shelf down to the deeper waters of the Iapetus Ocean at the start of the deposition of the Langøyene Formation. The author considers the present data as being insufficient to show the character and location of such a sand source. However, even though a development of a sand shoal seems viable, a eustatic fall in sea-level could probably have resulted in a forced regression where the shoreline prograded basinwards. This is discussed further in Chapter 6.6.

There is a gradual transition, from observed bedding in the successions below and above the "brown weathered" calcareous siltstone/very fine sandstone unit, to the middle of the facies association where no bedding is observed. The sample slab surface scans (see APPENDIX C) collected from this facies association on Langøyene Profile 1 show an increase in grade of bioturbation from the lower part with alternating limestone and structureless siltstone beds (grade 5) to the "brown weathered" unit (grade 6). The succession overlying the "brown weathered" unit has a bioturbation grade of 5. This most likely strengthens the interpretation by Brenchley and Newall (1975), that a pause or a low rate in sedimentation may have occurred during deposition of facies association FA4 in this profile. This is also reflected in the abundance of fossil content recorded in this facies association.

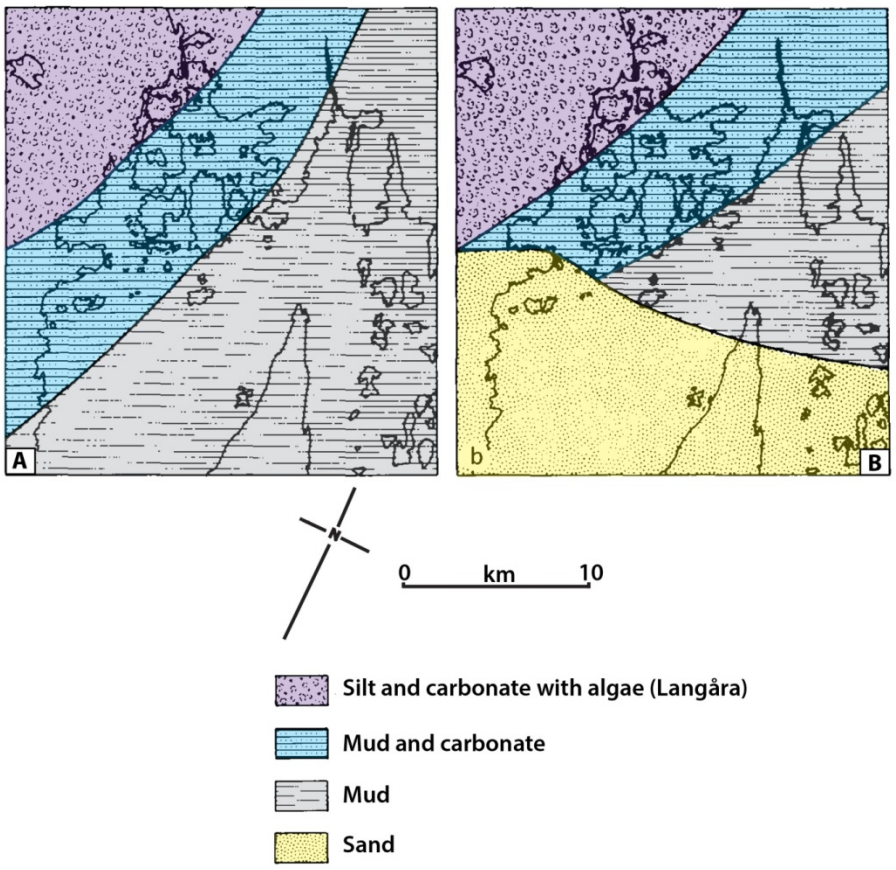

Figure 6.4: Palinspatic map of the lithofacies distribution within Husbergøya Formation and the Lower part of Langøyene Formation with the interpretation by Brenchley et al. (1979) that a possible sand shoal may have developed. A: Lithofacies distribution during the deposition of the Husbergøya Formation. B: Lithofacies distribution during the deposition of the lower part of Langøyene Formation. Modified from Brenchley et al. (1979).

6.4.5 FA5 (Lower to Middle Hirnantian)

As described in Chapter 5.2.5, the thickness of these sandstone beds in this facies association increases markedly within just a few meters. These are often graded, are medium grained and no sand/mud interlamination is observed. This is interpreted as reflecting higher current velocities and a proximal position to the shoreline or possible sand shoal (sand barrier). Stanistreet (1989) interpreted the succession from the "brown weathered" sandstone unit up to the conglomerates in the upper part of the Langøyene Formation as deposition from the lower to upper shoreface. The increased energy is reflected in the sharp erosional boundaries of the storm-deposited sandstone beds. The preservation of fine lamination in black shale (Facies Ic) may indicate that the frequency of sand influx was too high for settling of bottom-living fauna and thus prevented bioturbation. A shift in the slope direction from the gently inherited southeastward facing slope of the stable craton to a northwards facing slope induced by the

sand shoal was suggested by Brenchley et al. (1979). This could explain the occurrence of the many slumped sandstone layers observed in this facies association. Liquefaction and instability of the sediment could be caused by seismic activity due to the ongoing orogenesis in the Caledonides in the west. If this northward facing slope had a higher gradient than described earlier, the liquefied sediments would be affected by the increased force of gravity. Another explanation of the abundant slumped layers could be the development of a foreland bulge as a result of the advancing orogen, which may have increased the slope gradient. The rapid increase in amount of siliciclastic detritus, increase in sandstone bed thickness and a measured dominance of sand sized grains (Figure 5.29) clearly indicate that this is a regressive sequence.

6.5 Fossil content

The trace fossils described in this study (Chapter 5.4) correspond to the Thalassinoides association described by Stanistreet (1989) which represents the open part of the shallow platform. Many of the fossils observed in the mudstones and during facies association FA4 are well preserved, reflecting a tranquil environment. Reworking and transportation during severe storms can though be reflected in the many unidentified shell fragments observed in the coarser siltstone/very fine sandstone beds throughout the succession. Other explainations for the disturbance of shells prior to fossilization are suggested by Brenchley and Cocks (1982) to may have been wind-driven bottom currents or bioturbation.

According to (Flügel, 2004), trilobites and brachiopods often tolerate a muddy substrate. This corresponds well to the tranquil environment in which the studied successions reflect. Gastropods are mainly benthic herbivores and detritus feeders, but there is also some who has adapted to pelagic and sedentary life. According to the study of ecological associations in the latest Ordovician by Brenchley and Cocks (1982), the abundance of the trace fossil *Chondrites,* trilobites, and gastropods in the Husbergøya indicates the dominance of deposit-feeders. As described in Chapter 5.4, there is observed some brachiopods and crinoids higher up in the succession. These were, according to Brenchley and Cocks (1982), filter-feeders. Crinoids need a harder surface to grow, and their occurrence higher up in the succession coincides with the observed shallowing upwards trend of this succession.

Even though there is not especially high fossil abundance in the studied succession compared to higher up in the Langøyene Formation, there is observed fossils almost continuously

throughout the logged successions and the diversity is high. The general trend is an upwards increase in the fossil content with a maximum abundance in facies association FA4. The increase in fossil content from facies association FA1 to FA4 is suggested to be a result of the slight upward shallowing with a gradual change from anoxic to more oxic bottow waters. The abundance of fossil observations in facies association FA4 is suggested to be a result of a pause in sedimentation (see Chapter 6.4.4). Vertical burrows are observed in some of the beds belonging to Facies Ia. These are most likely escape-burrows due to a rapid deposition of these storm-deposited beds. The thin sections did not reveal high abundance in fossil content. This is reflected in the lack of observed orientation of the fossils.

6.6 Depositional environment and climate

The main part of the successions studied in this master thesis are interpreted as being deposited on intermediate to proximal parts on the stable platform of the Baltoscandian Epicontinental Sea, at or above storm wave base. Harwood (1985) suggested that deposition of the Upper Ordovician successions took place in a silled basin. This can be reflected in the abundance of limestone, and Harwood (1985) explained this type of basin as being nutrient traps that induced high surface productivity. He also pointed out that a high surface productivity would increase the oxygen consumption, and thus an oxygen minimum layer could have been formed in some periods (Harwood, 1985). As described in Chapter 5.4, the abundance of *Chondrites* types of burrows facies association FA1 and FA2 are suggested to represent anoxic bottom conditions. This may coincide with the development of an oxygen minimum layer.

As described in Chapter 6.4.1, a possible explanation for the observed silt fraction in the studied limestone beds may be that the micrite may have formed *in situ* on the shelf, but later have been transported and deposited together with the silt fraction during storm events. Dronov et al. (2011) observed invasion of limestone facies into the a deeper environment and argued that this could be explained by a mechanism described by Schlager (2005) as “highstand shedding”. This mechanism, according to Schlager (2005), is the transport of carbonates from a shallow-water environment to deeper environments in the time of maximum carbonate production in the shallow-water environment when the vertical accommodation is low and the excess carbonate produced has to be deposited in laterally located accommodation. This could be during a sea level highstand. Facies association FA1 is interpreted as deposition in most distal depositional environment occurring in this study.

There are observed some small (~2 centimeters in diameter) limestone nodules in that facies association, approximately 20 centimeters above point zero on Langøyene Profile 1 in which could have been transported by this mechanism. The author considers the data presented in this study insufficient to prove that the "highstand shedding" mechanism would be viable in this depositional environment, but is suggested as a possible explanation. A more detailed study on this subject would be needed.

The input of the progressively coarser siliciclastic material from point zero and upward in the succession (see Figure 5.30) indicates a slight upward shallowing during Facies association FA1, FA2, FA3 and FA4. Facies association FA5 is marked with rapid influx of coarser siliciclastic detritus in facies association FA5, which most likely represent a eustatic sea-level fall. According to Berner (1991), the CO_2 levels during the Late Ordovician times could have been 14-16 times higher that present day values, and one might expect that this prevented any glacial episode. A short lived drawdown in atmospheric CO_2 have been proposed in various papers, e.g Brenchley et al. (1994), Kulp (1995) and (Marshall et al., 1997), as explaining the Upper Ordovician glaciation of Gondwana. A study done by Crowley and Baum (1995) demonstrated that the Gondwana continent may well have triggered glaciation in the Upper Ordovician. This was based on the unique configuration and the presence of a major relief in some parts of the continent. There has also been suggested by various authors such as Eyles (1993) that the glaciation began in the early Late Ordovician with a maximum in the Hirnantian. This was also supported by (Herrmann et al., 2004). The occurrence of the Late Ordovician glaciation of the Gondwana continent is now well supported and accepted based on the information we now hold on this subject (Ettensohn, 2010). The rapid regression observed in facies association FA5 is believed to have been controlled by this glaciation. There is also reason to believe that overall shallowing of the studied succession could to some degree have been controlled by the glaciation of the Gondwana continent if this glaciation began earlier than Hirnantian times.

An increase in the input of siliciclastic sediments during a regressive sequence is common. According to (Meyers and Milton, 1996), an actual drop in sea-level might in some cases cause forced regression where the shoreline protrudes basinwards. The separation of aggradational and progradational portions of the highstand may be separated by an erosional surface on a condensed bed, and this bed is typically overlain by successions that show marked shallowing upwards trends (Brett, 1998). There is observed sharp erosional surfaces in the lowest part of facies association FA5, and the sudden increase in siliciclastic input are

considered to coincide well the forced regression and progradation of the shoreline that are suggested in Chapter 6.4.5.

8 Conclusion

- The studied Upper Ordovician successions on the islands Hovedøya, Rambergøya and Langøyene in the inner part of the Oslo Fjord was deposited in the Baltoscandian Epicontinental Sea, a tectonically stable platform, both below, at, or above storm wave base in distal to proximal positions relative to coast- and shoreline.

- The succession represents a mixed siliciclastic-carbonate sedimentary system. The siliciclastic detritus was transported in suspension from nearshore areas to the deeper parts of the shelf during major storms, with addition of windborn particles. Internally laminated siltstone/very fine sandstone beds represent tempestites.

- Siliciclastic silt grains in micritic limestone beds may have been transported by wind and deposited contemporaneous with the formation of carbonate mud, or the micrite sediment, mixed with terrigenous silt, was transported from other carbonate producing parts of the shelf/platform by reworking processes during storm events.

- Limestone nodules were formed by dissolution of originally continuous micritic beds or early lithified limestone beds, primarily due to variation in pH of the sea water controlled by variation in dissolved CO_2, as a function of changes in the sea water temperature, driven by climatic changes.

- In the uppermost part of the Skogerholmen Formation a limestone conglomerate with rip-up clasts indicates that there might have been a shallowing, followed by a flooding event represented by the dominance of mud in the lowest part of the Husbergøya Formation.

- Sea level fluctuations are reflected in the rhythmic occurrence and thickness of the storm-deposited beds. These fluctuations may represent Milankovic cycles.

- A marked increase in very fine sand fraction in the top section of the logged successions indicates a rapid fall in sea-level. This sea level fall was most likely glacioeustatic, controlled by the Late Ordovician glaciation in Gondwana. The increase in sand fraction is thought to be due to a forced regression and basinward

progradation of the shoreline. The increase in very fine sand fraction may also be explained with the development of a sand shoal/barrier.

References

FINN Kart 2014. *FINN kart - en ledende norsk karttjeneste Available at http://kart.finn.no/*

[Online]. [Accessed 08.06 2014].

BÁDENAS, B. & AURELL, M. 2001. Proximal–distal facies relationships and sedimentary processes in a storm dominated carbonate ramp (Kimmeridgian, northwest of the Iberian Ranges, Spain). *Sedimentary Geology,* 139**,** 319-340.

BATHURST, R. 1964. The replacement of aragonite by calcite in the molluscan shell wall. *Approaches to paleoecology***,** 357-376.

BERNER, R. A. 1991. A model for atmospheric CO 2 over Phanerozoic time. *American Journal of Science,* 291**,** 339-376.

BJØRLYKKE, K. 1973. Origin of limestone nodules in the lower Palaeozoic of the Oslo region. *Norsk geologisk tidsskrift. Supplement,* 53**,** 419-431.

BJØRLYKKE, K. 1974a. Geochemical and mineralogical influence of Ordovician Island Arcs on epicontinental clastic sedimentation. A study of Lower Palaeozoic sedimentation in the Oslo Region, Norway. *Sedimentology,* 21**,** 251-272.

BJØRLYKKE, K. 1974b. A reply. Origin of limestone nodules in the Lower Palaeozoic of the Oslo Region. *Norsk Geologisk Tidsskrift,* 54**,** 397-399.

BLATT, H., MIDDLETON, G. V. & MURRAY, R. C. 1972. Origin of limestones. *Origin of sedimentary rocks.* Prentice-Hall, INC.

BOCKELIE, J. F. 1981. Functional morphology and evolution of the cystoid Echinosphaerites. *Lethaia,* 14**,** 189-202.

BOCKELIE, J. F. 1982. THE ORDOVICIAN OF OSLO-ASKER. *INTERNATIONAL SYMPOSIUM ON THE ORDOVICIAN SYSTEM. FIELD EXCURSION GUIDE,* IV**,** 106-121.

BRENCHLEY, P. & COCKS, L. 1982. Ecological associations in a regressive sequence: the latest Ordovician of the Oslo-Asker district, Norway. *Palaeontology,* 25**,** 783-815.

BRENCHLEY, P., MARSHALL, J., CARDEN, G., ROBERTSON, D., LONG, D., MEIDLA, T., HINTS, L. & ANDERSON, T. 1994. Bathymetric and isotopic evidence for a short-lived Late Ordovician glaciation in a greenhouse period. *Geology,* 22**,** 295-298.

BRENCHLEY, P. J., MARSHALL, J. D., HARPER, D. A., BUTTLER, C. J. & UNDERWOOD, C. J. 2006. A late Ordovician (Hirnantian) karstic surface in a submarine channel, recording glacio‐eustatic sea‐level changes: Meifod, central Wales. *Geological Journal,* 41**,** 1-22.

BRENCHLEY, P. J. & NEWALL, G. 1975. The stratigraphy of the Upper Ordovician Stage 5 in the Oslo-Asker district, Norway. *Norsk Geologisk Tidsskrift,* 55**,** 243-275.

BRENCHLEY, P. J. & NEWALL, G. 1977. The significance of contorted bedding in upper Ordovician sediments of the Oslo region, Norway. *Journal of Sedimentary Research,* 47.

BRENCHLEY, P. J. & NEWALL, G. 1980. A facies analysis of Upper Ordovician regressive sequences in the Oslo region, Norway—A record of glacio-eustatic changes. *Palaeogeography, Palaeoclimatology, Palaeoecology,* 31**,** 1-38.

BRENCHLEY, P. J., NEWALL, G. & STANISTREET, I. G. 1979. A storm surge origin for sandstone beds in an epicontinental platform sequence, Ordovician, Norway. *Sedimentary geology,* 22**,** 185-217.

BRETT, C. E. 1998. Sequence stratigraphy, paleoecology, and evolution; biotic clues and responses to sea-level fluctuations. *Palaios,* 13**,** 241-262.

BROMLEY, R. G. & EKDALE, A. 1984. Chondrites: a trace fossil indicator of anoxia in sediments. *Science,* 224**,** 872-874.

BRUTON, D. L., GABRIELSEN, R. H. & LARSEN, B. T. 2010. The Caledonides of the Oslo Region, Norway–stratigraphy and structural elements. *Norwegian Journal of Geology,* 90**,** 93-121.

BRUTON, D. L. & WILLIAMS, S. H. 1982. Field Excursion Guide IV International Symposium on the Ordovician System. *Paleontological Contributions from the University of Oslo 279***,** 1-217.

BRØGGER, W. C. 1882. *Die silurischen Etagen 2 und 3 im Kristianiagebiet und auf Eker*, AW Brögger.

BUTMAN, B., NOBLE, M. & FOLGER, D. W. 1979. Long‐term observations of bottom current and bottom sediment movement on the mid‐Atlantic continental shelf. *Journal of Geophysical Research: Oceans (1978–2012),* 84**,** 1187-1205.
COCKS, L. & TORSVIK, T. 2006. European geography in a global context from the Vendian to the end of the Palaeozoic. *MEMOIRS-GEOLOGICAL SOCIETY OF LONDON,* 32**,** 83.
COLLINSON, J. D., THOMPSON, D. B. & MOUNTNEY, N. 2006. *Sedimentary structures,* Harpenden, Terra Publishing.
CROWLEY, T. J. & BAUM, S. K. 1995. Reconciling Late Ordovician (440 Ma) glaciation with very high (14X) CO2 levels. *Journal of Geophysical Research: Atmospheres (1984–2012),* 100**,** 1093-1101.
DRONOV, A., AINSAAR, L., KALJO, D., MEIDLA, T., SAADRE, T. & EINASTO, R. 2011. Ordovician of Baltoscandia: facies, sequences and sea-level changes. *Ordovician of the World,* 14**,** 143-150.
DROSER, M. L. & BOTTJER, D. J. 1986. A semiquantitative field classification of ichnofabric: Research method paper. *Journal of Sedimentary Research,* 56.
DUKE, W. L., ARNOTT, R. & CHEEL, R. J. 1991. Shelf sandstones and hummocky cross-stratification: new insights on a stormy debate. *Geology,* 19**,** 625-628.
DUMAS, S. & ARNOTT, R. 2006. Origin of hummocky and swaley cross-stratification—the controlling influence of unidirectional current strength and aggradation rate. *Geology,* 34**,** 1073-1076.
DUMAS, S., ARNOTT, R. & SOUTHARD, J. B. 2005. Experiments on oscillatory-flow and combined-flow bed forms: implications for interpreting parts of the shallow-marine sedimentary record. *Journal of Sedimentary research,* 75**,** 501-513.
DUNNING, G. & PEDERSEN, R. 1988. U/Pb ages of ophiolites and arc-related plutons of the Norwegian Caledonides: implications for the development of Iapetus. *Contributions to Mineralogy and Petrology,* 98**,** 13-23.
ERIKSSON, P., BOSE, P. K., CATUNEANU, O., SARKAR, S. & BANERJEE, S. 2008. Precambrian clastic epeiric embayments: examples from South Africa and India. *Dynamics of Epeiric Seas. Geological Association of Canada Spec. Pap,* 48**,** 119-136.
ETTENSOHN, F. R. 2010. Origin of Late Ordovician (mid-Mohawkian) temperate-water conditions on southeastern Laurentia: Glacial or tectonic? *Geological Society of America Special Papers,* 466**,** 163-175.
EYLES, N. 1993. Earth's glacial record and its tectonic setting. *Earth-Science Reviews,* 35**,** 1-248.
FINNEGAN, S., BERGMANN, K., EILER, J. M., JONES, D. S., FIKE, D. A., EISENMAN, I., HUGHES, N. C., TRIPATI, A. K. & FISCHER, W. W. 2011. The magnitude and duration of Late Ordovician–Early Silurian glaciation. *Science,* 331**,** 903-906.
FLÜGEL, E. 2004. Microfacies of Carbonate Rocks - Analysis, Interpretation and Application. 976 pp.
FOLK, R. L. 1954. The distinction between grain size and mineral composition in sedimentary-rock nomenclature. *The Journal of Geology***,** 344-359.
FOLK, R. L. 1962. Spectral subdivision of limestone types. *American Association of Petroleum Geologists Memoir.***,** 62-84.
GOLDRING, R. & BRIDGES, P. 1973. Sublittoral sheet sandstones. *Journal of Sedimentary Research,* 43.
HARMS, J. 1975. Shallow Marine Sands.
HARWOOD, C. 1985. *A facies analysis of shale-nodular limestone cycles from the Upper Ordovician of the Oslo region, Norway,* Liverpool, [C. Harwood].
HAYES, M. O. 1967. Hurricanes as Geological Agents, South Texas Coast: GEOLOGICAL NOTES. *AAPG Bulletin,* 51**,** 937-942.
HECKEL, P. H. 1972. Recognition of ancient shallow marine environments.
HENNINGSMOEN, G. 1974. A comment. Origin of limestone nodules in the Lower Palaeozoic of the Oslo Region. *Norsk Geologisk Tidsskrift,* 54**,** 401-412.
HERRMANN, A. D., HAUPT, B. J., PATZKOWSKY, M. E., SEIDOV, D. & SLINGERLAND, R. L. 2004. Response of Late Ordovician paleoceanography to changes in sea level, continental drift, and

atmospheric< i> p</i> CO< sub> 2</sub>: potential causes for long-term cooling and glaciation. *Palaeogeography, Palaeoclimatology, Palaeoecology,* 210**,** 385-401.
HESSLAND, I. 1949. Investigations of the Lower Ordovician of the Siljan District, Sweden, II. Lower Ordovician penetrative and enveloping algae from the Siljan District. *Bull,* 33**,** 409-428.
HOBDAY, D. & READING, H. 1972. Fair weather versus storm processes in shallow marine sand bar sequences in the late Precambrian of Finnmark, North Norway. *Journal of Sedimentary Research,* 42**,** 318-324.
IRWIN, M. 1965. General theory of epeiric clear water sedimentation. *AAPG Bulletin,* 49**,** 445-459.
JAANUSSON, V. 1973. Aspects of carbonate sedimentation in the Ordovician of Baltoscandia. *Lethaia,* 6**,** 11-34.
JAANUSSON, V. 1984. *What is so special about the Ordovician*, Palaeontological Contributions from the University of Oslo.
JONES, B. 2010. Warm-water neritic carbonates. *In:* JAMES, N. P. & DALRYMPLE, R. W. (eds.) *Facies Models.* Geological Association of Canada.
KELLING, G. & MULLIN, P. R. 1975. Graded limestones and limestone-quartzite couplets: possible storm-deposits from the Moroccan Carboniferous. *Sedimentary geology,* 13**,** 161-190.
KJERULF, T. & DAHL, T. 1857. *Ueber die Geologie des südlichen Norwegens*, J. Dahl.
KOBLUK, D. R. & RISK, M. J. 1977. Micritization and carbonate-grain binding by endolithic algae. *AAPG Bulletin,* 61**,** 1069-1082.
KREISA, R. D. 1981. Storm-generated sedimentary structures in subtidal marine facies with examples from the Middle and Upper Ordovician of southwestern Virginia. *Journal of Sedimentary Research,* 51.
KULP, M. A. 1995. *Paleoenvironmental Interpretation of the Brannon Member of Middle-Upper Ordovician Lexington Limestone, Central Bluegrass Region of Kentucky.* University of Kentucky.
LEE, Y. I. & KIM, J. C. 1992. Storm‐influenced siliciclastic and carbonate ramp deposits, the Lower Ordovician Dumugol Formation, South Korea. *Sedimentology,* 39**,** 951-969.
MARSHALL, J. D., BRENCHLEY, P. J., MASON, P., WOLFF, G. A., ASTINI, R. A., HINTS, L. & MEIDLA, T. 1997. Global carbon isotopic events associated with mass extinction and glaciation in the late Ordovician. *Palaeogeography, Palaeoclimatology, Palaeoecology,* 132**,** 195-210.
MEYERS, K. J. & MILTON, N. J. 1996. Principles of sequence stratigraphy. *In:* EMERY, D. & MEYERS, K. J. (eds.) *Sequence stratigraphy.* Oxford: Blackwell Science.
MILLER, K. B., CARLTON, E. B. & PARSONS, K. M. 1988. The Paleoecologic Significance of Storm-Generated Disturbance within a Middle Devonian Muddy Epeiric Sea. *PALAIOS,* 3**,** 35-52.
MOLINA, J., RUIZ-ORTIZ, P. & VERA, J. 1997. Calcareous tempestites in pelagic facies (Jurassic, Betic Cordilleras, southern Spain). *Sedimentary Geology,* 109**,** 95-109.
MORLEY, C. 1986. The Caledonian thrust front and palinspastic restorations in the southern Norwegian Caledonides. *Journal of Structural Geology,* 8**,** 753-765.
MORSE, J. W., ARVIDSON, R. S. & LÜTTGE, A. 2007. Calcium carbonate formation and dissolution. *Chemical reviews,* 107**,** 342-381.
MUCCI, A. 1983. The solubility of calcite and aragonite in seawater at various salinities, temperatures, and one atmosphere total pressure. *American Journal of Science,* 283**,** 780-799.
MYROW, P. M. & SOUTHARD, J. B. 1996. Tempestite deposition. *Journal of Sedimentary Research,* 66.
MÖLLER, N. K. & KVINGAN, K. 1988. The genesis of nodular limestones in the Ordovician and Silurian of the Oslo Region (Norway). *Sedimentology,* 35**,** 405-420.
NIELSEN, A. T. Ordovician sea-level changes: potential for global event stratigraphy. Ordovician from the Andes: Proceedings of the 9th International Symposium on the Ordovician System. INSUGEO: Serie Correlación Geológica, 2003. 445-449.
NIELSEN, A. T. 2004. Ordovician sea level changes: a Baltoscandian perspective. *The great Ordovician biodiversification event***,** 84-93.
OFTEDAHL, C. 1943. Oerskyvininger in den norske fjellkjede. *Naturen,* Oslo 5**,** 243-250.

OWEN, A. W., BRUTON, D. L., BOCKELIE, J. F. & BOCKELIE, T. G. 1990. *The Ordovician Successions of the Oslo Region, Norway*, Norges Geologiske Undersokelse.
OWEN, G., MORETTI, M. & ALFARO, P. 2011. Recognising triggers for soft-sediment deformation: Current understanding and future directions. *Sedimentary Geology,* 235**,** 133-140.
PIA, J. 1937. Die kalklosenden Thallophyten: Arch. Hydrobiol.,. 31**,** 264-328, 341-398.
PLINT, A. 2010. Wave-and storm-dominated shoreline and shallow-marine systems. *Facies models,* 4**,** 167-200.
PRATSON, L. E., IMRAN, J., PARKER, G., SYVITSKI, J. P. & HUTTON, E. 2000. Debris flows vs. turbidity currents: a modeling comparison of their dynamics and deposits. *SPECIAL PUBLICATION-SEPM,* 68**,** 57-72.
PURKIS, S. J., ROWLANDS, G. P. & KERR, J. M. 2014. Unravelling the influence of water depth and wave energy on the facies diversity of shelf carbonates. *Sedimentology*.
RAMBERG, I. B. & BOCKELIE, J. F. 1981. Geology and tectonics around Oslo. *Guide to excursion B-4. Nytt fra Oslofeltgruppen 7***,** 81-100.
READING, H. G. & COLLINSON, J. D. 1996. Clastic coasts *In:* READING, H. G. (ed.) *Sedimentary Environments: Processes, Facies and Stratigraphy.* Blackwell Science, Oxford.
REINECK, H. E. & SINGH, I. B. 1972. GENESIS OF LAMINATED SAND AND GRADED RHYTHMITES IN STORM-SAND LAYERS OF SHELF MUD. *Sedimentology,* 18**,** 123-128.
SCHLAGER, W. 2005. Concepts in Sedimentology and Paleontology. *In:* CROSSEY, L. J. (ed.) *Carbonate sedimentology and sequence stratigraphy.* SEPM (Society for Sedimentary Geology.
SEILACHER, A. & MEISCHNER, D. 1965. Fazies-Analyse im Paläozoikum des Oslo-Gebietes. *Geologische Rundschau,* 54**,** 596-619.
SHAW, A. B. 1964. *Time in stratigraphy*, McGraw-Hill New York.
SKJESETH, S. 1952. On the Lower Didymograptus Zone (3b) at Ringsaker, and contemporaneous deposits in Scandinavia. *Norsk Geologisk Tidsskrift,* 30**,** 138-182.
SPJELDNÆS, N. 1960. Ordovician climatic zones. *Norsk geologisk tidsskrift,* 41**,** 45-77.
SRAMEK, J. 1974. Origin of Limestone Nodules in the Lower Palaeozoic of the Oslo Region [discussion and reply]. *Norsk Geologisk Tidsskrift. Supplement,* 54**,** 395-399.
STANISTREET, I. G. 1983. Contemporaneous faulting in the Upper Ordovician of the Oslo-Asker District, Norway, and its significance in the development of the Oslo Basin. *Sedimentary geology,* 37**,** 133-150.
STANISTREET, I. G. 1989. Trace fossil associations related to facies of an upper Ordovician low wave energy shoreface and shelf, Oslo-Asker district, Norway. *Lethaia,* 22**,** 345-357.
STØRMER, L. 1967. Some aspects of the Caledonian geosyncline and foreland west of the Baltic Shield 20TH WILLIAM SMITH LECTURE. *Quarterly Journal of the Geological Society,* 123**,** 183-214.
SWIFT, D. J., HAN, G. & VINCENT, C. E. 1986. Fluid Processes and Sea-Floor Response on a Modern Storm-Dominated Shelf: Middle Atlantic Shelf of North America. Part I: The Storm-Current Regime.
SWIFT, D. J. P. & THORNE, J. A. 1991. Sedimentation on continental margins: I. A general model for shelf sedimentation. *Shelf sand and sandstone bodies,* 14**,** 3-31.
THORNE, J., GRACE, E., SWIFT, D. & NIEDORODA, A. 1991. Sedimentation on continental margins, III: the depositional fabric—an analytical approach to stratification and facies identification. *Shelf Sand and Sandstone Bodies: Geometry, Facies and Sequence Stratigraphy***,** 59-87.
UDDEN, J. A. 1914. Mechanical Composition of clastic sediments. *Bull. Geol. Soc. Amer.,* XXV**,** 655-744.
WENTWORTH, C. K. 1922. A scale of grade and class terms for clastic sediments. *The Journal of Geology***,** 377-392.
WORSLEY, D., AARHUS, N. & BASSETT, M. 1983. *The Silurian succession of the Oslo region*, Universitetsforl. Trondheim et al.

APPENDIX A

SEDIMENTARY LOGS

Legend

Lithology:


Sandstone


Silt


Sandy or silty shale

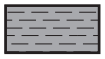
Shale

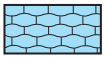
Nodular limestone

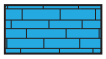
Limestone


Limestone conglomerate

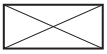
No exposed outcrops

Fossils:


Crinoid


Brachiopods


Blastoid


Shell fragments


Rugose coral


Cornulites

Sedimentary structures


Asymmetrical /current ripple


Vertical burrows


Horizontal burrows


Soft sediment deformation


Slump structures


Convolute bedding


Little bioturbation


Medium biuturbation


Heavy bioturbation


Limestone nodules


Lenticular bedding

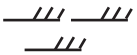
Cross-lamination

Symmetrical lamination


Wave/current-ripple lamination

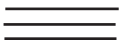
Parallel/horizontal lamination


Flazer bedding


Cross-bedding


Hummocky cross stratification


Loading structures


Pinching silt/sand layer

Erosional surface

HOVEDØYA PROFILE 1

SEDIMENTARY LOG

Scale: 1:10

LOCATION: *Hovedøya S.W* **SECTION NO:** *Profile 1* **SHEET NO:** *15/15* **DATE:** *20.10.2013* **BY:** *Martin Kjærsgaard*

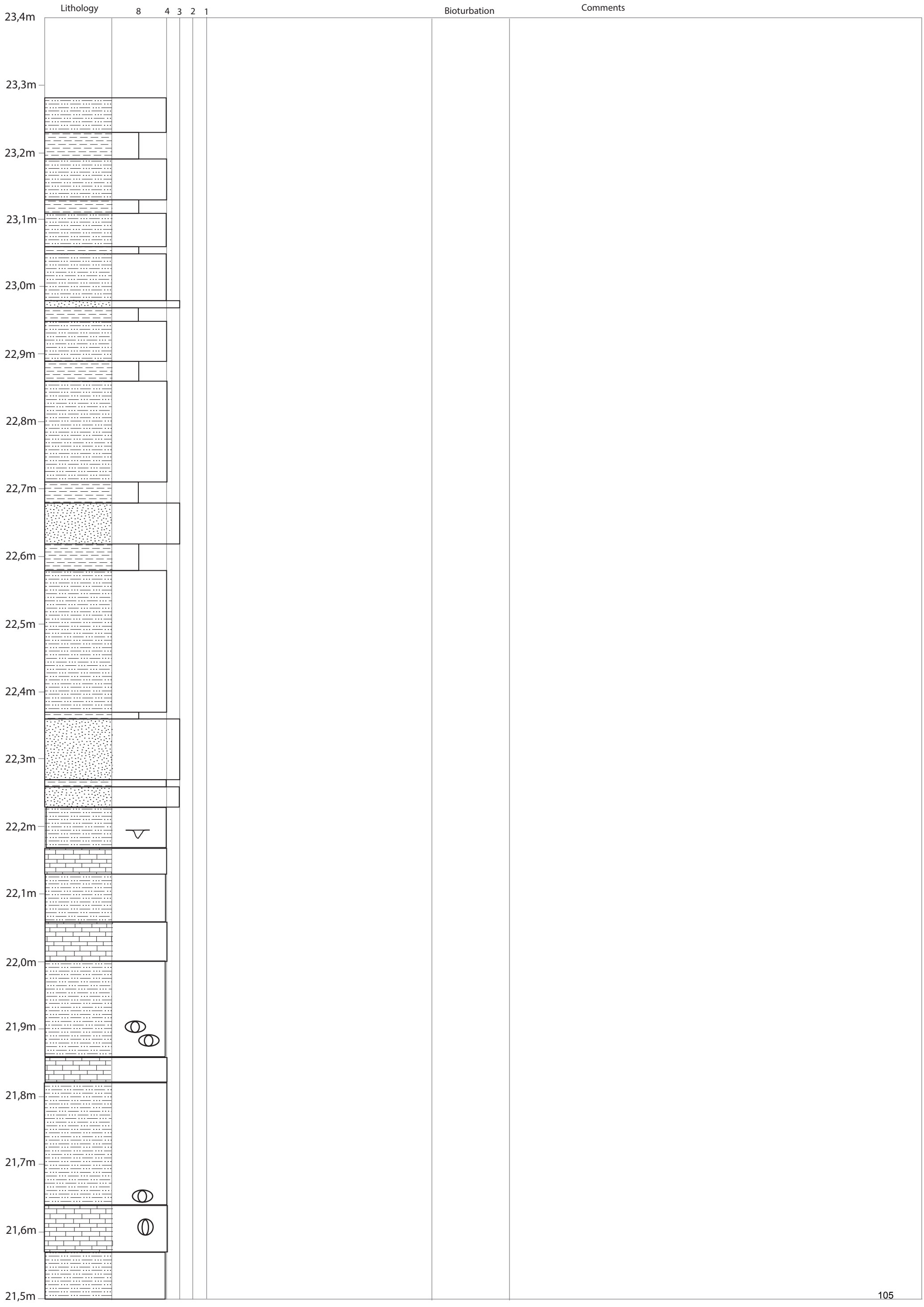

LOCATION: *Hovedøya S.W* **SECTION NO:** *Profile 1* **SHEET NO:** *14/15* **DATE:** *19.10.2013* **BY:** *Martin Kjærsgaard*

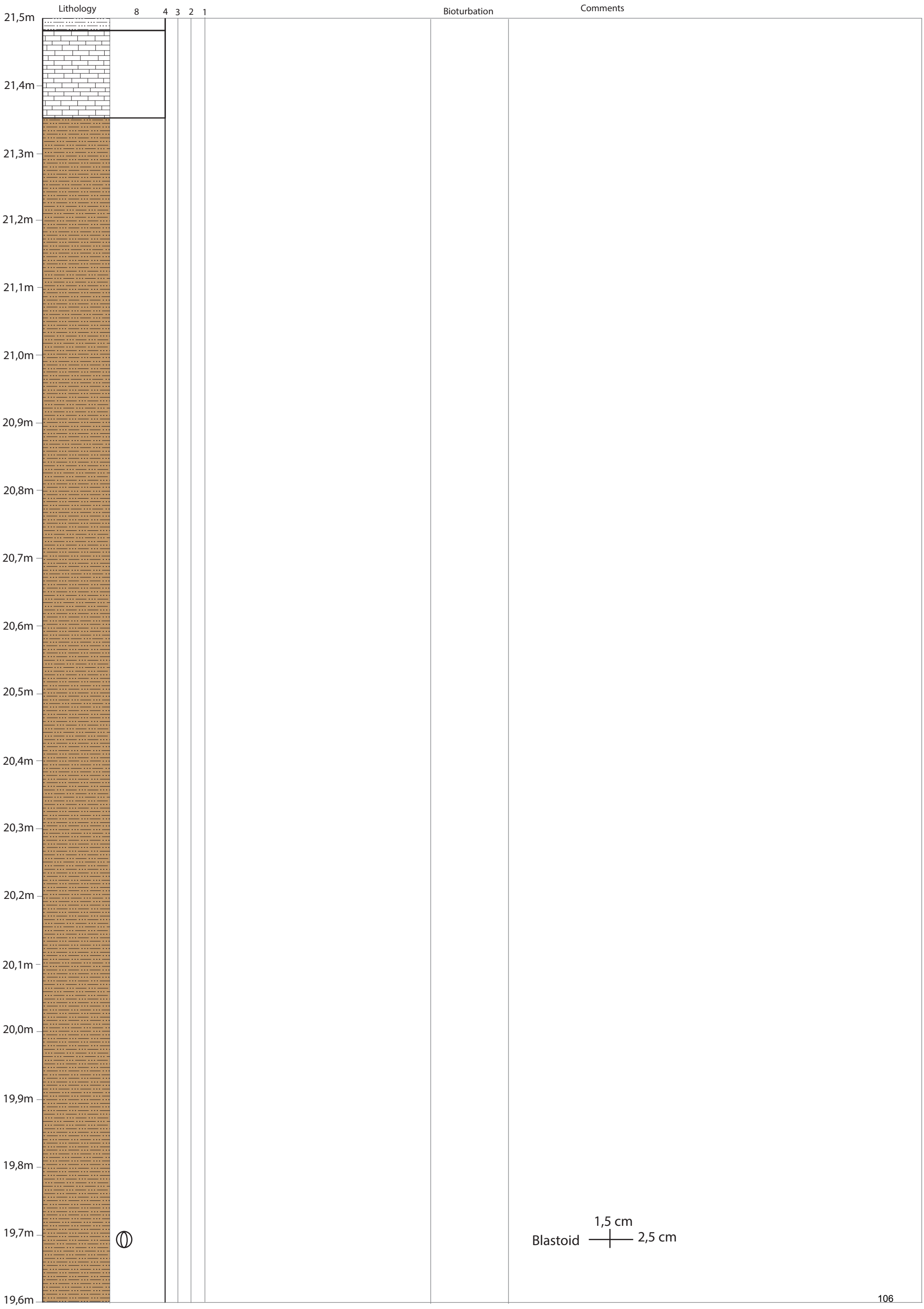

LOCATION: *Hovedøya S.W* **SECTION NO:** *Profile 1* **SHEET NO:** *13/15* **DATE:** *19.10.2013* **BY:** *Martin Kjærsgaard*

LOCATION: *Hovedøya S.W* **SECTION NO:** *Profile 1|* **SHEET NO:** *12/15* **DATE:** *19.10.2013* **BY:** *Martin Kjærsgaard*

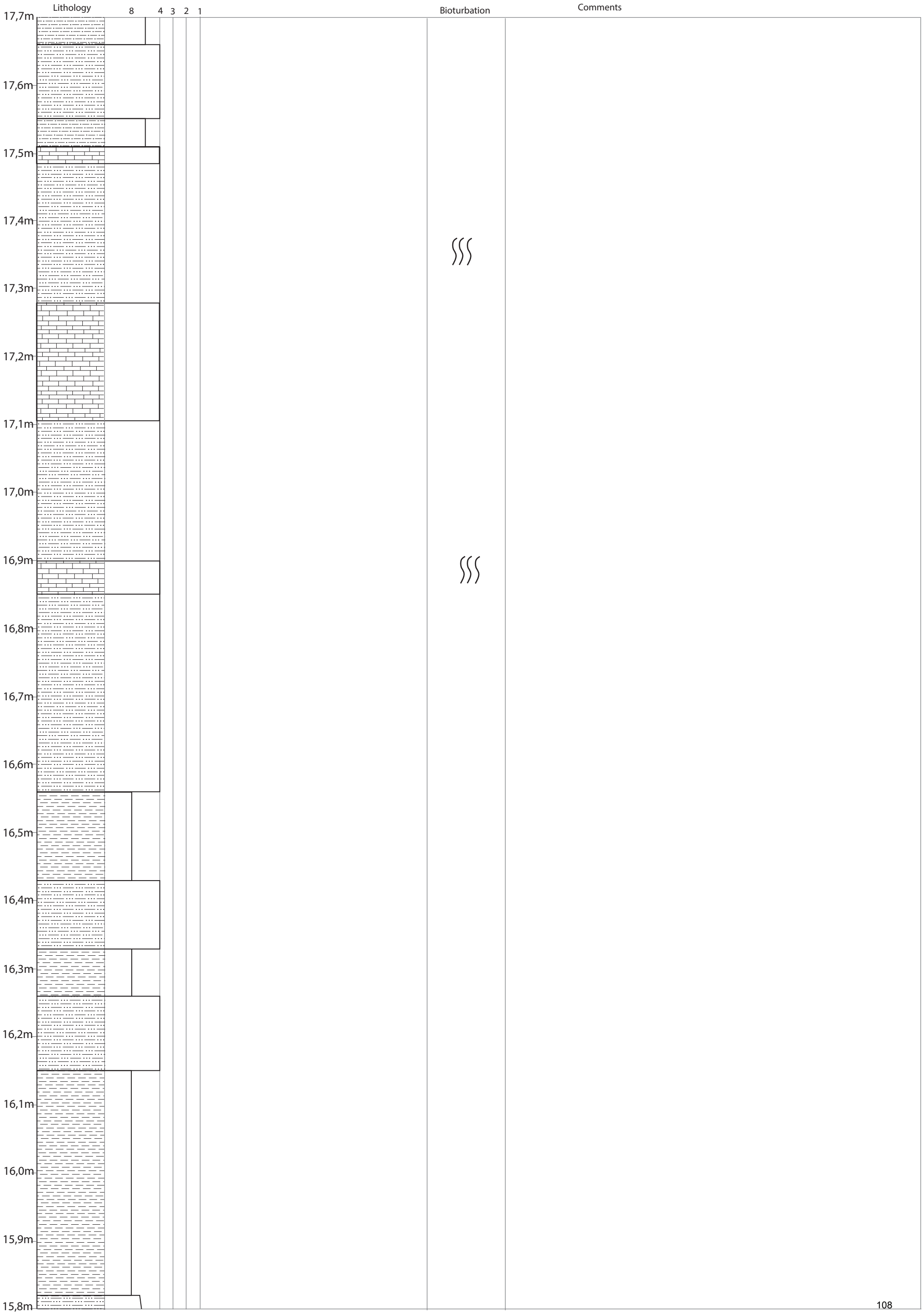

LOCATION: *Hovedøya S.W* **SECTION NO:** *Profile 1* **SHEET NO:** *11/15* **DATE:** *19.10.13* **BY:** *Martin Kjærsgaard*

Lithology 8 4 3 2 1 | Bioturbation | Comments

15,8m
15,7m
15,6m
15,5m
15,4m
15,3m
15,2m
15,1m
15,0m
14,9m
14,8m
14,7m
14,6m
14,5m
14,4m
14,3m
14,2m
14,1m
14,0m
13,9m

230
76

Contains 3 layers. Bottom layer is limestone, middle layer is silt and top layer is limestone.

Beach zone - no visible outcrops

LOCATION: *Hovedøya S.W* **SECTION NO:** *Profile 1* **SHEET NO:** *10/15* **DATE:** *19.10.2013* **BY:** *Martin Kjærsgaard*

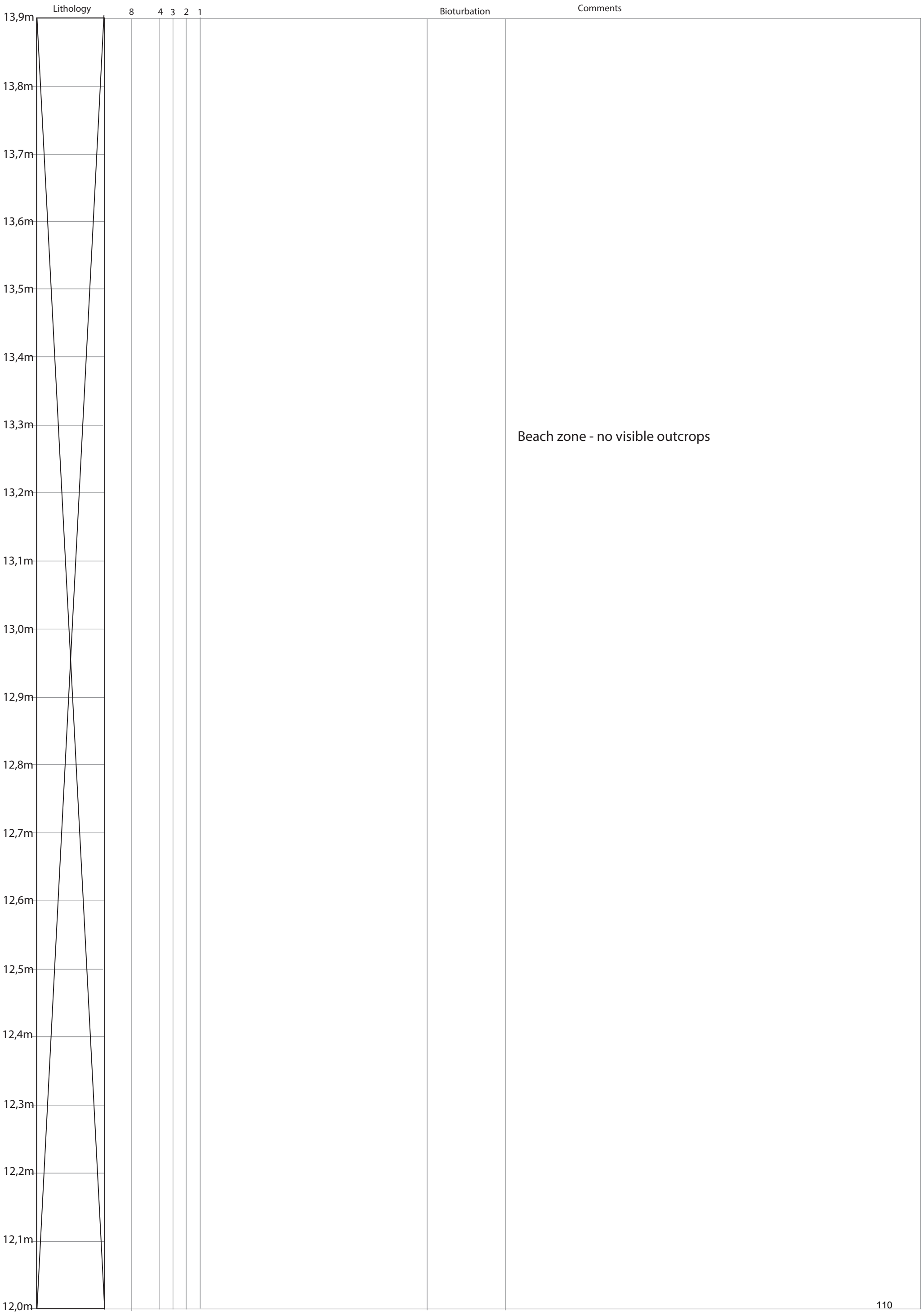

LOCATION: *Hovedøya S.W* **SECTION NO:** *Profile 1* **SHEET NO:** *9/15* **DATE:** *19.10.2013* **CONDITIONS:** *Cloudy, no rain* **BY:** *Martin Kjærsgaard*

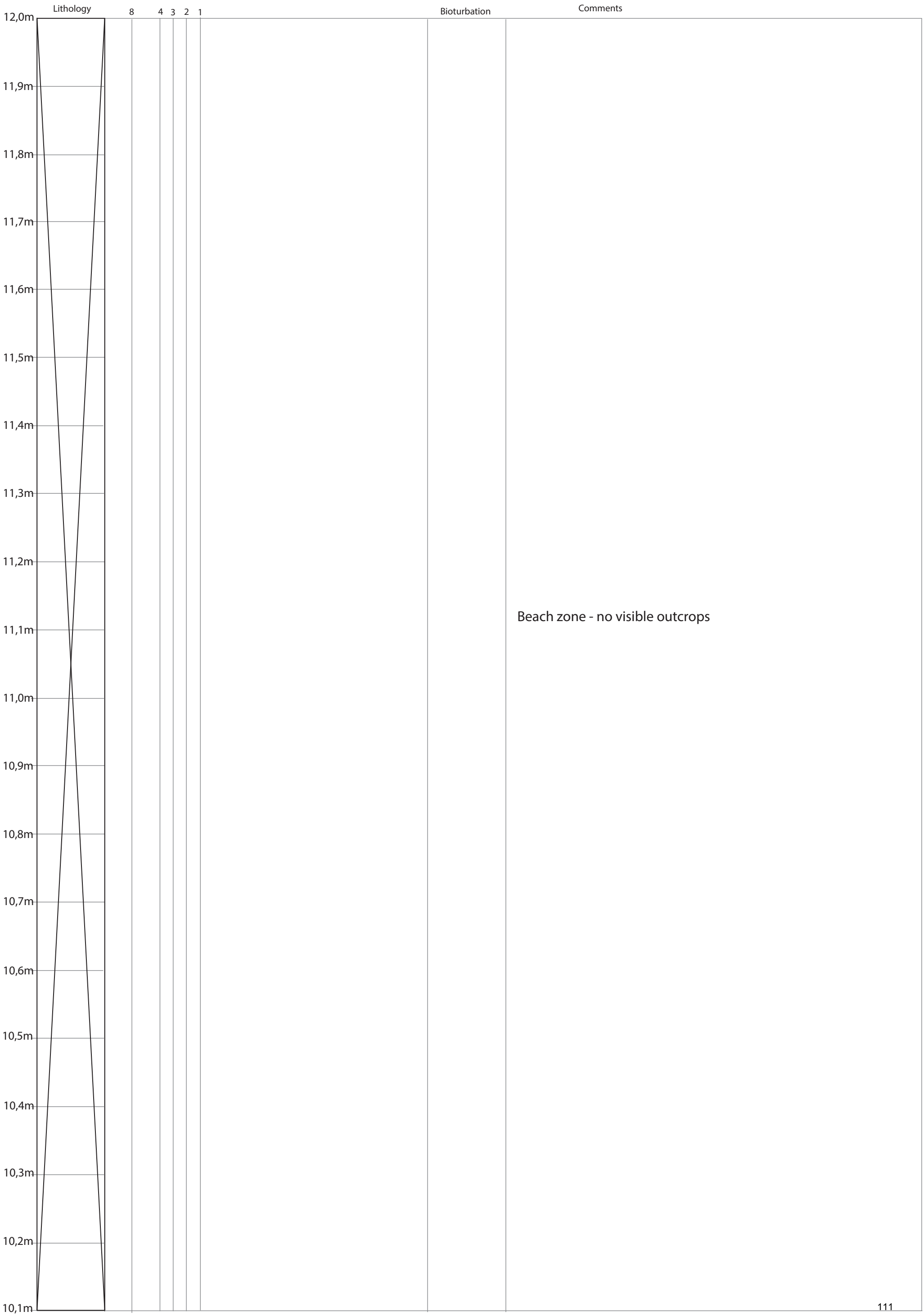

LOCATION: *Hovedøya S.W* **SECTION NO:** *Profile 1* **SHEET NO:** *8/15* **DATE:** *19.10.2013* **BY:** *Martin Kjærsgaard*

Lithology | 8 | 4 | 3 | 2 | 1 | Bioturbation | Comments

10,1m
10,0m
9,9m
9,8m
9,7m
9,6m
9,5m
9,4m
9,3m
9,2m
9,1m
9,0m
8,9m
8,8m
8,7m
8,6m
8,5m
8,4m
8,3m
8,2m

Beach zone - no visible outcrops

LOCATION: *Hovedøya S.W* **SECTION NO:** *Profile 1* **SHEET NO:** *7/15* **DATE:** *19.10.2013* **BY:** *Martin Kjærsgaard*

Lithology | 8 | 4 | 3 | 2 | 1 | Bioturbation | Comments

8,2m
8,1m
8,0m
7,9m
7,8m
7,7m
7,6m
7,5m
7,4m
7,3m
7,2m
7,1m
7,0m
6,9m
6,8m
6,7m
6,6m
6,5m
6,4m
6,3m

Beach zone - no visible outcrops

LOCATION: *Hovedøya S.W* **SECTION NO:** *7* **SHEET NO:** *6/15* **DATE:** *19.10.2013* **BY:** *Martin Kjærsgaard*

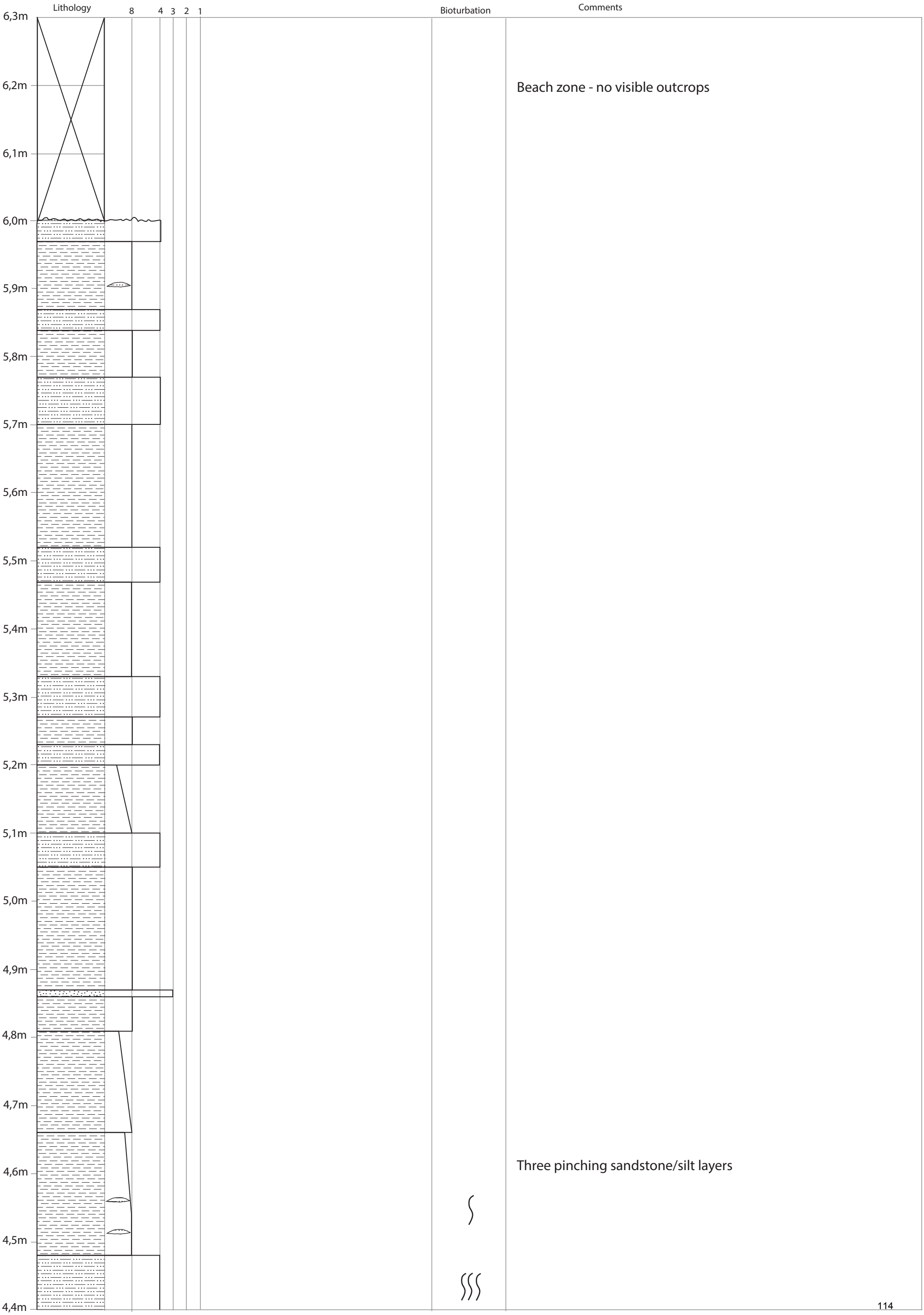

LOCATION: *Hovedøya S.W* **SECTION NO:** *Profile 1* **SHEET NO:** *5/15* **DATE:** *19.10.2013* **BY:** *Martin Kjærsgaard*

Lithology 8 4 3 2 1 Bioturbation Comments

4,4m
4,3m
4,2m
4,1m
4,0m
3,9m
3,8m
3,7m
3,6m
3,5m
3,4m
3,3m
3,2m
3,1m
3,0m
2,9m
2,8m
2,7m
2,6m
2,5m

230
68

115

LOCATION: *Hovedøya S.W* **SECTION NO:** *Profile 1* **SHEET NO:** *4/15* **DATE:** *19.10.2013* **BY:** *Martin Kjærsgaard*

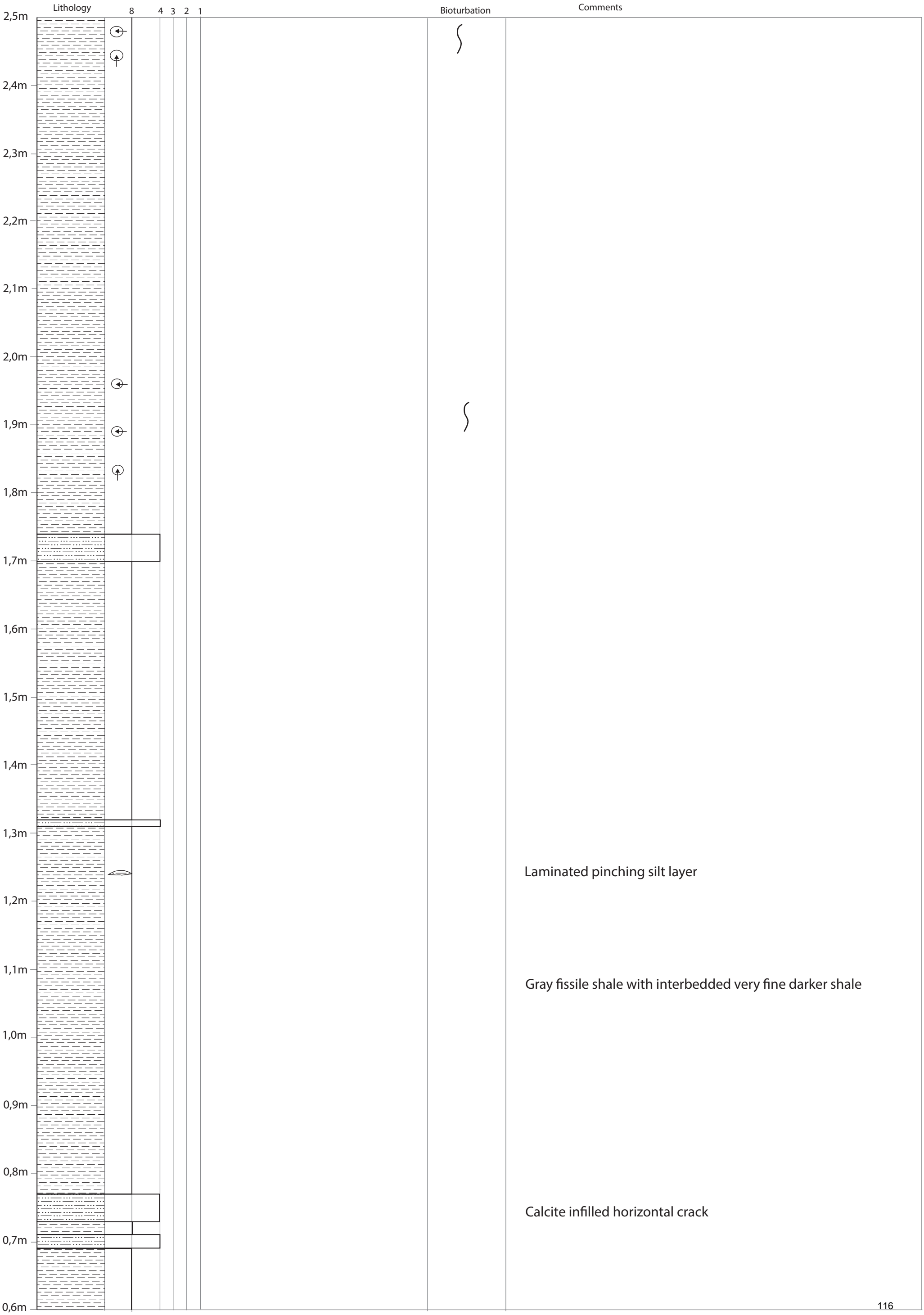

LOCATION: *Hovedøya S.W* **SECTION NO:** *Profile 1* **SHEET NO:** *3/15* **DATE:** *18.10.2013* **BY:** *Martin Kjærsgaard*

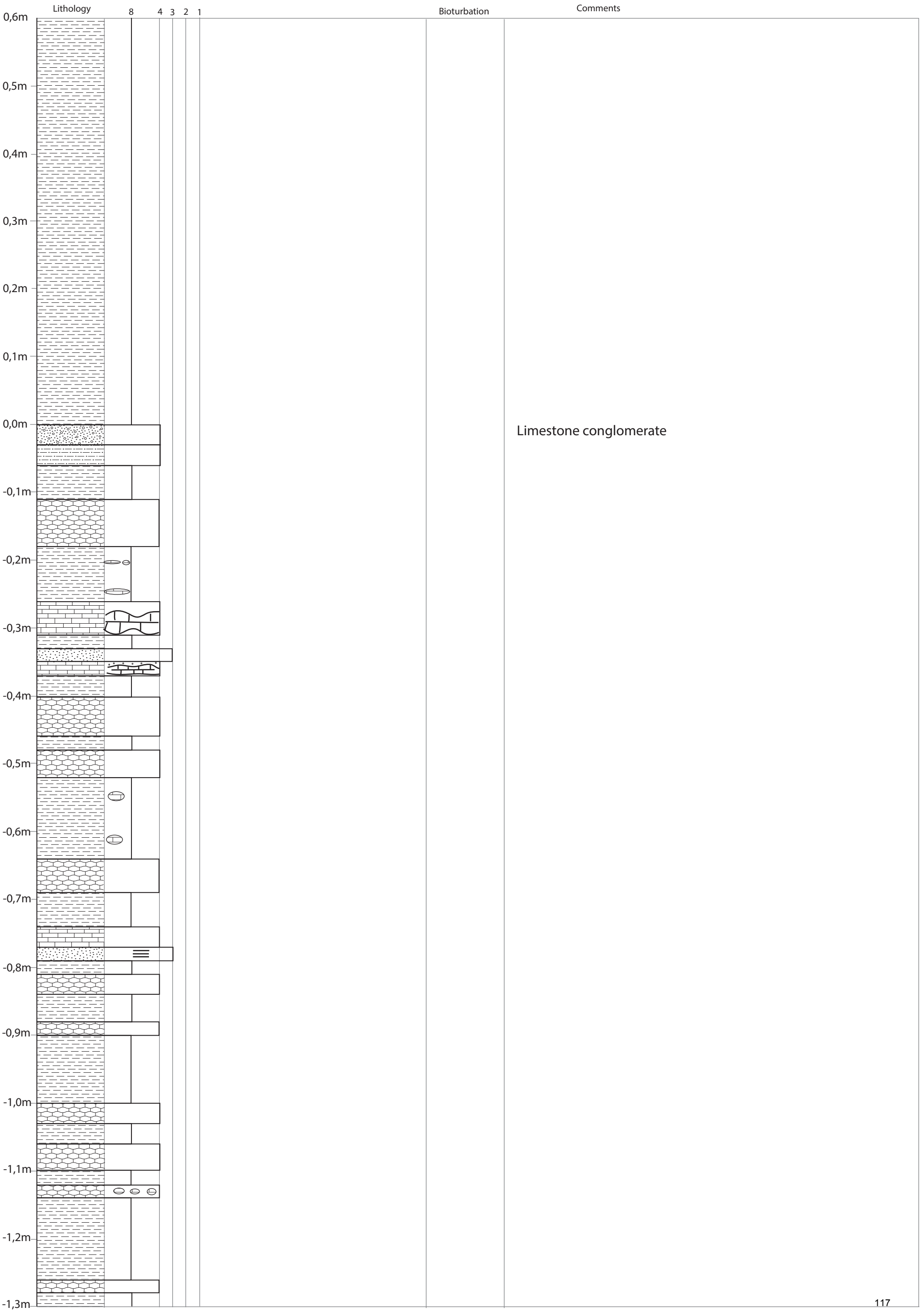

LOCATION: *Hovedøya S.W* **SECTION NO:** *Profile 1* **SHEET NO:** *2/15* **DATE:** *18.10.2013* **BY:** *Martin Kjærsgaard*

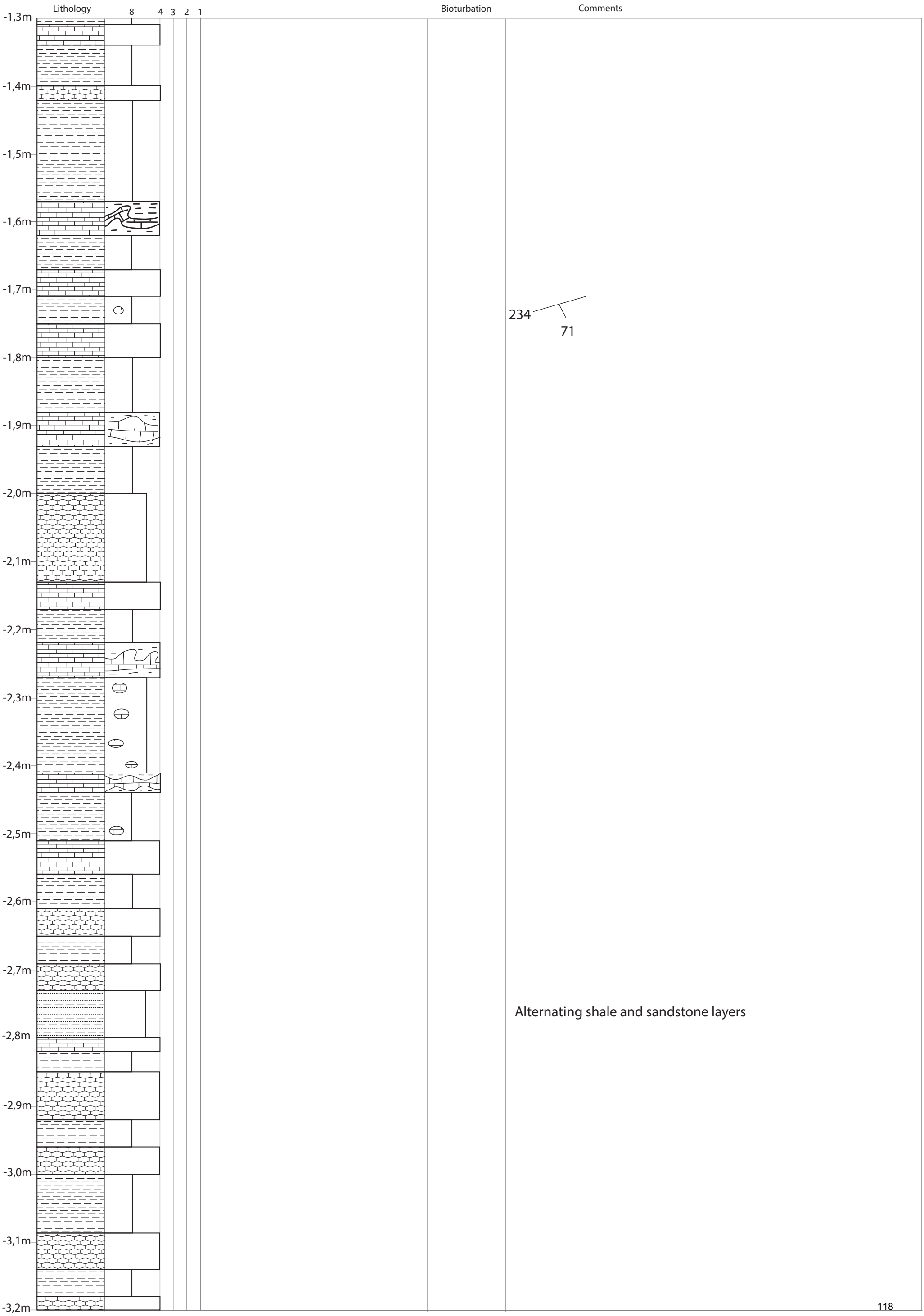

LOCATION: *Hovedøya S.W* **SECTION NO:** *Profile 1* **SHEET NO:** *1/15* **DATE:** *18.10.2013*

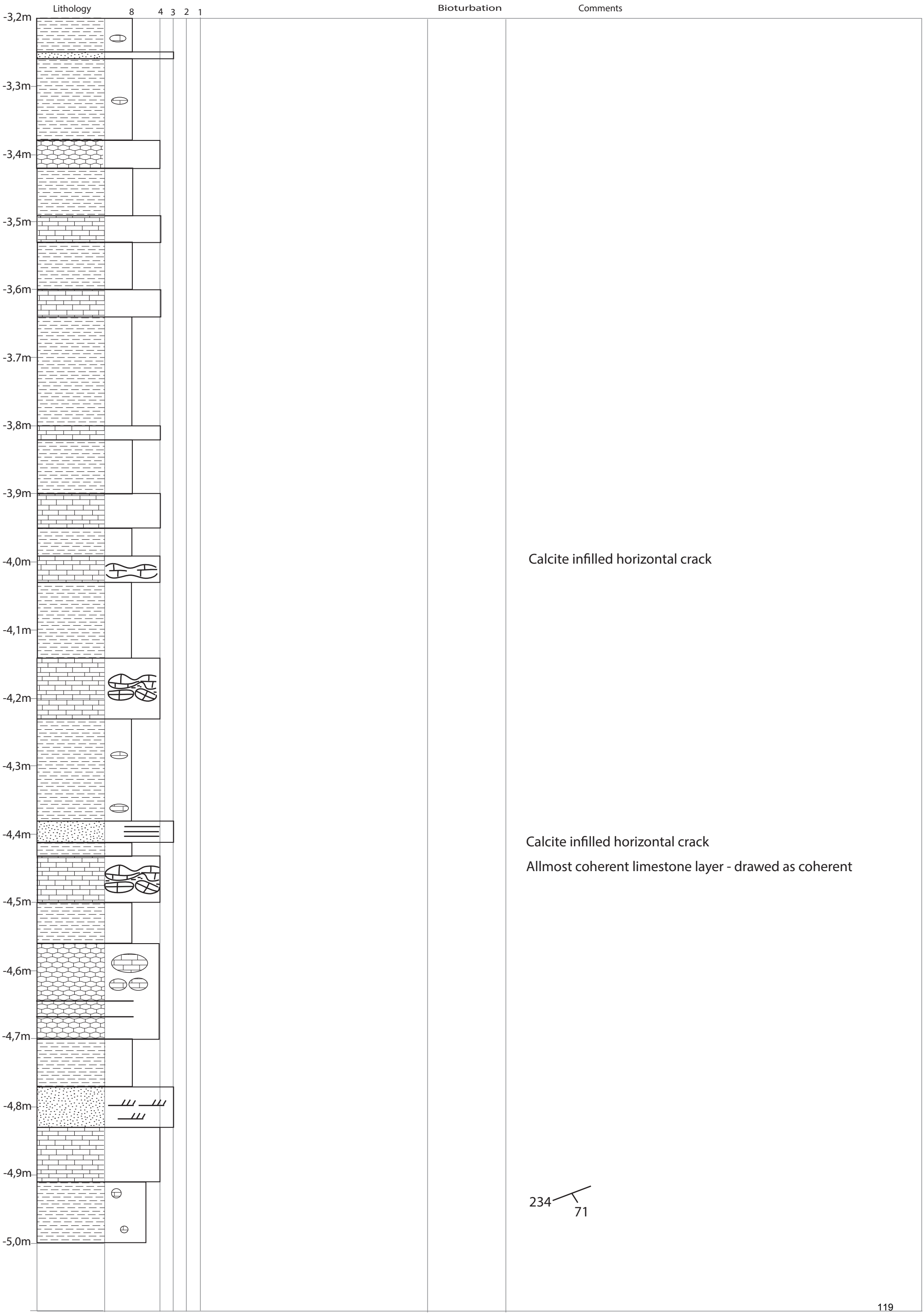

RAMBERGØYA PROFILE 1

SEDIMENTARY LOG

Scale: 1:10

LOCATION: *Rambergøya* **SECTION NO:** *Profile 1* **SHEET NO:** *16/16* **DATE:** *04.10.2013* **BY:** *Martin Kjærsgaard*

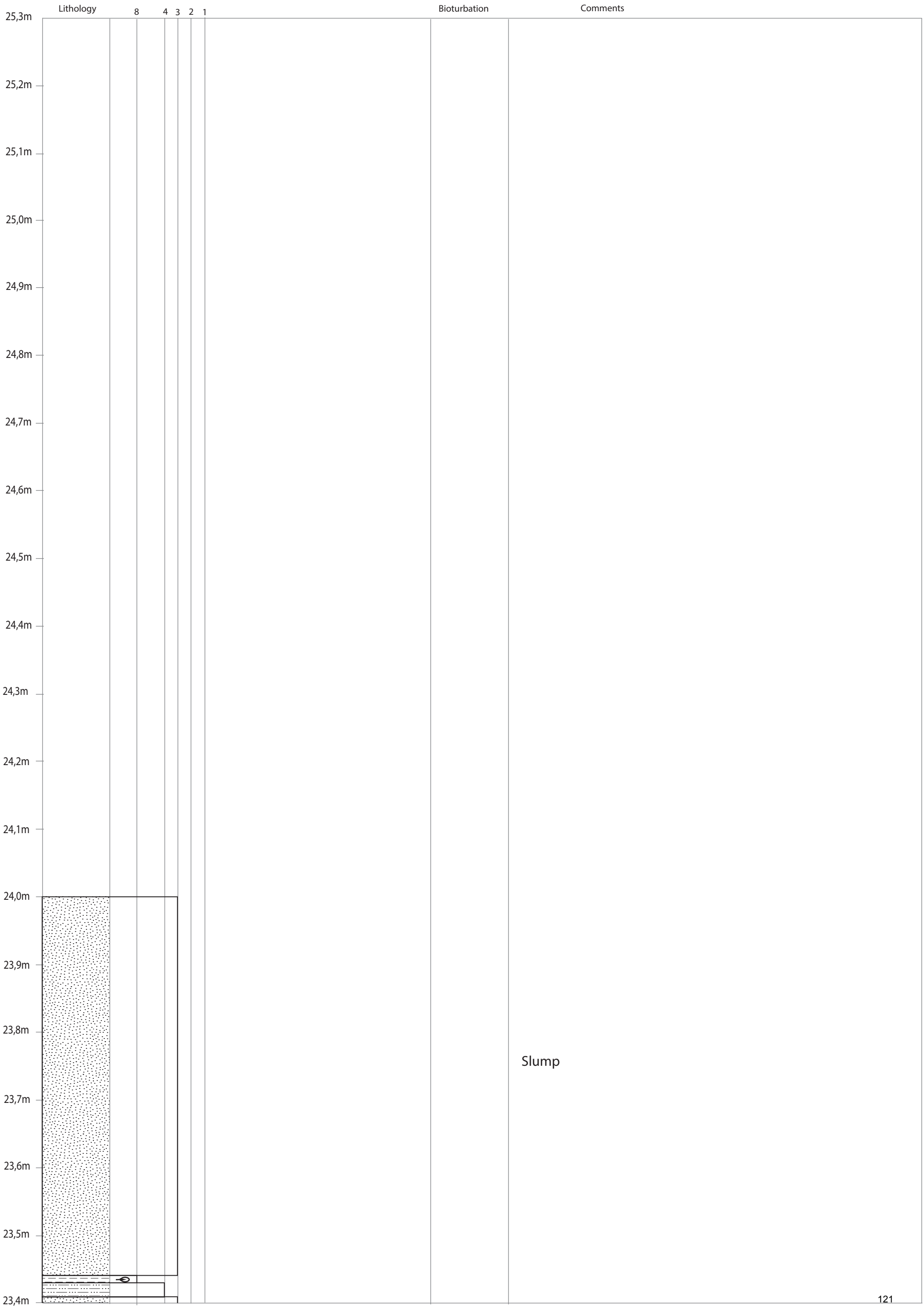

LOCATION: *Rambergøya* **SECTION NO:** *Profile 1* **SHEET NO:** *15/16* **DATE:** *04.10.2013* **BY:** *Martin Kjærsgaard*

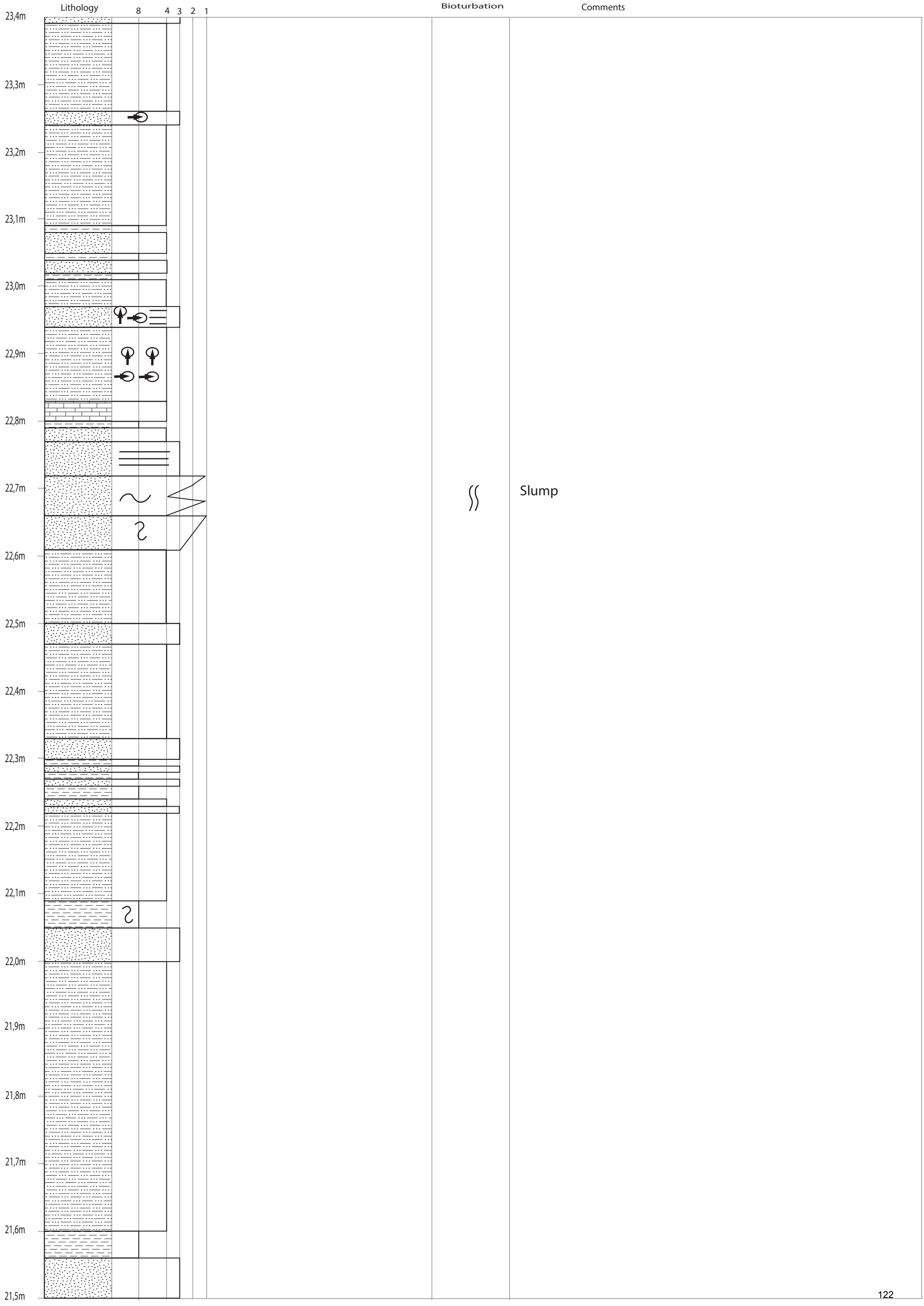

LOCATION: *Rambergøya* **SECTION NO:** *Profile 1* **SHEET NO:** *14/16* **DATE:** *04.10.2013* **BY:** *Martin Kjærsgaard*

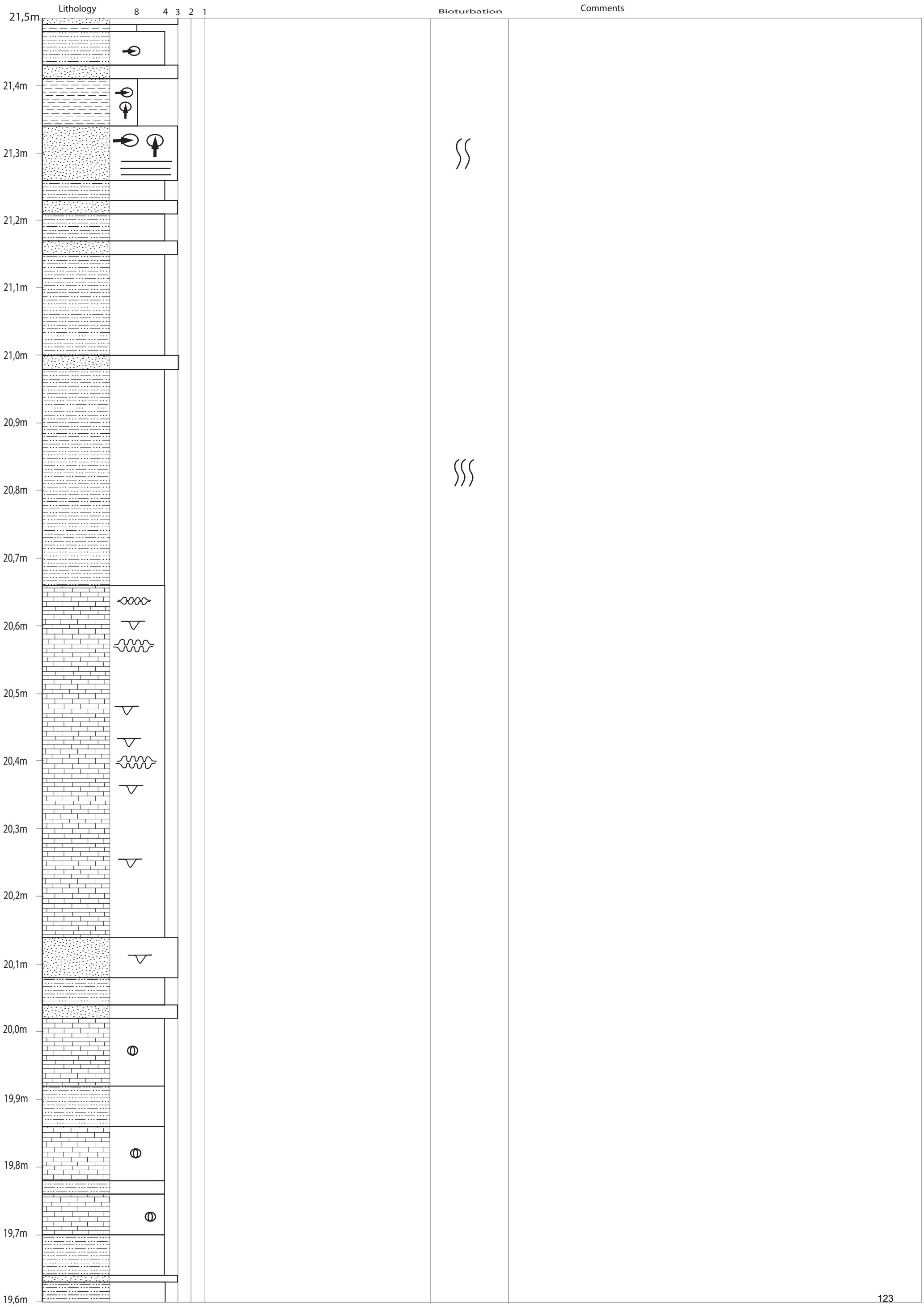

LOCATION: *Rambergøya* **SECTION NO:** *Profile 1* **SHEET NO:** *13/16* **DATE:** *23.09.2013* **BY:** *Martin Kjærsgaard*

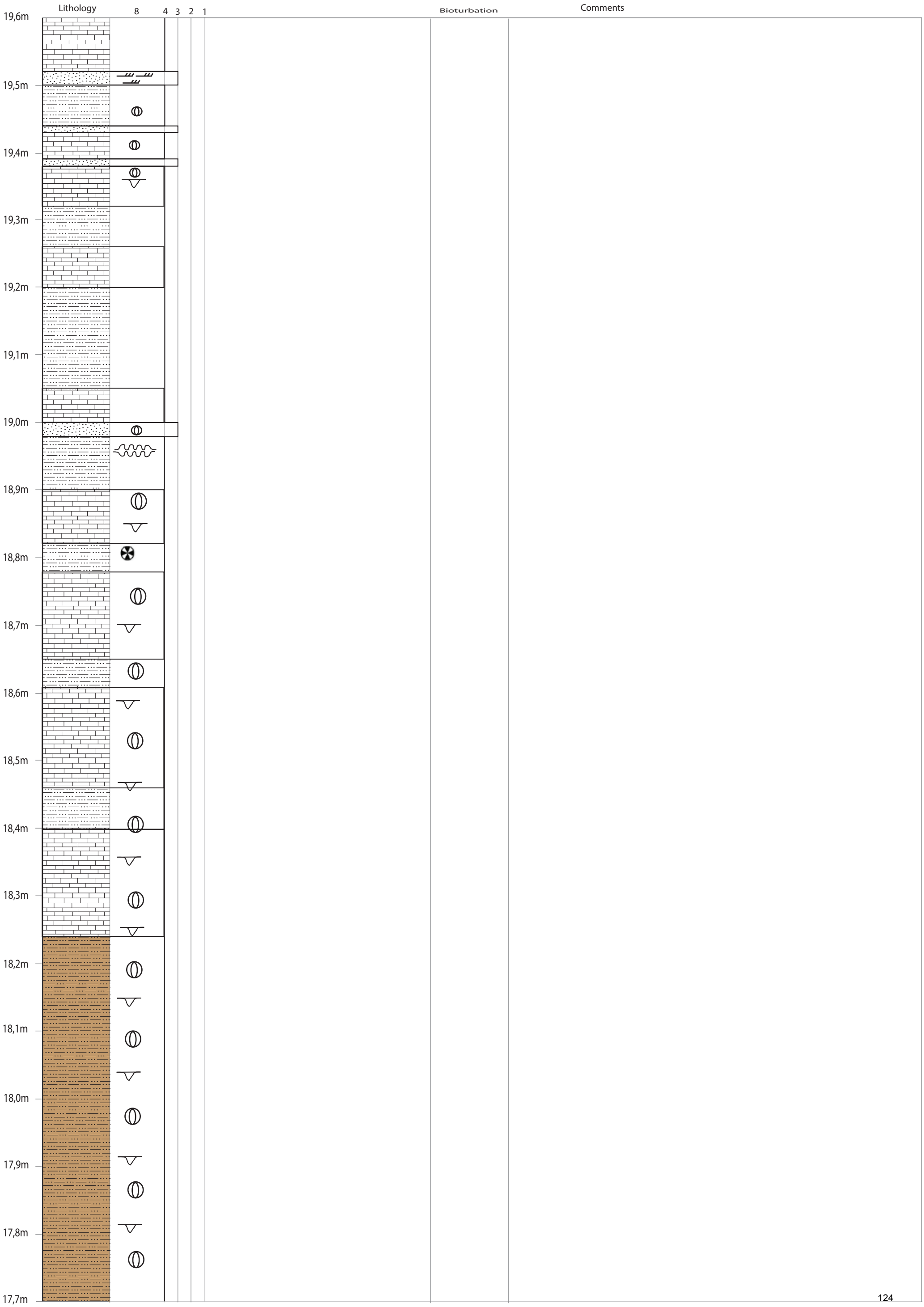

LOCATION: *Rambergøya* **SECTION NO:** *Profile 1* **SHEET NO:** *12/16* **DATE:** *23.09.2013* **BY:** *Martin Kjærsgaard*

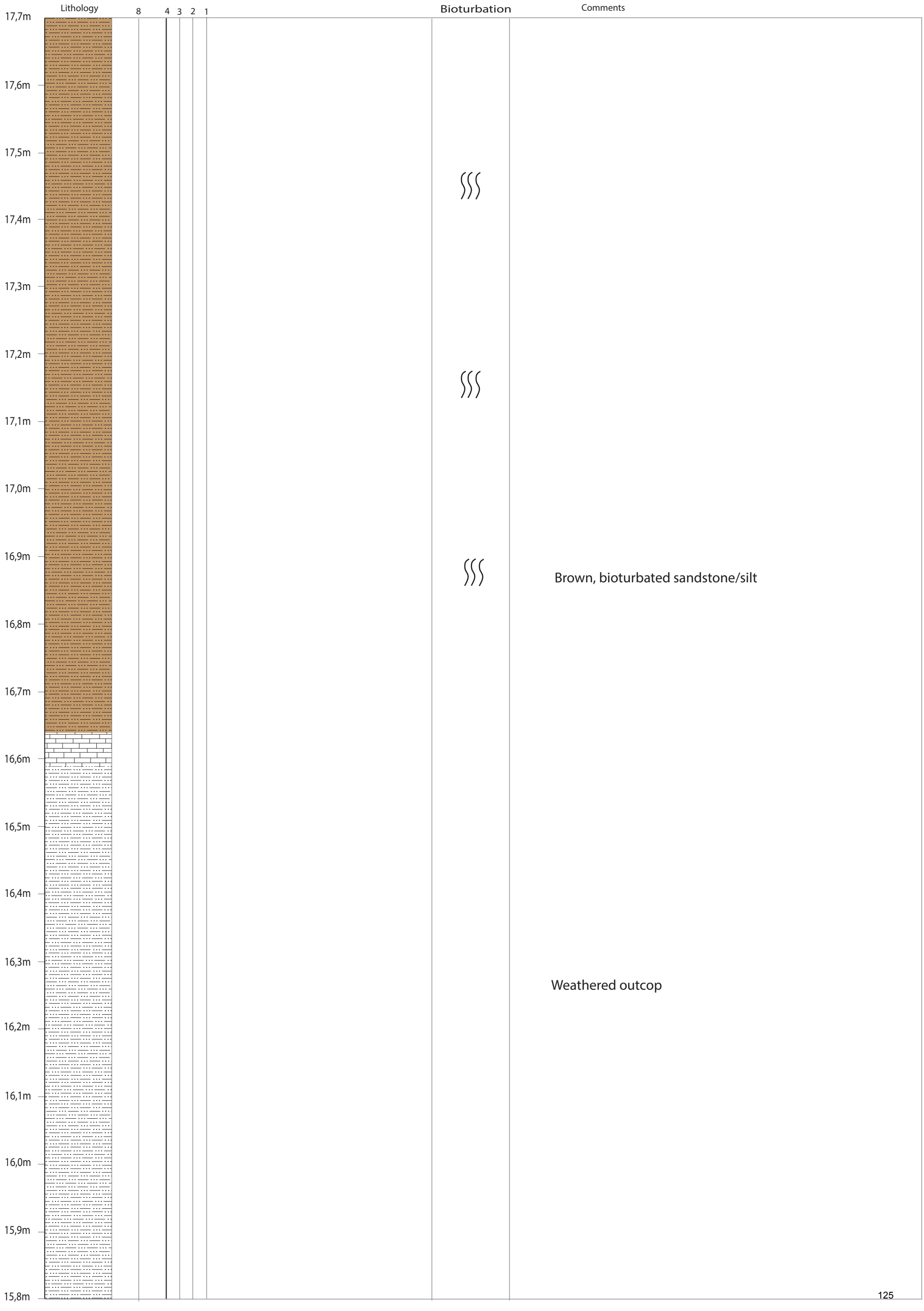

LOCATION: *Rambergøya* **SECTION NO:** *Profile 1* **SHEET NO:** *11/16* **DATE:** *23.09.2013* **BY:** *Martin Kjærsgaard*

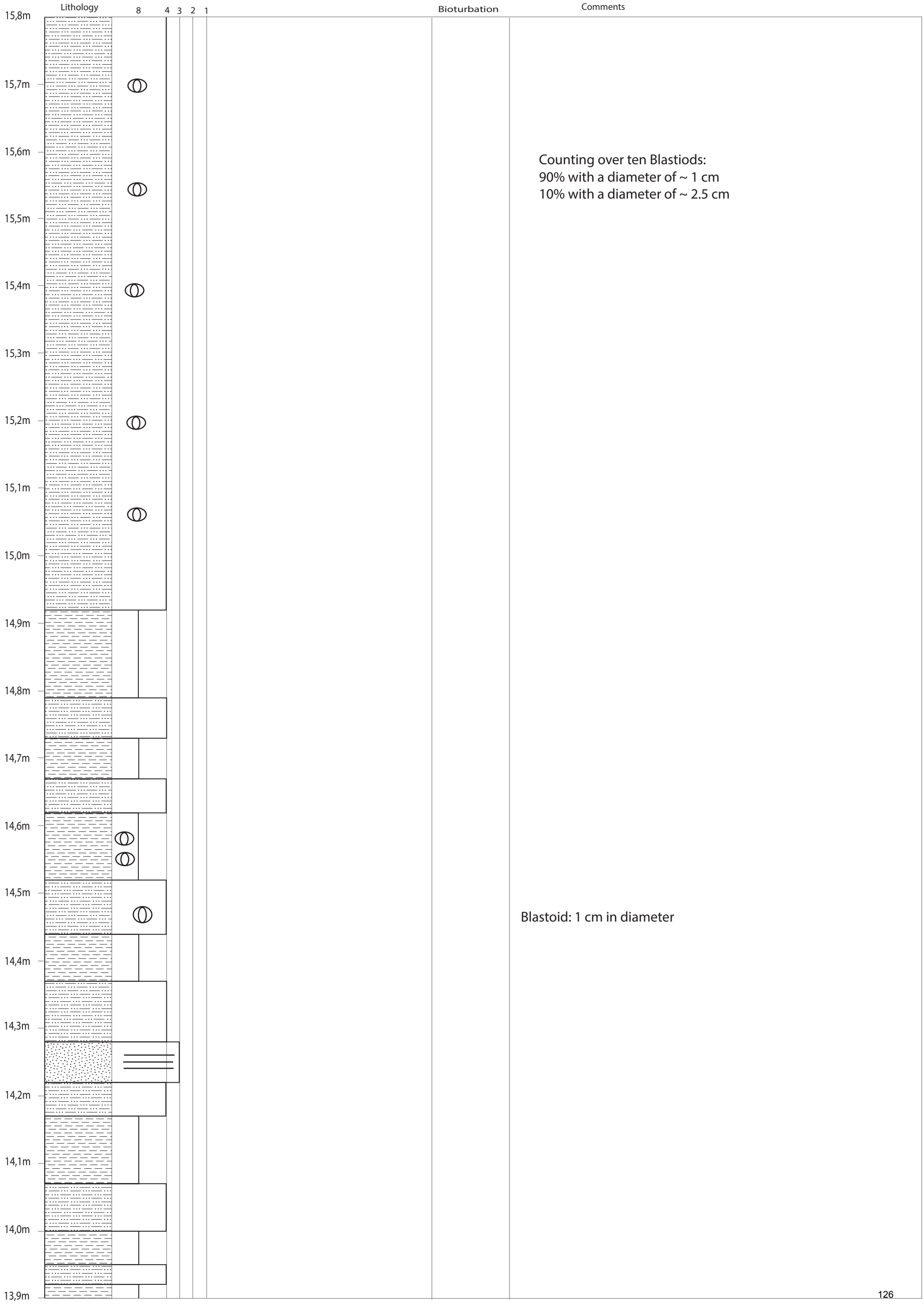

LOCATION: *Rambergøya* **SECTION NO:** *Profile 1* **SHEET NO:** *10/16* **DATE:** *23.09.2013* **BY:** *Martin Kjærsgaard*

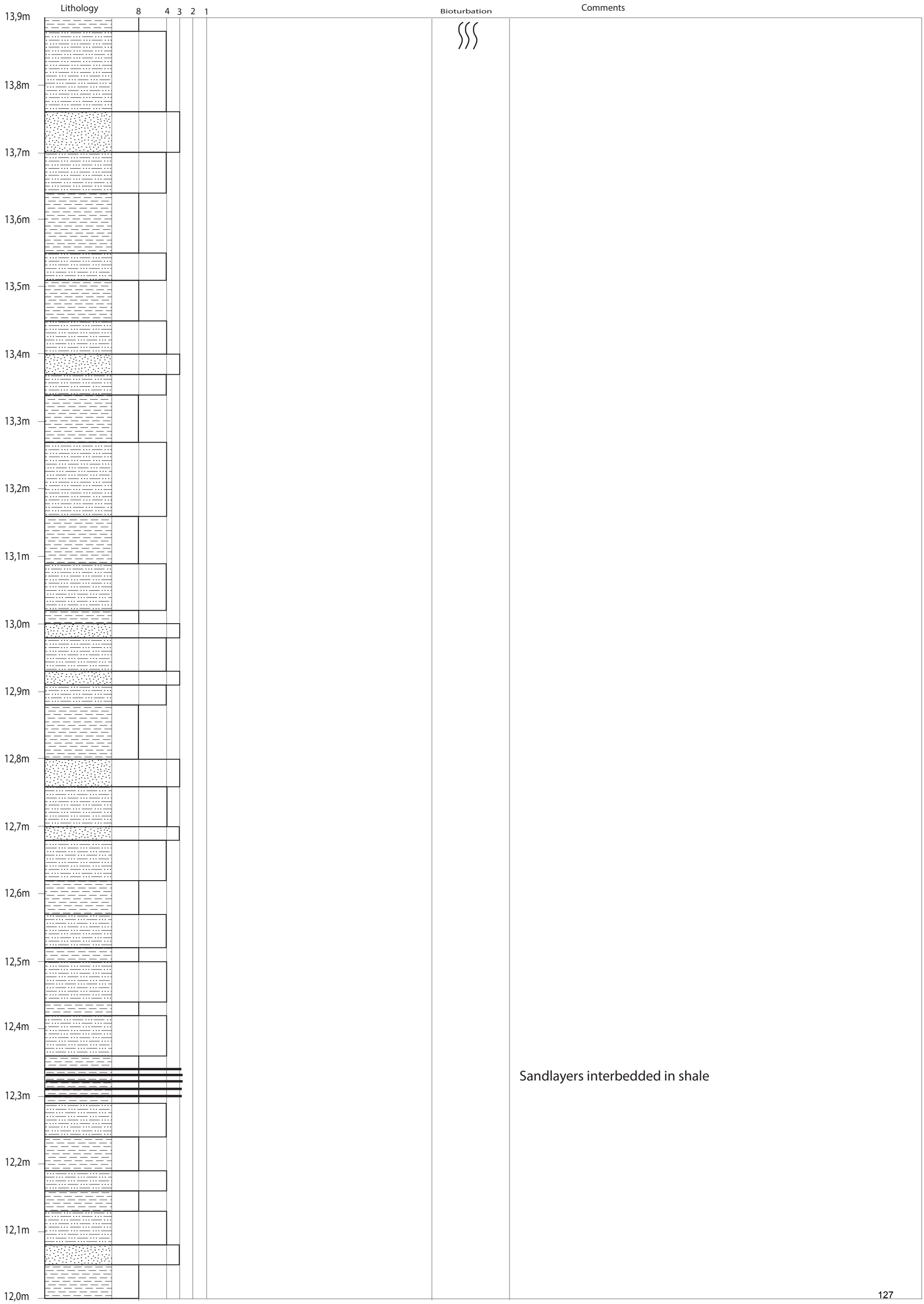

LOCATION: *Rambergøya* **SECTION NO:** *Profile 1* **SHEET NO:** *9/16* **DATE:** *23.09.2013* **BY:** *Martin Kjærsgaard*

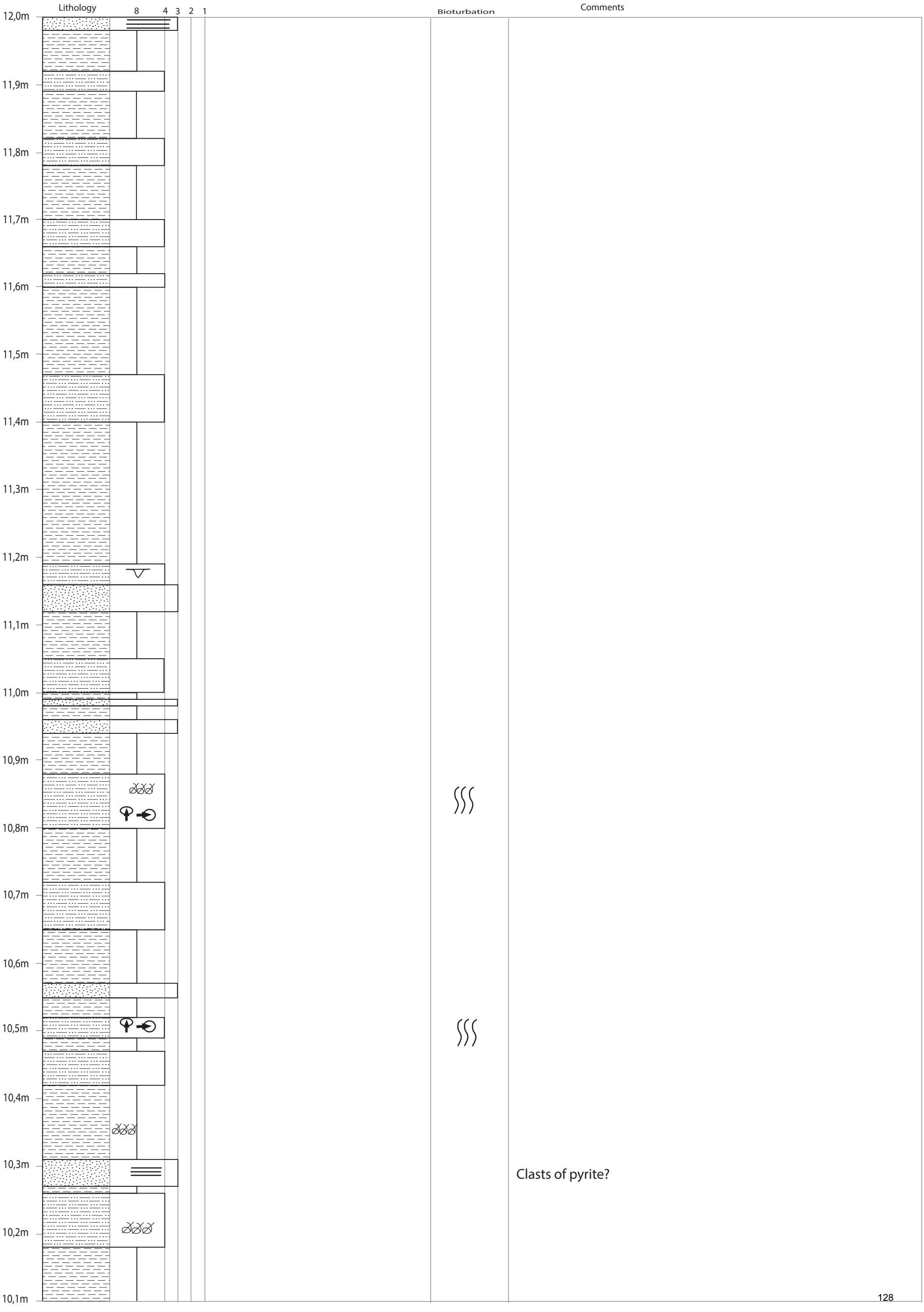

LOCATION: *Rambergøya* **SECTION NO:** *Profile 1* **SHEET NO:** *8/16* **DATE:** *23.09.2013* **BY:** *Martin Kjærsgaard*

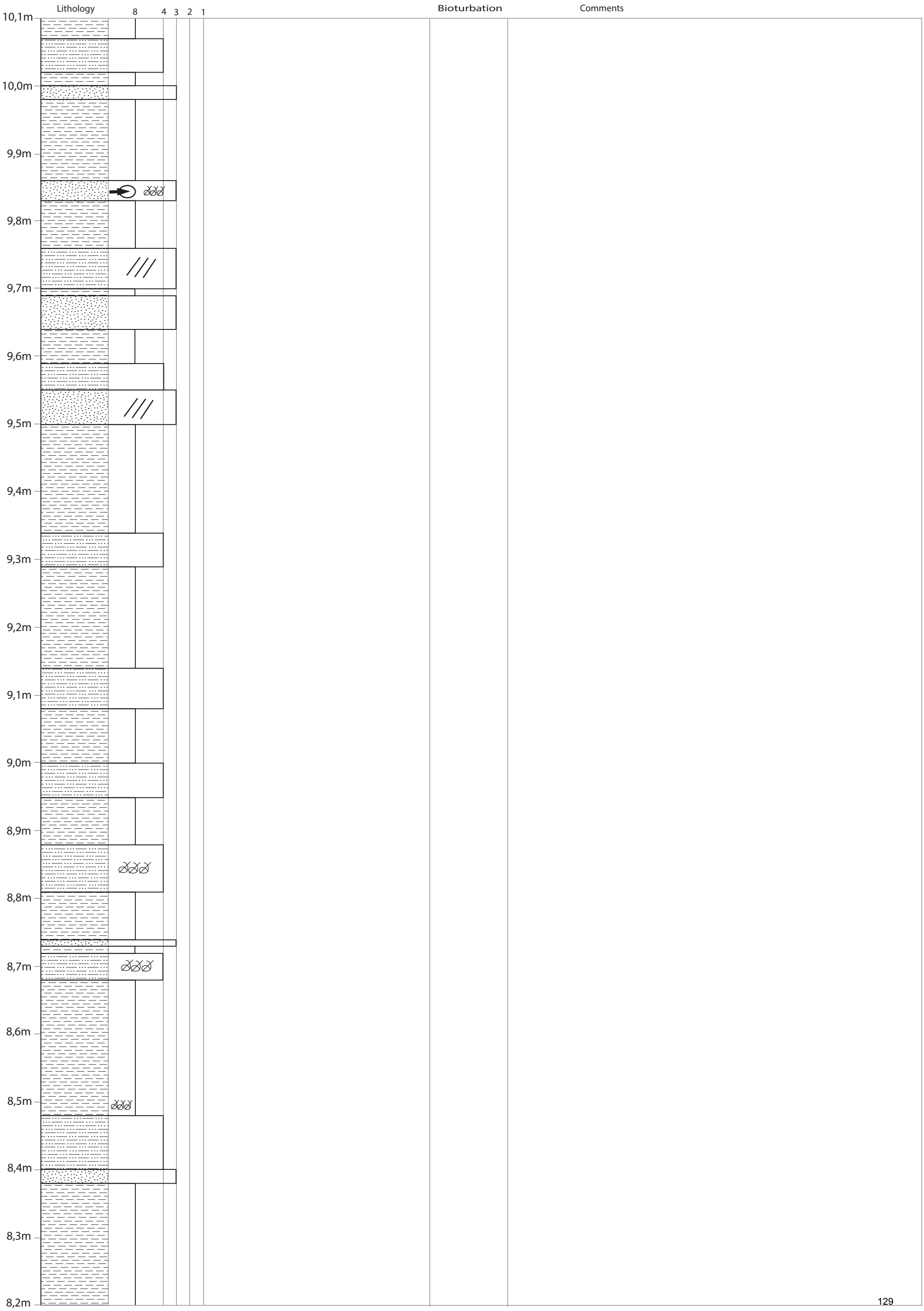

LOCATION: *Rambergøya* **SECTION NO:** *Profile 1* **SHEET NO:** *7/16* **DATE:** *23.09.2013* **BY:** *Martin Kjærsgaard*

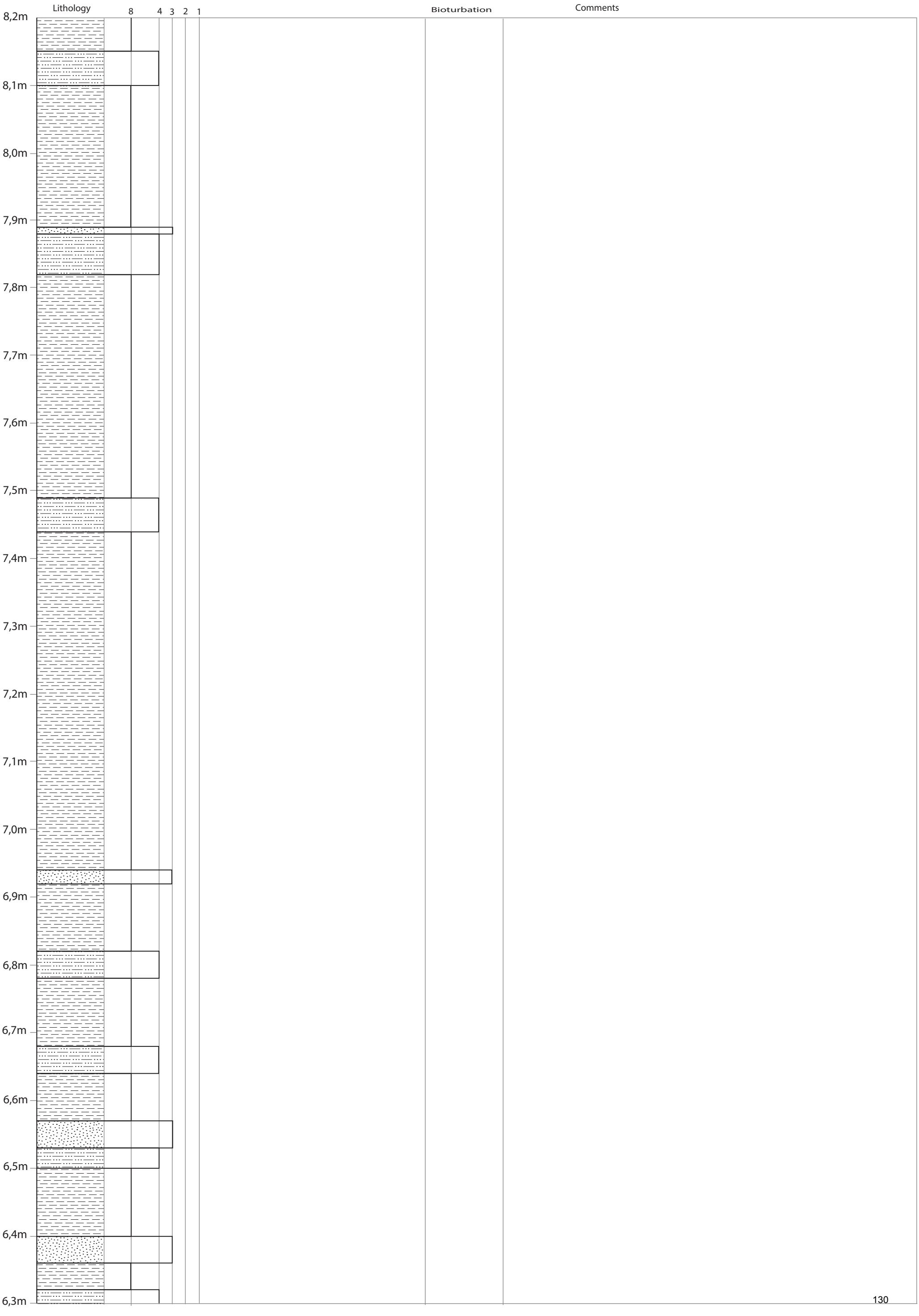

LOCATION: *Rambergøya* **SECTION NO:** *Profile 1* **SHEET NO:** *6* **DATE:** *21.09.2013* **BY:** *Martin Kjærsgaard*

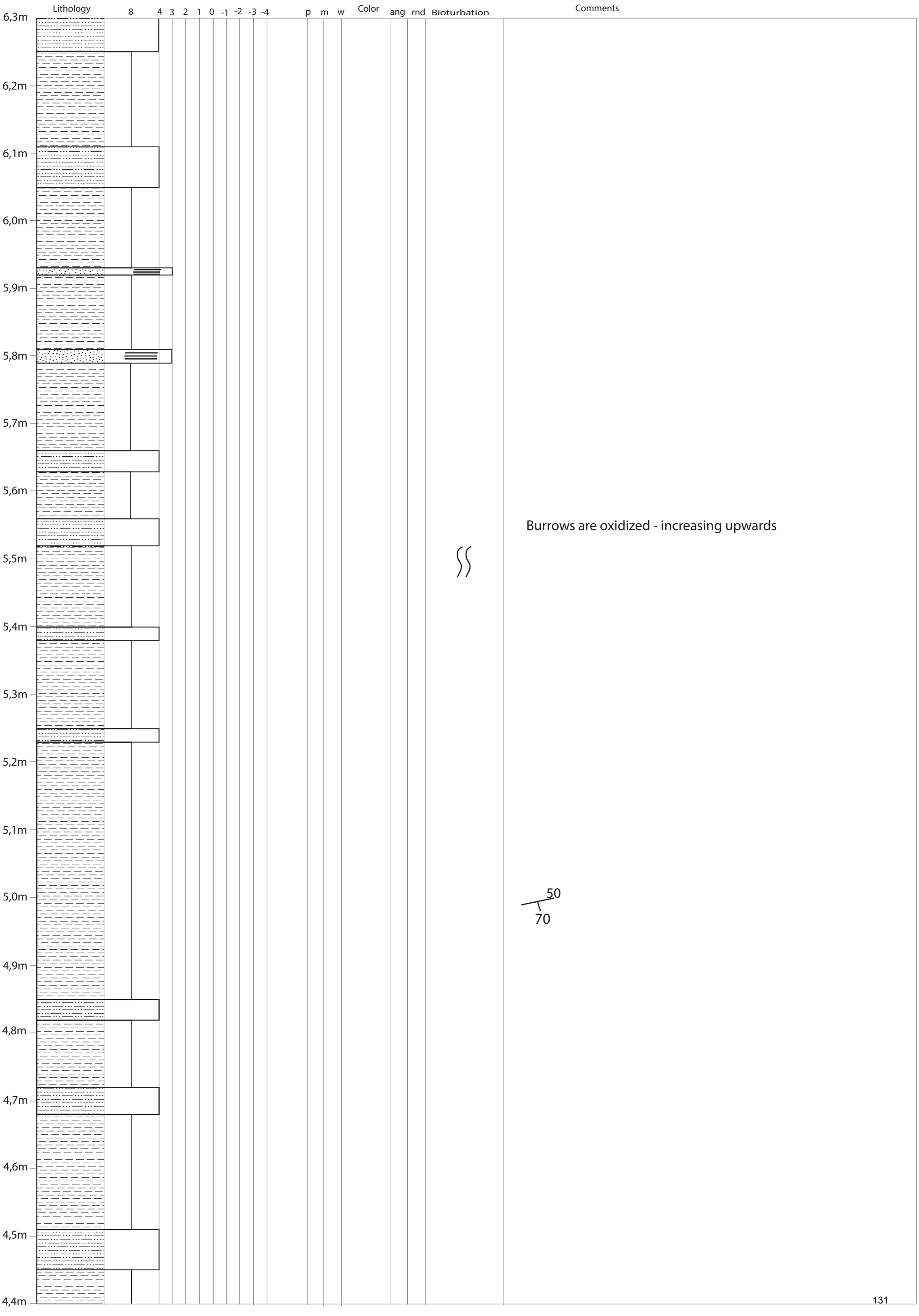

LOCATION: *Rambergøya* **SECTION NO:** *Profile 1* **SHEET NO:** *5/16* **DATE:** *21.09.2013* **BY:** *Martin Kjærsgaard*

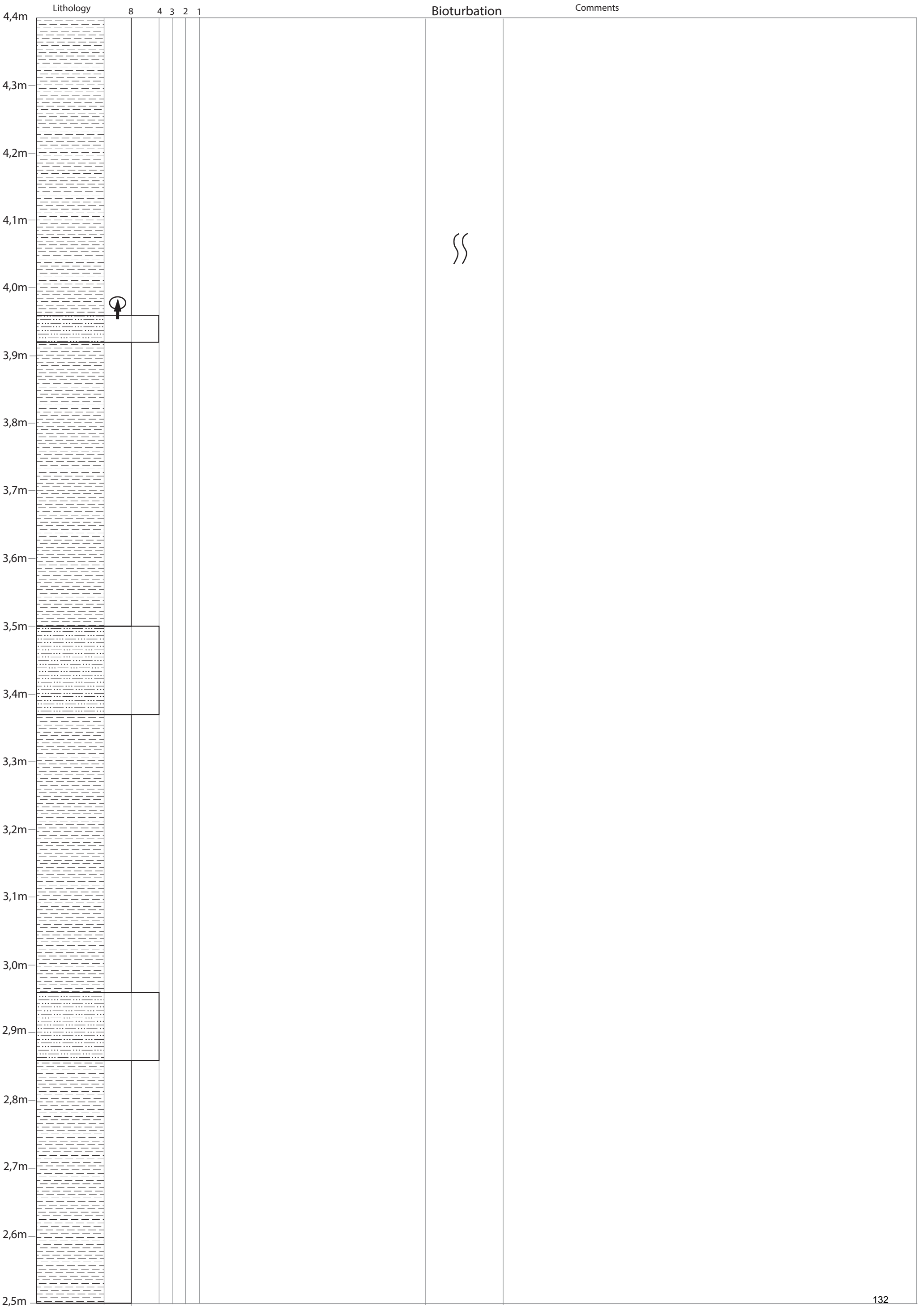

LOCATION: *Rambergøya* **SECTION NO:** *Profile 1* **SHEET NO:** *4/16* **DATE:** *21.09.2013* **BY:** *Martin Kjærsgaard*

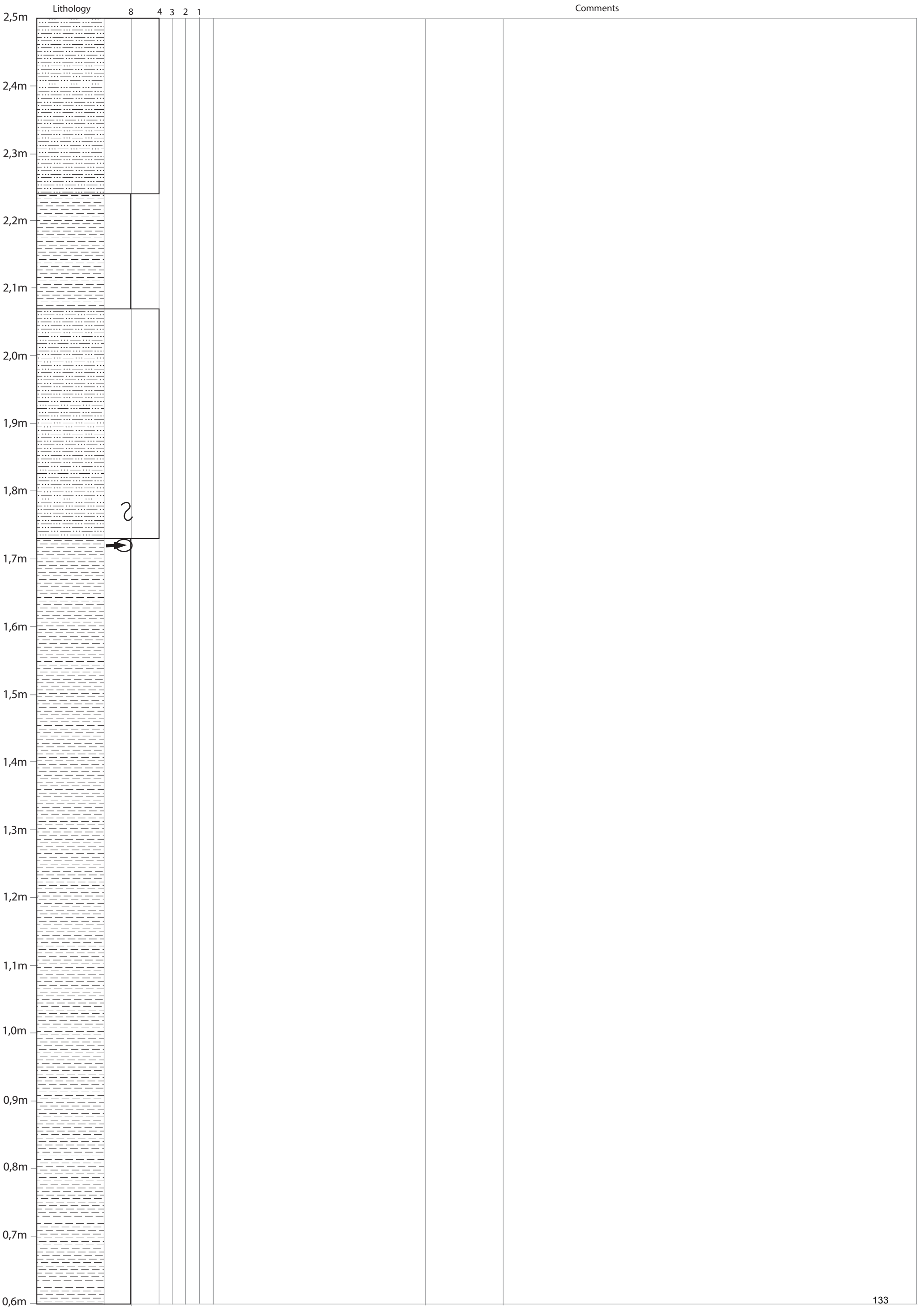

LOCATION: *Rambergøya* **SECTION NO:** *Profile 1* **SHEET NO:** *3/16* **DATE:** *21.09.2013* **BY:** *Martin Kjærsgaard*

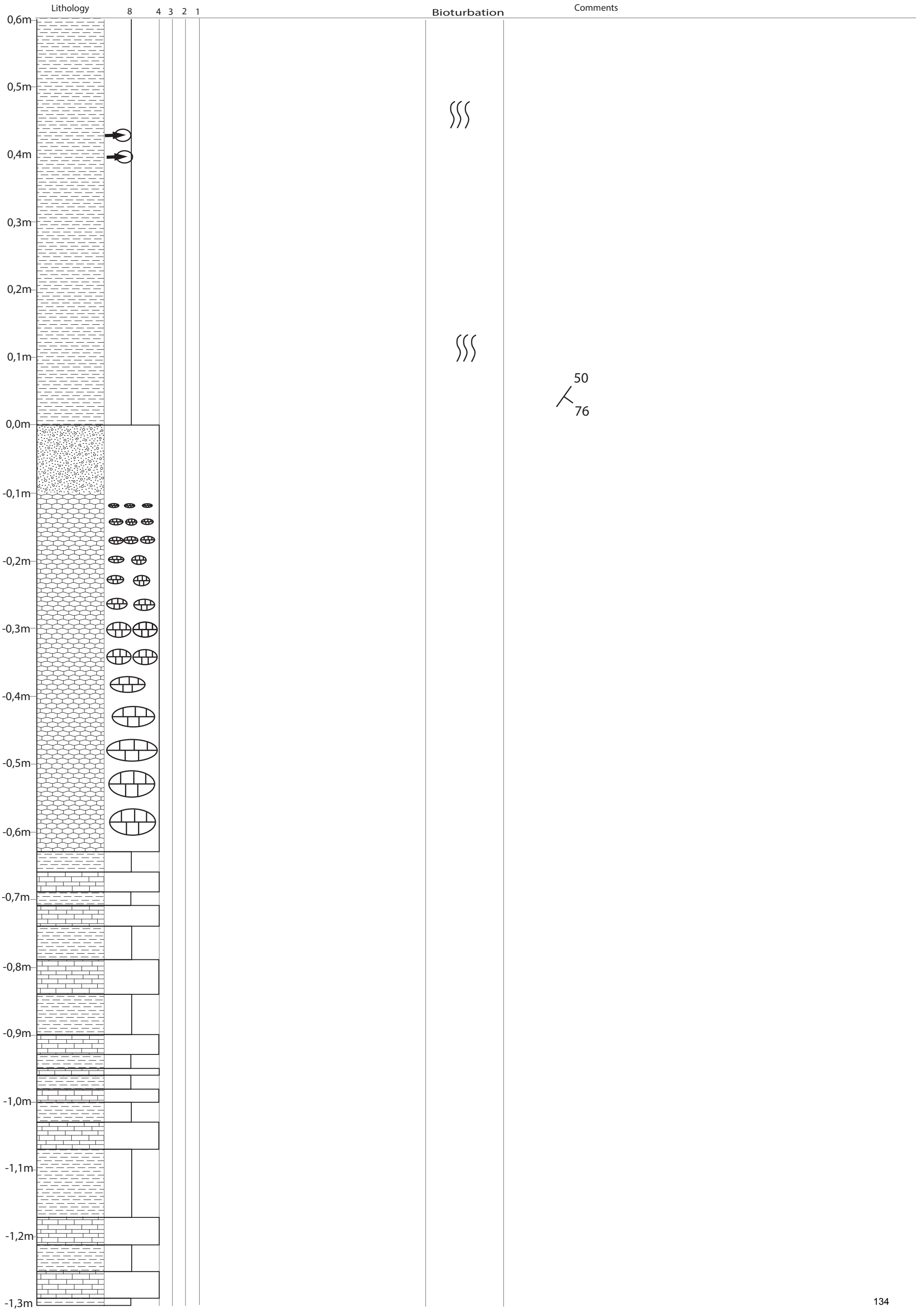

LOCATION: *Langøyene* **SECTION NO:** *Profile 1* **SHEET NO:** *2/16* **DATE:** *08.09.2013* **BY:** *Martin Kjærsgaard*

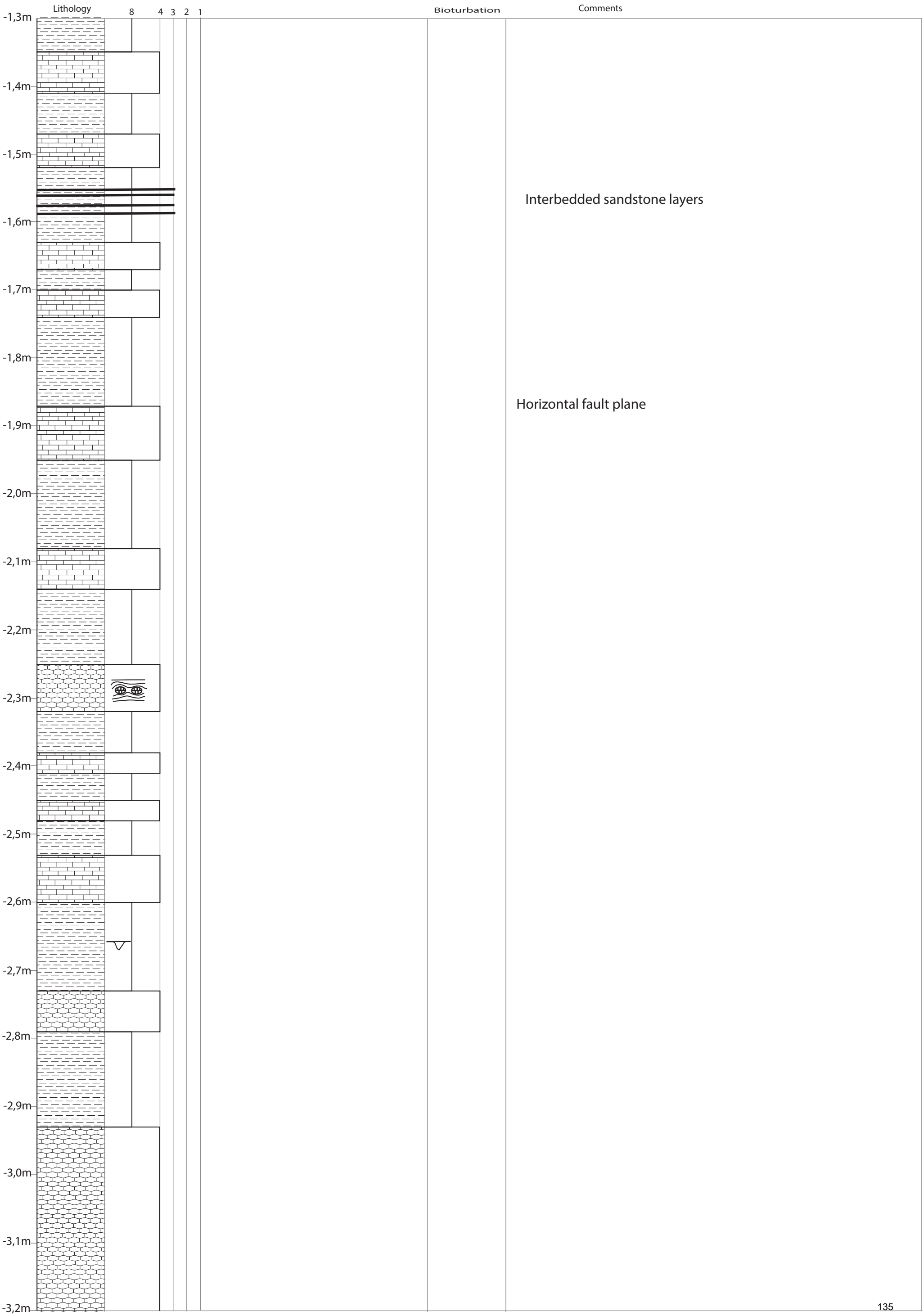

LOCATION: *Rambergøya* **SECTION NO:** *Profile 1* **SHEET NO:** *1/16* **DATE:** *21.09.2013* **BY:** *Martin Kjærsgaard*

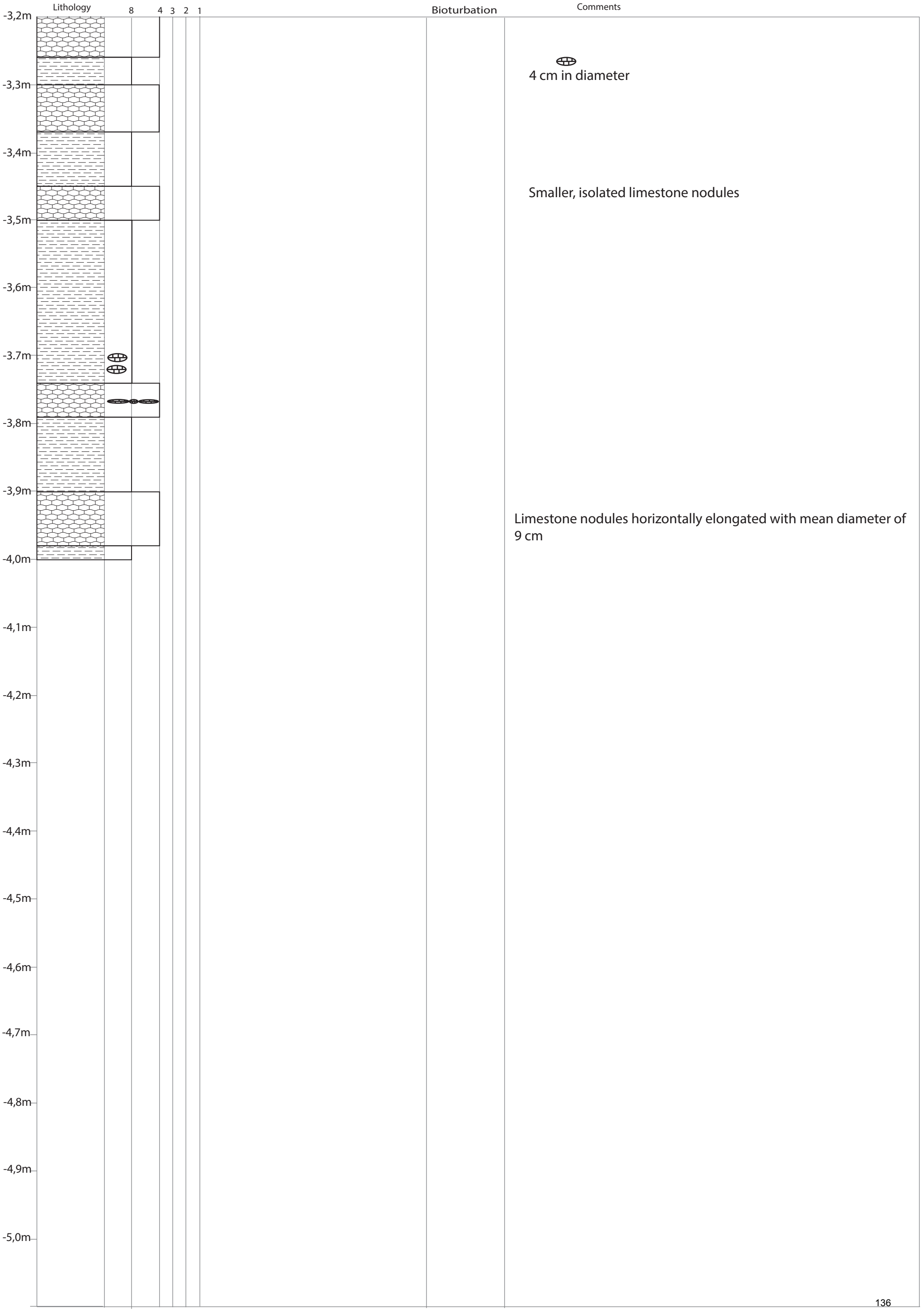

LANGØYENE PROFILE 1

SEDIMENTARY LOG

Scale: 1:10

LOCATION: *Langøyene* **SECTION NO:** *Profile 1* **SHEET NO:** *16/16* **DATE:** *13.09.2013* **BY:** *Martin Kjærsgaard*

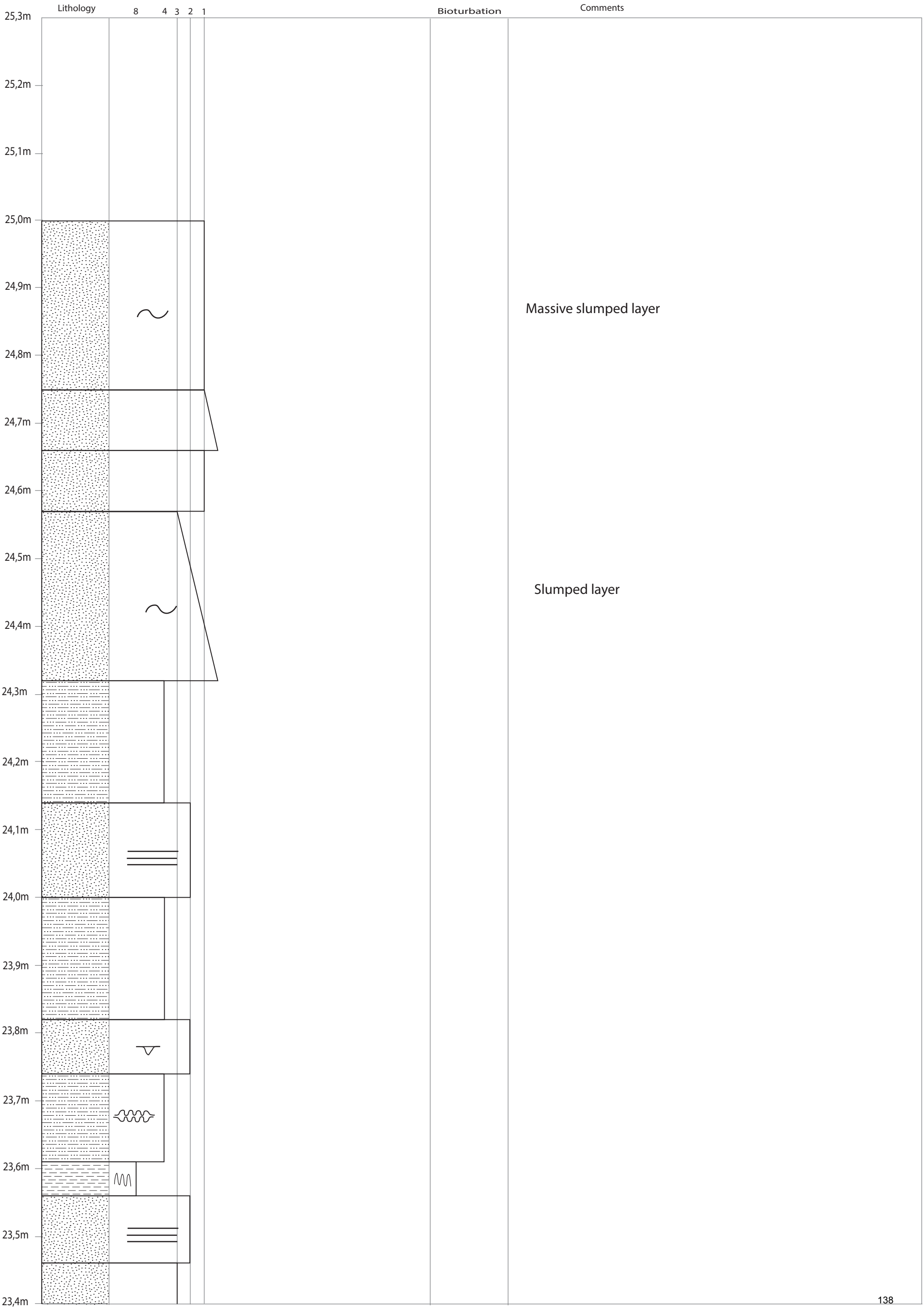

LOCATION: *Langøyene* **SECTION NO:** *Profile 1* **SHEET NO:** *15/16* **DATE:** *13.09.2013* **BY:** *Martin Kjærsgaard*

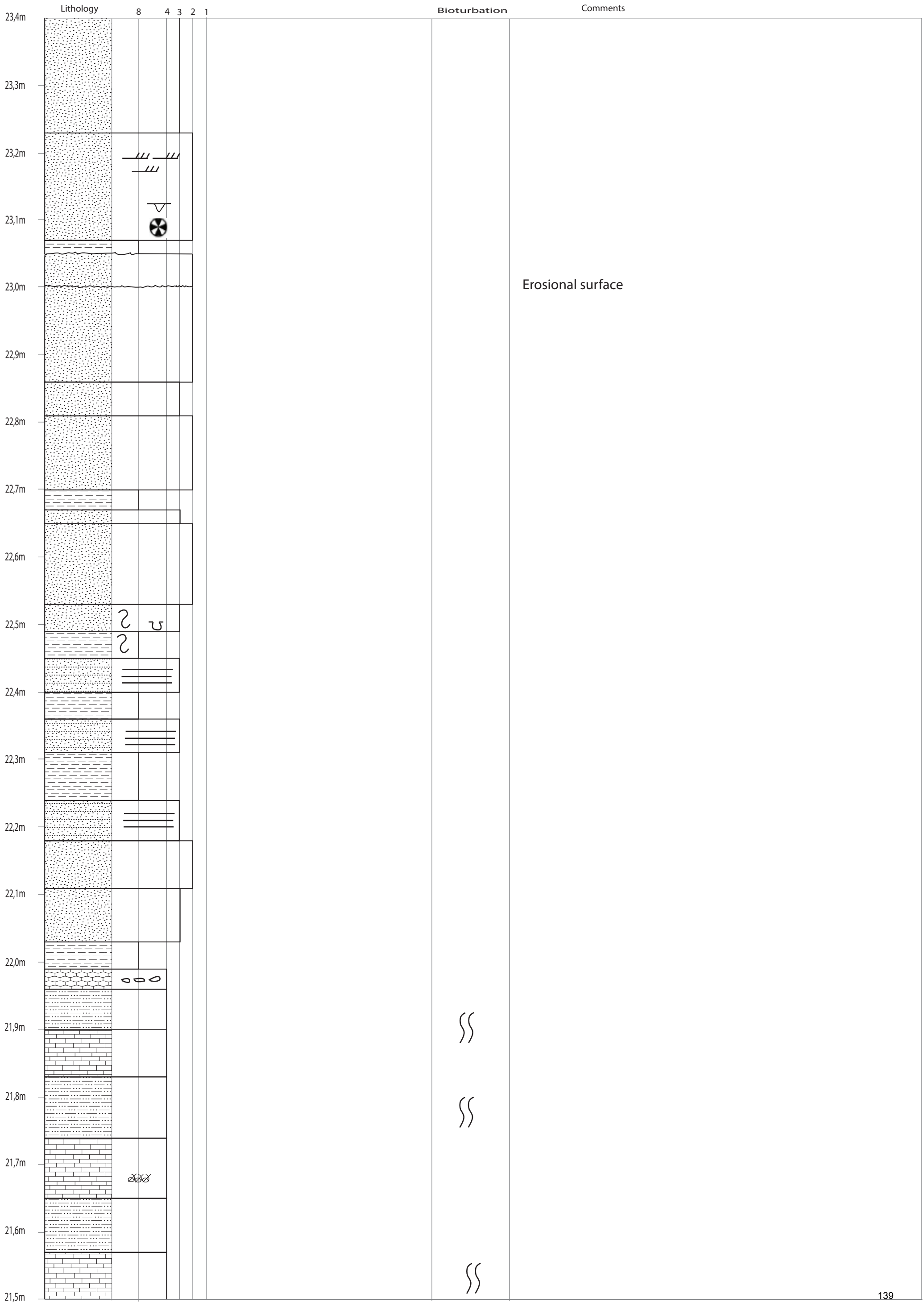

LOCATION: *Langøyene* **SECTION NO:** *Profile 1* **SHEET NO:** *14/16* **DATE:** *13.09.2013* **BY:** *Martin Kjærsgaard*

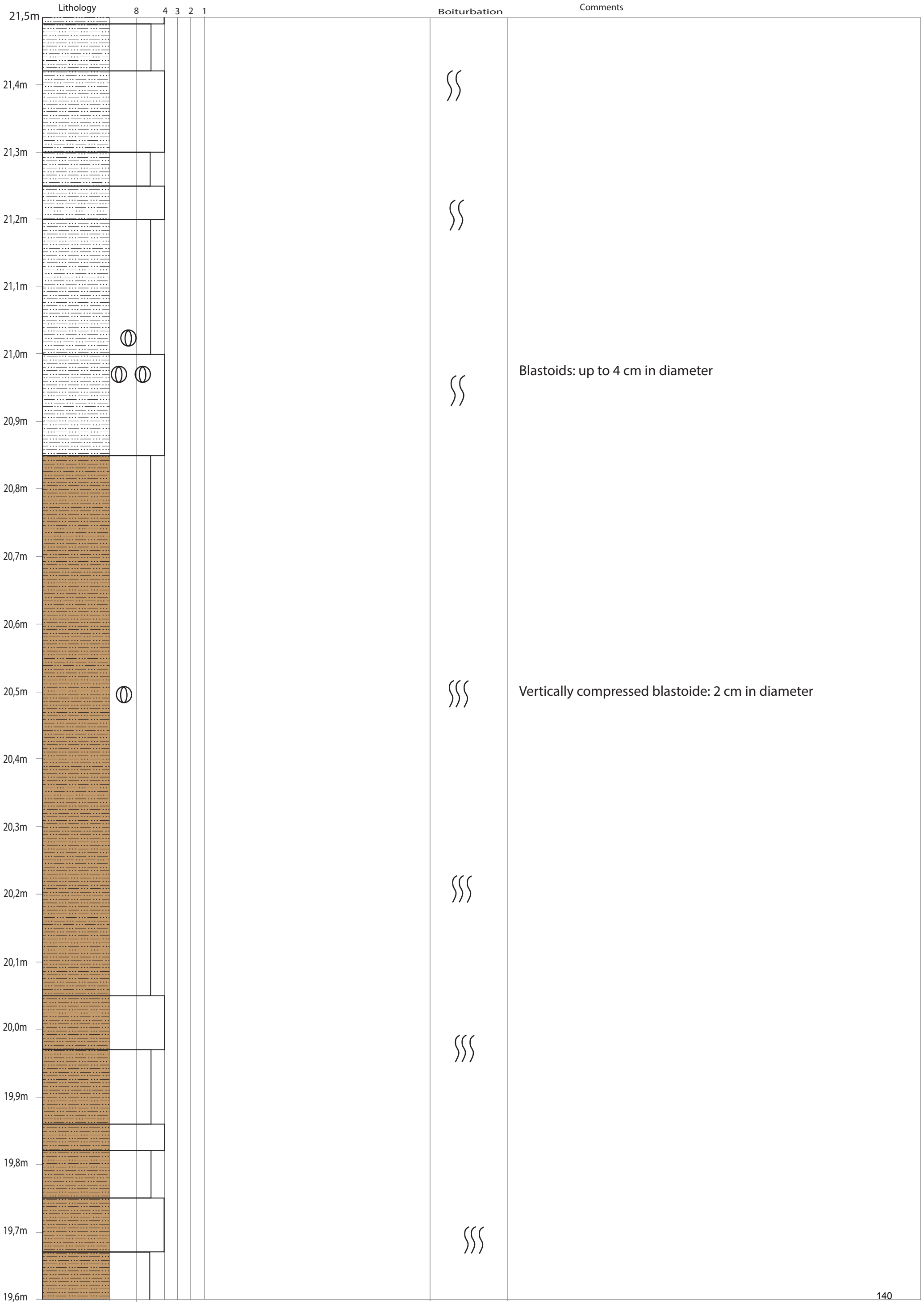

LOCATION: *Langøyene* **SECTION NO:** *Profile 1* **SHEET NO:** *13/16* **DATE:** *13.09.2013* **BY:** *Martin Kjærsgaard*

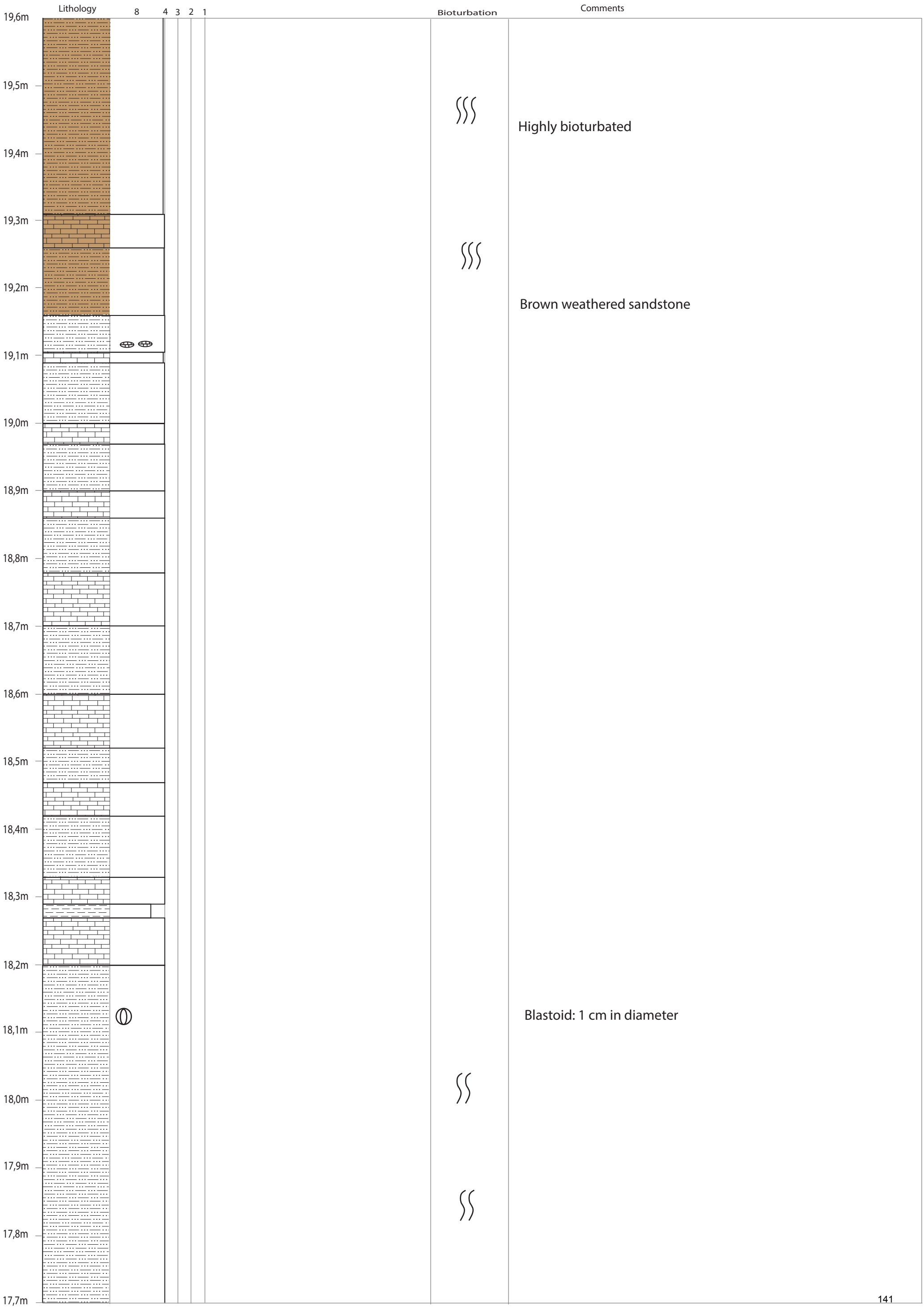

LOCATION: *Langøyene* **SECTION NO:** *Profile 1* **SHEET NO:** *12/16* **DATE:** *13.09.2013* **BY:** *Martin Kjærsgaard*

Lithology	Bioturbation	Comments
17,7m – 17,6m – 17,5m – 17,4m – 17,3m – 17,2m – 17,1m – 17,0m – 16,9m – 16,8m – 16,7m – 16,6m – 16,5m – 16,4m – 16,3m – 16,2m – 16,1m – 16,0m – 15,9m – 15,8m		Pinching sand layers in the silt
16,7m – 16,6m – 16,5m		Internal lamination. Ripple drift lamination on top. Little bioturbation in the sand layer: 1.

LOCATION: *Langøyene* **SECTION NO:** *Profile 1* **SHEET NO:** *11/16* **DATE:** *13.09.2013* **BY:** *Martin Kjærsgaard*

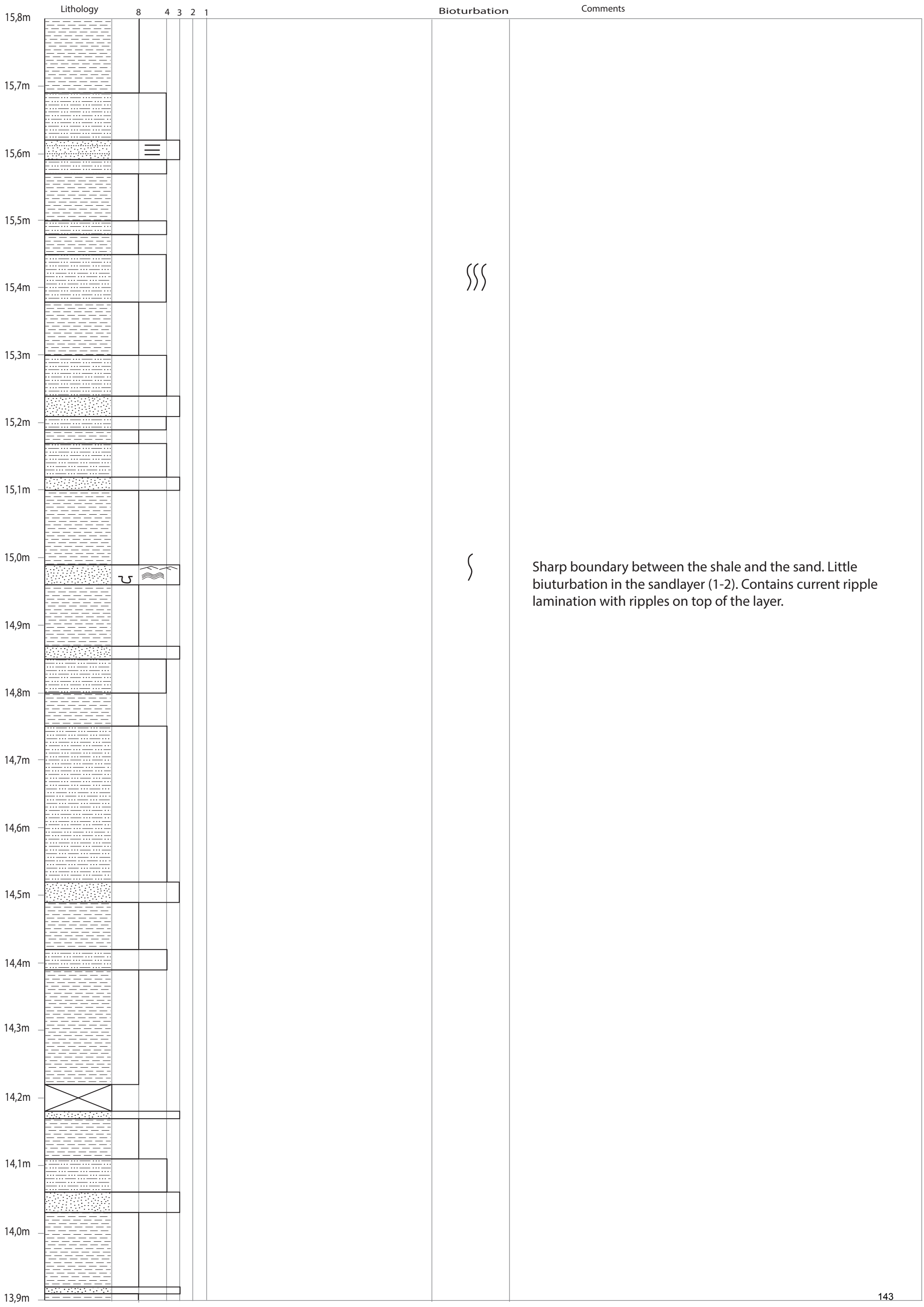

LOCATION: *Langøyene* **SECTION NO:** *Profile 1* **SHEET NO:** *10/16* **DATE:** *13.09.2013* **BY:** *Martin Kjærsgaard*

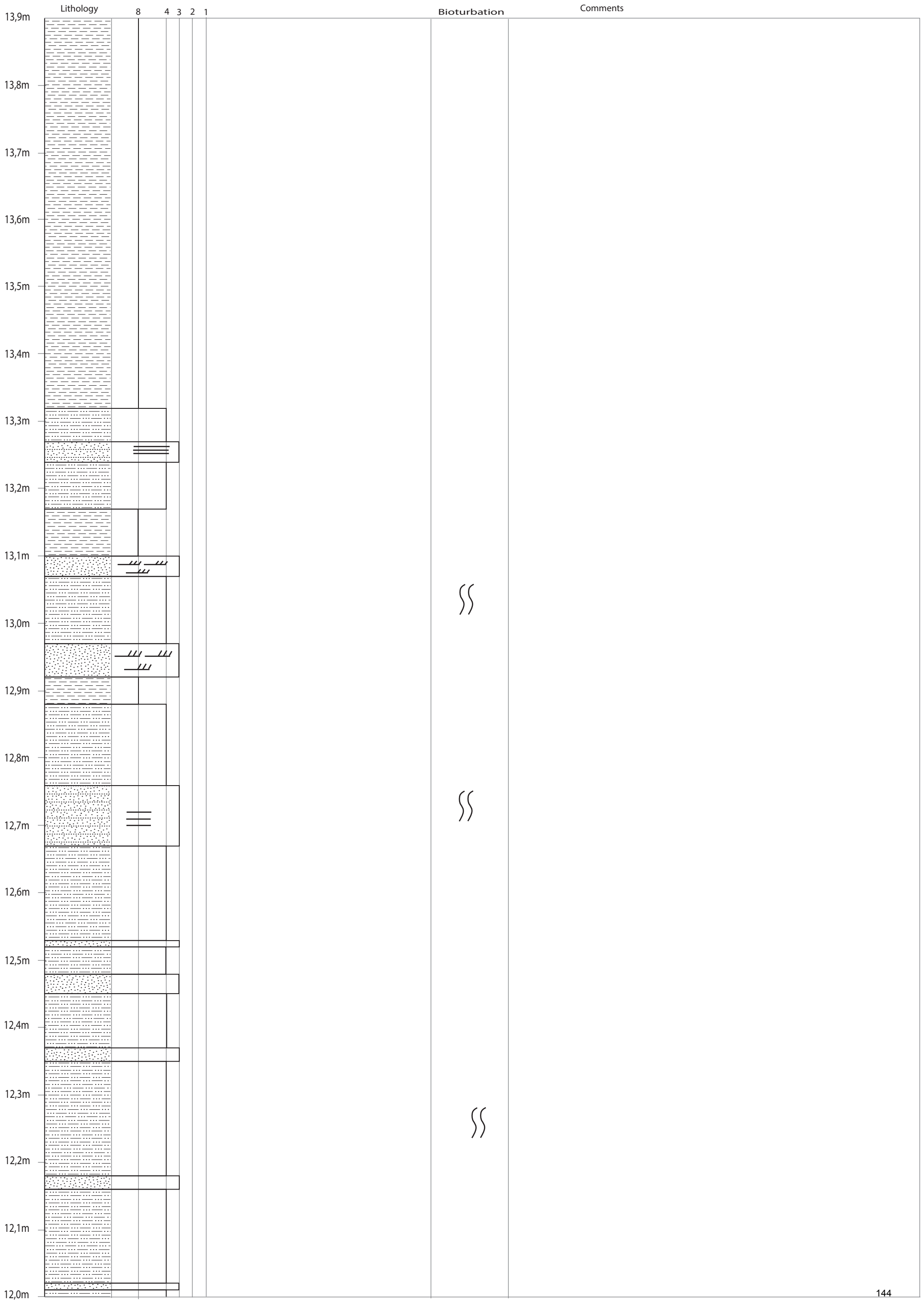

LOCATION: *Langøyene* **SECTION NO:** *Profile 1* **SHEET NO:** *9/16* **DATE:** *08.09.2013* **BY:** *Martin Kjærsgaard*

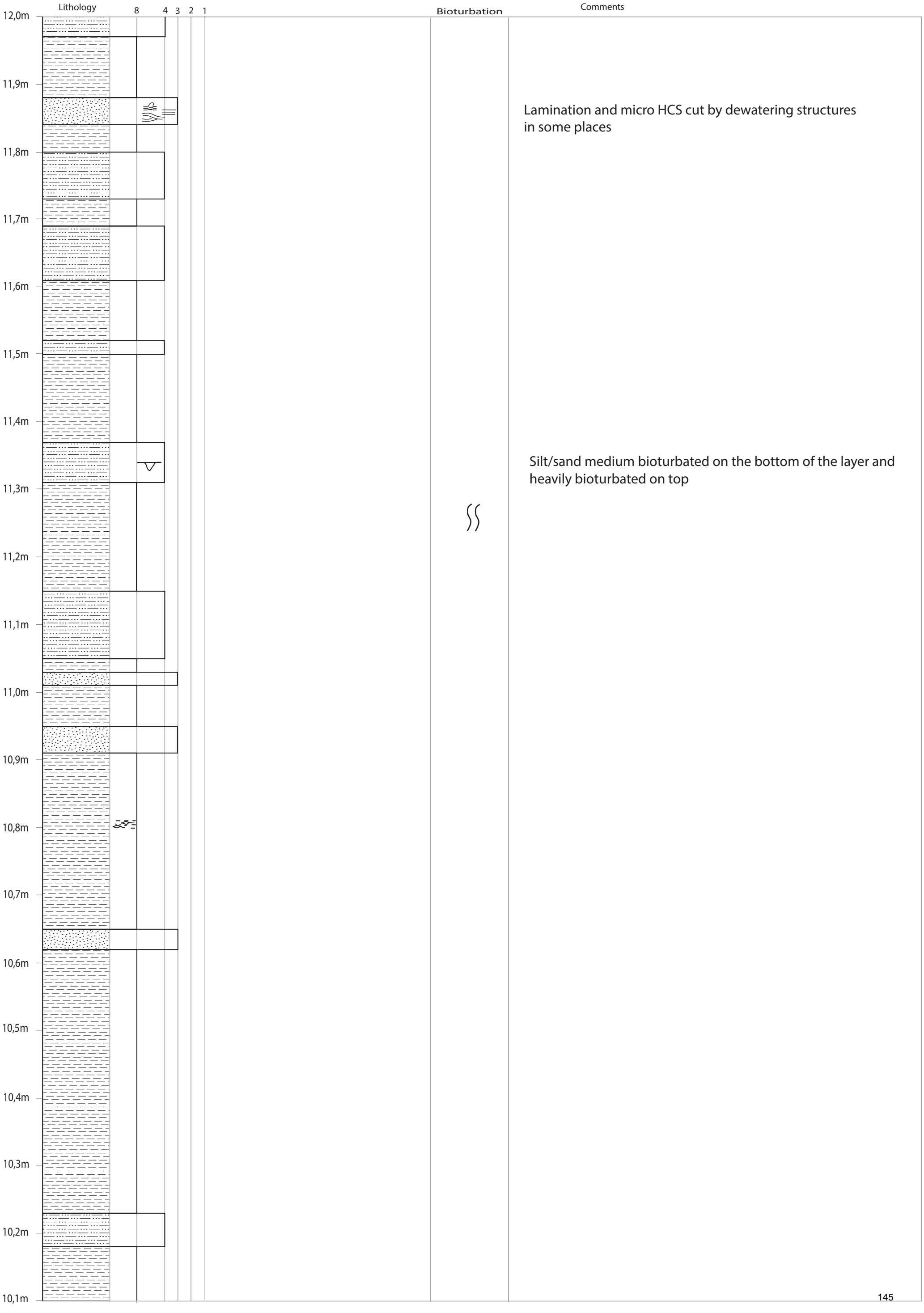

LOCATION: *Langøyene* **SECTION NO:** *Profile 1* **SHEET NO:** *8/16* **DATE:** *08.09.2013* **BY:** *Martin Kjærsgaard*

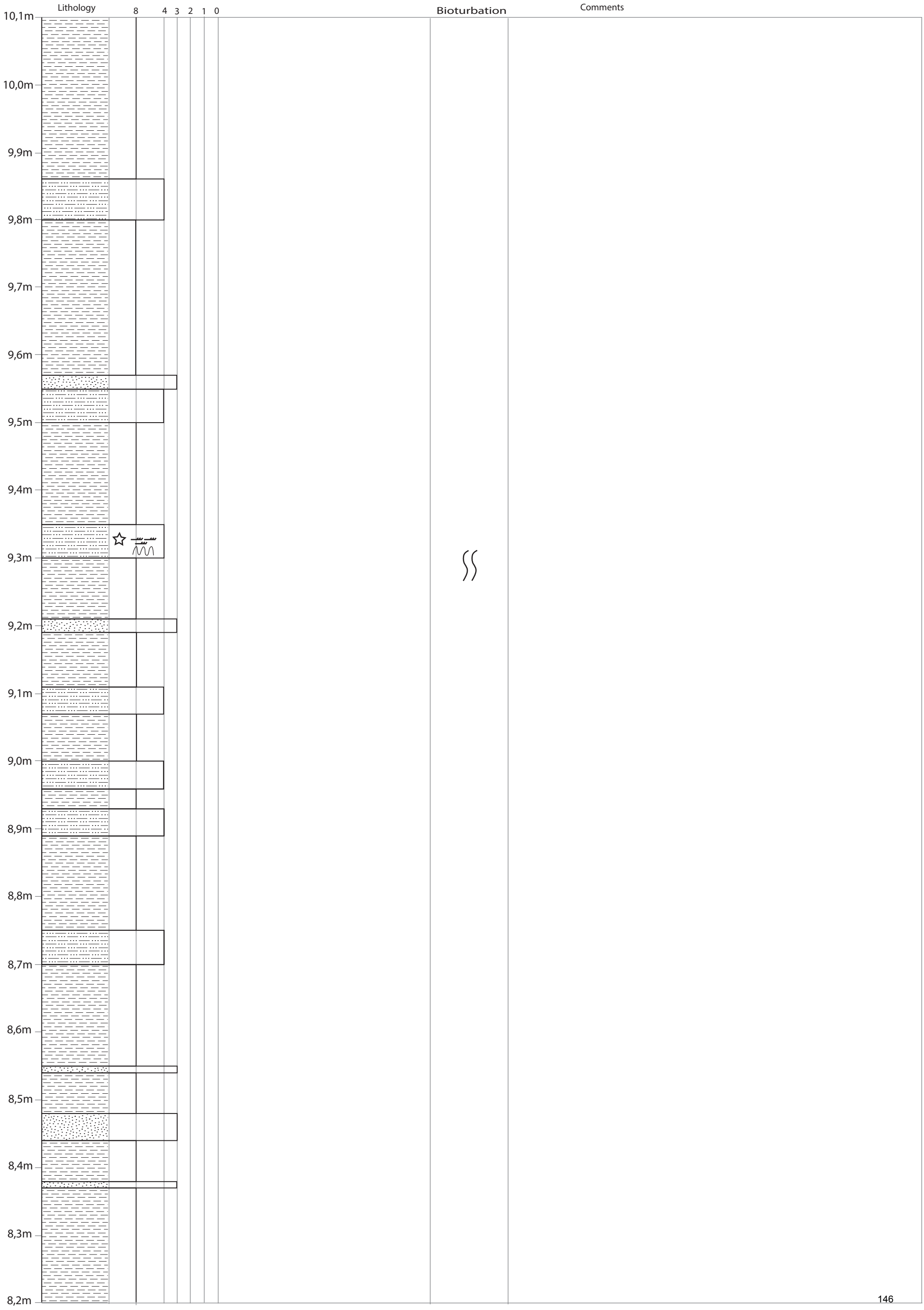

LOCATION: *Langøyene* **SECTION NO:** *Profile 1* **SHEET NO:** *7/16* **DATE:** *08.09.2013* **BY:** *Martin Kjærsgaard*

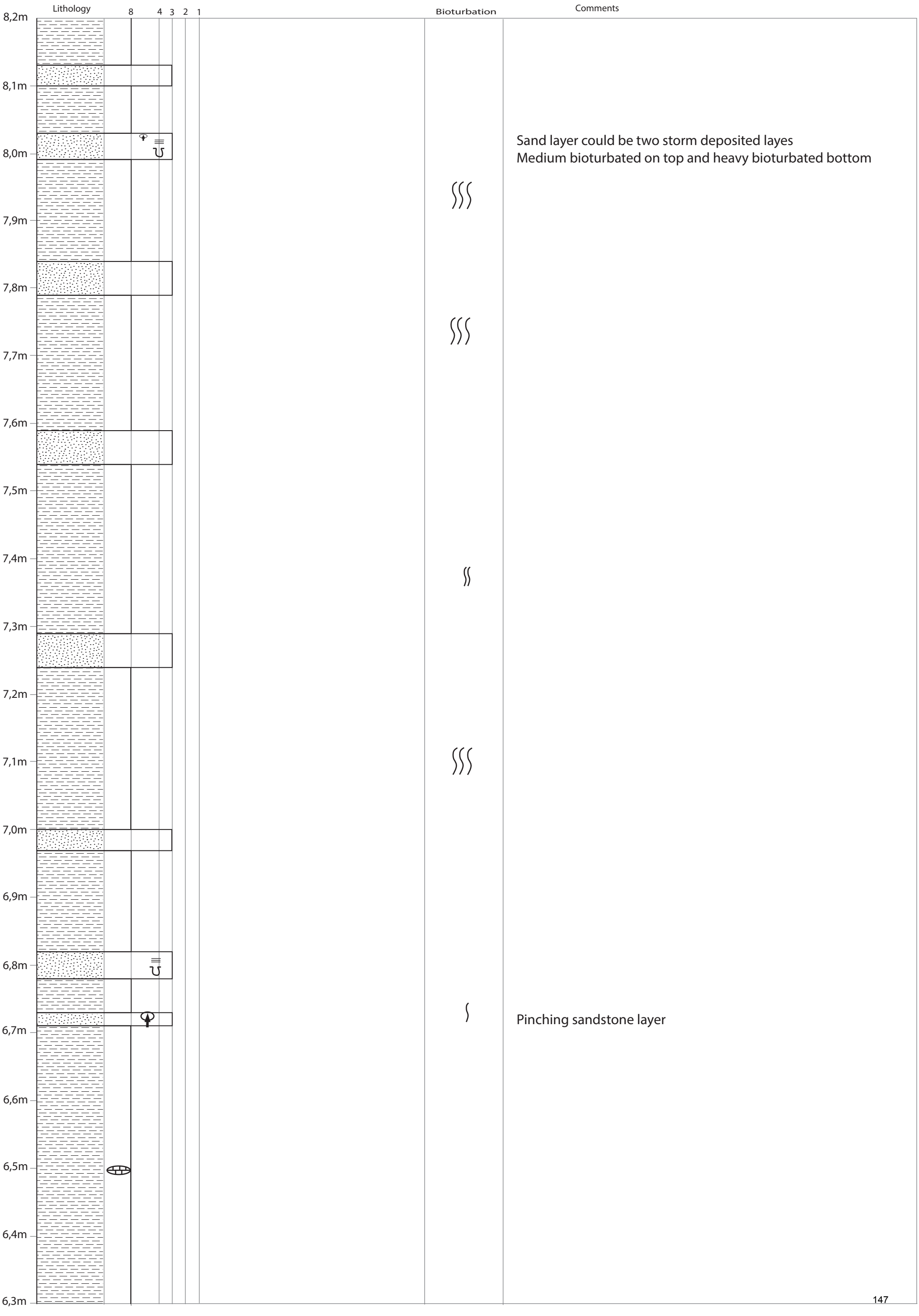

LOCATION: *Langøyene* **SECTION NO:** *Profile 1* **SHEET NO:** *6* **DATE:** *08.09.2013* **BY:** *Martin Kjærsgaard*

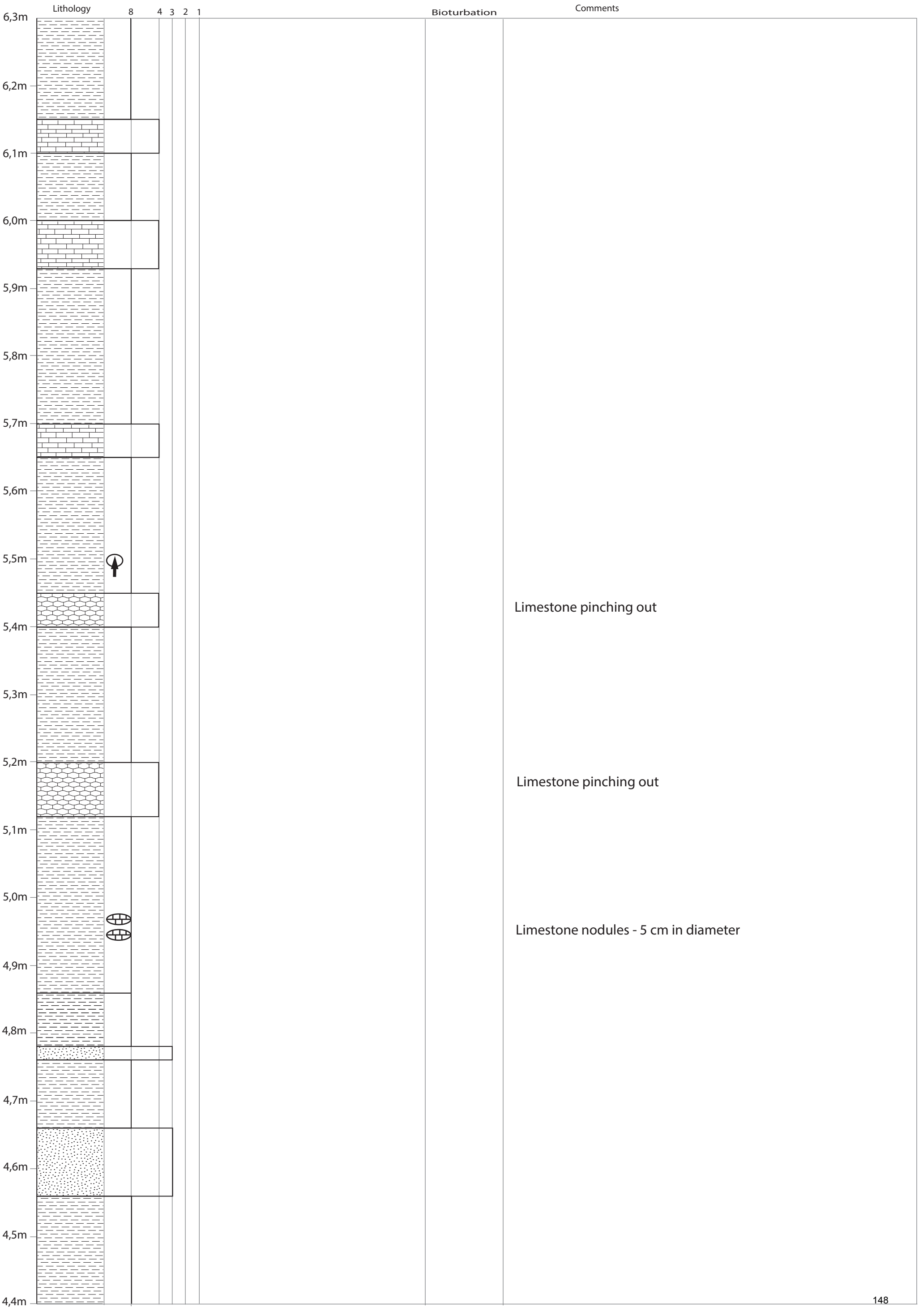

LOCATION: *Langøyene* **SECTION NO:** *Profile 1* **SHEET NO:** *5/16* **DATE:** *08.09.2013* **BY:** *Martin Kjærsgaard*

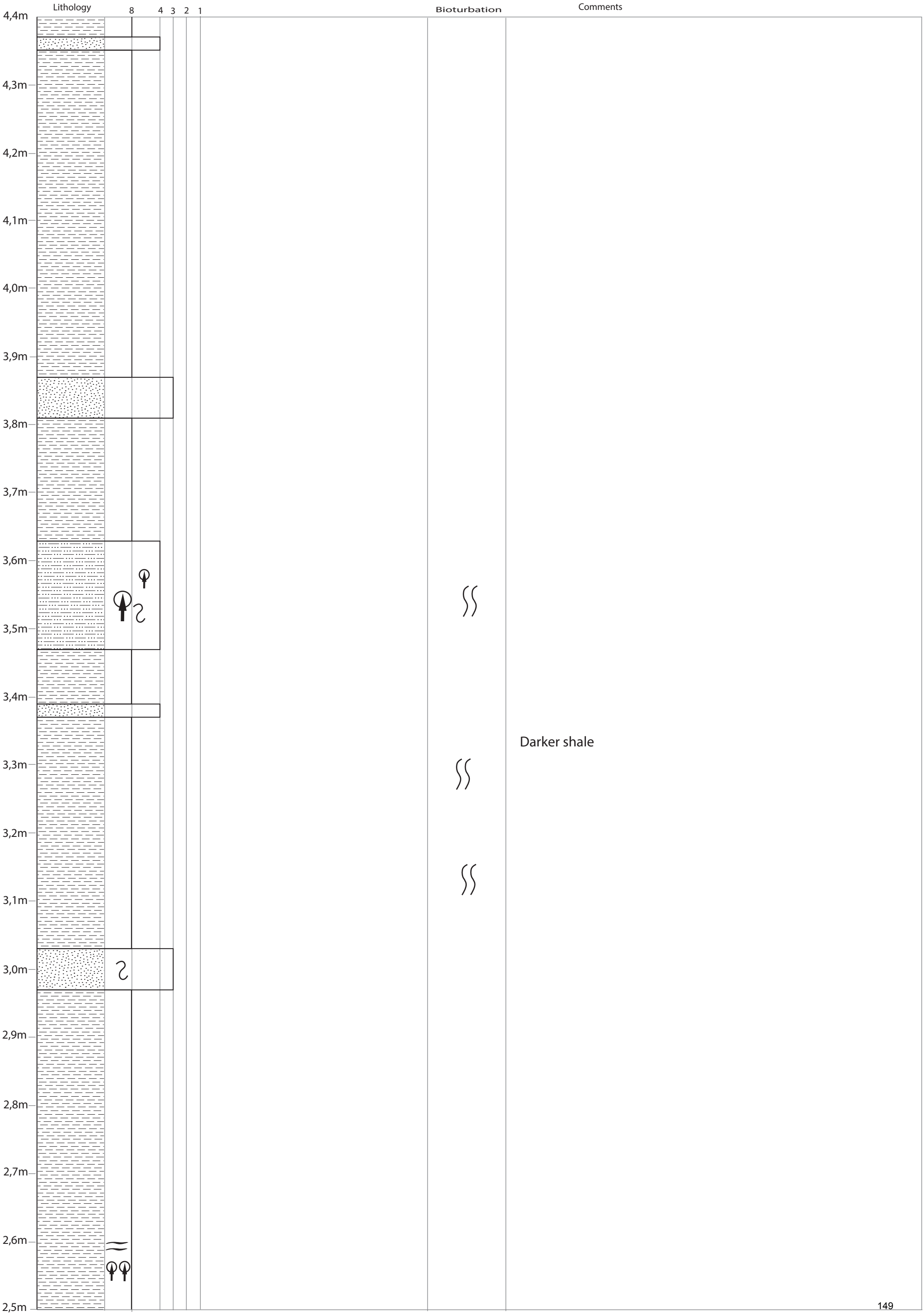

LOCATION: *Langøyene* **SECTION NO:** *Profile 1* **SHEET NO:** *4/16* **DATE:** *08.09.2013* **BY:** *Martin Kjærsgaard*

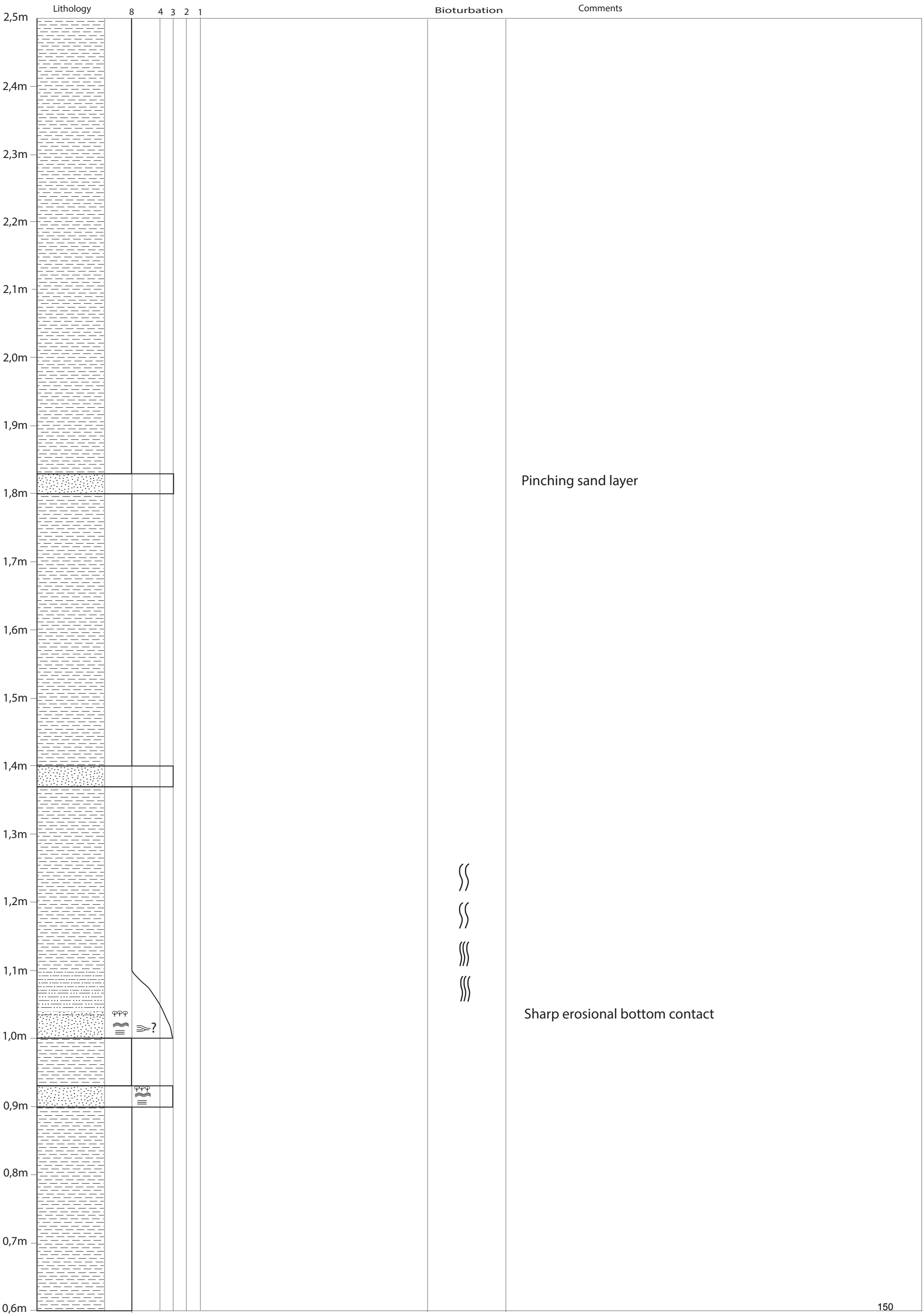

LOCATION: *Langøyene* **SECTION NO:** *Profile 1* **SHEET NO:** *3/16* **DATE:** *08.09.2013* **BY:** *Martin Kjærsgaard*

LOCATION: *Langøyene* **SECTION NO:** *Profile 1* **SHEET NO:** *2/16* **DATE:** *08.09.2013* **BY:** *Martin Kjærsgaard*

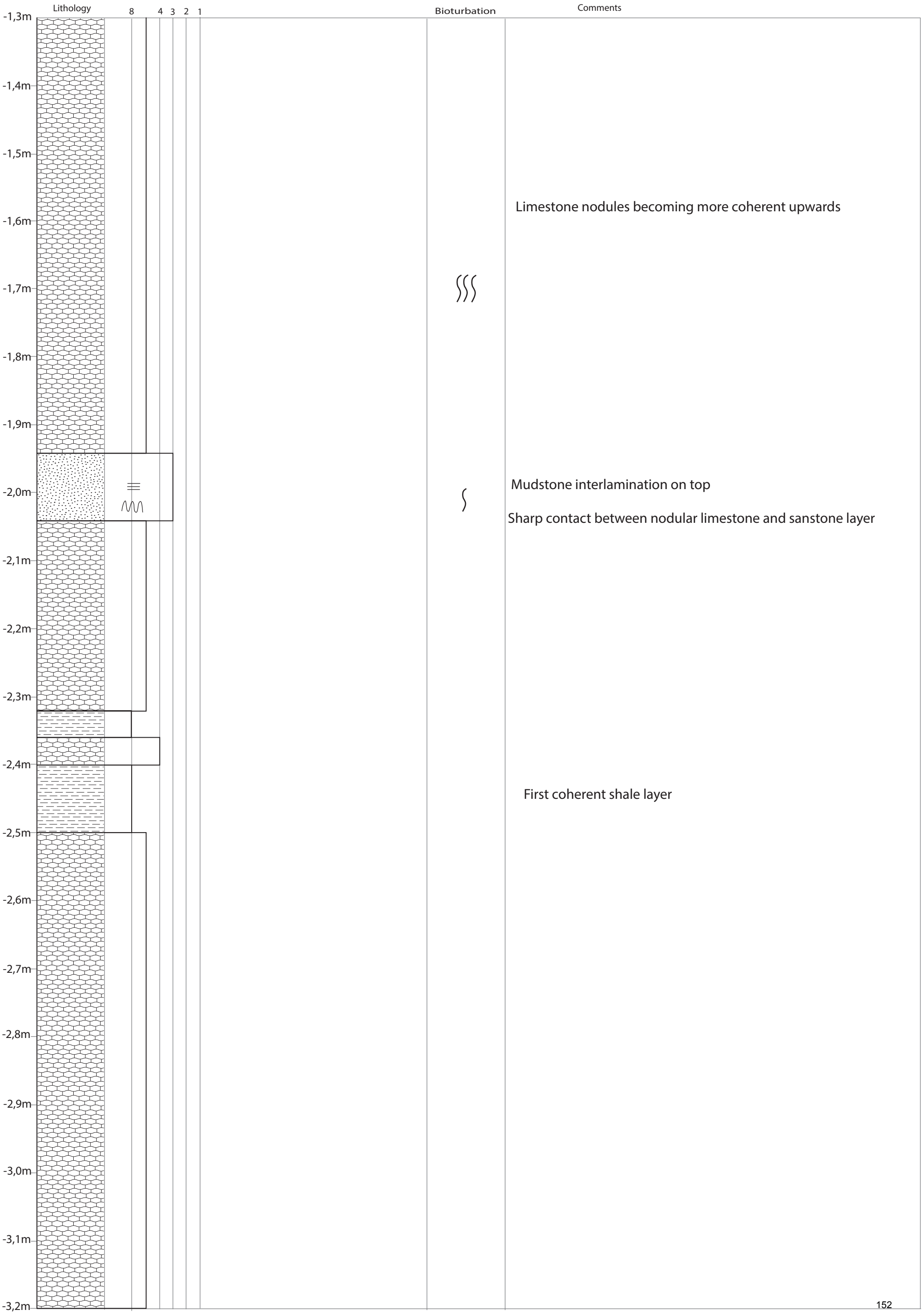

LOCATION: *Langøyene* **SECTION NO:** *Profile 1* **SHEET NO:** *1/16* **DATE:** *08.09.2013* **BY:** *Martin Kjærsgaard*

Utm 32
0596166
6637977

Lithology 8 4 3 2 1 Bioturbation Comments

-3,2m
-3,3m
-3,4m
-3,5m
-3,6m
-3.7m
-3,8m
-3,9m
-4,0m
-4,1m
-4,2m
-4,3m
-4,4m
-4,5m
-4,6m
-4,7m
-4,8m
-4,9m
-5,0m

Nodules between 3-4 cm in diameter.
Alternating nodular limestone and shale.

LANGØYENE PROFILE 2

SEDIMENTARY LOG

Scale: 1:100

Utm:
32 V
0596685N
6638310E

LOCATION: *Langøyene* **SECTION NO:** Profile 2 **SHEET NO:** *1/1* **DATE:** *07.09.2013* **BY:** *Martin Kjærsgaard*

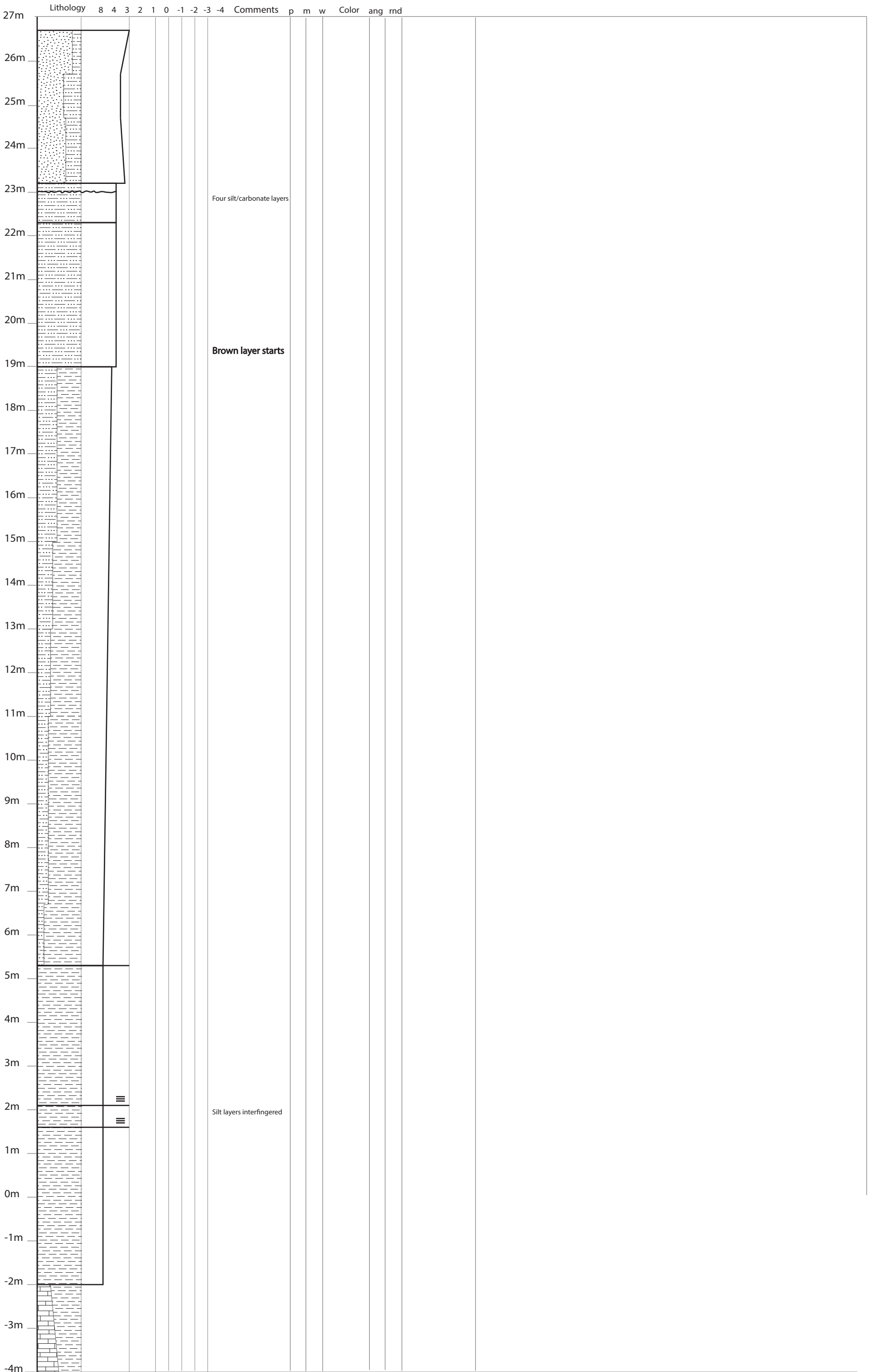

LANGØYENE PROFILE 3

SEDIMENTARY LOG

Scale: 1:100

LOCATION: *Langøyene* **SECTION NO:** *Profile 3* **SHEET NO:** *1/1* **DATE:** *18.09.2013* **BY:** *Martin Kjærsgaard*

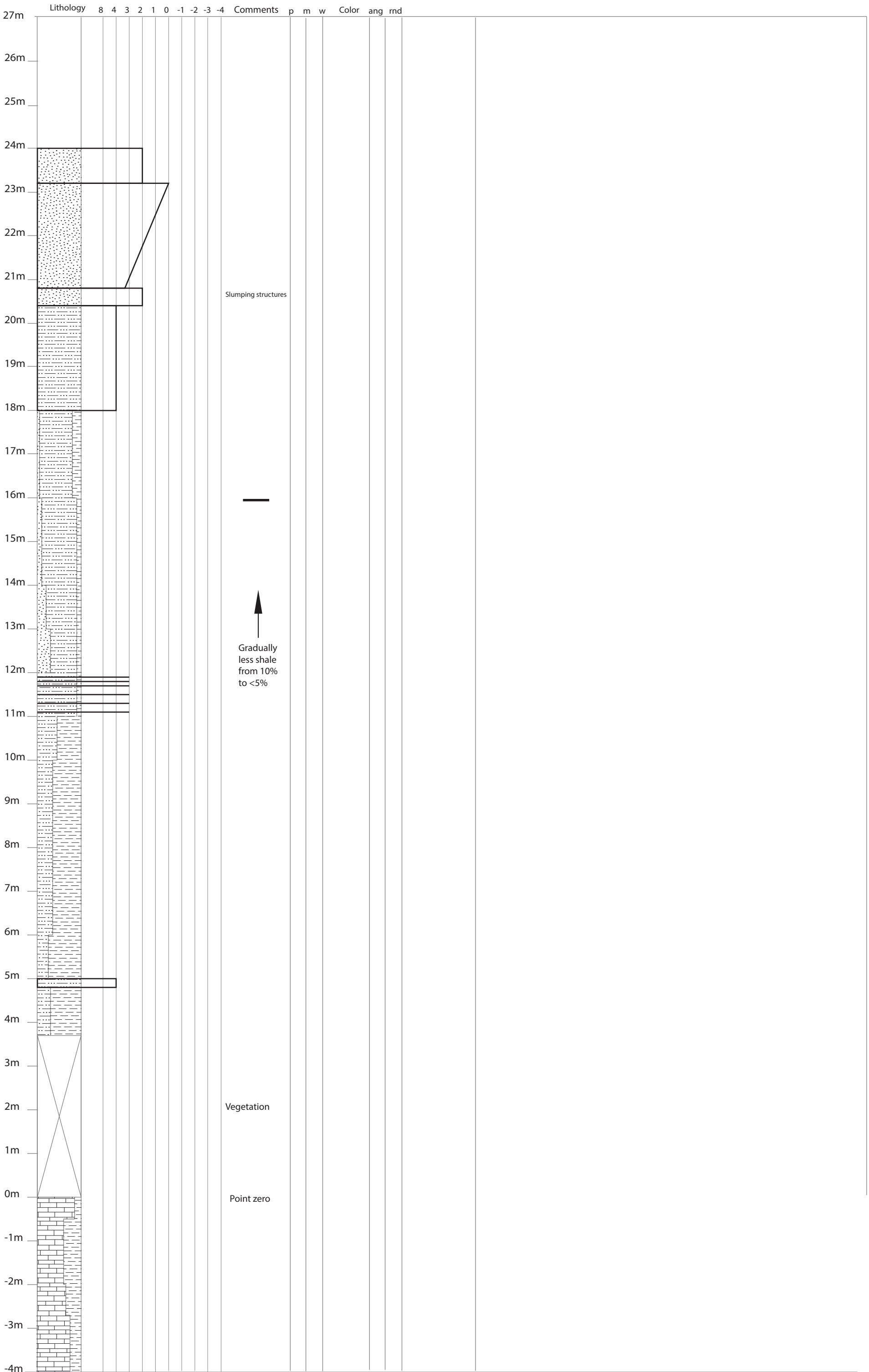

APPENDIX B

LIST OF “PMO” MATERIAL

Rambergøya Profile 1

	PMO-numbers		
Meter	**Rock samples**	**Sample scan pictures**	**Acetate peels**
21,10	227.485	227.485-SS	227.485-AP
20,60	227.484	227.484-SS	227.484-AP
19,10	227.483	227.483-SS	227.483-AP
18,00	227.482	227.482-SS	227.482-AP
17,10	227.481	227.481-SS	227.481-AP
16,20	227.480	227.480-SS	227.480-AP
16,00	227.479	227.479-SS	227.479-AP
15,00	227.478	227.478-SS	227.478-AP
14,00	227.477	227.477-SS	227.477-AP
13,05	227.476	227.476-SS	227.476-AP
12,00	227.475	227.475-SS	227.475-AP
10,40	227.474	227.474-SS	227.474-AP
10,00	227.473	227.473-SS	227.473-AP
9,00	227.472	227.472-SS	227.472-AP
6,80	227.471	227.471-SS	227.471-AP
5,90	227.470	227.470-SS	227.470-AP
4,00	227.469	227.469-SS	227.469-AP
1,80	227.468	227.468-SS	227.468-AP
1,30	227.467	227.467-SS	227.467-AP
-0,70	227.465	227.465-SS	227.465-AP
-1,00	227.466	227.466-SS	227.466-AP

LANGØYENE PROFILE 1

	PMO-numbers		
Meter	**Rock samples**	**Sample surface scan pictures**	**Thin sections**
23,2	227.464	227.464-SS	227.464-TS
22,5	227.463	227.463-SS	227.463A-TS/227.463B-TS/227.463C-TS/
22,4	227.462	227.462-SS	227.462A-TS/227.462B-TS
22	227.461	227.461-SS	227.461-TS
21,9	227.460	227.460-SS	227.460A-TS/227.460B-TS
21,75	227.459	227.459-SS	227.459A-TS/227.459B-TS
21,5	227.458	227.458-SS	227.458A-TS/227.458B-TS
21	227.457	227.457-SS	227.457A-TS/227.457B-TS
20,3	227.456	227.456-SS	227.456-TS
19,2	227.455	227.455-SS	227.455-TS
19	227.454	227.454-SS	227.454-TS
17,9	227.453	227.453-SS	227.453-TS
16,6	227.452	227.452-SS	227.452-TS
15,4	227.451	227.451-SS	227.451-TS
15	227.450	227.450-SS	227.450A-TS/227.450B-TS
13,05	227.449	227.449-SS	227.449-TS
11,85	227.448	227.448-SS	227.448-TS
11,25	227.447	227.447-SS	227.447-TS
9,35	227.446	227.446-SS	227.446A-TS/227.446B-TS/227.446C-TS
8	227.445	227.445-SS	227.445A-TS/227.445B-TS
7	227.444	227.444-SS	227.444-TS
6,8	227.443	227.443-SS	227.443-TS
5,5	227.442	227.442-SS	227.442-TS
3,5	227.441	227.441-SS	227.441-TS
1,25	227.440	227.440-SS	227.440-TS
1	227.439	227.439-SS	227.439-TS
0,8	227.438	227.438-SS	227.438-TS
0,37	227.437	227.437-SS	227.437A-TS/227.437B-TS
-0,6	227.436	227.436-SS	227.436-TS
-1,85	227.435	227.435-SS	227.435-TS
-1,9	227.434	227.434-SS	227.434-TS

APPENDIX C

SAMPLE SLAB SURFACE SCANS AND DESCRIPTIONS

RAMBERGØYA PROFILE 1

SAMPLE SLAB SURFACE SCANS AND DESCRIPTIONS

Rambergøya Profile 1 samples

Scale: 2 centimeters

227.485-SS	Original scan	Brightness and contrast modified scan	21,10m

227.484-SS	Original scan	Brightness and contrast modified scan	20,60m

227.483-SS	Original scan	Brightness and contrast modified scan	19,10m

227.482-SS | Original scan | Brightness and contrast modified scan | 18,00m

227.481-SS | Original scan | Brightness and contrast modified scan | 17,10m

227.480-SS | Original scan | Brightness and contrast modified scan | 16,20m

227.479-SS | Original scan | Brightness and contrast modified scan | 16,00m

227.478-SS | Original scan | Brightness and contrast modified scan | 15,00m

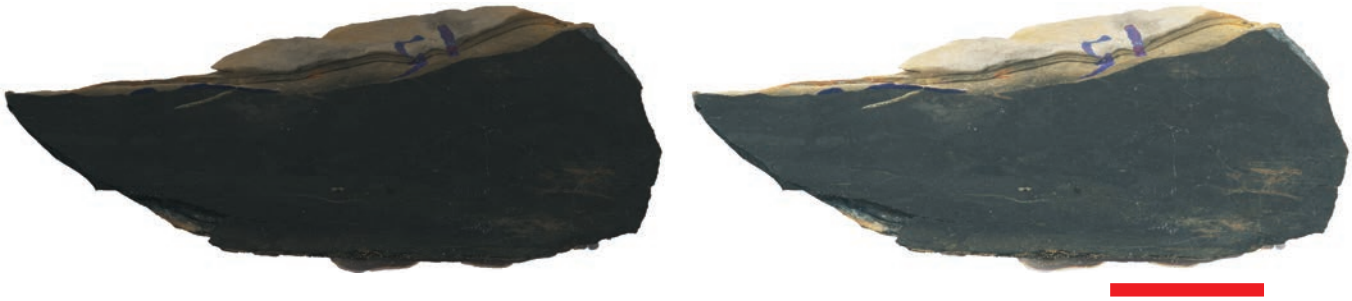

227.477-SS | Original scan | Brightness and contrast modified scan | 14,00m

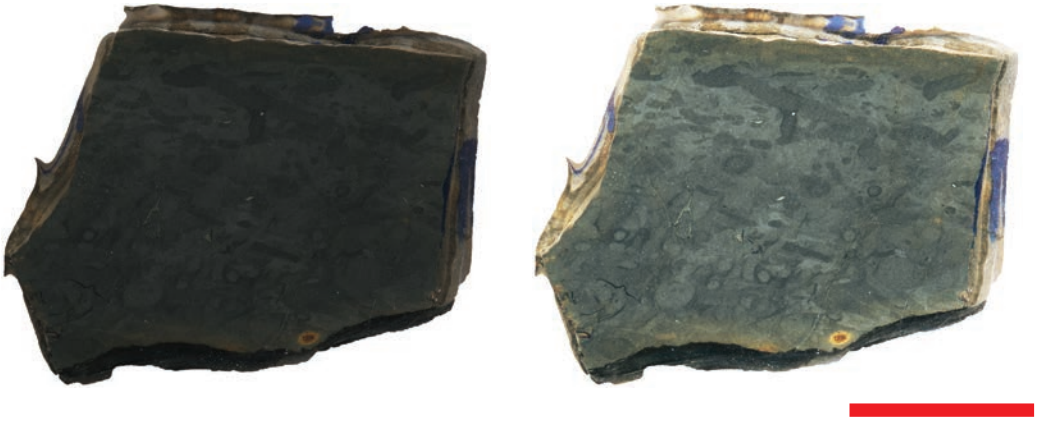

227.476-SS | Original scan | Brightness and contrast modified scan | 13,05m

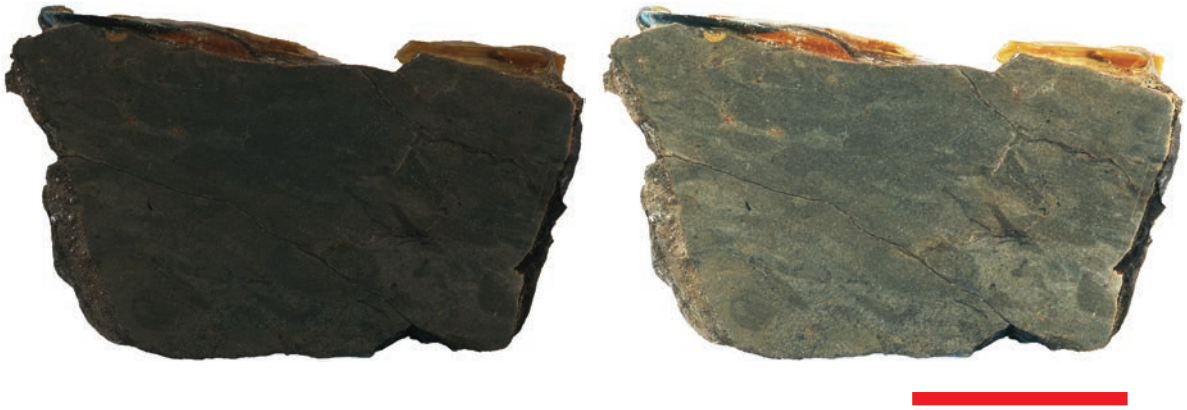

227.475-SS | Original scan | Brightness and contrast modified scan | 12,00m

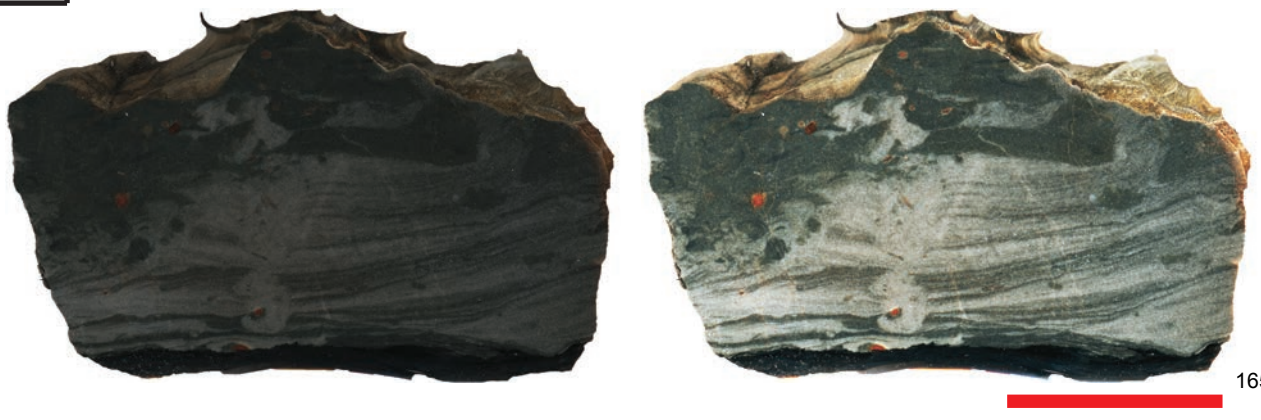

227.474-SS

Original scan

Brightness and contrast modified scan

10,40m

227.473-SS

Original scan

Brightness and contrast modified scan

10,00m

227.472-SS

Original scan

Brightness and contrast modified scan

9,00m

227.471-SS

Original scan

Brightness and contrast modified scan

6,80m

227.470-SS | Original scan | Brightness and contrast modified scan | 5,90m

227.469-SS | Original scan | Brightness and contrast modified scan | 4,00m

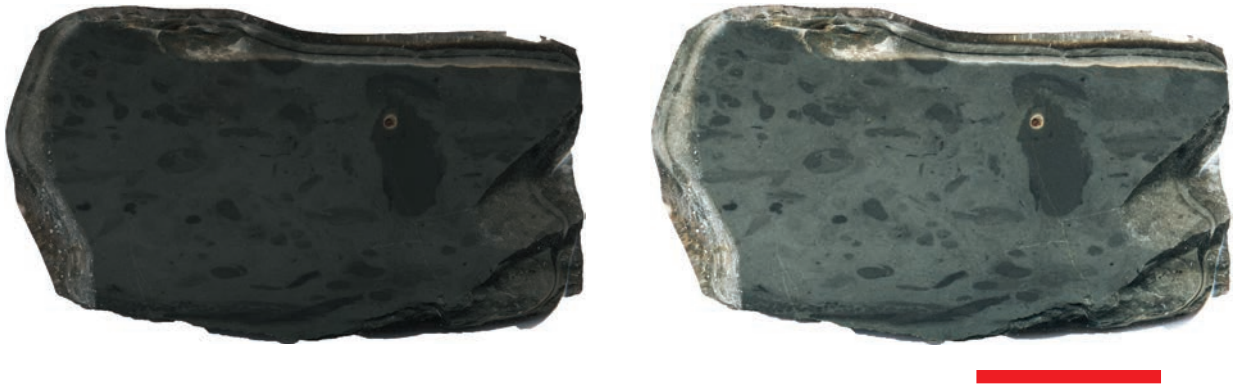

227.468-SS | Original scan | Brightness and contrast modified scan | 1,80m

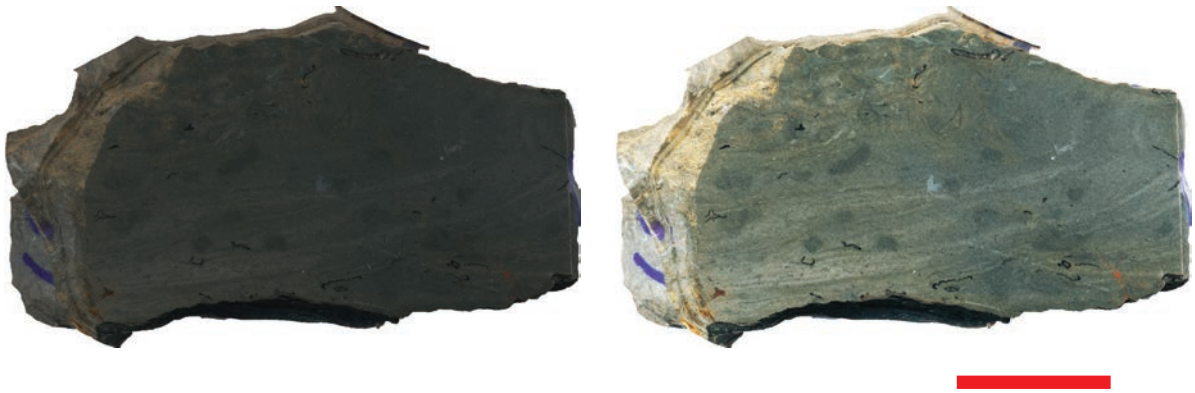

227.467-SS | Original scan | Brightness and contrast modified scan | 1,30m

227.466-SS

Original scan

Brightness and contrast modified scan

-0,70m

227.465-SS

Original scan

Brightness and contrast modified scan

-1,00m

Rambergøya Profile 1

Meter	PMO-number	Description
21,10	227.485-SS	Bioturbated siltstone. Bioturbation: 6.
20,60	227.484-SS	Bioturbated siltstone. Bioturbation: 6.
19,10	227.483-SS	Sandy, bioturbated siltstone. Bioturbation: 4-5.
18,00	227.482-SS	Structureless siltstone.Bioturbation: 4. Possibly some sand fractions (lighter color)
17,10	227.481-SS	Bioturbated siltstone. Bioturbation: 6. ("brown weathered" siltstone)
16,20	227.480-SS	Bioturbated siltstone. Bioturbation: 6. ("brown weathered" siltstone)
16,00	227.479-SS	Bioturbated siltstone. Bioturbation: 6.
15,00	227.478-SS	No internal structures. Heavily bioturbated. Black. Bioturbation: 6.
14,00	227.477-SS	Bioturbated siltstone. Bioturbation: 4.
13,05	227.476-SS	Bioturbated siltstone. Bioturbation: 4.
12,00	227.475-SS	Storm deposited sandstone layer with micro HCS structures. Vertical burrow through the sand.
10,40	227.474-SS	Structureless siltstone. Bioturbation: 4. Many shell fragments - allogenic? Could possibly be a storm deposited layer where bioturbation has altered primary laminae.
10,00	227.473-SS	Bioturbated storm deposited siltstone/sandstone layer. Ripples in the top section of the sample. Bioturbation: 3-4.
9,00	227.472-SS	Storm deposited layer (according to sedimentary log). See alot of cracks - could probably be calcite cementation that results in more brittle layers. Brown spots may be siderite.
6,80	227.471-SS	Bioturbated siltstone. Bioturbation: 5-6.
5,90	227.470-SS	Storm deposited layer. Horizontal lamination in the bottom and current ripple lamination on the top. Probably water-escape structures on top. Bioturbation from the overlying shale and downwards - this can possibly also be escape burrows.
4,00	227.469-SS	Bioturbated shale/siltstone. Bioturbation: 3.
1,80	227.468-SS	Storm deposited layer. Shell fragments - probably allogenic. Internally parallel laminated. Bioturbation: 1.
1,30	227.467-SS	Storm deposited layer. Some ripple lamination. Siderite or pyrite clast. Some lamination. Unidentified shell fragments. Bioturbation: 2-3.
-0,70	227.466-SS	Limestone. Micrite. Bioturbation: 5.
-1,00	227.465-SS	Black mudstone. Bioturbated. Brittle - several vertical cracks.

LANGØYENE PROFILE 1

SAMPLE SLAB SURFACE SCANS AND DESCRIPTIONS

Langøyene Profile 1 samples

Scale: 2 centimeters

227.464-SS

Original scan

Brightness and contrast modified scan

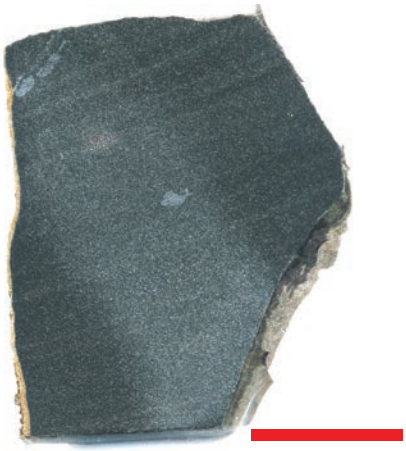

23,20m

227.463-SS

Original scan

Brightness and contrast modified scan

22,50m

227.462-SS

Original scan

Brightness and contrast modified scan

22,40m

227.461-SS

Original scan

Brightness and contrast modified scan

22,00m

227.460-SS

Original scan

Brightness and contrast modified scan

21,90m

227.459-SS

Original scan

Brightness and contrast modified scan

21,75m

227.458-SS

Original scan

Brightness and contrast modified scan

21,50m

227.457-SS

Original scan

Brightness and contrast modified scan

21,00m

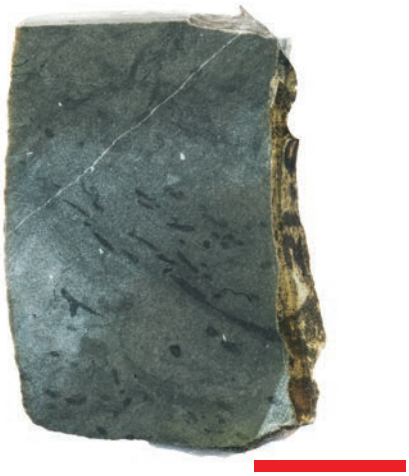

227.456-SS

Original scan

Brightness and contrast modified scan

20,30m

227.455-SS

Original scan

Brightness and contrast modified scan

19,20m

227.454-SS

Original scan

Brightness and contrast modified scan

19,00m

227.453-SS

Original scan

Brightness and contrast modified scan

17,90m

227.452-SS

Original scan

Brightness and contrast modified scan

16,60m

227.451-SS

Original scan

Brightness and contrast modified scan

15,40m

227.450-SS

Original scan

Brightness and contrast modified scan

15,00m

227.449-SS

Original scan

Brightness and contrast modified scan

13,05m

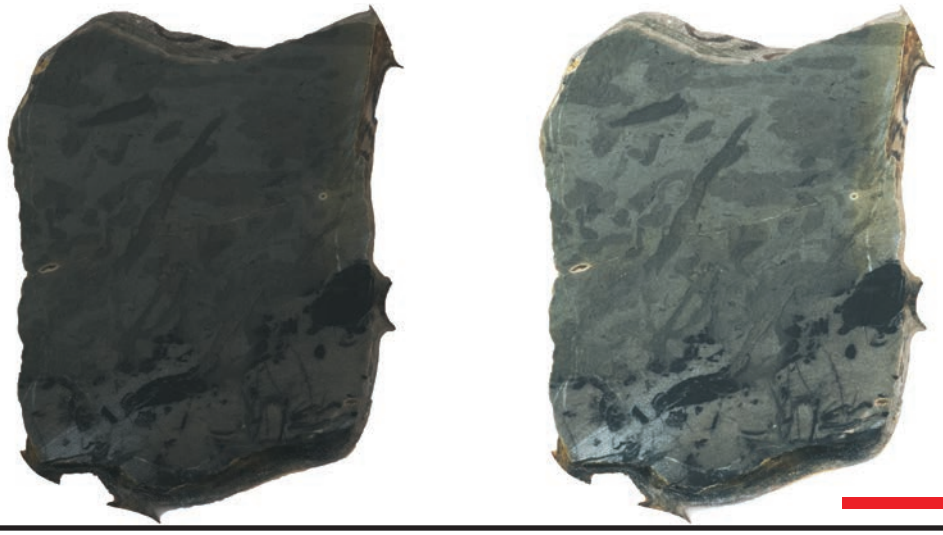

227.448-SS

Original scan

Brightness and contrast modified scan

11,85m

227.447-SS

Original scan

Brightness and contrast modified scan

11,25m

227.446-SS

Original scan

Brightness and contrast modified scan

9,35m

227.445-SS

Original scan

Brightness and contrast modified scan

8,00m

227.444-SS

Original scan

Brightness and contrast modified scan

7,00m

227.443-SS

Original scan

Brightness and contrast modified scan

6,80m

227.442-SS

Original scan

Brightness and contrast modified scan

5,50m

227.441-SS | Original scan | Brightness and contrast modified scan | 3,50m

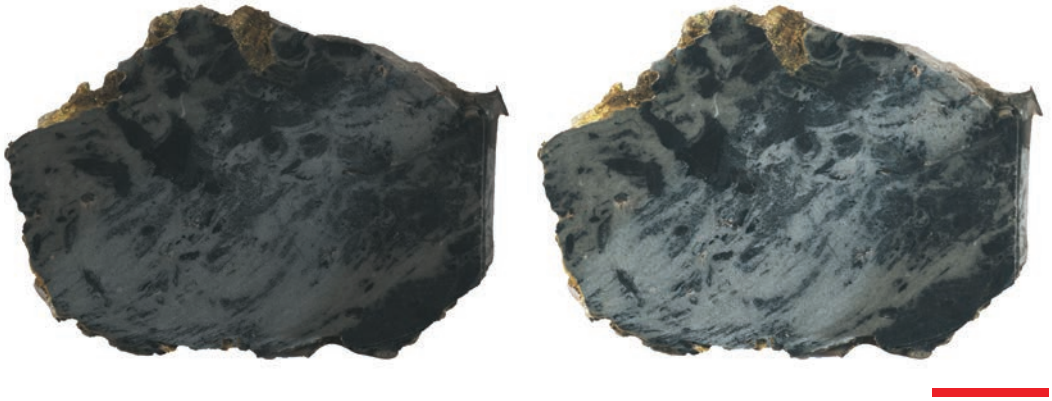

227.440-SS | Original scan | Brightness and contrast modified scan | 1,25m

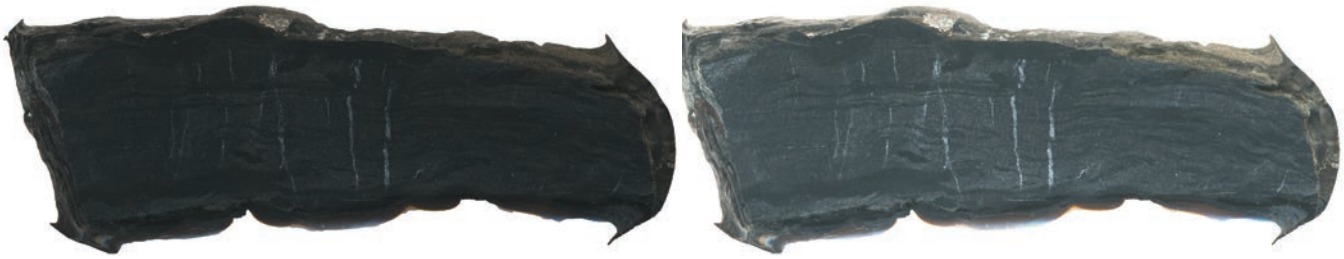

227.439-SS | Original scan | Brightness and contrast modified scan | 1,00m

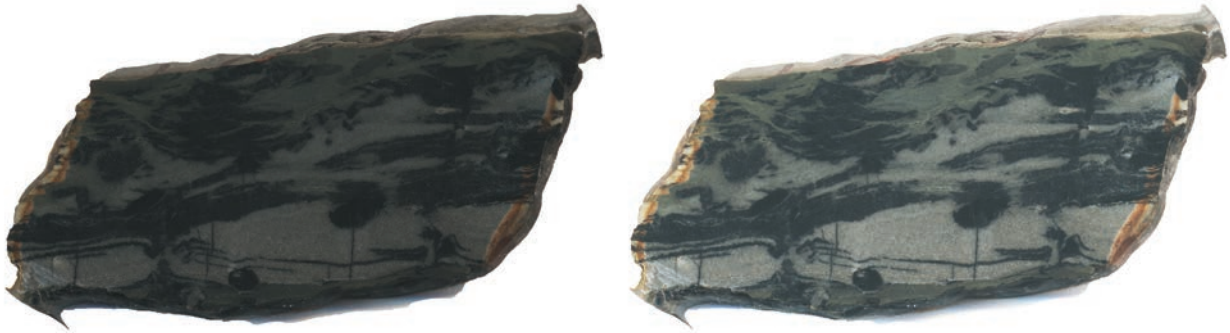

227.438-SS | Original scan | Brightness and contrast modified scan | 0,80m

227.437A-SS

Original scan

Brightness and contrast modified scan

0,37m

227.436-SS

Original scan

Brightness and contrast modified scan

-0,6m

227.435-SS

Original scan

Brightness and contrast modified scan

-1,85m

227.434-SS

Original scan

Brightness and contrast modified scan

-1,9m

Langøyene Profile 1

Meter	PMO-number	Description
23,20	227.464-SS	Some laminae.
22,50	227.463-SS	Stuctureless, bioturbated. Loading in the bottom part.
22,40	227.462-SS	Bioturbation: 6.
22,00	227.461-SS	Bioturbation: 6.
21,90	227.460-SS	"Brown weathered" siltstone facies. Bioturbation: 6.
21,75	227.459-SS	"Brown weathered" siltstone facies. Bioturbation: 6.
21,50	227.458-SS	"Brown weathered" siltstone facies. Bioturbation: 6.
21,00	227.457-SS	"Brown weathered" siltstone facies. Bioturbation: 6.
20,30	227.456-SS	Heavy bioturbated.
19,20	227.455-SS	"Brown weathered" siltstone facies. Bioturbation: 6.
19,00	227.454-SS	"Brown weathered" siltstone facies. Bioturbation: 6.
17,90	227.453-SS	Bioturbated siltstone. Bioturbation: 6.
16,60	227.452-SS	Storm deposited layer. Ripple drift lamination. Bioturbation:1.
15,40	227.451-SS	Bioturbated siltstone. Bioturbation: 5.
15,00	227.450-SS	Sharp erosional contact. Internally laminated, loading structures. Current ripple lamination in the top section.
13,05	227.449-SS	Bioturbated silt. Bioturbation: 3.
11,85	227.448-SS	Storm deposited sandstone layer. Internally laminated. Micro HSC. Dewatering structures that destroy primary laminae (water escape structures). Siderite concresions.
11,25	227.447-SS	Horisontal grazing of organisms on top. Bioturbation: Top: 3, bottom: 5.
9,35	227.446-SS	Bioturbation vertical into the sand layer. Ripple cross lamination and convolute lamination.
8,00	227.445-SS	Could be two storm deposited layers. Current ripple lamination in the sandstone and microloading on the bottom section of the sandstone into the shale. Bioturbation: Top: 3, Bottom: 5.
7,00	227.444-SS	Structureless. Bioturbation: 6.
6,80	227.443-SS	Storm deposited sandstone layer. Internally laminated and loading structures. Bioturbation: 2.
5,50	227.442-SS	Bioturbated mudstone. Diplocraterion burrow?
3,50	227.441-SS	Slump structures. Bioturbation: 4.
1,25	227.440-SS	Bioturbated, some observed laminae. Vertical calcite filled cracks.

1,00	227.439-SS	Parallel laminated storm deposited sandstone. Effective bioturbation on top.Sharp erosional contact on bottom of storm deposited layer. Possible micro HCS structures. Secondary grading by bioturbation. Mud and sand interlamination.
0,80	227.438-SS	Parallel laminated storm deposited sandstone. Mud and sand interlamination. Current ripple laminated. Bioturbation on top. Horizontal burrows.
0,37	227.437-SS	Bioturbated siltstone. Parallel lamination and current ripple lamination.
-0,60	227.436-SS	Bioturbation: 5-6. Brown clasts indicate siderite.
-1,85	227.435-SS	Structureless shale/siltstone. Bioturbation: 6.
-1,90	227.434-SS	Storm deposited layer. Weak grading. Laminated. Convolute bedding in the bottom.

APPENDIX D

SAMPLE POSITIONS IN SIMPLIFIED SEDIMENTARY LOGS

Rambergøya Profile 1

Scale: 2 centimeters

Bioturbation:

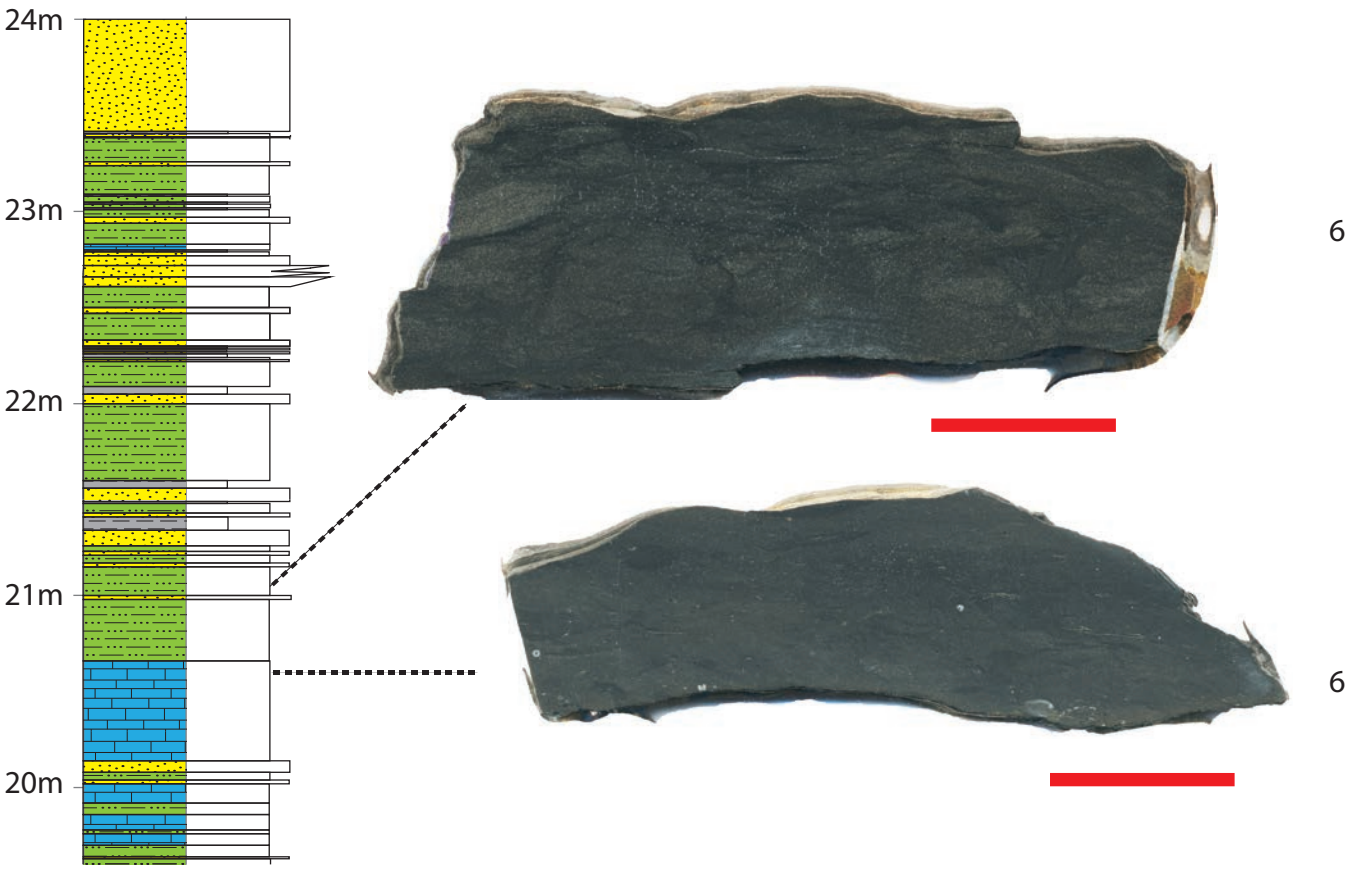

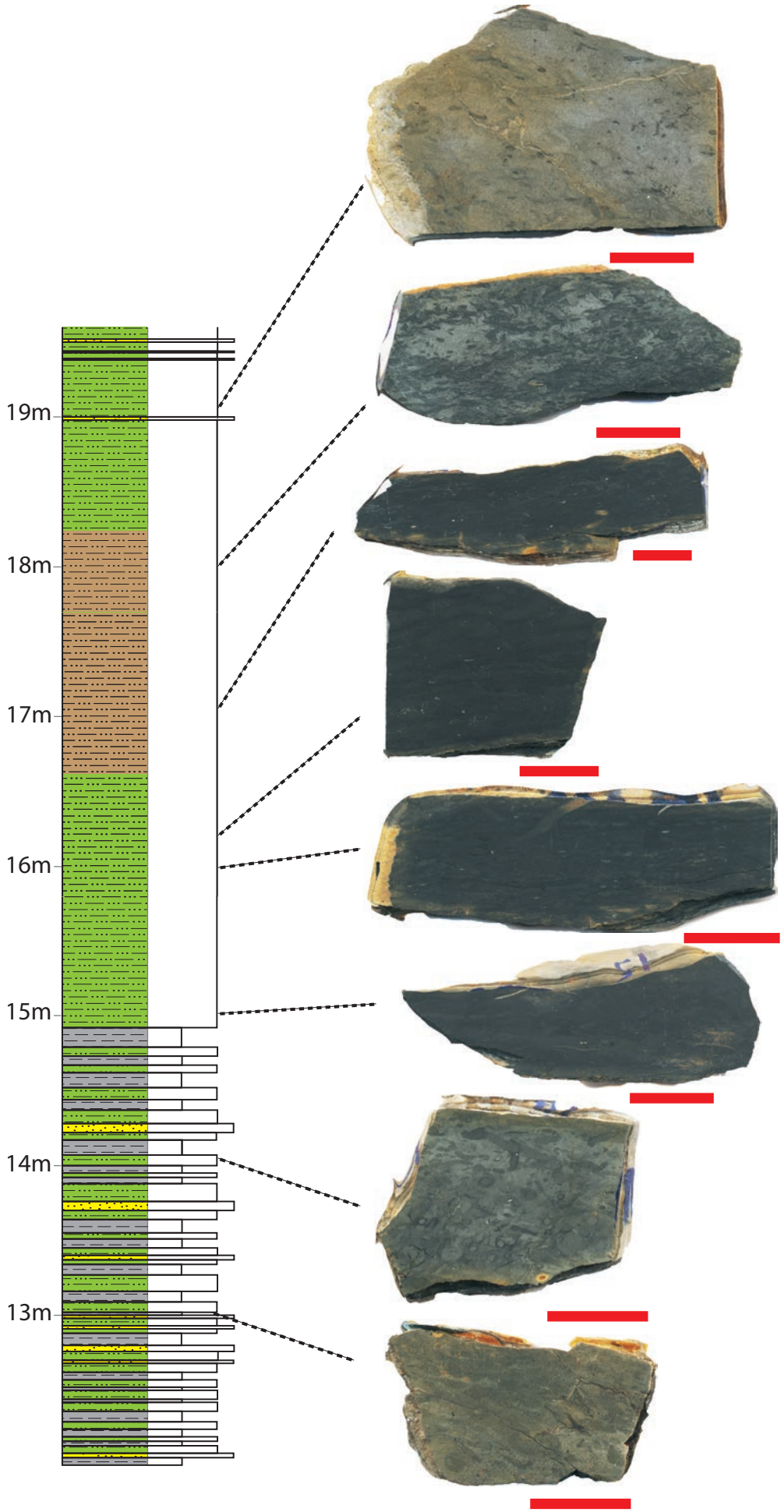
19m
18m
17m
16m
15m
14m
13m
5-6
5
6
6
6
6
5
4

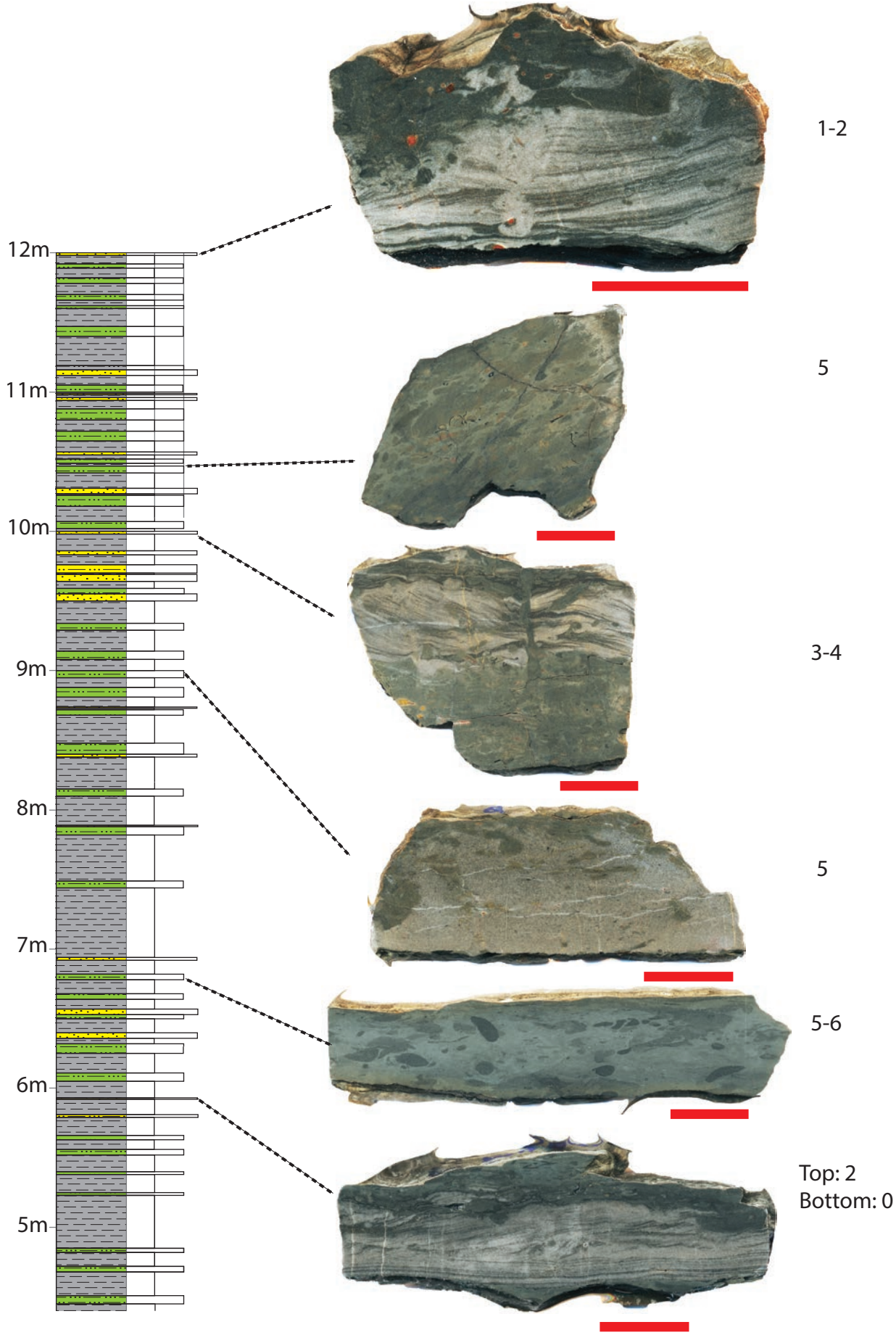
12m
11m
10m
9m
8m
7m
6m
5m
1-2
5
3-4
5
5-6
Top: 2
Bottom: 0

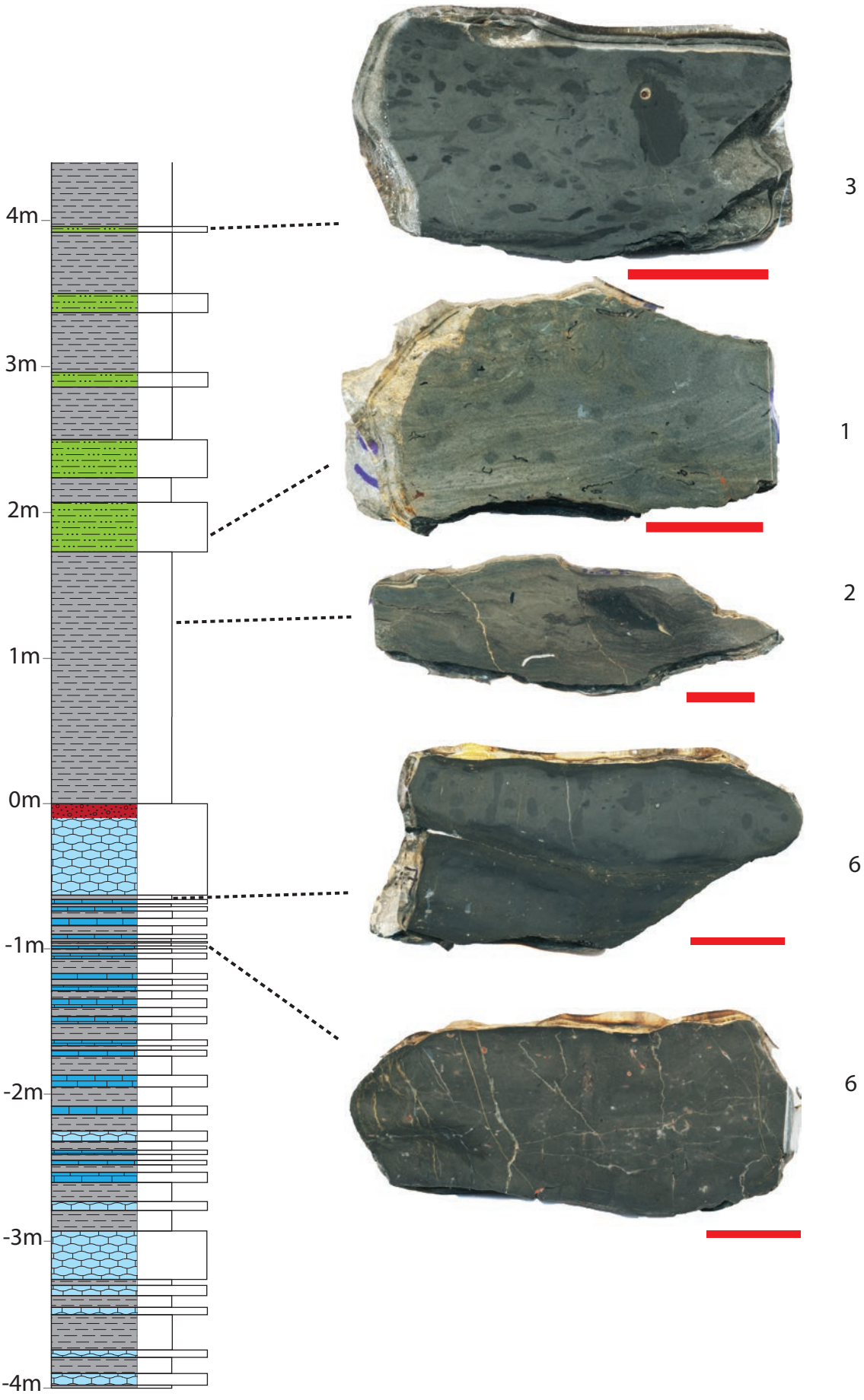
4m
3m
2m
1m
0m
-1m
-2m
-3m
-4m
3
1
2
6
6

Langøyene Profile 1

Scale: 2 centimeters

Bioturbation:

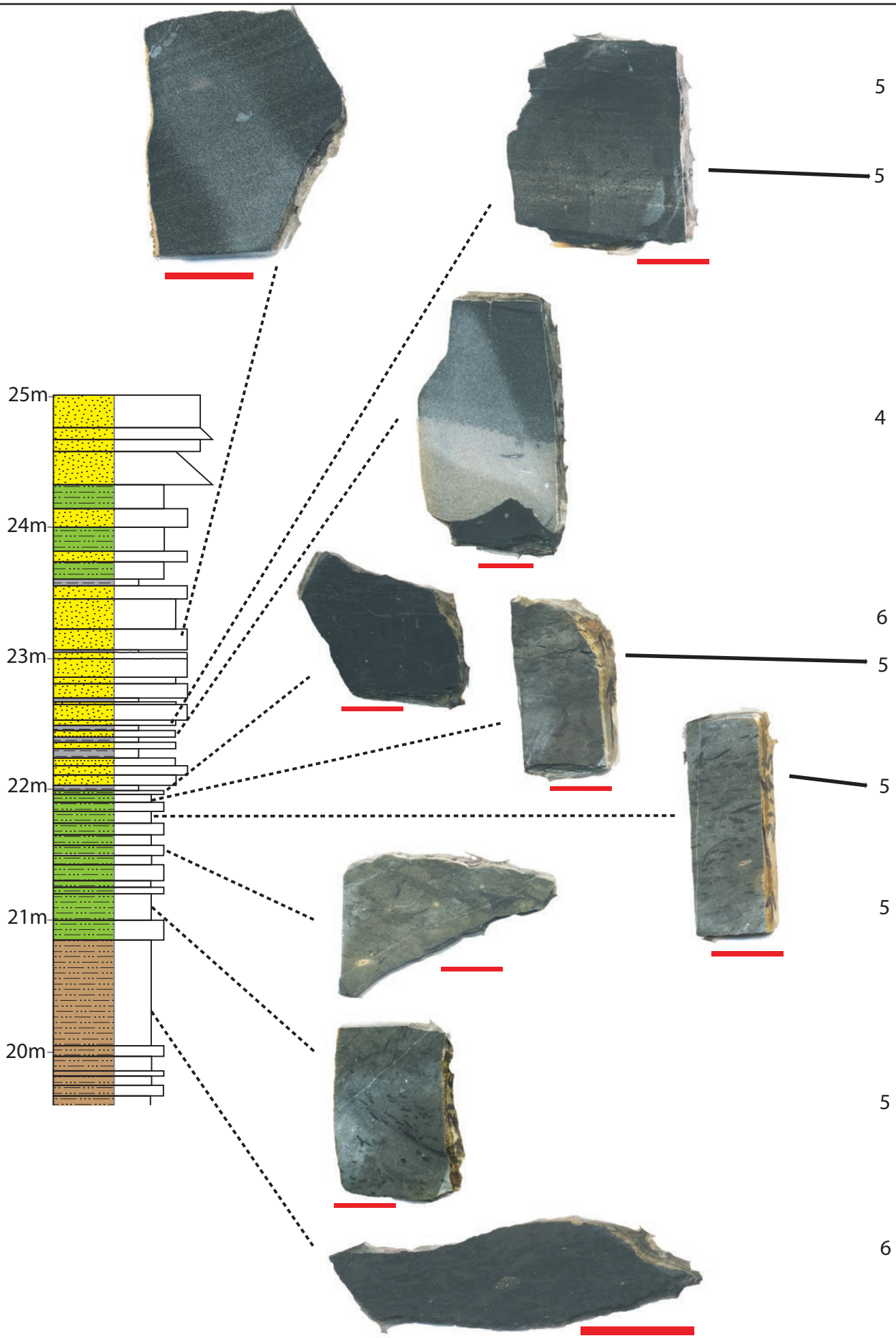

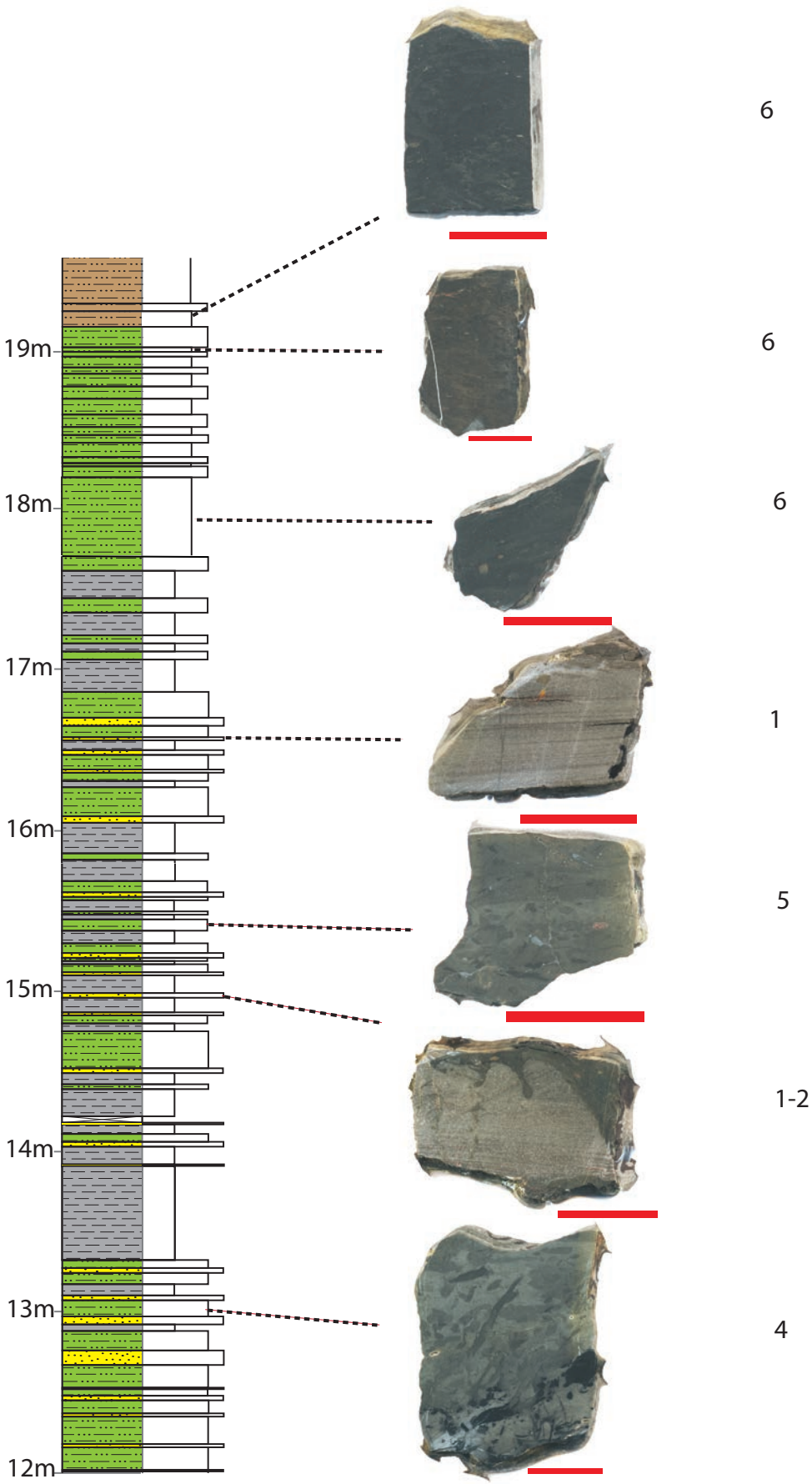
19m
18m
17m
16m
15m
14m
13m
12m
6
6
6
1
5
1-2
4

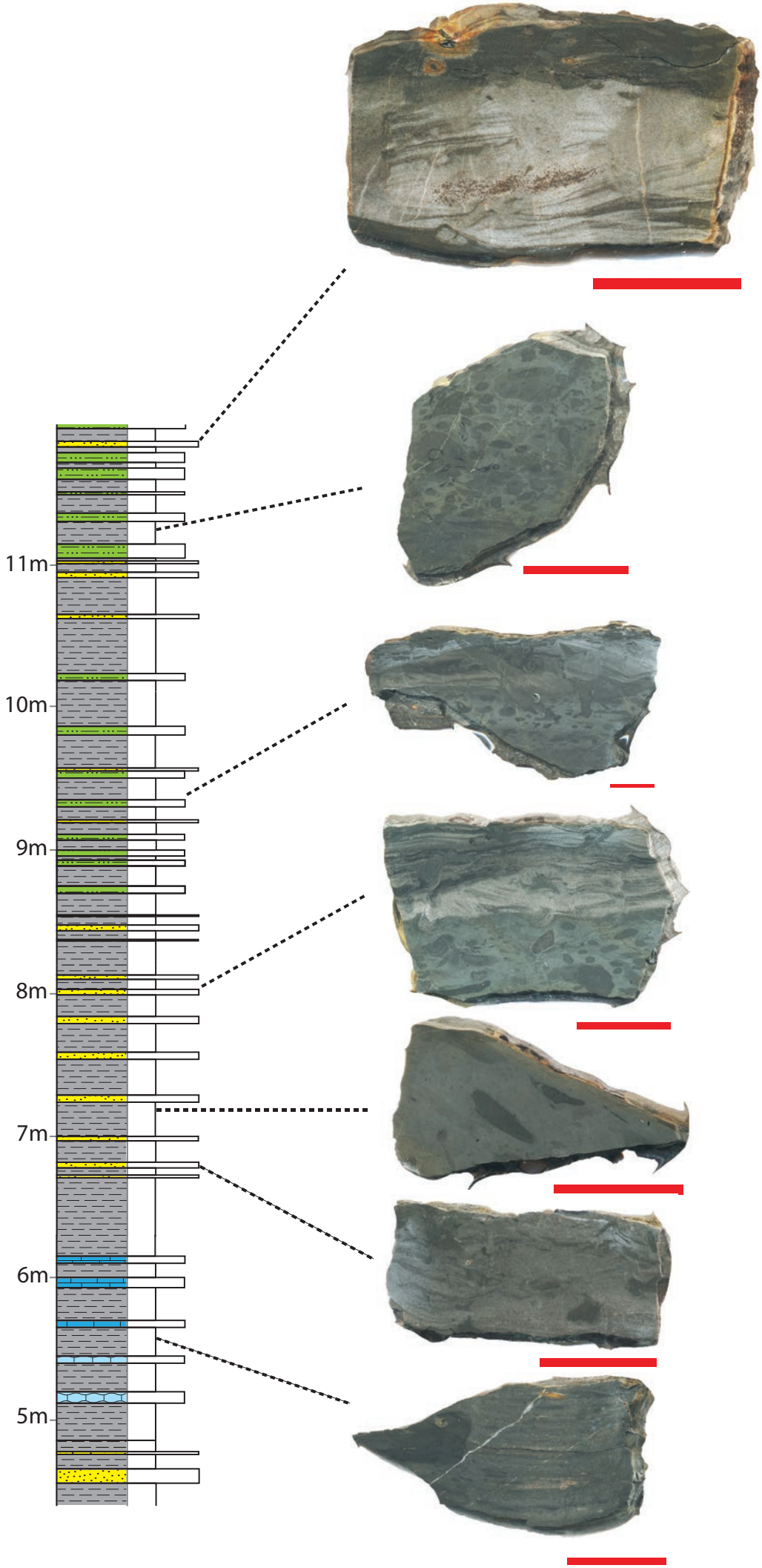

Top: 5
Bottom: 0

Top: 3
Bottom: 5

Top: 2
Bottom: 5

Top: 3
Bottom: 5

6

2

Veritical borrow with visible spreiten

Bioturbation:

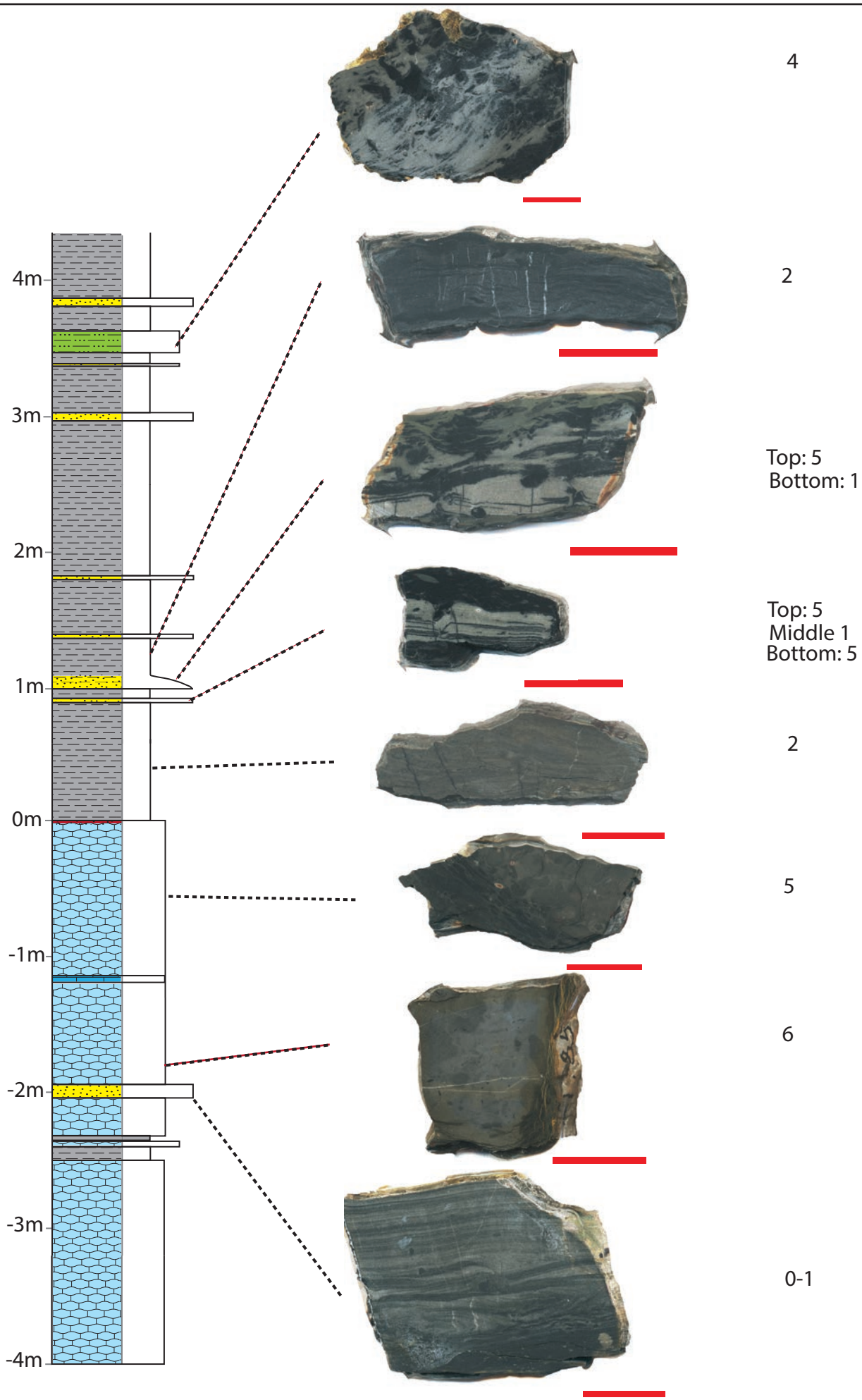

APPENDIX E

LOCATION OF FACIES ASSOCIATIONS IN SIMPLIFIED SEDIMENTARY LOGS

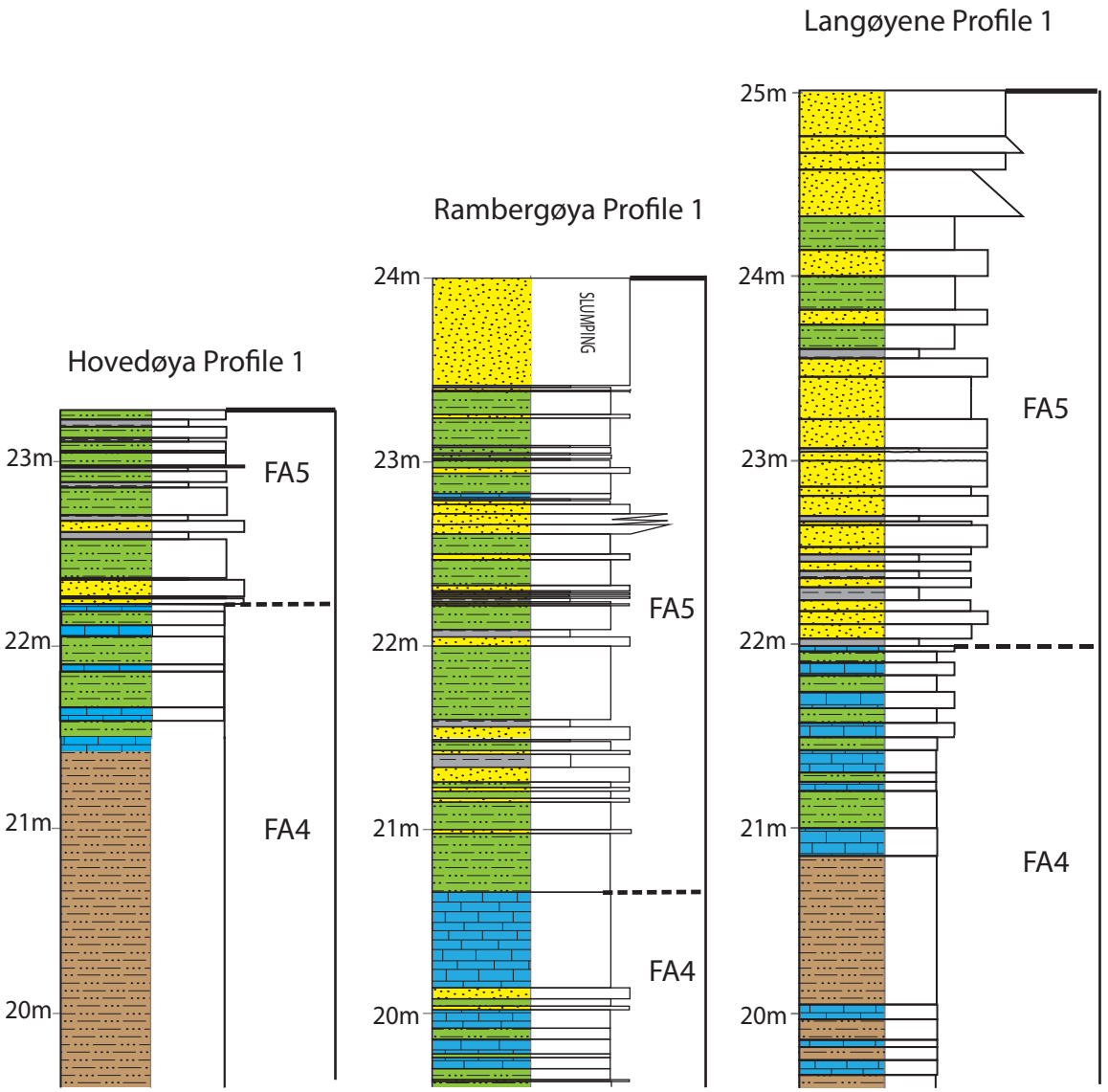
Hovedøya Profile 1
23m
22m
21m
20m
FA5
FA4
Rambergøya Profile 1
24m
23m
22m
21m
20m
SLUMPING
FA5
FA4
Langøyene Profile 1
25m
24m
23m
22m
21m
20m
FA5
FA4

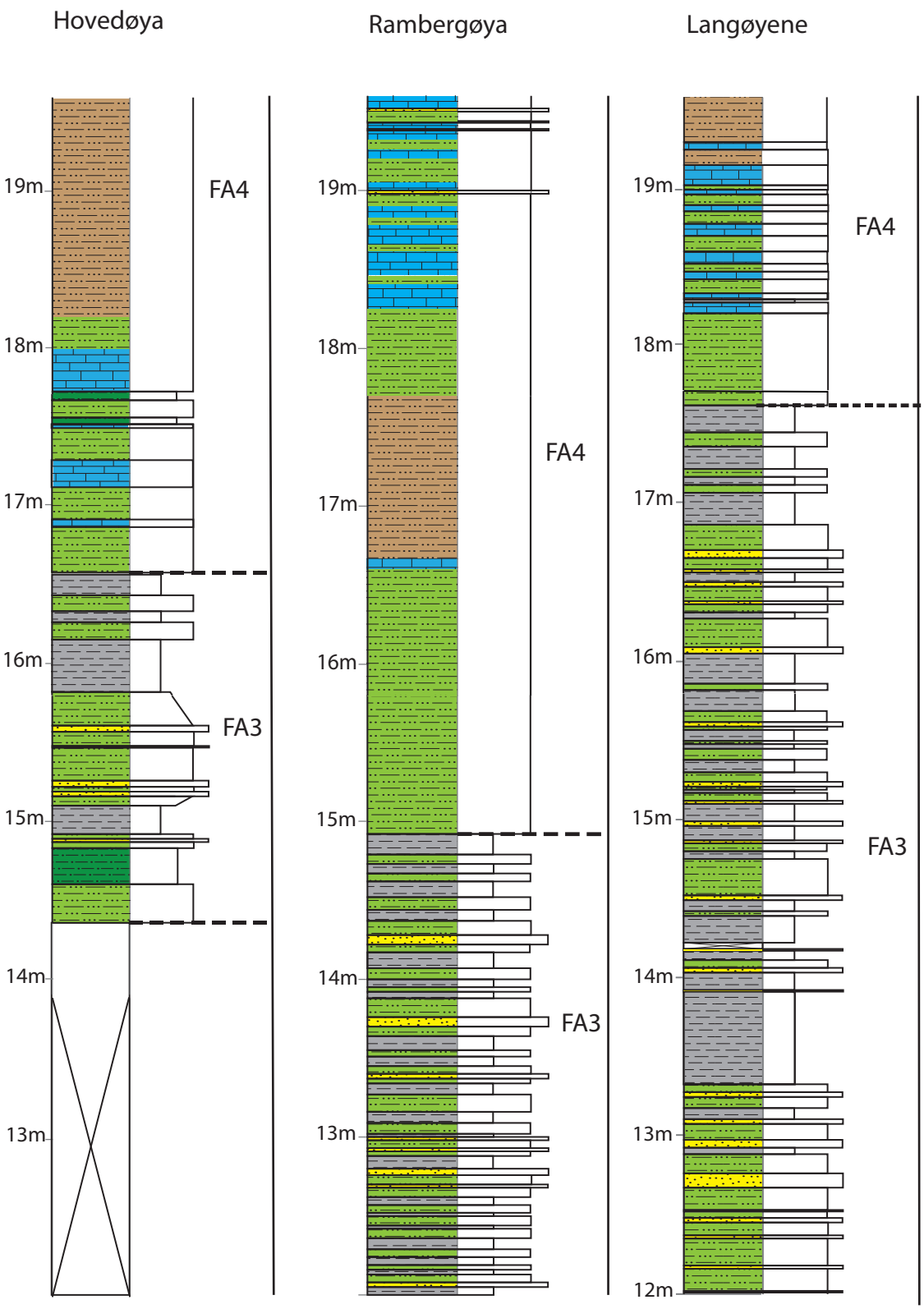
Hovedøya
Rambergøya
Langøyene
19m
18m
17m
16m
15m
14m
13m
12m
FA4
FA3

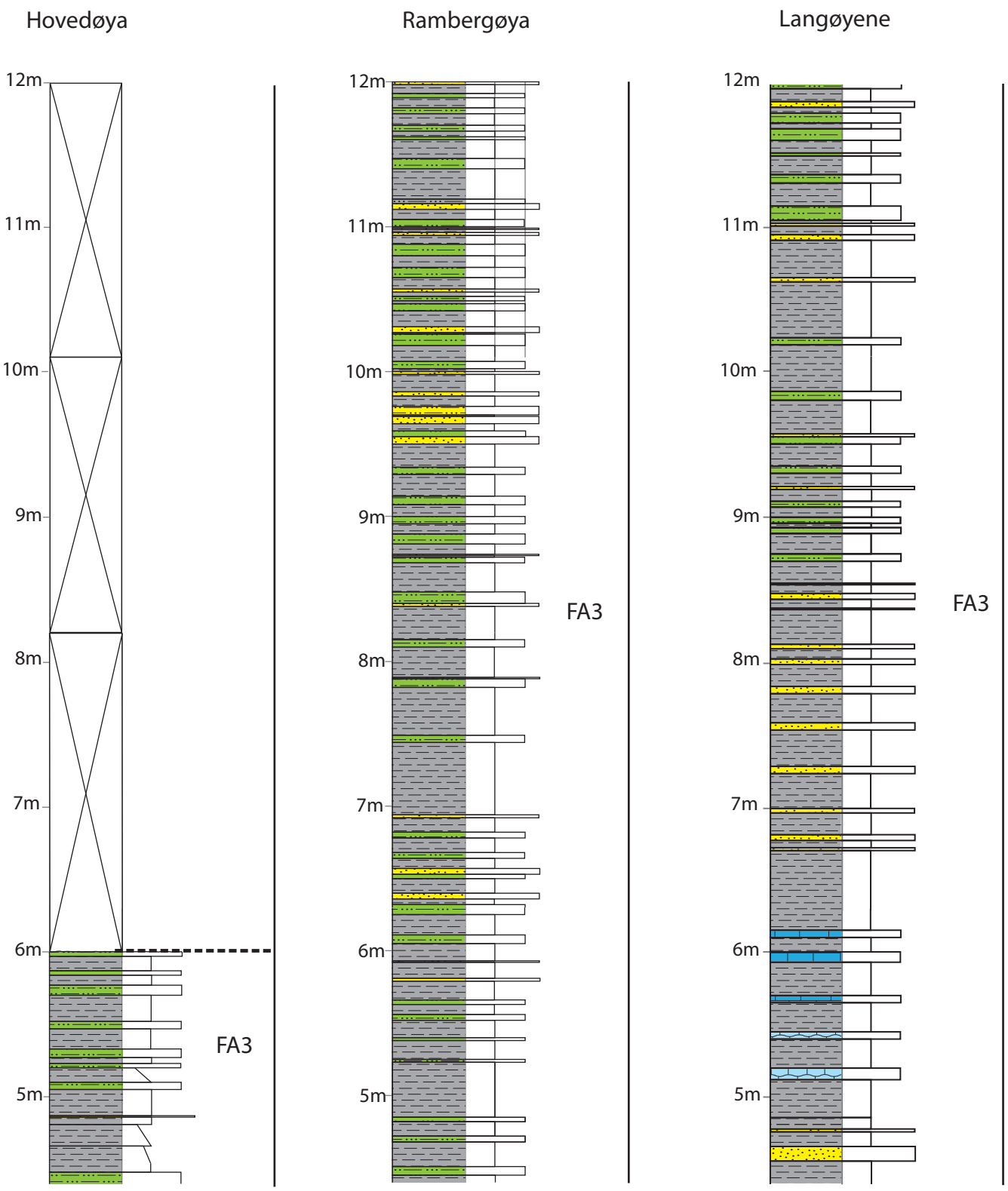
Hovedøya
Rambergøya
Langøyene
12m
11m
10m
9m
8m
7m
6m
5m
FA3
FA3
FA3

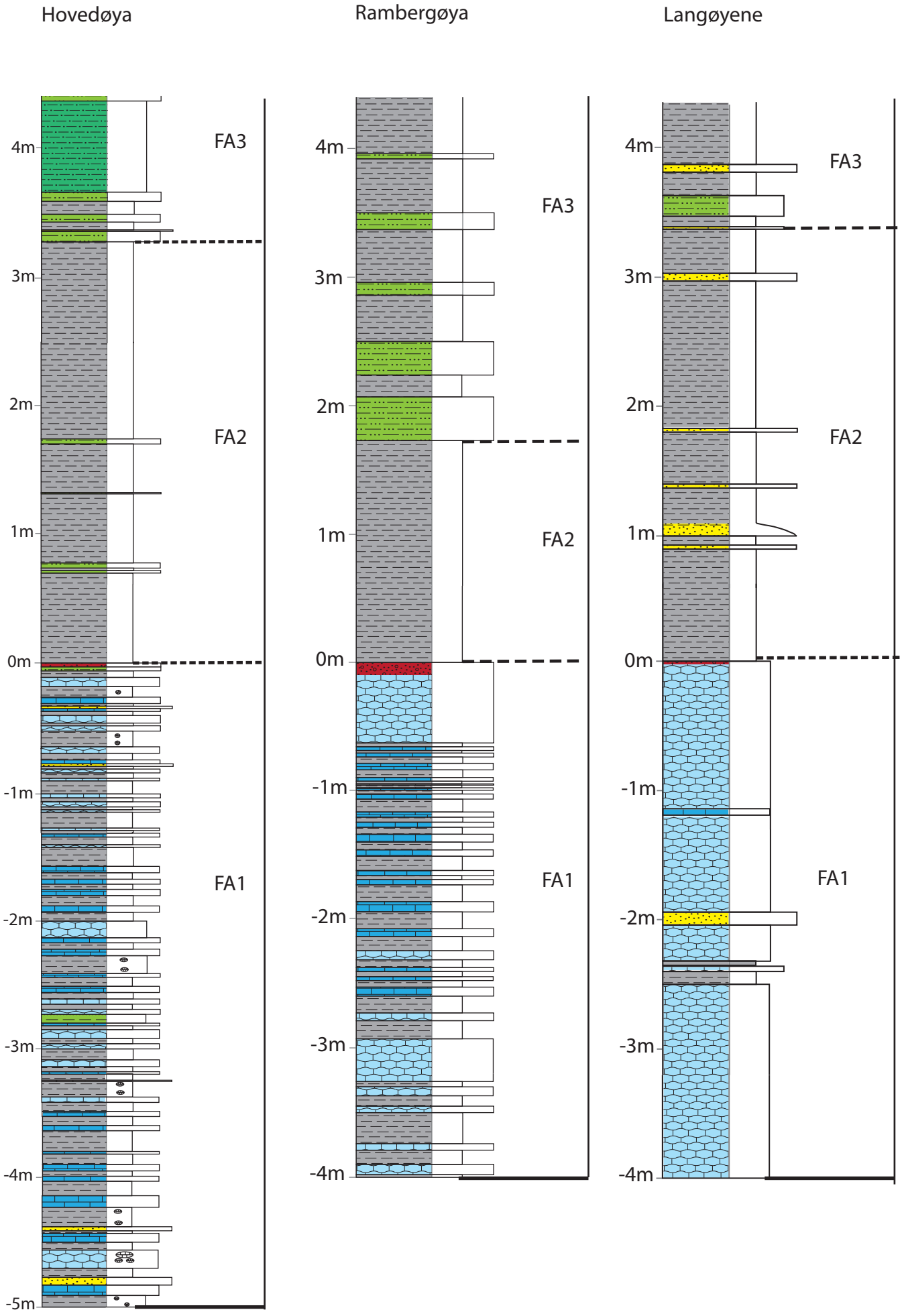
Hovedøya
Rambergøya
Langøyene
4m
3m
2m
1m
0m
-1m
-2m
-3m
-4m
-5m
FA3
FA2
FA1

APPENDIX F

SEDIMENTARY LOG TEMPLATES

LOCALITY SHEET OF DATE: SCALE:

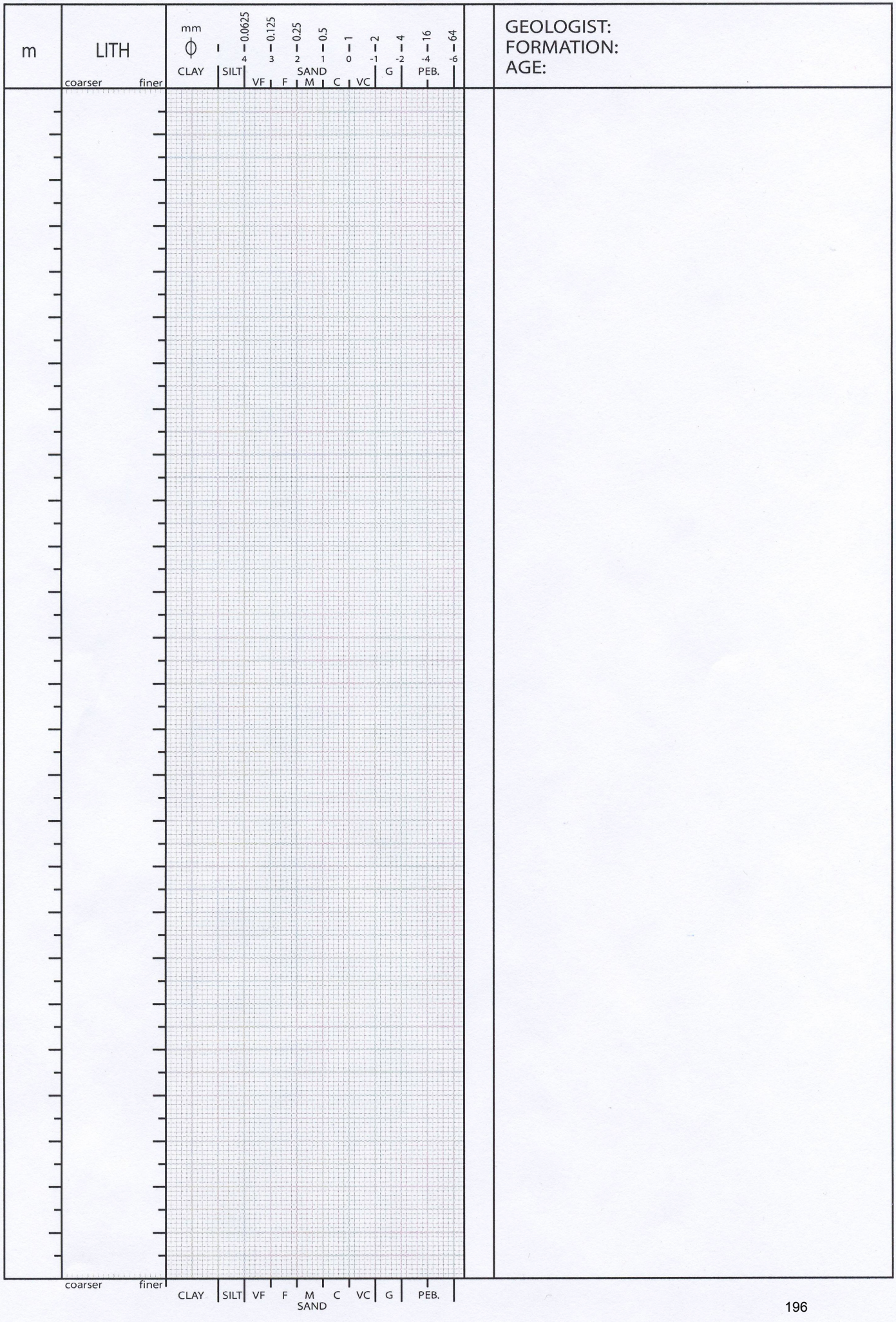

H.
O.
D.

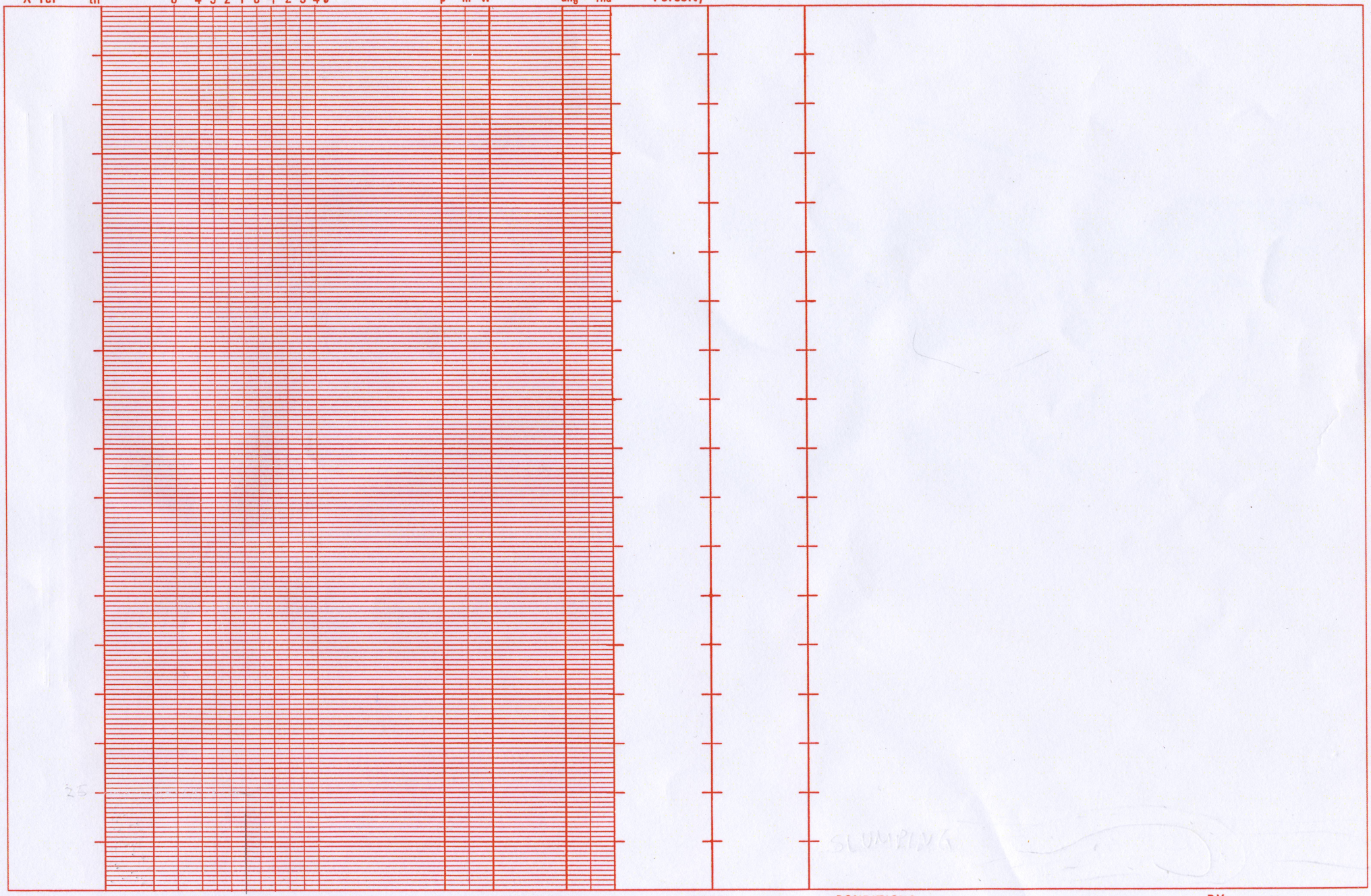

LOCATION SECTION NO. SHEET NO. DATE CONDITIONS BY

APPENDIX G - MAGNETIC SUSCEPTIBILITY

LOCALITY	PROFILE	Name	Measurement
RAMBERGØYA	PROFILE 1	Martin Kjærsgaard Martin Sandbakken	Suseptibility

Meter	Measurement 1	Measurement 2	Measurement 3	Average
-0,98	226	170	200	198,67
-0,93	192	64	211	155,67
-0,88	176	223	189	196,00
-0,83	150	158	158	155,33
-0,78	168	267	160	198,33
-0,73	183	138	151	157,33
-0,68	85	272	153	170,00
-0,63	287	241	256	261,33
-0,58	171	148	174	164,33
-0,53	195	191	250	212,00
-0,48	62	129	170	120,33
-0,43	235	208	210	217,67
-0,38	239	324	373	312,00
-0,33	253	141	256	216,67
-0,28	170	167	165	167,33
-0,23	213	225	292	243,33
-0,18	315	297	187	266,33
-0,13	242	245	216	234,33
-0,08	171	213	268	217,33
-0,03	156	217	183	185,33
0,03	392	312	365	356,33
0,08	245	311	450	335,33
0,13	319	531	327	392,33
0,18	355	348	233	312,00
0,23	357	405	429	397,00
0,28	371	410	367	382,67
0,33	393	440	313	382,00
0,38	374	439	396	403,00
0,43	351	381	369	367,00
0,48	368	384	340	364,00
0,53	367	364	365	365,33
0,58	359	428	387	391,33
0,63	397	434	381	404,00
0,68	328	453	415	398,67
0,73	377	386	434	399,00
0,78	360	412	401	391,00
0,83	356	361	378	365,00
0,88	435	411	451	432,33
0,93	368	405	353	375,33

0,98	380	442	350	390,67
1,03	428	369	349	382,00
1,08	397	434	319	383,33
1,13	443	368	596	469,00
1,18	339	340	379	352,67
1,23	392	384	365	380,33
1,28	344	347	360	350,33
1,33	308	314	383	335,00
1,38	330	398	311	346,33
1,43	369	250	290	303,00
1,48	386	313	292	330,33
1,53	282	227	395	301,33
1,58	348	388	267	334,33
1,63	311	268	272	283,67
1,68	305	369	206	293,33
1,73	179	317	309	268,33
1,78	240	294	314	282,67
1,83	253	261	292	268,67
1,88	222	250	250	240,67
1,93	226	187	216	209,67
1,98	278	219	220	239,00
2,03	182	197	230	203,00
2,08	422	333	393	382,67
2,13	315	288	280	294,33
2,18	197	214	247	219,33
2,23	251	201	171	207,67
2,28	191	200	217	202,67
2,33	168	174	172	171,33
2,38	187	188	174	183,00
2,43	228	173	151	184,00
2,48	229	238	194	220,33
2,53	294	225	262	260,33
2,58	270	272	316	286,00
2,63	307	343	277	309,00
2,68	244	262	284	263,33
2,73	226	301	315	280,67
2,78	289	258	320	289,00
2,83	289	349	320	319,33
2,88	287	308	254	283,00
2,93	314	308	355	325,67
2,98	328	320	414	354,00
3,03	312	277	297	295,33
3,08	299	312	315	308,67
3,13	303	362	318	327,67
3,18	324	326	313	321,00
3,23	317	339	315	323,67
3,28	297	344	285	308,67
3,33	313	345	339	332,33
3,38	233	317	371	307,00
3,43	212	223	200	211,67

3,48	245	229	256	243,33
3,53	258	265	253	258,67
3,58	332	248	347	309,00
3,63	368	448	415	410,33
3,68	321	544	431	432,00
3,73	368	411	474	417,67
3,78	436	366	306	369,33
3,83	363	399	340	367,33
3,88	328	233	284	281,67
3,93	282	271	256	269,67
3,98	228	272	295	265,00
4,03	247	264	282	264,33
4,08	261	306	345	304,00
4,13	256	285	284	275,00
4,18	326	350	382	352,67
4,23	390	326	373	363,00
4,28	309	314	379	334,00
4,33	426	331	417	391,33
4,38	397	441	346	394,67
4,43	345	388	413	382,00
4,48	381	365	312	352,67
4,53	416	385	404	401,67
4,58	421	377	393	397,00
4,63	412	374	386	390,67
4,68	439	410	412	420,33
4,73	280	213	269	254,00
4,78	390	370	380	380,00
4,83	277	223	239	246,33
4,88	478	508	388	458,00
4,93	288	390	445	374,33
4,98	346	285	384	338,33
5,03	377	359	359	365,00
5,08	363	343	350	352,00
5,13	338	315	356	336,33
5,18	388	370	413	390,33
5,23	387	363	375	375,00
5,28	404	393	324	373,67
5,33	378	382	433	397,67
5,38	339	344	409	364,00
5,43	294	318	291	301,00
5,48	280	300	347	309,00
5,53	425	332	337	364,67
5,58	449	356	362	389,00
5,63	375	226	336	312,33
5,68	286	340	316	314,00
5,73	301	310	356	322,33
5,78	193	333	295	273,67
5,83	280	371	229	293,33
5,88	298	309	321	309,33
5,93	344	383	445	390,67

5,98	305	332	289	308,67
6,03	288	317	194	266,33
6,08	256	231	222	236,33
6,13	334	394	372	366,67
6,18	316	307	357	326,67
6,23	311	316	372	333,00
6,28	264	302	230	265,33
6,33	430	233	315	326,00
6,38	209	379	237	275,00
6,43	286	253	289	276,00
6,48	258	296	289	281,00
6,53	183	262	145	196,67
6,58	317	248	297	287,33
6,63	229	251	259	246,33
6,68	246	356	327	309,67
6,73	323	400	316	346,33
6,78	266	233	318	272,33
6,83	307	328	306	313,67
6,88	260	279	242	260,33
6,93	337	348	277	320,67
6,98	306	247	364	305,67
7,03	333	351	339	341,00
7,08	403	437	327	389,00
7,13	404	418	259	360,33
7,18	306	305	308	306,33
7,23	306	325	423	351,33
7,28	371	378	351	366,67
7,33	369	361	418	382,67
7,38	368	360	475	401,00
7,43	302	271	314	295,67
7,48	320	360	332	337,33
7,53	352	377	345	358,00
7,58	344	352	333	343,00
7,63	339	340	343	340,67
7,68	343	389	349	360,33
7,73	362	345	370	359,00
7,78	295	327	398	340,00
7,83	286	316	293	298,33
7,88	337	296	373	335,33
7,93	430	307	384	373,67
7,98	318	302	305	308,33
8,03	347	346	354	349,00
8,08	372	369	411	384,00
8,13	380	401	405	395,33
8,18	476	369	381	408,67
8,23	368	326	354	349,33
8,28	319	395	319	344,33
8,33	306	331	316	317,67
8,38	354	226	179	253,00
8,43	206	235	228	223,00

8,48	258	396	215	289,67
8,53	287	290	390	322,33
8,58	303	409	277	329,67
8,63	290	311	368	323,00
8,68	292	335	278	301,67
8,73	244	246	261	250,33
8,78	263	259	253	258,33
8,83	357	284	251	297,33
8,88	209	248	195	217,33
8,93	264	255	265	261,33
8,98	212	232	185	209,67
9,03	242	239	251	244,00
9,08	257	238	252	249,00
9,13	268	281	221	256,67
9,18	253	326	344	307,67
9,23	275	260	288	274,33
9,28	190	162	200	184,00
9,33	275	253	295	274,33
9,38	305	268	260	277,67
9,43	262	329	241	277,33
9,48	53	181	166	133,33
9,53	174	210	232	205,33
9,58	204	248	239	230,33
9,63	63	89	96	82,67
9,68	202	200	209	203,67
9,73	267	251	261	259,67
9,78	239	183	248	223,33
9,83	175	183	194	184,00
9,88	223	240	155	206,00
9,93	212	177	186	191,67
9,98	229	233	223	228,33
10,03	216	220	198	211,33
10,08	167	182	137	162,00
10,13	193	159	209	187,00
10,18	212	35	276	174,33
10,23	245	259	230	244,67
10,28	214	235	173	207,33
10,33	199	201	204	201,33
10,38	263	210	245	239,33
10,43	206	206	211	207,67
10,48	243	213	213	223,00
10,53	250	252	277	259,67
10,58	219	256	215	230,00
10,63	299	221	228	249,33
10,68	273	170	260	234,33
10,73	200	271	238	236,33
10,78	204	176	209	196,33
10,83	198	256	228	227,33
10,93	213	207	236	218,67
10,98	249	266	228	247,67

11,03	172	256	206	211,33
11,06	275	193	268	245,33
11,12	73	68	48	63,00
11,17	276	175	201	217,33
11,22	302	332	338	324,00
11,27	330	343	295	322,67
11,32	386	259	312	319,00
11,27	315	274	213	267,33
11,42	250	286	226	254,00
11,47	222	324	211	252,33
11,52	276	352	378	335,33
11,57	299	258	332	296,33
11,62	220	275	375	290,00
11,67	226	230	224	226,67
11,72	289	236	243	256,00
11,77	207	237	220	221,33
11,82	190	77	32	99,67
11,87	342	303	217	287,33
11,92	247	304	288	279,67
11,97	247	166	78	163,67
12,02	226	205	208	213,00
12,07	197	277	240	238,00
12,13	194	212	230	212,00
12,17	223	215	199	212,33
12,22	236	285	224	248,33
12,27	263	214	319	265,33
12,34	209	288	210	235,67
12,39	232	220	300	250,67
12,43	198	275	212	228,33
12,48	271	211	338	273,33
12,53	244	263	199	235,33
12,58	372	264	240	292,00
12,63	215	209	253	225,67
12,68	209	163	199	190,33
12,73	291	296	205	264,00
12,78	287	191	244	240,67
12,83	212	271	348	277,00
12,88	209	208	218	211,67
12,93	231	191	311	244,33
12,98	262	231	248	247,00
13,03	248	327	323	299,33
13,08	351	212	253	272,00
13,13	339	373	347	353,00
13,17	250	248	279	259,00
13,23	224	277	277	259,33
13,28	262	311	230	267,67
13,33	357	239	252	282,67
13,38	192	204	166	187,33
13,43	201	166	186	184,33
13,48	280	314	365	319,67

13,53	286	252	291	276,33
13,58	171	264	266	233,67
13,63	245	242	289	258,67
13,68	171	218	197	195,33
13,73	197	232	163	197,33
13,78	303	215	324	280,67
13,83	316	272	191	259,67
13,88	201	219	259	226,33
13,93	235	339	248	274,00
13,98	237	212	248	232,33
14,03	157	203	187	182,33
14,08	230	277	213	240,00
14,13	211	145	236	197,33
14,18	206	178	214	199,33
14,23	139	153	143	145,00
14,28	246	277	246	256,33
14,33	207	218	220	215,00
14,38	262	287	255	268,00
14,43	255	264	230	249,67
14,48	214	204	215	211,00
14,53	287	210	282	259,67
14,58	253	186	292	243,67
14,63	198	234	298	243,33
14,68	273	254	241	256,00
14,73	204	286	246	245,33
14,78	23	222	209	151,33
14,83	268	198	273	246,33
14,93	206	201	183	196,67
14,98	165	180	159	168,00
15,03	166	264	217	215,67
15,08	240	216	261	239,00
15,13	190	220	166	192,00
15,18	225	209	226	220,00
15,23	236	250	211	232,33
15,28	272	232	246	250,00
15,33	195	175	240	203,33
15,38	178	201	227	202,00
15,43	293	239	299	277,00
15,48	212	240	191	214,33
15,53	233	229	225	229,00
15,58	220	207	249	225,33
15,63	233	171	203	202,33
15,68	219	226	196	213,67
15,73	214	206	220	213,33
15,78	259	242	211	237,33
15,83	254	220	213	229,00
15,88	280	249	247	258,67
15,93	228	219	239	228,67
15,98	261	223	197	227,00
16,03	220	199	221	213,33

16,08	184	188	183	185,00
16,13	175	189	229	197,67
16,18	182	226	233	213,67
16,23	185	194	166	181,67
16,28	191	192	175	186,00
16,33	215	192	187	198,00
16,38	217	176	194	195,67
16,43	167	195	187	183,00
16,48	177	180	168	175,00
16,53	200	170	171	180,33
16,58	203	165	177	181,67
16,63	201	154	186	180,33
16,68	189	202	178	189,67
16,73	229	184	211	208,00
16,78	178	250	179	202,33
16,83	206	186	184	192,00
16,88	165	181	161	169,00
16,93	190	194	179	187,67
16,98	166	238	174	192,67
17,03	191	165	249	201,67
17,08	194	186	185	188,33
17,13	164	227	183	191,33
17,18	168	179	182	176,33
17,23	159	159	178	165,33
17,28	169	198	167	178,00
17,33	203	207	216	208,67
17,38	170	182	194	182,00
17,43	170	157	197	174,67
17,48	172	173	157	167,33
17,53	181	177	162	173,33
17,58	164	159	153	158,67
17,63	174	167	193	178,00
17,68	176	165	156	165,67
17,73	197	169	190	185,33
17,78	180	163	187	176,67
17,83	188	202	154	181,33
17,88	164	190	163	172,33
17,93	213	161	170	181,33
17,98	202	192	195	196,33
18,03	172	239	225	212,00
18,08	217	198	277	230,67
18,13	231	199	199	209,67
18,18	248	189	266	234,33
18,23	205	247	195	215,67
18,28	174	168	183	175,00
18,33	197	183	177	185,67
18,38	176	161	189	175,33
18,43	174	192	180	182,00
18,48	168	201	205	191,33
18,53	213	201	184	199,33

18,58	188	193	202	194,33
18,63	213	213	204	210,00
18,68	190	149	165	168,00
18,73	181	154	183	172,67
18,78	152	162	179	164,33
18,83	198	198	187	194,33
18,88	160	160	179	166,33
18,93	173	140	169	160,67
18,98	134	133	139	135,33
19,03	60	54	48	54,00
19,08	79	76	79	78,00
19,13	157	162	158	159,00
19,18	182	156	276	204,67
19,23	155	155	152	154,00
19,28	157	142	142	147,00
19,33	180	151	172	167,67
19,38	152	193	158	167,67
19,43	193	187	174	184,67
19,48	175	175	178	176,00
19,53	160	172	170	167,33
19,58	183	162	194	179,67
19,63	183	185	165	177,67
19,68	234	195	257	228,67
19,73	197	196	184	192,33
19,78	169	165	196	176,67
19,83	166	152	183	167,00
19,88	169	160	158	162,33
19,93	203	179	197	193,00
19,98	169	166	163	166,00
20,03	63	61	171	98,33
20,08	61	54	53	56,00
20,13	87	58	176	107,00
20,18	194	84	61	113,00
20,23	70	182	65	105,67
20,28	81	77	155	104,33
20,33	171	171	72	138,00
20,38	198	172	184	184,67
20,43	77	156	184	139,00
20,48	197	48	182	142,33
20,53	137	217	228	194,00
20,58	174	184	213	190,33
20,63	58	169	166	131,00
20,68	166	158	71	131,67
20,73	170	161	152	161,00
20,78	72	148	182	134,00
20,83	188	143	186	172,33
20,88	187	201	214	200,67
20,93	162	162	194	172,67
20,98	177	177	144	166,00
21,03	67	152	57	92,00

21,08	138	159	222	173,00
21,13	186	179	140	168,33
21,18	206	164	57	142,33
21,23	191	168	219	192,67
21,28	181	245	153	193,00
21,33	224	174	156	184,67
21,38	137	145	211	164,33
21,43	182	62	178	140,67
21,48	138	232	176	182,00
21,53	209	172	149	176,67
21,58	140	251	210	200,33
21,63	205	226	193	208,00
21,68	178	158	199	178,33
21,73	167	183	214	188,00
21,78	186	192	154	177,33
21,83	181	166	177	174,67
21,88	135	131	142	136,00
21,93	181	207	259	215,67
21,98	230	164	165	186,33
22,03	142	171	178	163,67
22,08	144	114	156	138,00
22,13	138	162	75	125,00
22,18	153	148	198	166,33
22,23	68	190	151	136,33
22,28	60	67	51	59,33
22,33	63	152	159	124,67
22,38	63	135	44	80,67
22,43	146	156	62	121,33
22,48	58	53	57	56,00
22,53	37	54	77	56,00
22,58	47	61	60	56,00
22,63	44	71	65	60,00
22,68	186	192	150	176,00
22,73	61	69	57	62,33
22,78	168	209	226	201,00
22,83	183	243	154	193,33
22,88	266	257	213	245,33
22,93	170	60	79	103,00
22,98	210	190	188	196,00
23,03	194	238	209	213,67
23,08	250	238	237	241,67
23,13	200	168	172	180,00
23,18	210	191	292	231,00
23,23	191	160	168	173,00
23,28	140	66	166	124,00
23,33	251	243	267	253,67
23,38	247	285	201	244,33
23,43	186	180	183	183,00
23,48	172	169	154	165,00
23,53	171	155	158	161,33

23,58	194	167	144	168,33
23,63	162	179	158	166,33
23,68	170	166	167	167,67
23,73	164	176	165	168,33
23,78	175	146	174	165,00
23,83	192	220	156	189,33
23,88	241	158	147	182,00
23,93	155	144	202	167,00
23,98	159	167	173	166,33